

**Analysis of changes in monthly and m-daily maximum discharges using the MPI and KNMI climate scenarios in the Myjava and Hron river basins in Slovakia**

Zuzana SABOVÁ\*, Silvia KOHNOVÁ, Kamila HLAVČOVÁ

The paper is focused on an evaluation of changes in average monthly discharges and selected characteristics of maximum discharges (m-daily maximum discharges and the occurrence of maximum discharges) in the selected gauging station of Myjava in the Jablonica profile (5022) and the Hron gauging station in the Banská Bystrica profile (7160). The Indicators of Hydrological Alteration (IHA) software analyzed the data modelled using the MPI and the KNMI climate scenarios. The researched time period from 1981 to 2100 was divided into 4 thirty-year periods, i.e., 1981–2010, 2011–2040, 2041–2070, and 2071–2100. The paper aims to evaluate the changes in monthly discharges and m-daily maximum discharges in the future as well as to determine the suitability of the simulated scenario, which describes the results from the observed data. The results showed that droughts will continue to occur in the summer months and that the winter months will be accompanied by higher total precipitation in the future.

KEY WORDS: Myjava River, Hron River, IHA program, hydrological regime

### Introduction

As a result of global climate change induced by increased greenhouse gas concentrations, temperatures are expected to rise; precipitation trends will evolve; and the frequency of extreme occurrences is likely to increase. Flooding and droughts may cause considerable economic, social, and environmental damage as well as injuries and fatalities, which call for the use of reliable and accurate water supply systems (Booij, 2005).

Floods are an inherent and natural component of river geosystems, but they can also result in severe effects in urbanized landscapes. In Europe, and especially in Slovakia, the intensity and frequency of precipitation events capable of triggering excessive runoff and floods have increased dramatically in recent years (Pišút, 2011). Flooding can cause substantial damage or disruption to commodities, services, human health, and crops. Despite massive investments in flood-control infrastructures such as levees and dams, flood losses have remained significant over the years (Kozłowski, 1984).

Many kinds of flood analyses have treated events in a hydrological time series as a set of variable time-order numerical values until relatively recently. The approaches for modifying, modelling, and predicting flood values that have been created and refined over time have become more sophisticated (Hirschboeck, 1988).

The management of flows and the fragmentation of major global river systems are attracting notice. Riverine flow

variability is acknowledged as a driving force of biotic and abiotic conditions (Zhou et al., 2020). Hydrological changes and their effects on ecosystems are critical to the long-term development of water resources. Analyzing current regime changes is an important step that necessitates the use of suitable indicators (Yang et al., 2017).

River ecosystems are organized and defined by their natural flow regimes. Physical processes, particularly the movement of water and sediment inside a channel and between the channel and a floodplain, establish the physical structure of an environment and, as a consequence, of the habitats in rivers. The quantity and heterogeneity of sediments, the shapes of channels and floodplains, and other geomorphic characteristics all contribute to a river's physical environment. As a result, the habitat conditions of channels and floodplains differ for each river, depending on the flow parameters and the kind and the presence of moving materials. Different habitat characteristics are produced and maintained by a wide variety of flows within a river (Zeiringer et al., 2018).

For establishing the parameters of environmental flows, a lot of methods have been devised; each has its own set of advantages and disadvantages, as well as requiring varying levels of work. Some of these methodologies use a wide range of scientific skills along with complex software models and tools (Mathews and Richter, 2007). Historical tools may be used to address the issue of how

many hydrological alterations are too excessive for river systems. Historical approaches may concentrate on specific aspects of an ecosystem, including aquatic biology or riparian functions, instead of an overall system (Swanson, 2002). A streamflow regime is fundamental for stabilizing biodiversity and ecological integrity. Extreme occurrences such as floods and droughts are the most serious dangers to rivers caused by climate change (Lopéz-Ballesteros et al., 2020).

According to the Nature Conservancy (TNC, 2009), large floods have the following impacts on an ecosystem: a new phase in the life cycle can be a trigger (insects); they allow fish to survive and reproduce in a floodplain, as well as offer a nursery habitat for young fish; they ensure new food sources for fish and waterfowl; they create diversity in types of floodplain forests through long-term flooding (various plant species have varying levels of tolerance); plant distribution and abundance in a floodplain can be controlled, etc.

The identification of long-term changes in a hydrological regime was dealt with by Pekárová et al. (2016), who studied spatial and temporal changes in the magnitude, duration, and frequency of high flows in the Danube River basin. Pramuk et al. (2016) dealt with the analysis of long-term changes in flows in selected Slovak rivers that do not have large reservoirs (e.g., the Váh, Belá, Kysuca, Nitra, Hron, Topľa, Ipeľ and Krupinica rivers). This work focused on the average annual flows and the analysis of changes in the rising and falling rate of flow waves. Halmová et al. (2011) focused on an evaluation of changes in the minimum daily flows at selected stations on the Danube River. Other authors have also dealt with the indicators of hydrologic alteration issue, i.e., Byung-Sik et al. (2011) and Bing et al. (2012).

The aim of the paper is to identify long-term changes in the hydrological regime in the selected Slovak rivers (the Myjava and Hron) using the MPI and KNMI climate

scenarios models until 2100. We focused on changes in the characteristics of average monthly discharges and selected characteristics of the maximum discharges (monthly maximum discharges and the occurrence of maximum discharges). The first part of the paper reviews the literature relating to the problem. The second part deals with a description of the IHA program, the selection of sub-basins, the input data, and the methodology. The third part consists of the resulting values of the monthly discharges and characteristics of maximum discharges.

## Material and methods

### Study site

The research area of the study is the Myjava River basin in the Jablonica profile (5022) and the Hron River basin in the Banská Bystrica profile (7160) (Fig. 1).

The Myjava River is a left-hand tributary of the Morava River that flows through western Slovakia and a small portion of the Czech Republic. The Myjava River is 79 km long and has an area of 806 km<sup>2</sup>. It rises near the Moravian settlement of Nová Lehota in the White Carpathians, but soon crosses the Czech-Slovak boundaries and flows south until it reaches the town of Myjava, where it enters the Myjava Hills and turns west. It comes into the Záhorie Lowlands at Sobotište and goes south until it reaches the village of Jablonica; it then swings northwest until it reaches Senica, when it turns west, passes through Šaštín-Stráže and finally empties into the Morava River near Kúty.

The Hron River springs in the Horehronie at an altitude of approximately 980 m.a.s.l. It is the second-longest Slovak river with a length of 289 km; the catchment area is 5 465 km<sup>2</sup>. It is mostly a torrential river with a rapid increase in runoff along with the flow's longitudinal profile.

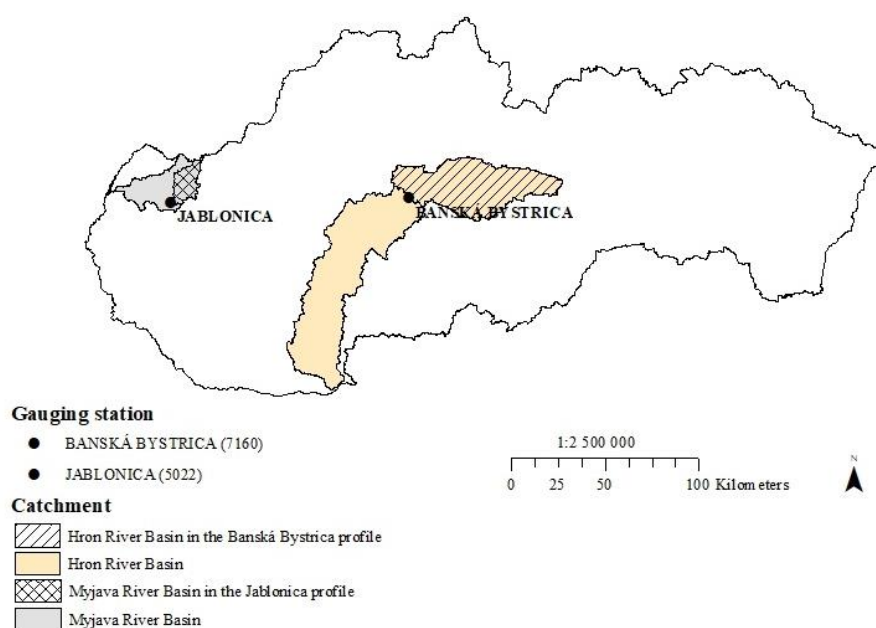


Fig. 1. Location of the Myjava and Hron River basins in Slovakia.

The selection of the river basins was based on the availability of data, their location in Slovakia, and the rate of streamflow of the river. The Hron River has higher flow rates than the Myjava River, especially in the winter and spring months, when the watercourse is affected by heavy rainfall in the form of snow or ice. There is an increased incidence of ice floods on the Hron River.

### Methodology and input data

The Indicators of Hydrologic Alteration (IHA) software was created by Brian Richter and colleagues between 1996 and 1998. It contains important information for anyone attempting to comprehend the hydrological impacts of human activities or make environmental references to watercourses. The IHA software is mostly used to examine how human activity has changed rivers, lakes, and river basins over time and analyzes scenarios for future water management (Hersh and Maidment, 2006).

To compare the features of natural and changed hydrological modes, the IHA software version 7.1.0.10 is employed. The program can accept many forms of daily hydrological data (e.g., water levels, groundwater levels, discharges). The ability to summarize long series of daily hydrological data into useable and significant hydrological parameters is a significant advantage of using this application (Pramuk et al., 2016). It is based on hydrological data within an ecosystem or data derived by a model (Yang, 2008).

A total of 67 parameters of the IHA program are split into two groups, i.e., 33 IHA parameters and 34 Environmental Flow Component (EFC) parameters. These hydrological indicators were identified for their ecological significance and capacity to represent human-induced changes in flow regimes along with a wide variety of factors, such as water retraction, dam operations, groundwater pumping, and landscape modifications (Gao et al., 2009).

The 33 IHA criteria are separated into five categories:

- the volume of monthly discharges,
- the magnitude of extremes (3-, 7-, 30-, and 90-day minimum and maximum flows; the base flow index (BFI), the number of days with zero discharges),
- yearly extremes and their timing (days of occurrences of extremes),
- high and low pulse frequencies and durations (a day is defined as a pulse if the value of a discharge is more significant or lower than the present threshold),
- changes in the flow rate and frequency (based on changes in the sequential daily discharges) (Halmová et al., 2011).

The five categories of the IHA EFC parameters are extreme low flows, low flows, high flow pulses, small floods, and large floods (Hersh and Maidment, 2006):

- **Low flows** - In most rivers, this is the most common flow state. A river's low-flow levels are maintained by groundwater discharges, which have a significant

impact on the quantity and diversity of species that may exist in the river;

- **Extreme low flows** – During droughts, water levels decrease to critical levels, which can be stressful for many species but maybe inevitable for others (TNC, 2009);
- **High-flow pulses** – These situations occur, for example, when heavy rains or snowmelt causes rising water to surpass low flow levels but not the banks of rivers;
- **Small floods** – This value accounts for all rises in the water level during a main overflow, but excludes extreme floods (Halmová et al., 2011);
- **Large floods** – Large floods usually reorganize a river's biological and physical structure, including its floodplain. These extreme floods flush out many life forms, reducing certain populations while simultaneously providing new competitive advantages for other species. Large floods may also have a role in the formation of critical ecosystems, such as oxbow lakes and floodplain wetlands (TNC, 2009).

The National Research Council of the National Academy of Sciences in USA (The National Research Council, 2005) developed a conceptual model to classify the natural flow regime into four components (Fig. 2):

- **Subsistence flow:** during extreme drought situations, the minimum streamflow required to maintain acceptable water quality and allow a minimal aquatic habitat space for the survival of aquatic species is known as subsistence flow.
- **Base flow:** the normal discharge conditions observed in a river between storms in the base flow, and it provides enough habitats for varied, native aquatic species while also maintaining groundwater levels to sustain riparian vegetation.
- **High flow pulses:** are of short duration, but are high discharges inside a stream channel that occur during or shortly after a storm event discharges fine sediment deposits and waste products; they restore the normal water quality after continuous low flows and offer longitudinal connections for the migration of species throughout the river.
- **Overbank flows:** are rare, high-flow occurrences that cause riverbanks to be destroyed. Overbank flows can reshape channels and floodplains, restore groundwater tables, provide nutrients to riparian plants, and connect channels to floodplain ecosystems that provide extra food for aquatic species (Hersh and Maidment, 2006).

In this study, the input data consists of average daily discharge data observed (OBS) from the 1981–2010 period. The observed data were provided by the Slovak Hydrometeorological Institute. We also modelled the average daily discharge data using the MPI and the KNMI scenarios in the time period of 1981–2100. The methodological approach of the non-parametric statistical processing of the daily series of flows

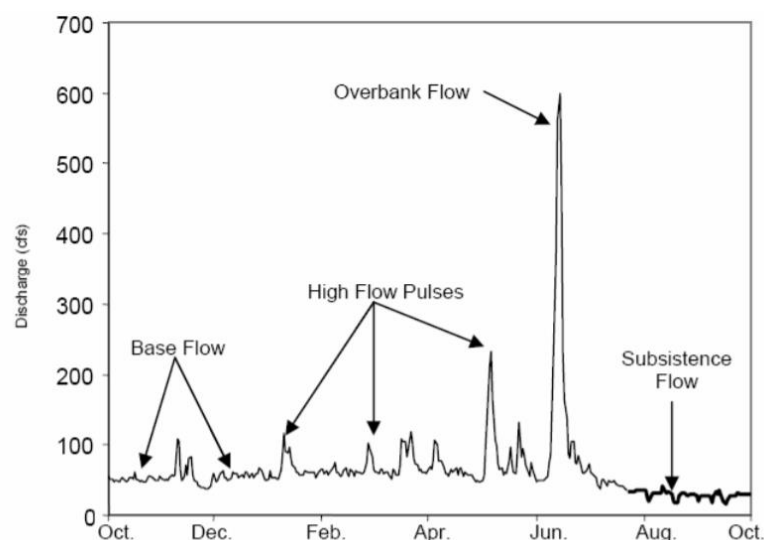


Fig. 2. Example of a daily streamflow hydrograph depicting flow components (Hersh and Maidment, 2006).

**Table 1.** Selected time periods used in the study

	Data	Time period
First period	OBS, MODEL, MPI and KNMI	1.1.1981 – 31.10.2010
Second period	MPI and KNMI	1.11.2010 – 31.10.2040
Third period	MPI and KNMI	1.11.2040 – 31.10.2070
Fourth period	MPI and KNMI	1.11.2070 – 31.10.2100

measured at the gauging stations in the Hron River and Myjava River sub-basins was used. The hydrological characteristics of the daily discharges were calculated for four periods, i.e., 1981–2010, 2011–2040, 2041–2070, and 2071–2100, which we can see in Table 1. We used modelled data (MODEL) in the first period to a comparison with both climate scenarios. To model the average daily discharges, the HBV rainfall-runoff model was used (Výleta et al., 2020).

The hypothetical climate scenarios used in this study are the Dutch KNMI (with the A1B emission scenario) and the German MPI (with the A1B emission scenario). These regional circulation models use the ECHAM5 global model's outputs as the boundary terms for solving equations. Both models are linked, i.e., they are atmosphere-ocean cycle models with gas emissions and aerosol effects on changes in radiative forcing (Rončák and Šurda, 2019).

In Slovakia, the MPI and the KNMI regional climate models have 19x10 grid points with a precise topography and a suitable representation of all the topographic features greater than 25 km. The daily means, the maximum and lowest air temperatures, the daily means of the relative air humidity, the total daily precipitation, the daily wind speed means, and the daily totals of the global radiation are among the variables for which scenarios have been developed (Rončák et al., 2021).

## Results

First, we focused on an analysis of the changes in monthly discharges in both gauging stations selected. We looked at the resulting discharge values from several points of view:

- A comparison of the simulated monthly discharges using the MPI scenario and modelled data (MODEL) in the first time period (1981–2010),
- A comparison of the simulated monthly discharges using the KNMI scenario and modelled data (MODEL) in the first time period (1981–2010),
- A comparison of the changes in the simulated monthly discharges using the MPI and the KNMI scenarios until 2100.

The analyses of the changes in the monthly discharges at the Jablonica (5022) gauging station revealed (Table 2):

- The highest mean monthly discharges are concentrated for the MODEL data ( $2.65 \text{ m}^3 \text{ s}^{-1}$ ) and simulated data using the MPI scenario ( $2.99 \text{ m}^3 \text{ s}^{-1}$ ) in March in the first period. The largest differences between the MODEL and simulated data using the MPI scenario occur in April and June.
- When we compared the MODEL and simulated data using the KNMI scenario, the highest monthly discharge also occurs in March ( $2.65 \text{ m}^3 \text{ s}^{-1}$ ). The simulated data using the KNMI scenario are

close to the MODEL data, that's why the KNMI scenario is a better choice for similar analyses in the future at the Jablonica gauging station.

c) If we focus on the results of the simulated data using the MPI and the KNMI climate scenarios throughout the period under study, we observed that the simulated data using the MPI scenario have an upward trend in the second period, but in the following period, the average monthly values of the discharges decrease. This decline continues until 2100, with the exceptions of November, February, March, and June. On the other hand, the modelled data using the KNMI scenario show a declining trend in the second time period (except for the months of December, January, February, September, and October). In the third period, according to this scenario, the average monthly values of the discharges will average 1:1 (decrease:increase). In the last research period up to 2100, the mean monthly discharges will decrease, especially in the summer months. The decreases occurring in the mean monthly discharges may be due to a higher incidence of drought in the study area in the future.

Using the IHA method (Table 3), it was determined for the Banská Bystrica (7160) gauging station that:

- a) According to the simulated data using the MPI scenario, the highest average monthly discharges occur in April ( $42.94 \text{ m}^3 \text{ s}^{-1}$ ), and in the same month we record the highest mean monthly discharges of the MODEL data ( $36.26 \text{ m}^3 \text{ s}^{-1}$ ) in the first period. For the average monthly discharges, the use of simulated data using the MPI scenario is also a better choice for similar analyses in the future because the scenario describes the closest reality.
- b) The simulated data using the KNMI scenario show the highest monthly discharges also in April ( $32.27 \text{ m}^3 \text{ s}^{-1}$ ).

c) In terms of their future changes, the simulated data using the MPI and the KNMI scenarios in December, March, April, May, and September show the same trend, i.e., an increase in the values of the average discharges in the second period examined, a decrease in the next period, and again, in the fourth time period, an increase in the values of the average discharges. The simulated data using the MPI scenario show an increase by 2100 in January and February. Within the simulated data using the KNMI scenario, we can observe a decrease in the average monthly discharges up to 2100 in June and July.

The second part of the analysis deals with changes in the m-daily maximum discharges and the occurrence of maximum discharges.

We found that the MODEL data of m-daily maximum discharges at Jablonica (5022) gauging station, see Table 4, are underestimated in the first time period compared to the simulated data using MPI and KNMI scenarios in the 1-daily and 3-daily maximum discharges. With a view to the future, the simulated data of the m-daily maximum discharges using the MPI will increase in the first thirty years, then decrease and increase again by 2100. The simulated data using the KNMI scenario have approximately the same average final values of the m-daily maximum discharges until 2040, and by 2100, its values will also increase.

The occurrence of the maximum discharge until 2010 was in March. According to the scenarios, it will be moved to February by 2040, and by 2070, the maximum discharges will occur again in March. In the last thirty-year period surveyed, the occurrence of maximum discharges is divided into two months, i.e., February and March.

The greatest changes in the m-daily maximum discharges occurred in the course of the 1-day maximum discharge. In Fig. 3, we can see the course of the 1-daily yearly

**Table 2. Median values of the mean monthly discharges at the Jablonica (5022) gauging station [ $\text{m}^3 \text{ s}^{-1}$ ] for the selected period**

Myjava – Jablonica (5022)	OBS	MODEL	MPI	KNMI	MPI	KNMI	MPI	KNMI	MPI	KNMI
	1981–2010				2011–2040		2041–2070		2071–2100	
November	0.58	0.50	0.60	0.60	0.72	0.58	0.50	0.52	0.64	0.59
December	0.63	0.88	0.99	0.84	1.48	1.89	1.38	1.88	1.31	1.87
January	0.72	1.19	1.22	1.17	1.48	2.02	2.21	2.67	1.89	2.81
February	1.21	1.53	1.62	1.61	2.70	2.17	2.59	2.54	3.05	3.42
March	1.48	2.65	2.99	2.65	3.01	2.39	2.64	2.91	3.84	3.03
April	1.34	2.21	2.62	2.27	2.68	1.89	3.20	2.66	2.59	3.31
May	1.15	1.26	1.60	1.58	1.49	1.35	1.86	1.51	1.51	1.66
June	0.85	0.92	1.36	1.08	1.11	0.94	0.90	0.83	0.95	0.72
July	0.65	0.69	0.67	0.77	0.83	0.51	0.62	0.43	0.48	0.31
August	0.41	0.44	0.39	0.37	0.41	0.34	0.33	0.41	0.28	0.26
September	0.44	0.35	0.56	0.39	0.56	0.46	0.31	0.28	0.26	0.27
October	0.42	0.30	0.37	0.33	0.55	0.61	0.48	0.54	0.43	0.47

**Table 3. Median values of the mean monthly discharges at the Banská Bystrica (7160) gauging station [ $\text{m}^3 \text{s}^{-1}$ ] for the selected period**

Hron – Banská Bystrica (7160)	OBS	MODEL	MPI	KNMI	MPI	KNMI	MPI	KNMI	MPI	KNMI
	1981–2010				2011–2040		2041–2070		2071–2100	
November	12.63	10.93	11.61	12.61	15.31	13.77	11.01	11.22	14.36	11.12
December	14.28	13.30	12.16	14.51	20.25	24.18	18.46	22.64	24.89	27.44
January	11.82	11.60	10.59	13.83	13.98	21.14	20.09	26.38	24.43	24.42
February	11.57	11.17	13.10	17.37	16.38	25.44	26.56	23.79	28.58	31.69
March	23.29	24.58	24.60	23.97	24.61	27.86	31.60	31.50	34.74	32.01
April	40.96	36.26	42.94	32.27	37.93	27.71	39.87	34.60	38.63	37.48
May	30.61	26.72	28.34	25.18	25.00	23.60	28.84	26.48	25.38	22.00
June	21.30	25.38	27.61	25.61	23.77	19.45	23.78	17.88	22.48	15.35
July	16.35	19.00	17.50	17.81	19.95	15.50	17.19	13.12	13.05	10.34
August	12.12	12.85	13.76	13.54	13.18	9.90	11.71	11.92	10.61	9.02
September	10.06	10.69	11.36	10.30	12.11	12.44	10.22	9.49	9.48	8.73
October	9.98	10.39	10.54	9.93	14.54	12.67	11.19	10.43	12.56	9.82

**Table 4. M-daily maximum discharges and the occurrence of maximum discharges for the Jablonica (5022) gauging station for the selected period**

Myjava – Jablonica (5022)	OBS	MODEL	MPI	KNMI	MPI	KNMI	MPI	KNMI	MPI	KNMI	
	1981–2010				2011–2040		2041–2070		2071–2100		
1-day maximum	8.92	6.09	6.80	6.48	9.06	6.53	6.70	7.19	6.96	8.64	
3-day maximum	6.72	5.84	6.58	6.29	8.61	6.31	6.30	6.87	6.84	8.27	
7-day maximum	[ $\text{m}^3 \cdot \text{s}^{-1}$ ]	4.54	5.47	6.11	5.93	7.87	5.79	5.87	6.50	6.62	7.75
30-day maximum		3.13	4.07	4.52	4.79	5.74	4.42	4.49	5.02	5.58	5.78
90-day maximum		2.12	2.69	3.07	3.11	4.11	3.27	3.64	3.62	4.09	4.01
Date of maximum	[month]	March	March	March	March	February	February	March	March	March	February

maximum discharges of the MODEL data until 2010, and the simulated 1-daily yearly maximum discharges from the MPI and the KNMI climate scenarios models until 2100.

Within the 7-day maximum discharge characteristics, the changes in flow rates decreased in the first period examined (Fig. 4). According to the simulated data using the MPI and the KNMI climate scenarios better, the resulting values of the 7-day maximum discharges describe the MODEL data. The simulated data using the KNMI scenario show a calmer course in the future than the MPI scenario.

The second gauging station discussed is the Banská Bystrica (7160), in which the following results were determined by analyses of changes in the m-daily maximum discharges (Table 5): using the MPI scenario in the period 1981–2010, the simulated m-daily maximum discharges contain the lowest resulting values

(compared to the MODEL and simulated data using the KNMI scenario). The discharges modelled using the MPI scenario will increase in the second time period, but the simulated discharges using the KNMI scenario will decrease. The occurrence of the maximum discharges is in March. Maximum discharges may also occur in April until 2100.

Even in this case, figures were created to better represent changes for 1-day yearly maximum discharges (Fig. 5) and 7-day yearly maximum discharges (Fig. 6) for the Banská Bystrica (7160) gauging station. The simulated data using MPI and KNMI scenarios show extremes for 1-day yearly maximum discharges in 1987. The simulated MPI scenario is more suitable for the Banská Bystrica (7160) gauging station than to examine other analyses because his course of 7-day yearly maximum discharges is more extreme than the simulated KNMI scenario.

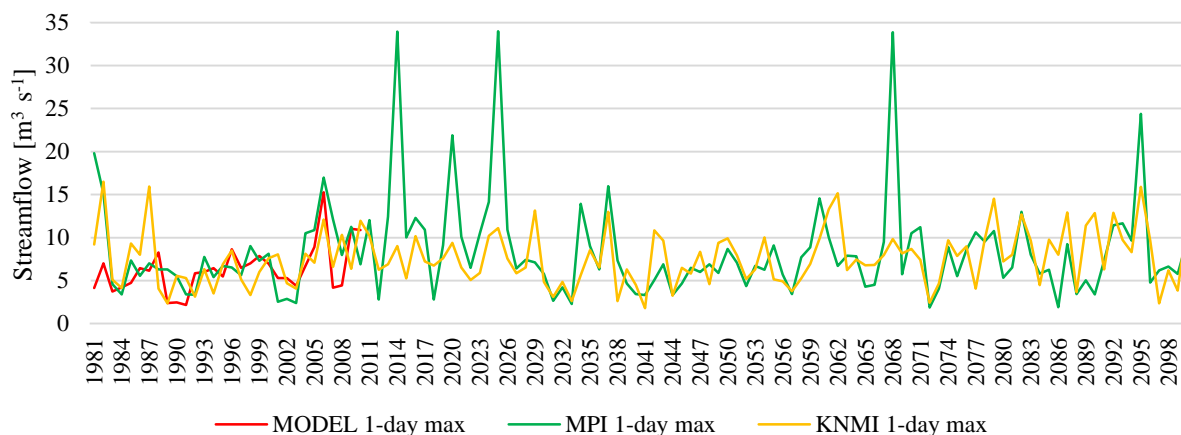


Fig. 3. 1-day yearly maximum discharges for the MODEL (1981–2010) and the simulated data using the MPI and the KNMI scenarios (1981–2100) for the Jablonica (5022) gauging station.

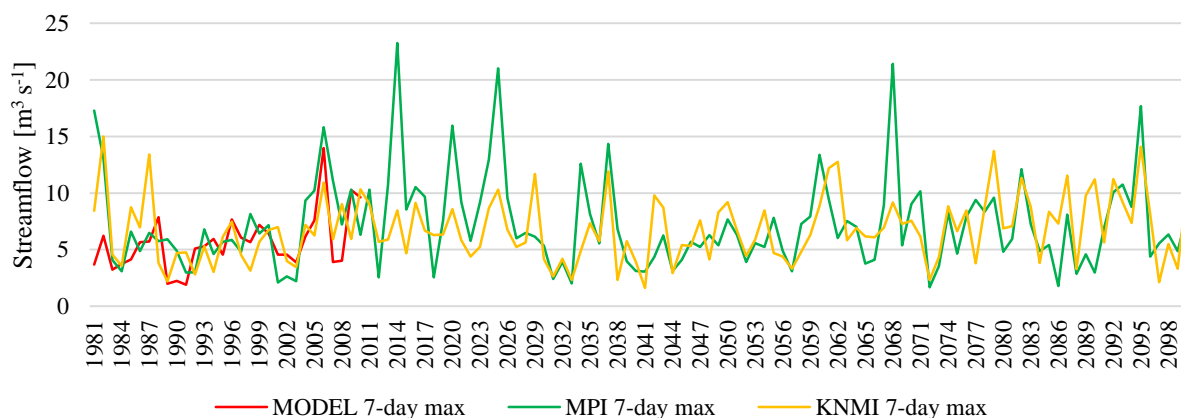


Fig. 4. 7-day yearly maximum discharges for the MODEL data (1981–2010) and the simulated data using the MPI and the KNMI scenarios (1981–2100) for the Jablonica (5022) gauging station.

**Table 5. M-daily maximum discharges and the occurrence of maximum discharges for the Banská Bystrica (7160) gauging station during the studied period**

Hron – Banská Bystrica (7160)		OBS	MODEL	MPI	KNMI	MPI	KNMI	MPI	KNMI	MPI	KNMI
		1981–2010				2011–2040		2041–2070		2071–2100	
1-day maximum		116.10	87.23	79.21	92.09	95.36	86.51	82.83	85.18	82.70	94.85
3-day maximum		97.90	83.35	76.01	84.59	92.05	81.96	79.08	80.47	79.23	91.41
7-day maximum	[m <sup>3</sup> s <sup>-1</sup> ]	81.01	78.13	70.74	78.86	86.84	72.17	69.40	71.35	74.66	83.04
30-day maximum		59.38	55.63	52.28	55.25	62.43	50.57	51.09	56.72	58.03	56.51
90-day maximum		40.53	39.66	39.65	39.36	41.86	36.03	39.75	40.52	43.04	44.63
Date of maximum	[month]	May	April	April	May	April	April	March	March	April	March

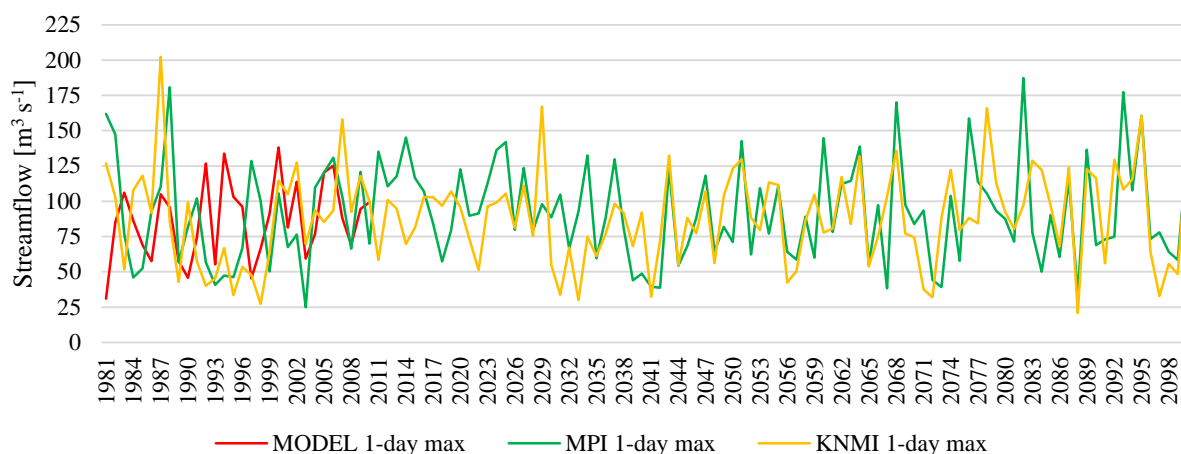


Fig. 5. 1-day yearly maximum discharges for the MODEL data (1981–2010) and the simulated data using the MPI and the KNMI scenarios (1981–2100) for the Banská Bystrica (7160) gauging station.

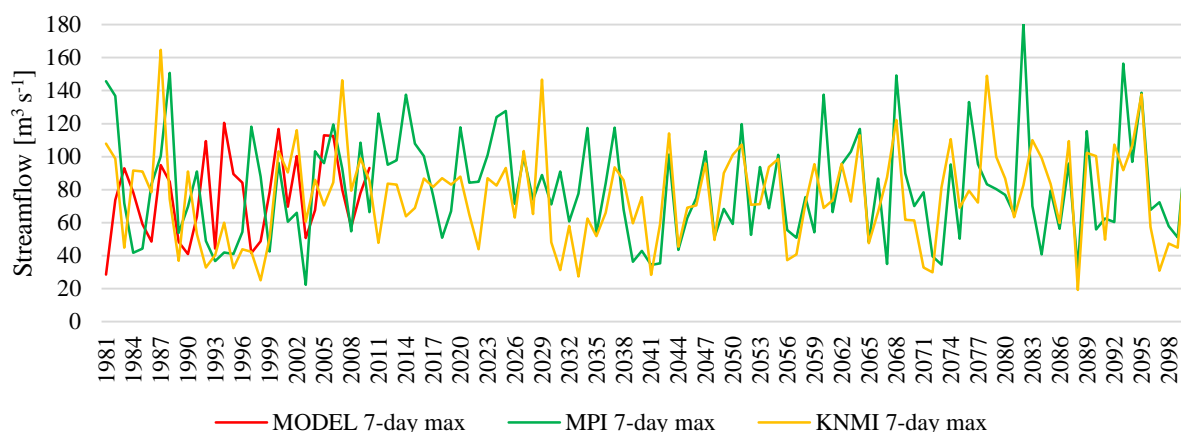


Fig. 6. 7-day yearly maximum discharges for the MODEL data (1981–2010) and the simulated data using the MPI and the KNMI scenarios (1981–2100) for the Banská Bystrica (7160) gauging station.

## Conclusion and discussion

In our work, we dealt with changes in the average monthly discharges until 2100, changes in the m-daily maximum discharges, and the occurrence of maximum discharges until 2100 in the Jablonica (5022) gauging station and in the Banská Bystrica (7160) gauging station. We used the IHA program, version 7.1.0.10, in which we focused on the characteristics of the m-daily maximum discharges, i.e., 1-day, 3-day, 7-day, 30-day and 90-day maximums, and the occurrence of maximum discharges. We worked with three groups of data, i.e., the observed data, the MODEL data and simulated data using the MPI and KNMI scenarios until 2100. The time period of 1981–2100 was divided into 4 groups, i.e., 1981–2010, 2011–2040, 2041–2070, and 2071–2100, in which we monitored changes in the hydrological characteristics investigated.

The following characteristics were noted at the Jablonica (5022) gauging station:

- The highest average monthly discharges occur in the months of February, March, and April. The simulated average monthly discharges using the MPI scenario increase until 2040 and then decrease until 2100 (except for November, February, March, and June). The simulated average monthly discharges using the KNMI model scenario decrease until 2040; by 2070, the final values of the average monthly discharges do not significantly differ, and by 2100, their values will decrease, especially in the summer months.
- Within the m-daily maximum discharges, it was determined in this study that there are no significant differences in the first time period between the MODEL and simulated data using the MPI and the KNMI scenarios. The occurrence of maximum

discharges is in February and March. The most extreme fluctuations of the resulting m-daily maximum discharges occur from 2080 to 2100.

For the Banská Bystrica (7160) gauging station it was determined in this work that:

- The highest monthly discharges occur in the months of March and April. The simulated monthly discharges using the MPI and the KNMI scenarios have similar course in December, March, April, May, and September: they increase by 2040, decrease by 2070, and increase by 2100.
- At this gauging station, we see more extreme fluctuations of the m-daily maximum discharges than at the Jablonica (5022) gauging station investigated. The occurrence of maximum discharges is concentrated in the months of March, April, and May.

In general, it was found that the simulated data using the KNMI scenario are more suitable for the Jablonica (5022) gauging station because it shows the smallest differences in the resulting values from the observed and MODEL data compared to the MPI scenario. At the Banská Bystrica (7160) gauging station, on the contrary, the simulated data using MPI scenario are more suitable for the future predictions.

A significant finding is that the maximum discharges at the Banská Bystrica (7160) gauging station occur in April and May and that their occurrence will shift by 2100 for the months of March, and April. This can be caused by warming of the climate (rapid melting of snow in the winter months) and an increase in total precipitation in the colder period of the year. The model outputs assume that the summer precipitation regime should change to periods of more frequent droughts (a decrease in the average monthly discharges).

In the summer months, such changes, i.e., a reduction in total precipitation and an increase in the variability of total precipitation are expected to last longer. The aspects noted are the reason for the emergence of dry periods and the emergence of short-term rainy periods (Mind'áš et al., 2011). According to the study "Climate change and its possible consequences in cities" (Lapin et al., 1997), the increase in winter runoff by 2075 may change as follows: northern Slovakia 10–40%, central Slovakia: 20–50%, and southern Slovakia 30–80%.

With the help of the IHA program, it is possible to investigate further changes in the characteristics of a hydrological regime, and changes in the basic settings of the IHA program can achieve the results desired for various watercourses around the world.

### Acknowledgement

The study was supported by the VEGA Agency No. 1/0782/21 and by APVV No. 19-0340, APVV No. 20-0374. The authors are very grateful for their research support.

### References

- Bing, G., Dawen, Y., Tongtiengang, Z., Hanbo, Y. (2012): Changes in the eco-flow metrics of the Upper Yangtze River from 1981 to 2008. *Journal of Hydrology*. vol. 448–449, 30–38.
- Booij, M. J. (2005): Impact of climate change on river flooding assessed with different spatial model resolutions. *Journal of Hydrology*, vol. 303, 176–198.
- Byung-Sik, K., Bo-Kyung, K., Hyun-Han, K. (2011): Assessment of the impact of climate change on the flow regime of the Han River basin using indicators of hydrologic alteration. *Hydrological Processes*. vol. 25, 691–704.
- Gao, Y., Vogel, R. M., Kroll, CH. N., Poff, N. L., Olden, J. D. (2009): Development of representative indicators of hydrologic alteration. *Journal of Hydrology*. vol. 374, 136–147.
- Halmová, D., Pekárová, P., Meszároš, I. (2011): Low flow change analysis in selected gauging stations on the Danube River. *Acta Hydrologica Slovaca*. vol. 12, no. 2, 286–295.
- Hersh, E., Maidment, D. (2006): Assessment of Hydrologic Alteration software. CRWR Online Report 06-11, TX 78712-4497.
- Hirschboeck, K. K. (1988): Flood Hydroclimatology. *Flood Geomorphology*. 27–49.
- Kozłowski, T. T. (1984): Extent, Causes, and Impacts of Flooding. *Flooding and plant growth*. 1–6.
- Lopéz-Ballesteros, A., Senent-Aparicio, J., Martínéz, C., Peréz-Sánchez, J. (2020): Assessment of future hydrologic alteration due to climate change in the Arachos River Basin (NW Greece). *Science of the Total Environment*. vol. 733, 13 p.
- Mathews, R., Richter, B. D. (2007): Application of the indicators of hydrologic alteration software in environmental flow setting. *Journal of the American Water Resources Association*. vol. 43, no. 6, 1400–1413.
- Mind'áš, J., Páleník, V., Nejedlík, P. (2011): Consequences of climate change and possible adaptation measures in individual sectors. EFRA – Scientific Agency for Forestry and Ecology. Zvolen, 253 p.
- Pekárová, P., Pramuk, B., Halmová, D., Miklánek, P., Prohaska, S., Pekár, J. (2016): Identification of long-term high-flow regime changes in selected stations along the Danube River. *Journal of Hydrology and Hydromechanics*. vol. 64, no. 4, 393–403.
- Pišút, P. (2011): The 1787 flood of the River Danube in Bratislava. *Geographical Journal*, vol. 63, no. 1, 87–109.
- Pramuk, B., Pekárová, P., Škoda, P., Halmová, D., Bačová Mítková, V. (2016): Identification of the Slovak rivers daily discharge regime changes. *Acta Hydrologica Slovaca*. vol. 17, no. 1, 65–77.
- Rončák, P., Šurda, P. (2019): Water balance estimation under a changing climate in the Turiec River basin. *Acta Hydrologica Slovaca*. vol. 20, no. 2, 160–165.
- Rončák, P., Šurda, P., Vitková, J. (2021): The impact of climate change on the hydropower potential: a case study from Topľa River basin. *Acta HS* vol. 22, no. 1, 22–29.
- Swanson, S. (2002): Indicators of Hydrologic Alteration. Resource notes. vol. 58, 2 p.
- The National Research Council, 2005: The Science of Instream Flows: A Review of the Texas Instream Flow Program. The National Academies Press, Washington, D. C, 126 p.
- TNC (2009): Indicators of Hydrologic Alteration Version 7 User's Manual. 76 p.
- Výleta, R., Hlavčová, K., Szolgay, J., Kohnová, S., Valent, P., Danáčová, M., Kandra, M., Alekšič, M. (2020): Reassessment of the structure and methodology of the quantitative water balance of the surface water. Bratislava, 282 p.
- Yang, T., Cui, T., Xu, Ch., Ciais, P., Shi, P. (2017): Develop-

- ment of a new IHA method for impact assessment of climate change on flow regime. *Global and Planetary Change*, vol. 156, 68–79.
- Yang, T., Zhang, Q., Chen, Y. D., Tao, X., Xu, CH., Chen, X. (2008): A spatial assessment of hydrologic alteration caused by dam construction in the middle and lower Yellow River, China. *Hydrological Processes*. vol. 22, 3829–3843.
- Zeiringer, B., Seliger, C., Greimel, F., Schmutz, S. (2018): River Hydrology, Flow Alteration, and Environmental Flow (Chapter 4). *Aquatic Ecology Series*. vol. 8, 67–89.
- Zhou, X., Huang, X., Zhao, H., Ma, K. (2020): Development of a revised method for indicators of hydrologic alteration for analyzing the cumulative impacts of cascading reservoirs on flow regime. *Hydrology and Earth System Sciences*. vol. 24. 4091–4107.

Ing. Zuzana Sabová (\*corresponding author, e-mail: zuzana.sabova@stuba.sk  
prof. Ing. Silvia Kohnová, PhD.  
prof. Ing. Kamila Hlavčová, PhD.  
Department of Land and Water Resources Management  
Faculty of Civil Engineering  
Slovak University of Technology in Bratislava  
Radlinského 11  
811 07 Bratislava  
Slovak Republic

### Peak maxima on the rivers of the Prut and Siret basins (within Ukraine)

Stanislav MOSKALENKO, Liudmyla MALYTSKA \*

The study performed in the article revealed how the daily mean maximum discharge of water runoff and peak discharge of water runoff corresponding to this day on the rivers in the Prut and Siret basins are correlated. There are only the upper reaches of these rivers with a total catchment area of 11300 km<sup>2</sup> within Ukraine. Climatic (significant precipitation) and orographic (35% of the territory of these basins is mountain Carpathians) conditions of the Prut and Siret basins contribute to the formation of significant maxima on rivers during rain floods, which often become dangerous with devastating effects and provide the highest peaks in the year. The analysis of maxima is based on the use of historical series of observations at 12 hydrometric gauges. As a result, we found that for small rivers in the mountains, maximum peaks exceed the daily mean maximum discharges on average by 1.8–2.0 times. In the foothills with an increase in the area of the studied catchments and with a decrease in slopes and heights they exceed by 1.4–1.7 times, and with access to the plain – by 1.0–1.3 times. Such research is influential in assessing and forecasting the hazard of the hydrological situation on rivers.

KEY WORDS: Prut and Siret rivers basins, Ukraine, maximum river runoff, daily mean maximum discharge of water runoff, peak discharge of water runoff

#### Introduction

The maximum river runoff is one of the important extreme regime characteristics of river water runoff. It causes various manifestations of catastrophic situations (flooding of territories, settlements, destruction of bridges, buildings, hydraulic structures, etc.). High rises in water levels and a corresponding increase in water discharges are observed on rivers during periods of spring freshets and floods. They depend on the intensity and duration of water supply to the watershed basin surface, also the flow rates and the state of the catchment. The maximum river runoff is observed at the peak of the main wave of floods or freshets. The maximums on the rivers are characterized by the daily mean maximum discharge of water runoff (defined as an average over the periods daily measurement) or peak discharge of water runoff (the absolute maximum of the day). On small rivers, there could be significant differences in values between these maximum values, but the larger the river, the smaller these differences. Especially, such differences can be traced in mountainous regions, where, flowing from mountains with large slopes, rivers pass into the foothills and then go to the plain or lowland (Lukianets and Moskalenko, 2019b; Lukianets et al., 2019).

The main purpose of the study is to identify how the daily

mean maximum and peak maximum of water runoff of the day on the rivers in the Prut and Siret basins are related. This is an influential issue in assessing and forecasting the hazard of the hydrological situation on rivers.

Prut and Siret are the rivers in southeastern Europe (Fig. 1). They belong to the Danube river basin (Black Sea basin) and they are its left tributaries. Only the upper reaches of the Prut and Siret rivers are located within Ukraine. They originate in the Carpathian Mountains. The length of the Prut River in Ukraine is 272 km, the Siret River is 115 km. The total catchment area of these rivers in Ukraine is 11300 km<sup>2</sup> (Lukianets and Moskalenko, 2019a). The heights of the terrain in these basins are distributed as follows: 55% of the study area is within the heights of 200–400 m a.s.l., 16% – 400–800 m a.s.l. and 29% – above 800 m a.s.l.

The Prut and Siret river basins (within Ukraine) belong to areas with a complex nature of atmospheric processes and weather conditions that associated with the location of the watershed basins on the border of circulating systems of temperate and subtropical latitudes and with a pronounced influence of mountain systems. For the south of Eastern Europe, Ukraine, and for the basins of the Prut and Siret rivers, the following circulation features are most characteristic: the predominance of the anticyclonic circulation during the year; increased

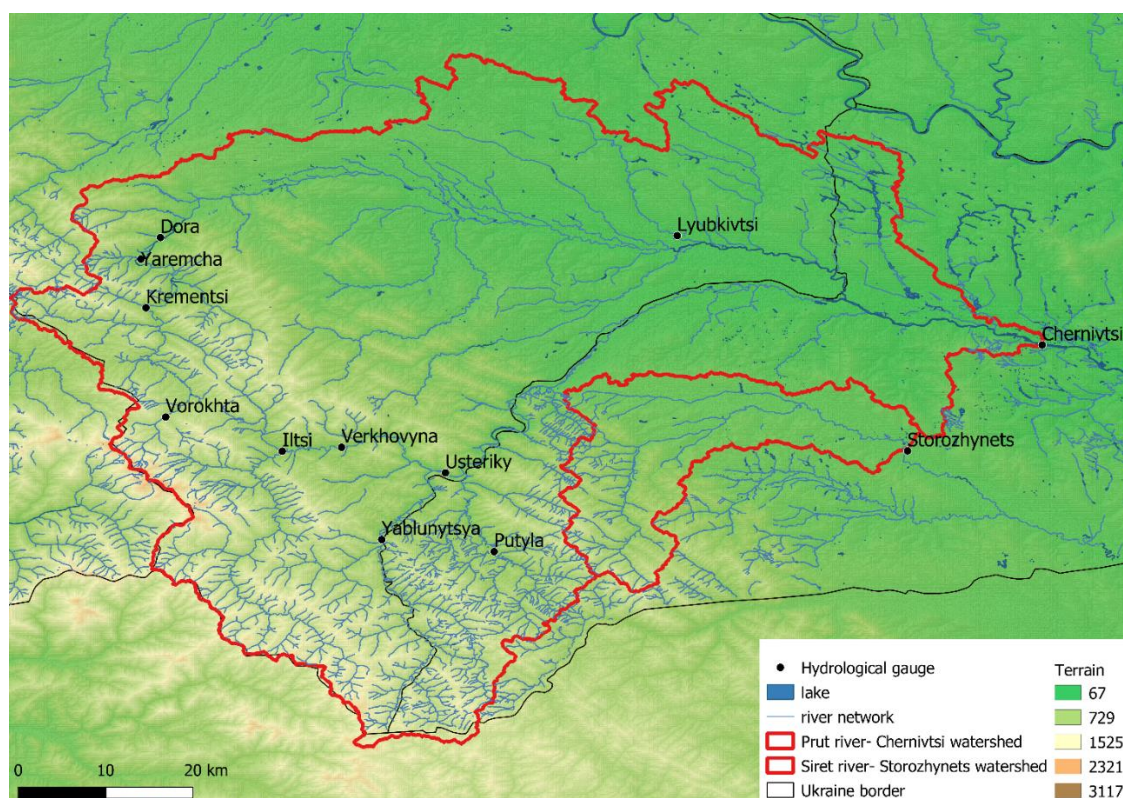


Fig. 1. Area of investigation.

activity of atmospheric processes and sudden changes in weather in the cold season; weakening of the activity of atmospheric processes and the development of intensive convection in the warm season.

Average annual precipitation in the Prut and Siret basins generally increases with the height of the area from 630–660 mm to 1400–1420 mm (Balabukh and Lukianets, 2011). In some years, the annual amount of precipitation can reach from 940 to 1850 mm (also according to the altitude of the territory). However, there were years when they did not exceed 370–560 mm in most parts of basin, and 1000 mm at an altitude above 1000 m.

In the water regime, spring floods are observed, but rain floods prevail in the warm season. They are those who acquire the nature of dangerous phenomena with destructive consequences and provide high maximums per year. Snow – rain floods of the cold period occur on the studied rivers, but they are not typical.

The intensity of the development of rain floods in the basins of the Prut and Siret rivers can be represented by the following data. In the section of the gauging station on mountain rivers, the time interval between the onset of the precipitation core and the flood maximum from a drainage area of 1000–1200 km<sup>2</sup> is 6–10 hours (Grebin et al., 2012). The mountainous part of the basins belongs to the main flow formation zone.

### Material and methods

To accomplish the tasks set, statistical methods for

processing hydrometeorological information were used (determining the numerical characteristics of random variables, testing statistical hypotheses for the homogeneity of data series, statistical analysis of dependencies between variables, etc.).

A database has been created for a long-term period – the daily mean maximum water discharge and the maximum peak water discharge corresponding them on the rivers of the Prut and Siret river basins. There are 12 gauging stations in the study area, which monitor the flow of water in rivers. Eleven of them are located in the Prut basin and 1 gauging station is in the Siret basin. Table 1 lists the hydrological gauges, periods of water flow monitoring, and hydrographic characteristics of rivers and their catchment areas.

Analyzing the hydrographic characteristics (Table 1), we see that the watersheds in the Prut basin have a fairly large range of their average heights – 450–1200 m. The average height of the Siret – Storozhynets' river basin is 590 m. The areas of the studied watersheds in the Prut basin vary from 18.1 km<sup>2</sup> (Kam'yanka river – Dora) to 1500 km<sup>2</sup> (Cheremosh river – Usteriky). The point to the outlet of the Prut River basin within Ukraine is the city of Chernivtsi (Prut river- Chernivtsi) with a catchment area of 6890 km<sup>2</sup>. The catchment area of the Siret river – Storozhynets' is 672 km<sup>2</sup>.

The source data bank (daily mean maximum water discharge and corresponding them the maximum peak water discharge) was created from the beginning of observations up to 2016 inclusive. At 83% of

**Table 1. Hydrographic characteristics of rivers and their catchments of the Prut and Siret river basins**

River – Hydrological gauge	Observation period (number of years)	Fall of the river [‰]		River basin				
		Average	Weighted average	Area [km <sup>2</sup> ]	Mean altitude [m a.s.l.]	Average fall [%]	Waterlogged [%]	Wooded [%]
Siret river – Storozhynets'	1953–2016 (64)	9.3	4.7	672	590	144	<1	51
Prut river – Vorokhta	1978–2016 (39)	–	–	48.3	–	–	–	–
Prut river – Kremetsi	1959–2016 (57)	27.5	11.9	366	1000	285	0	85
Prut river – Yaremcha	1950–2016 (67)	21.8	9.6	597	990	281	0	87
Prut river – Chernivtsi	1895–1911, 1920–1924, 1926–1935, 1945–2016 (109)	7.8	3.6	6890	450	–	<1	42
Kam'yanka river – Dora	1946–2016 (71)	111	66.4	18.1	870	446	0	76
Chornyava river – Lyubkivtsi	1984–2016 (32)	–	–	333	–	–	–	–
Cheremosh river – Usteriky	1957–2016 (59)	9.8	9.0	1500	1100	–	0	51
Bilyy Cheremosh river – Yablunytsya	1958–2016 (59)	19.0	10.2	552	1200	334	0	56
Chornyy Cheremosh river – Verkhovyna	1958–2016 (59)	16.7	11.4	657	1200	321	0	57
Il'tsya river – Il'tsi	1959–2016 (58)	40.2	30.5	86.1	1100	303	0	52
Putyla river – Putyla	1963–2016 (54)	24.2	15.8	181	960	325	0	50

hydrological stations on the rivers of the Prut and Siret basins have observation periods for water runoff of 54–72 years, only 2 stations have an observation period less than 40 years.

## Results and discussion

Statistical parameters were determined for the series of maximum peak water discharge, as the most important in practical application in hydrological calculations and forecasts. Variation coefficient of maximum annual peak water runoff on the rivers of the Prut and Siret basins in the vast majority vary in the range of 0.8–1.0. The skewness coefficients have positive values and they are generally in the range of 1.8–2.5 (Table 2).

Relative values of root mean square errors  $\sigma_n$  [%] for each gauge is determined by the Eq. (1):

$$\sigma_n = \pm(100 \cdot C_v) / \sqrt{n} \quad (1)$$

where

$C_v$  – variation coefficient,

$n$  – number of years of continuous observations.

The relative values of the root mean square errors do not exceed 15–20%. The highest value  $\sigma_n=19.8\%$  was obtained for Chornyava river – Lyubkivtsi, which is explained by a short series of observations. But in general, the series of observations of the maximum water runoff on the studied rivers are representative.

A quantitative assessment of the temporally homogeneity of the maximum annual water discharges at a 5% significance level on the rivers of the Prut and Siret

basins was carried out according to the standard parametric criteria of Student and Fisher (Table 3). One of the most stringent, the Wilcoxon test, was used from nonparametric criteria (Table 4).

Checking the equality of mean values by Student's test (statistics  $t$ ) and equality of variance by Fisher's test (statistics  $F$ ) showed that the hypothesis of homogeneity of samples of the maximum annual water runoff for all rivers of the Prut and Siret basins is accepted. The result is the same for Wilcoxon's test (statistics of the number of inversions  $U$ ).

Due to the fact that water discharge is directly dependent on the catchment area of the river, the water discharge of two or more different rivers is incomparable, because their catchment areas are not the same. To enable a spatial comparison of the maximum values on the rivers of the Prut and Siret basins, was used such characteristic as the specific discharge of water runoff. This indicator shows the amount of water ( $\text{dm}^3$  or liter) flowing down in one second (1 s) from a unit area (1  $\text{km}^2$ ) of the river basin. Or, we can say that the specific discharge of water runoff is the discharge rate from 1  $\text{km}^2$  of the basin as shown in Eq. (2):

$$q = 1000 \cdot Q \cdot F^{-1} \quad (2)$$

where

$q$  – specific discharge of water runoff [ $1 \text{ s}^{-1} \text{ km}^{-2}$ ],

1000 – conversion factor from cubic meters to cubic decimeters or liters,

$Q$  – discharge of water runoff [ $\text{m}^3 \text{ s}^{-1}$ ],

$F$  – catchment area [ $\text{km}^2$ ].

To clarify the differences in the values of the specific discharge of water runoff (daily mean maximum via with the corresponding peak maximum) on the rivers of the Prut and Siret basins, we constructed dependences between the indicated characteristics.

Fig. 2 shows that the relationships between the maximum mean daily specific discharge and the corresponding maximum peak specific discharge on the rivers of the investigated catchments are quite significant. The approximation coefficients  $R^2$  vary from 0.59 to 0.97, which corresponds to the correlation coefficients  $r$

– from 0.77 to 0.98. But the ratios themselves between the daily mean maximums and the corresponding peak maxima on the rivers of the Prut and Siret basins are different.

To identify patterns in detected differences graphs of relations between the maxima and the mean altitude of the catchments and their areas were constructed. (Fig. 3). As follows from Fig. 3 the greatest ratio between the peak maximum and daily mean maximum of water discharge is observed in small mountain watersheds with mean altitude of 1000–1200 m a.s.l. where, the peak maxima

**Table 2. Statistical parameters of the maximum peak water runoff on the rivers of the Prut and Siret basins**

River – Hydrological gauge	Catchment area [km <sup>2</sup> ]	Maximum annual water runoff (peak values)				
		Discharge of water runoff [m <sup>3</sup> s <sup>-1</sup> ]	Normals Specific discharge of water runoff [l s <sup>-1</sup> km <sup>-2</sup> ]	Variation coefficient $C_v$	Skewness coefficient $C_s$	Relative root mean square error $\sigma_n$ [%]
Siret river – Storozhynets'	672	177	265	0.96	2.62	12.0
Prut river – Vorokhta	48,3	31.6	666	0.56	1.42	8.92
Prut river – Kremetsi	366	121	331	0.72	2.17	9.55
Prut river – Yaremcha	597	309	518	0.84	2.26	10.3
Prut river – Chernivtsi	6890	1131	164	0.83	1.99	9.84
Kam'yanka river – Dora	18.1	15.2	855	0.83	1.55	9.88
Chornyava river – Lyubkivtsi	333	22.7	68.2	1.12	2.22	19.8
Cheremosh river – Usteriky	1500	393	261	0.60	2.05	7.80
Bilyy Cheremosh river – Yablunyt'sya	552	158	285	0.84	1.80	11.0
Chornyy Cheremosh river – Verkhovyna	657	164	250	0.85	2.91	11.0
Il'tsya river – Il'tsi	86.1	42.1	489	0.99	2.06	13.0
Putyla river – Putyla	181	62.0	343	0.94	1.86	12.8

**Table 3. Results of the test for the temporal homogeneity of the maximum water runoff of the rivers of the Prut and Siret basins according to parametric criteria (Student's and Fisher's) at a significance level of  $2\alpha = 5\%$**

River – Hydrological gauge	Homogeneity criteria					
	Student's, statistics t			Fisher's, statistics F		
	Statistics value		Results of hypothesis test	Statistics value		Results of hypothesis test
	empirical	analytical		empirical	analytical	
$t_e$	$t_a$	$t_e < t_a$	$F_e$	$F_a$	$F_e < F_a$	
Siret river – Storozhynets'	0.15	2.00	homogenous	1.26	2.14	homogenous
Prut river – Vorokhta	0.13	2.04	homogenous	3.49	2.86	heterogeneous
Prut river – Kremetsi	0.67	2.01	homogenous	1.94	2.19	homogenous
Prut river – Yaremcha	1.56	2.00	homogenous	3.37	2.10	heterogeneous
Prut river – Chernivtsi	0.94	2.00	homogenous	2.02	2.06	homogenous
Kam'yanka river – Dora	0.81	2.00	homogenous	1.46	2.06	homogenous
Chornyava river – Lyubkivtsi	0.48	2.07	homogenous	3.18	3.33	homogenous
Cheremosh river – Usteriky	0.82	2.01	homogenous	1.38	2.17	homogenous
Bilyy Cheremosh river – Yablunyt'sya	0.16	2.01	homogenous	2.01	2.17	homogenous
Chornyy Cheremosh river – Verkhovyna	0.88	2.01	homogenous	1.96	2.18	homogenous
Il'tsya river – Il'tsi	1.51	2.01	homogenous	1.46	2.19	homogenous
Putyla river – Putyla	1.25	2.01	homogenous	1.46	2.25	homogenous

**Table 4.** Results of the test for the temporal homogeneity of the maximum water runoff of the rivers of the Prut and Siret basins according to nonparametric criteria (Wilcoxon's) at a significance level of  $2\alpha = 5\%$ 

River – Hydrological gauge	Empirical quantity of inversions, $U_e$	analytical critical values of statistics, $U_a$		Results of hypothesis test
		lower $U_{a,L}$	upper $U_{a,U}$	
Siret river – Storozhynets'	528	366	658	homogenous
Prut river – Vorokhta	150	120	260	homogenous
Prut river – Kremetsi	438	283	529	homogenous
Prut river – Yaremcha	648	405	718	homogenous
Prut river – Chernivtsi	680	474	822	homogenous
Kam'yanka river – Dora	565	460	800	homogenous
Chornyava river – Lyubkivtsi	127	76.0	180	homogenous
Cheremosh river – Usteriky	490	306	564	homogenous
Bilyy Cheremosh river – Yablunytsya	366	306	564	homogenous
Chornyy Cheremosh river – Verkhovyna	474	306	564	homogenous
Il'tsya river – Il'tsi	331	294	547	homogenous
Putyla river – Putyla	309	251	478	homogenous

typically exceed in 1.8–2.0 times the daily ones. From catchments with mean altitude of 400 m a.s.l. such ratios decrease to 1.1–1.3 with increasing catchment area.

Mentions of catastrophic floods in the area of investigative appear in chronicles and in literary sources from the 12th century (1229, 1230, 1464, 1668, 1674, 1700, 1730, 1750). The longest series of observations of the maximum water runoff has a hydrological gauge on the Prut River near the city of Chernivtsi (since 1895). See Table 1. But such observations are intermittent. According to the available data (Fig. 4) it can be stated that for the last 120 years in the Prut and Siret basins high maxima during floods were observed in 1897, 1908, 1911, 1930, 1941, 1948, 1955, 1969, 1974, 1996, 2008, 2010 (Tymulyak, 2012).

There is not enough information about the characteristics of some floods, for example, about the flood in September 1941, but it is known from the literature that then flood waters flooded settlements in the river valleys of the Prut basin, and led to significant destruction and casualties.

At other hydrological stations, systematic observations of maximum water runoff began mainly in the 1950s (Table 1).

To be able to compare the intensity of formation of maximum peak values on the rivers of the Prut and Siret basins we performed a standard conversion of maximum peak specific discharge to modular coefficient through the process of normalization  $k_q$  (3):

$$k_{(q,i)} = q_i / \bar{q} \quad (3)$$

where

$q_i$  – maximum peak specific discharge for long-term period [ $l\ s^{-1}\ km^{-2}$ ],

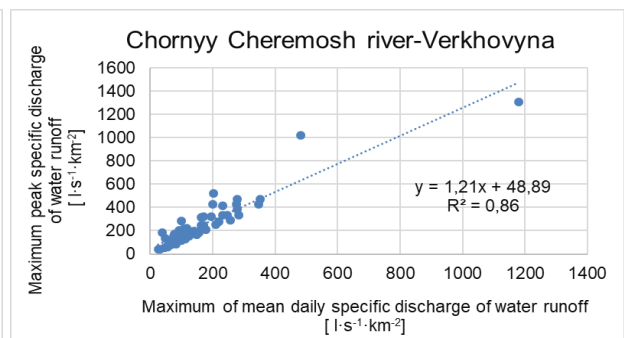
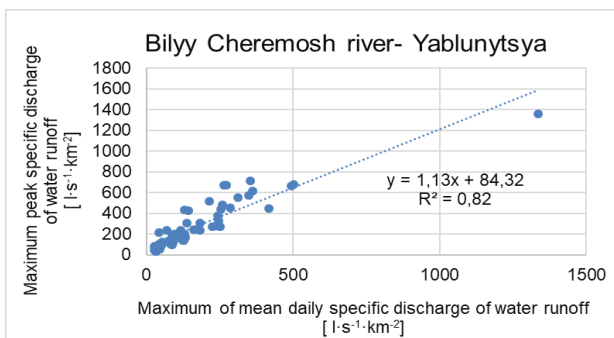
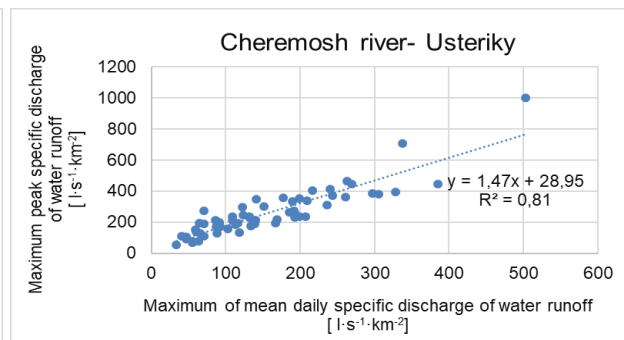
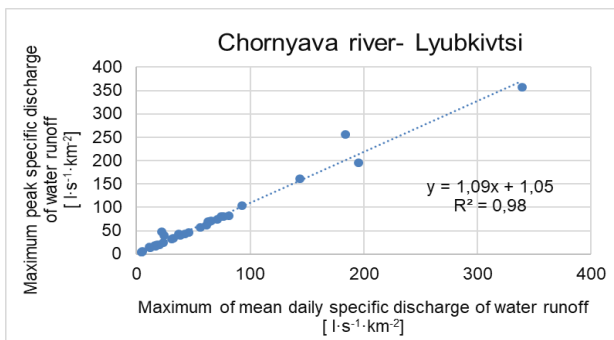
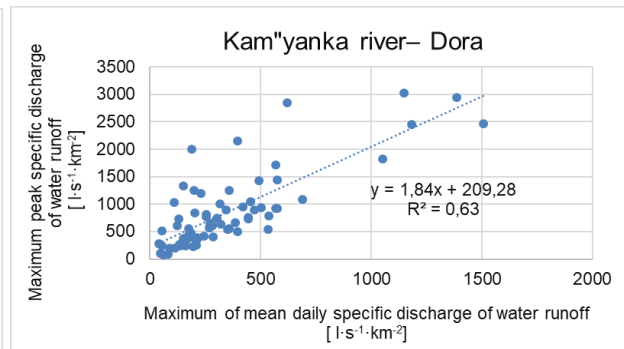
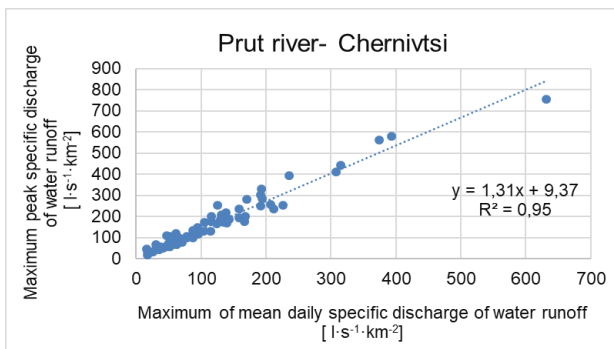
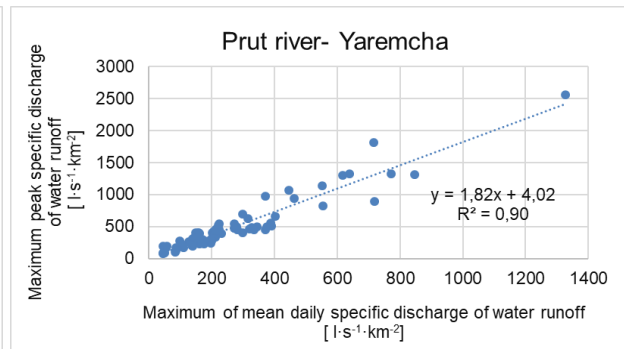
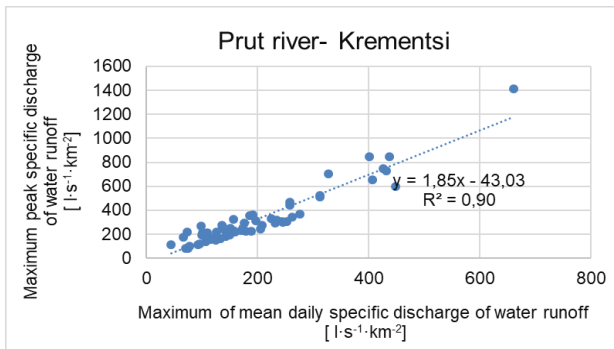
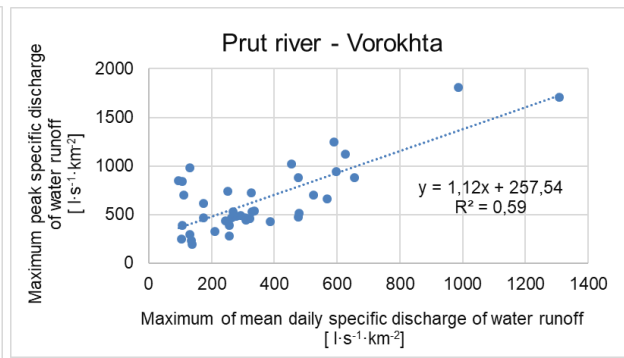
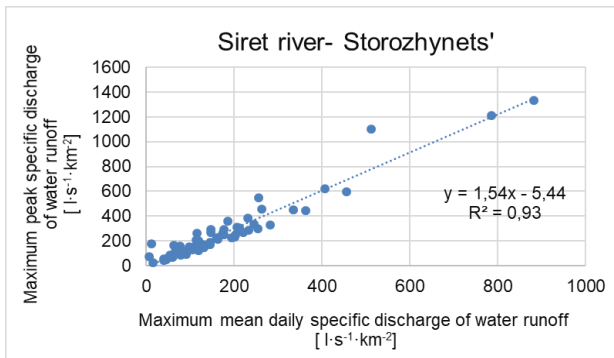
$\bar{q}$  – normal value of maximum peak specific discharge [ $l\ s^{-1}\ km^{-2}$ ].

Fig. 5 shows temporal change of modular coefficients in different regions of the investigated area for the period of observations 1945–2016.

As we can see, in the spatial relation (Fig. 5A-B) high floods (at  $k_q \geq 2$ ) occur synchronously in both regions of the study area, although different intensity of peak peaks is noticeable. Over the past 60–70 years in the Prut river basin extremely high peak runoff ( $k_q \approx 5$ ) was noted in 1969 and currently it remains the absolute maximum (Fig. 5A). In the basin of the Cheremosh and Siret rivers, an extremely high maximum, which was reached during the observation period (Fig. 5B), was recorded in 2008 ( $k_q \approx 5$  as well).

Fig. 5C presents temporal change of modular coefficients for small mountain rivers. Their catchment areas do not exceed 180  $km^2$ , and the mean altitude of the basins is 900–1100 m a.s.l. On such rivers it is possible to allocate many equivalent high peak maxima in different years. It is caused by sensitivity of small mountain catchments and their fast reaction to heavy local rains in mountains. Table 5 contains values of extremely high maximum peak specific discharge which were formed during the observation period (1969–2008) on the rivers of the Prut and Siret basins. Their comparison is shown in Fig. 6. The largest maximum peak specific discharges associated with small mountain catchments and reach values 3000–3500  $l\ s^{-1}\ km^{-2}$ .

On the rivers of the Prut and Siret basins maximum values are ten times higher than the average annual runoff. To identify the influence of the maximum peak runoff at an average annual runoff of the rivers of Siret and Prut basins we constructed correlations between them. The generalization of such influence is carried out by the coefficient of determination denoted  $R^2$  and presented on Fig. 7. It is an indicator of the degree of connection between variables and shows the share of the scatter relative to the mean value, which is "explained" by the constructed regression.



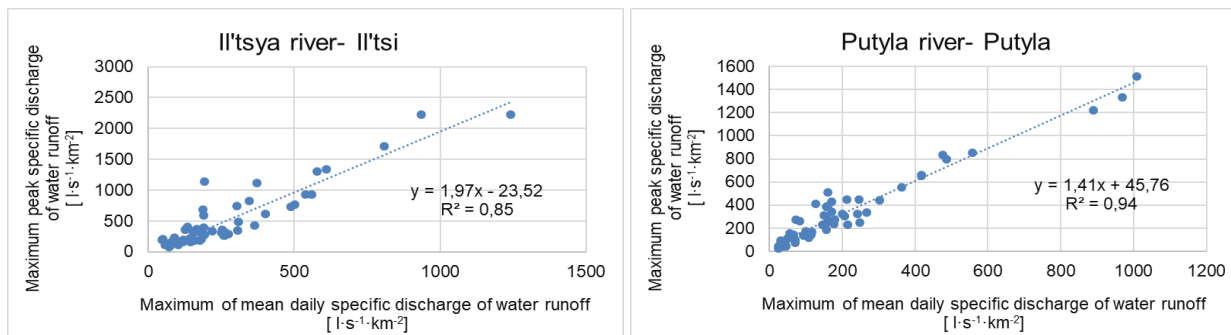


Fig. 2. Ratios between the maximum mean daily specific discharge and the corresponding maximum peak specific discharge on the rivers of Prut and Siret basins.

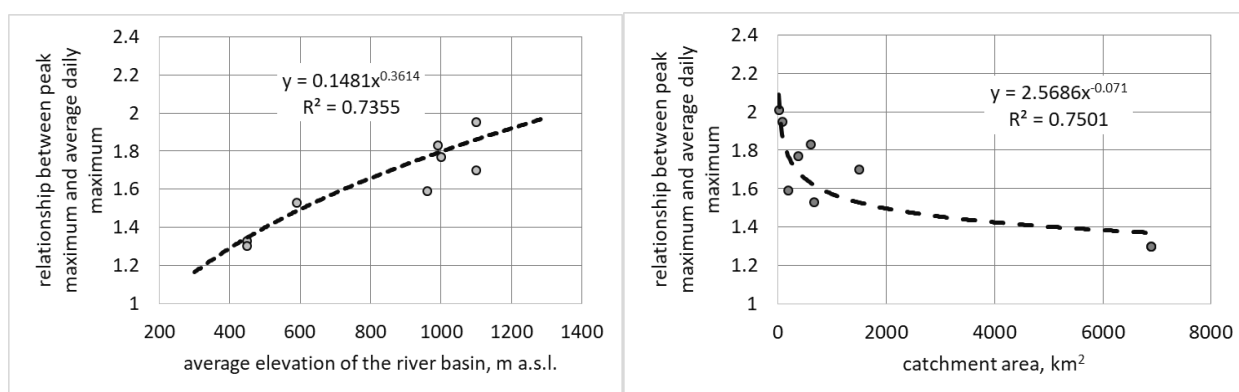


Fig. 3. Dependencies of ratios between peak maximum and average daily maximum to: a) average elevations, b) catchment area in the rivers of the Prut and Siret basins.

Table 5. Maximum peak water runoff on the rivers of the Prut and Siret basins

River – Hydrological gauge	Area of the river basin [km <sup>2</sup> ]	Mean altitude [m a.s.l.]	Maximum peak specific discharge [l s <sup>-1</sup> km <sup>-2</sup> ]	
			1969 p.	2008 p.
Siret river – Storozhynets'	672	590	1214	1336
Prut river – Vorokhta	48.3	–	–	1805
Prut river – Kremetsi	366	1000	1413	746
Prut river – Yaremcha	597	990	2563	1327
Prut river – Chernivtsi	6890	450	755	579
Kam"yanka river – Dora	18.1	870	2939	3028
Chornyava river – Lyubkivtsi	333	–	–	161
Cheremosh river – Usteriky	1500	1100	707	1000
Bilyy Cheremosh river – Yablunytysya	552	1200	672	1359
Chorny Cheremosh river – Verkhovyna	657	1200	1304	1018
Il'tsya river – Il'tsi	86.1	1100	2230	1707
Putyla river – Putyla	181	960	652	1331

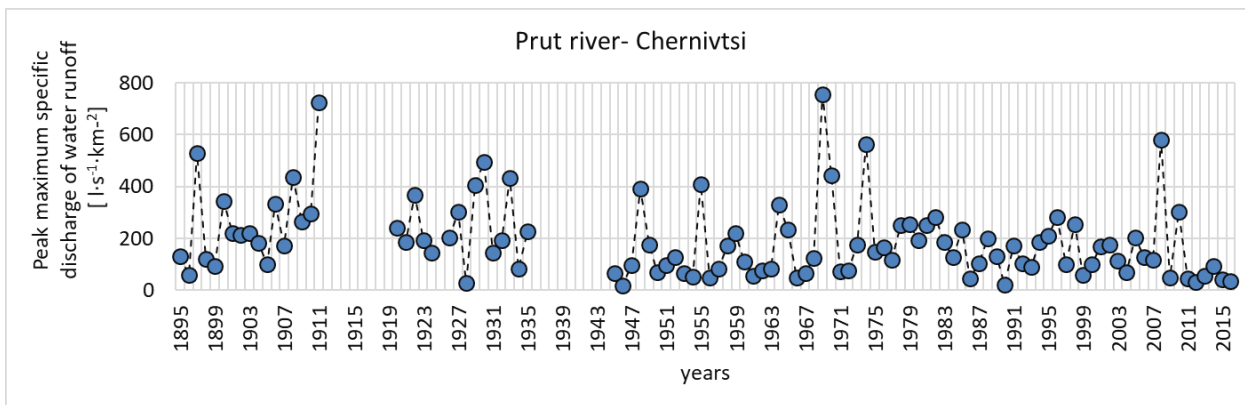


Fig. 4. Peak maxima according to observations (1895–2016). Prut River – Chernivtsi.

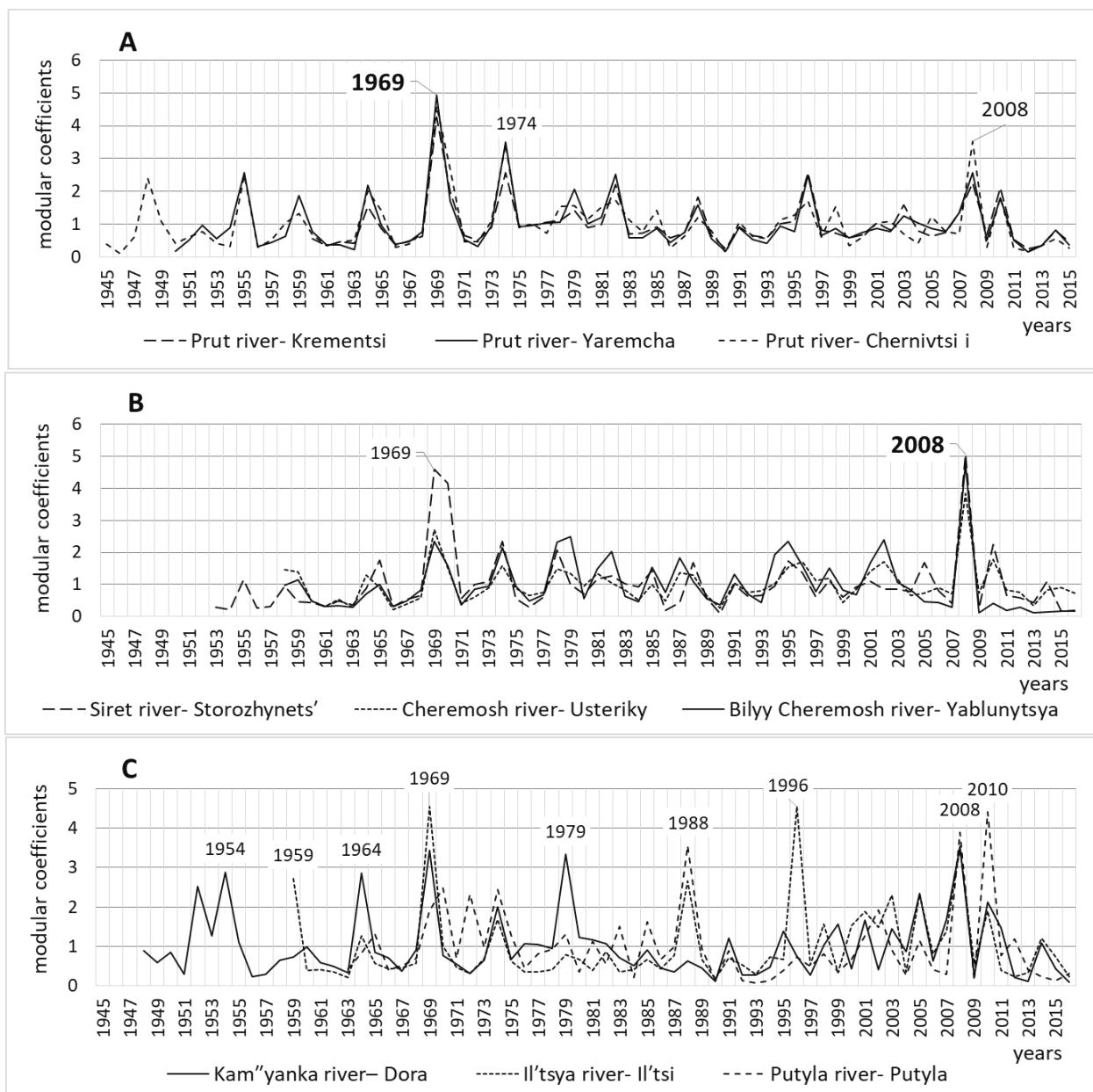


Fig. 5. Temporal change of modular coefficients in different regions of the investigated area. 1945–2016. A) – in the Prut river basin (to Chernivtsi city), B) – in the basin of the river Cheremosh (tributaries of the river Prut), C) – in the basin of the Siret river.

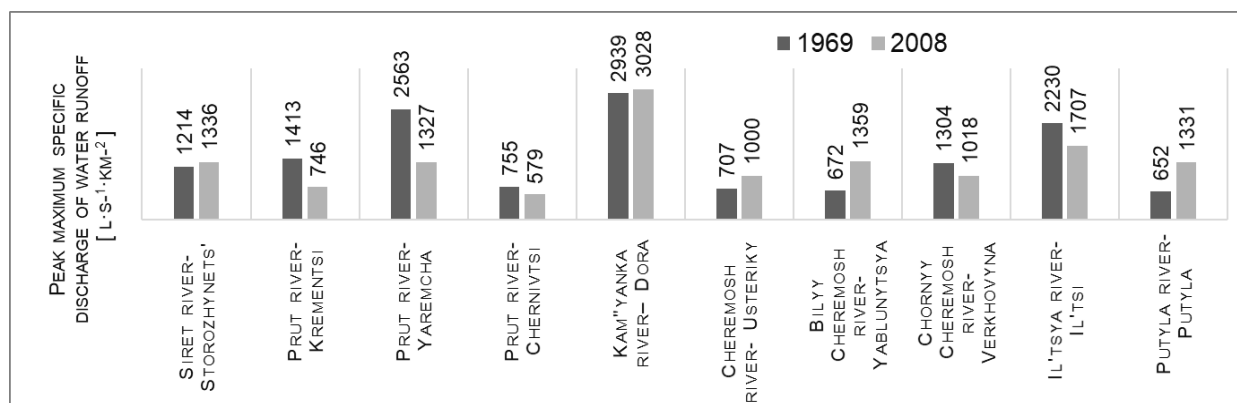


Fig. 6. Comparison of maximum peak specific discharge on the rivers of the Prut and Siret basins. 1969–2008.

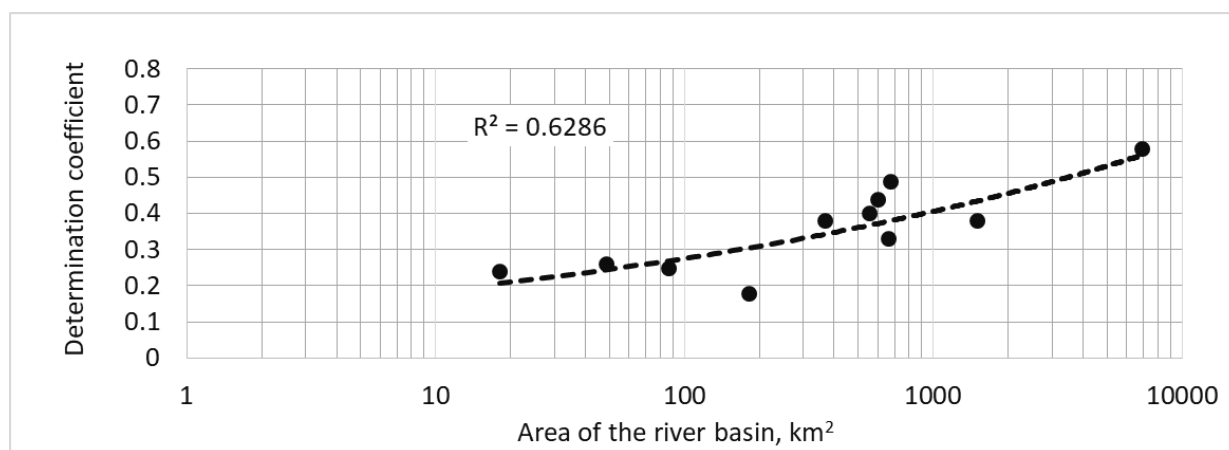


Fig. 7. Changes in the degree of influence (based on the values of the determination coefficients  $R^2$ ) of the peak runoff on the average annual runoff of the rivers of the Prut and Siret basins, depending on the areas of their basins.

Maximum peak annual water runoff in small river (from catchment areas of 100–200 km<sup>2</sup>) has little effect on the value of the average annual, only 15–20% (Fig. 7). For rivers with catchment areas of 500–2000 km<sup>2</sup>, the formation of the average annual runoff by 30–50% determines the values of maximum peak. For hydrological gauge on the Prut river that is located near the city of Chernivtsi (Prut river – Chernivtsi) with the largest catchment area of 6890 km<sup>2</sup> the degree of such impact increases to 60%.

### Conclusion

The physical and geographical conditions of the Prut and Siret river basins (first of all, climatic and orographic) contribute to the formation of significant maxima on the rivers. The study area has elements of mountain and foothill orography. The water regime of rivers is characterized by spring freshets, but rain floods in the warm period of the year predominate, and snow-rain

floods of the cold period are not inherent in these catchments. It is in the warm period we observe the greatest maximum peaks over the year, which have a rather intensive development during their formation. The time interval between the onset of the precipitation core and the maximum flood for the catchment area of 1000–1200 km<sup>2</sup> does not exceed 6–10 hours. Therefore, between the peak maximum and daily mean maximum on the rivers of Prut and Siret basins are observed significant differences in values. In mountain watersheds with mean altitude of 1000–1200 m a.s.l, the peak maxima typically exceed in 1.8–2.0 times the daily ones. From catchments with mean altitude of 400 m a.s.l. such ratios decrease to 1.1–1.3.

The highest maximum peaks of water runoff on the rivers in the Prut and Siret basins during the observation period were recorded in 1969 and 2008. The highest maximum peak specific discharge can reach 3000–3500 l s<sup>-1</sup> km<sup>-2</sup> on small mountain rivers with small-scale catchment areas.

## References

- Balabukh, V., Lukianets, O. (2011): Regional features of change of atmospheric processes in the river basins of overhead Prut-Siret and their influence on water regime of the rivers, XXVth Conference of the Danube Countries on Hydrological Forecasting and Hydrological Bases of Water Management, 98.
- Grebin, V. V., Lukianets, O. I., Tkachuk, I. I. (2012): An estimation of possibility of operative forecasting of rain floods is on the rivers of basins of Prut and Siret, Ukrainian Hydrometeorological Journal, 10, 164–175.
- Lukianets, O., Moskalenko, S. (2019a): Generalization and multi-annual variability of the maximum annual runoff river water in accordance with the hydrographic zoning of Ukraine, *Hidrolohiia, hidrokhiimia i hidroekolohiia*, 2(53), 6–20.
- Lukianets, O., Moskalenko, S. (2019b): Correlation between daily mean maximums and peak maximums on the rivers of the Tisza basin within Ukraine, *Hidrolohiia, hidrokhiimia i hidroekolohiia*, 3(54), 57–58.
- Lukianets, O., Malyska, L., Moskalenko, S. (2019): Maximum rivers runoff in the basin of Tysa and Prut within Ukraine, XXVIII Conference of the Danubian countries on hydrological forecasting and hydrological bases of water management, BOOK OF ABSTRACT, 47.
- Tymulyak, L. M. (2012): Comparative characteristics of the disastrous floods of the 20th and the beginning of the 21st century in the Pre-Carpathians, *Hidrolohiia, hidrokhiimia i hidroekolohiia*, 2(27), 65–73.

Moskalenko Stanislav, PhD.  
Taras Shevchenko National University of Kyiv  
Volodymyrska Street 60  
01033 Kyiv  
Ukraine

Malyska Liudmyla, PhD. (\* corresponding author, e-mail: malitska30@gmail.com)  
Ukrainian Hydrometeorological Institute  
Prospekt Nauky 37  
03028 Kyiv  
Ukraine

## Evaluation of flow frequency on streams in the South Moravian Region for the last 40 years

Pavel COUFAL\*

The aim of the mentioned article is to evaluate the flow frequency in selected water gauging stations in the South Moravian Region from the CHMI network over the last 40 years. Use derived series of M-day discharges for evaluation, which are based on the flow duration curves of the time series of mean daily discharges and the corresponding probabilities of exceeding. The series of M-day discharges in the observed profiles will be evaluated for the current reference period 1981–2010 and the newly proposed period 1991–2020. To orientate the trend analysis in the time series, use a mass curve of mean daily discharges. The result will therefore be to describe the changes in flow frequencies between these reference periods. The above-mentioned results and conclusions will serve for practical use in applied hydrology, e.g. as a basis for determining the minimum discharges in water management and other purposes within the provision of standard hydrological data of surface waters according to ČSN 75 1400.

KEY WORDS: South Moravia, flow frequency, minimum discharges, flow duration curve, Morava River

### Introduction

The South Moravian Region is specific in terms of hydrography in that most of it lies in flat depressions, where the largest watercourses in Moravia have their mouths. The Morava River, draining the Jeseníky and Beskydy Mountains, or Svratka, flowing through the city of Brno, brings water from areas of several thousand of these squares. These watercourses flow through larger cities, where a possible increase or longer decrease of flows to historical lows can have a significant impact on the socio-economic sphere. The aim of this concept is to evaluate the flow frequency at selected water gauging stations of the CHMI network for a period of 40 years. The findings are then used to compare the series of M-day discharges in the observed profiles between the current reference period 1981–2010 and the newly proposed period 1991–2020. Use a mass of curve of mean daily discharges to orientatively analyze the trend in time series. These evaluated time series are used in applied hydrology as a basis for providing standard hydrological data of surface waters according to ČSN 75 1400.

### Material and methods

#### *Selection of suitable water gauging stations*

Before the actual analysis of flow frequency on streams

in the South Moravian Region, it was first necessary to select suitable water gauging stations (see Fig. 1) to meet the criteria in the length of the time series of mean daily discharges of 40 years, i.e. from 1 November 1980 to 31 October 2020 (hydrological year used).

The length of the 40-year period was chosen because it corresponds to the beginning of the time series of daily mean discharges, which was used to evaluate the reference period 1981–2010, which is still used in applied hydrology in providing hydrological data according to ČSN 75 1400 to the overlap between the two reference periods addressed and the subsequent expression of the differences between them. Time series from Czech hydrometeorological institute were used for the mentioned analyzes (hereinafter only abbreviated as CHMI).

Characteristics of selected water gauging stations are given in Tab. 1. The specified elevation (above sea level) is defined as the zero line of a depth gauge at water gauging station (gauge zero level). Basin area (catchment area in km<sup>2</sup>) is derived from GIS. The Strážnice station has the largest catchment area and the Kyjov station has the smallest catchment area. The characteristics of mean discharge  $Q_a$  (meaning long-term mean discharge), the annual rainfall amounts (meaning the average amount of rainfall per catchment area) and the mean annual runoff (mm) are derived for the current reference period 1981–2010. The runoff coefficient is then determined as the ratio the runoff height to the amount of rainfall.

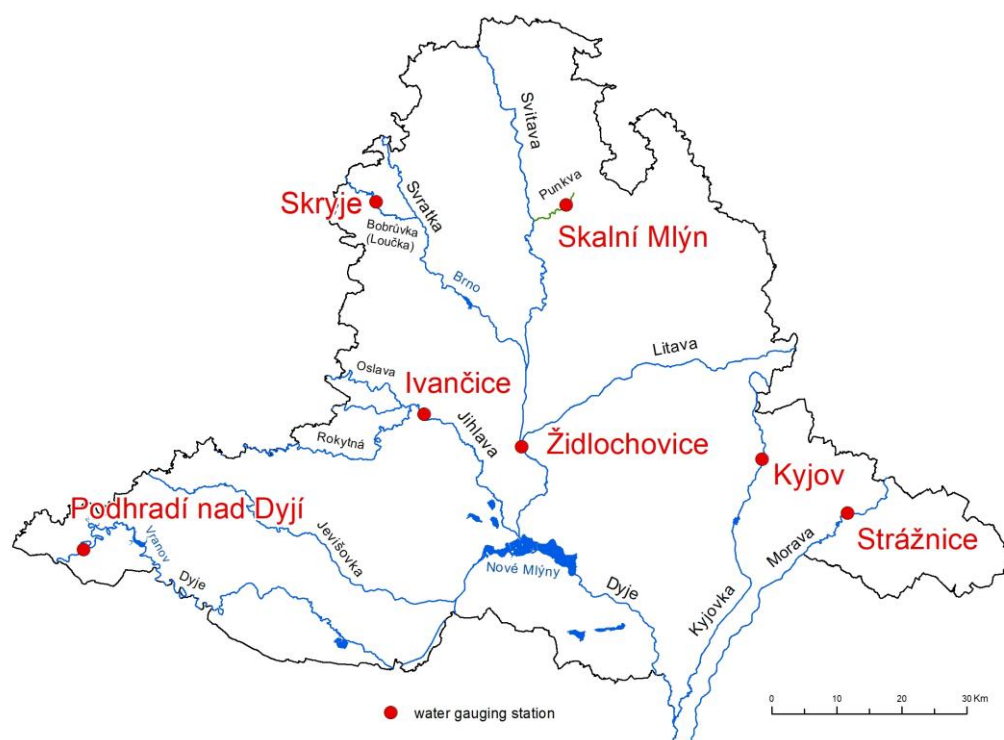


Fig. 1. Location of selected water gauging stations in the South Moravian Region.

Table 1. Characteristics of selected water gauging stations in the South Moravian Region

Gauging station	River	Elevation [m a. s. l.]	Basin area [km <sup>2</sup> ]	Mean discharge $Q_a$ [m <sup>3</sup> s <sup>-1</sup> ]	Annual Rainfall amounts [mm]	Mean Annual Runoff [mm]	Runoff coefficient
Strážnice	Morava	163.3	9144.83	59.33	718	205	0.29
Podhradí nad Dyjí	Dyje	348.4	1755.49	8.81	652	158	0.24
Skryje	Bobrůvka	310.1	222.01	1.45	687	206	0.30
Židlochovice	Svratka	177.9	3938.12	15.05	649	121	0.19
Skalní Mlýn	Punkva	342.5	154.17	0.93	644	191	0.30
Ivančice	Jihlava	194.0	2679.98	10.39	614	122	0.20
Kyjov	Kyjovka	185.9	117.49	0.26	621	68	0.11

The Kyjov station has the lowest value of the runoff coefficient, which is caused by a large loss of run-off water from rainfall.

#### Processing of time series and evaluation of a series of M-day discharges

For the sake of clarity and to provide an overview of flow frequency in the given years, flow frequency data were displayed graphically in mean annual discharges with indication of reference periods. The comparison of the series of M-day discharges will be displayed in tabular form. For the subsequent evaluation of the differences in the long-term mean discharge and the series of M-day discharges in water gauging stations between the currently used (1981–2010) and the newly designed reference period (1991–2020) determined according to the formula of Chegodaev (1).

$$p = \frac{m - 0,3}{n + 0,4} \quad (1)$$

where

$m$  – is the order of the given value in the time series, which is arranged in descending order (ie in the first place is the highest value of mean daily discharge in 30 years),

$n$  – is the number of values in the time series (in 30 years it is almost 10 960 values mean daily discharges).

Chegodaev's formula is used to calculate the probability of exceedance because we work with time series of mean daily discharges, which are almost always a sample from the basic statistical set, for which we do not know all the values that could probably occur in a given time series. Thus, the last value of the series does not have a probability of occurrence of 1 or 100 %, but has a lower probability of exceedance (Němec, 1964).

From the displayed flow duration curve (FDC) it is then possible to derive a discharge value for a given probability. So, for example, to express a 355-day discharge, we derive a value from the flow duration curve with a probability of occurrence of 97%. The value of the long-term mean discharge is then calculated as the arithmetic average of all mean daily discharges over 30 years. Evaluation of N-year discharges is not the aim of this concept.

To analyze the trend in the time series used, the method of a mass curve of mean daily discharges is used, where the trends of discharges over a period 40 years can be clearly displayed. The method of the mass curve consists in first converting the time series of mean daily discharges (according to Kaňok, 1999) into a cumulative form. The cumulative series is determined by successive addition of individual values, so that the last value of the cumulative series has the value of the sum of all values of mean daily discharges. By converting this cumulative series into a relative series by gradually dividing the individual values with the value of the sum of all daily discharges. For each value of the cumulative series, its share in the whole series is created as a percentage. We will convert this relative series of daily discharges into a graphical form with the interpolation of the trend line. From this graph, it is then possible to clearly derive how the daily discharges behaved over 40 years in terms of deviations (breaks) from the trend line.

## Results

### Morava River Basin

In the case of the Morava river basin in the South Moravian Region, the evaluated mean daily discharges from the Strážnice water gauging station for the last 40 years were used. The Strážnice station has a catchment area of 9145 km<sup>2</sup> and is located in the flat depression Dolnomoravský úval, where extensive outflows into floodplain forests occur at higher flows.

The graphical representation of the mean annual discharges shows the period of minimum flows 1989 to 1993, which contrasts sharply with the following period

1995 to 2002, when the mean annual discharges remained above 60 m<sup>3</sup> s<sup>-1</sup> (see Fig. 2). Above all, it is worth mentioning the extensive regional floods in July 1997, when discharges of more than a century occurred in the Morava river basin. If we focus on the subnormal period of flow frequencies (when discharges fell on average below 50 m<sup>3</sup> s<sup>-1</sup>), then from 1980 to 1990 there were several, but it was compensated by abnormally water years above 60 m<sup>3</sup> s<sup>-1</sup>. In the period of the last 10 years (2010 to 2020), however, these compensations did not occur; on the contrary, in the years 2017–2019 the annual discharges fell below 30 m<sup>3</sup> s<sup>-1</sup>. An example is the mean daily discharge in the Moravia river in Strážnice from 20 August 2018, which was only 3.2 m<sup>3</sup> s<sup>-1</sup> (see Fig. 4), which is below the level of even the lowest value of 364-day discharge in both solved reference periods of series of M-daily discharges. These facts were then reflected in a decrease in the long-term mean discharge ( $Q_a$ ) in Strážnice by 8%, in minimum discharges by up to 15%, which is evident from Table 2. From the analysis of the trend in the time series by the mass curve method, it was found that the mean daily discharges in the 80's are balanced around the trend line. From the 1990s onwards, there were first declines in the minimum flows, which were offset by increases between 1997 and 2014. Since 2015, the trend has been significantly declining (see Fig. 3).

### Dyje River Basin

On the example of the Podhradí nad Dyjí water gauging station over the last 40 years, periods with maximum and minimum annual discharges are evident (see Fig. 5). Significant decreases in annual flows at the turn of the 1980s and 1990s and also between 2016 and 2019 are most noticeable here. Here the flows fell to lows, when the mean annual discharge fell significantly below 4 m<sup>3</sup> s<sup>-1</sup> (in mean daily discharges, especially in August 2018, flows decreased to historical lows). Maximum discharges occurred during major flood events in 1985–1988, 1996, 2002–2006, 2009–2010 and also in 2013. In addition, compared to the reference period 1981–2010, the newly proposed period 1991–2020 includes a longer

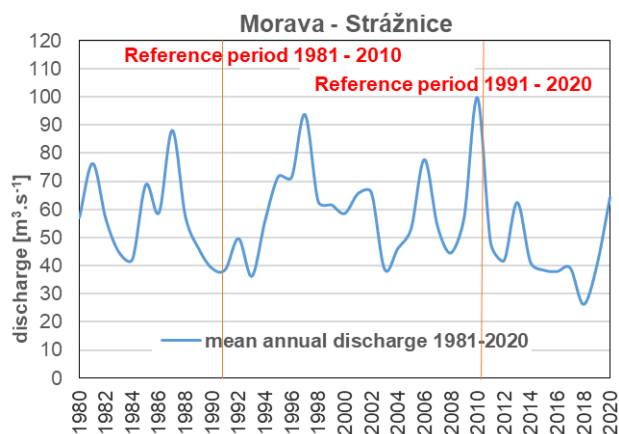


Fig. 2. Mean annual discharges in the water gauging station Strážnice (Morava) for the period from November 1980 to October 2020 with indication of reference periods. Source of used data: CHMI.

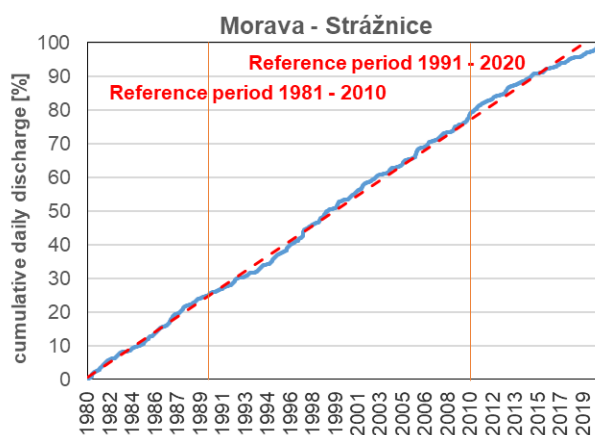


Fig. 3. Mass curve of mean daily discharges in the water gauging station Strážnice (Morava) for the period from November 1980 to October 2020 with indication of reference periods. Source of used data: CHMI.

**Table 2. Comparison of series of M-day discharges for the current and proposed reference period in the water gauging station Strážnice (Morava)**

	M-day discharges [ $\text{m}^3 \text{s}^{-1}$ ]		Difference [%]
	1981–2010	1991–2020	
$Q_a$	59.3	54.7	-8
$Q_{30d}$	135	124	-8
$Q_{60d}$	93.1	85.9	-8
$Q_{90d}$	72.6	66.2	-9
$Q_{120d}$	57.7	53.7	-7
$Q_{150d}$	47.5	44.4	-7
$Q_{180d}$	39.6	36.7	-7
$Q_{210d}$	33.5	31.0	-8
$Q_{240d}$	28.1	25.4	-9
$Q_{270d}$	23.3	20.8	-11
$Q_{300d}$	18.5	16.6	-10
$Q_{330d}$	14.1	12.6	-11
$Q_{355d}$	9.10	8.00	-12
$Q_{364d}$	5.30	4.49	-15



Fig. 4. The water level of Morava river in the Strážnice water gauging station on 20 August 2018 at a time when only about  $3 \text{ m}^3 \text{ s}^{-1}$  flowed here.

period with the occurrence of minimum flows (2014–2019) than in the previous case (here only in 1983/84 and

1989/90). In this case, we do not consider the overlapping period 1991–2010. From the results of the comparison of

the series of M-day discharges for both periods (see Table 3.) it is clear that the long-term mean discharge for the period 1991–2020 will be 11% lower than for the previous period. The minimum values in a number of M-day discharges will be lower by up to 45% (364-day discharge) precisely due to the already mentioned decreases in flows in the years 2016 to 2018 (mean daily discharges often fell below  $0.5 \text{ m}^3 \text{ s}^{-1}$ ).

From the analysis of the trend in time series by the mass curve method, it was found that the daily discharges compared to the Strážnice station in the period 1987–90 have an upward trend. Since the 1990s, there have been falls to the minimum discharges, which have been offset by increases between 2009 and 2014. Since 2015, the trend has been declining significantly (see Fig. 6).

### Svratka River Basin

Svratka is one of the most important watercourses in the region. It flows through the built-up area of the city of Brno and is the waterfront tributary to the Nové Mlýny reservoir system. In addition to the water meter station directly on Svratka (Židlochovice), a water meter station on a significant tributary of the Svratka – Bobruvka (Skryje) was used for water analysis. This more or less unaffected station was chosen both because it drains a significant part of the runoff from the adjacent Vysočina Region, but also because the flows in the period 2016–2018 dropped very significantly to the values of historical lows. According to data from hydrometric measurements of CHMI staff, only  $20 \text{ l s}^{-1}$  was measured here on 21 August 2018, which is, according to available records, the lowest measured instantaneous discharge in the history of this water gauging station. Thus, when we compare the reference period, it is clear that the years 1980 to 1987 were more watery in the first period, and only then at the turn of the 80s and 90s there was a significant decrease in annual flows below  $1 \text{ m}^3 \text{ s}^{-1}$  (see Fig. 7). In contrast, the years 2010 to 2019 in the newly proposed reference period were below normal in terms of flow frequency. The long-term mean discharge for the period 1991–2020 will therefore be 9% lower than for

the previous period and in minimum daily discharges there will be a decrease of up to 39% due to historical significant low water levels (see Table 4).

From the analysis of the trend in the time series by the mass curve method, it was found that the daily discharges in the period 1981–1986 and 1997–2000 are essentially balanced around the trend line. Between 1991 and 1996, there were decreases to minimum flows. To the upward trend then between 2009–2014. Since 2015, the trend is declining (see Fig. 8).

The Židlochovice water gauging station, which also includes the Svitava, Bobrava and Litava river basins, was used to evaluate changes in flow frequencies over 40 years directly at Svratka. From the course of the mean annual discharges, it is quite clear that the new reference period 1991–2020 will include significantly lower flow frequencies than in the current period 1981–2010 (see Fig. 9). This is mainly due to significant drops in flow frequencies in the period 2016–2018.

While in the years 1980–1990 the mean annual discharges reached over  $20 \text{ m}^3 \text{ s}^{-1}$ , in the years 2011–2020 this did not happen at all and the annual discharges reached the maximum level of the long-term mean discharge ( $Q_a$ ). From the results of the comparison of the series of M-day discharges (Table 4.) for both periods, it is clear that the long-term mean discharge for the period 1991–2020 will be 7% lower than for the previous period.

From the analysis of the trend in the time series by the mass curve method, it was found that the daily discharges in the period 1981–1986 and 1997–2009 are essentially balanced around the trend line. In other periods, the graphic representation is very similar to the Skryje station (see Fig. 10). The minimum values in the series of M-day discharges will be lower by up to 17% (364-day discharge) due to the already mentioned decreases in daily discharges in the years 2016 to 2018. It is clear that the occurrence of historically significant minimum discharges also affected the supply of large reservoirs in the Svratka river basin, which kept runoff at the necessary minimums so that they themselves had enough water for their own management.

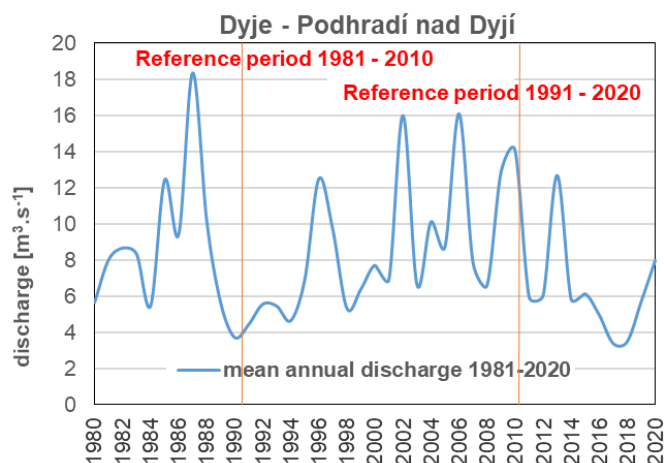


Fig. 5. Mean annual discharges in the water gauging station Podhradí nad Dyjí (Dyje) for the period from November 1980 to October 2020 with indication of reference periods. Source of used data: CHMI.

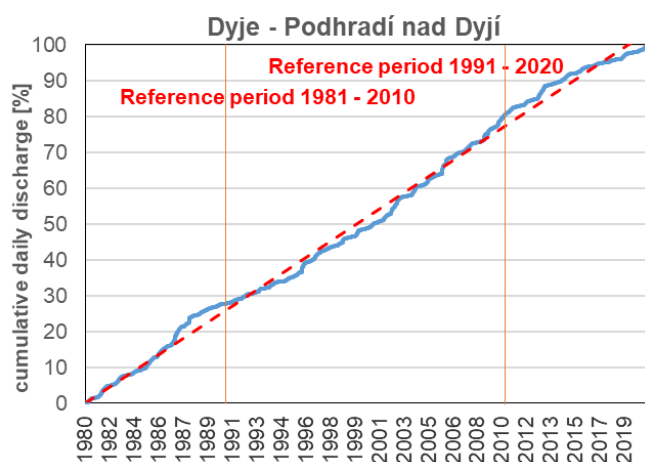


Fig. 6. Mass curve of mean daily discharges in the water gauging station Podhradí nad Dyjí (Dyje) for the period from November 1980 to October 2020 with indication of reference periods. Source of used data: CHMI.

Table 3. Comparison of series of M-day discharges for the current and proposed reference period in the water gauging station Podhradí nad Dyjí (Dyje)

	M-day discharges [ $\text{m}^3 \text{s}^{-1}$ ]		Difference [%]
	1981–2010	1991–2020	
$Q_a$	8.81	7.86	-11
$Q_{30d}$	20.2	18.5	-8
$Q_{60d}$	12.7	11.5	-9
$Q_{90d}$	9.25	8.40	-9
$Q_{120d}$	7.39	6.68	-10
$Q_{150d}$	6.05	5.42	-10
$Q_{180d}$	5.07	4.50	-11
$Q_{210d}$	4.30	3.78	-12
$Q_{240d}$	3.68	3.21	-13
$Q_{270d}$	3.11	2.73	-12
$Q_{300d}$	2.57	2.27	-11
$Q_{330d}$	1.97	1.72	-13
$Q_{355d}$	1.30	1.05	-19
$Q_{364d}$	0.80	0.437	-45

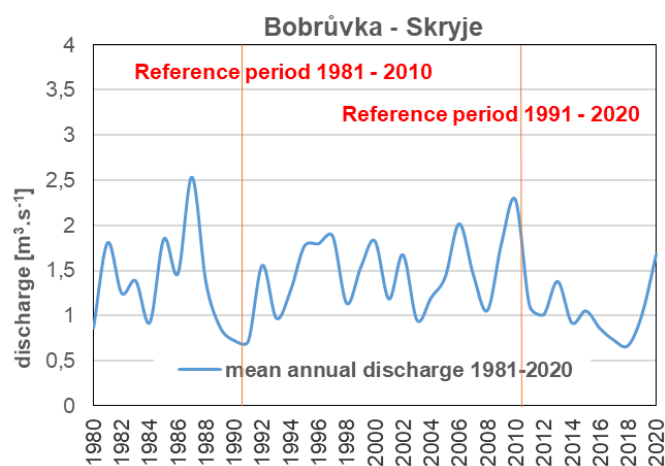


Fig. 7. Mean annual discharges in the water gauging station Skryje (Bobrůvka) for the period from November 1980 to October 2020 with indication of reference periods. Source of used data: CHMI.

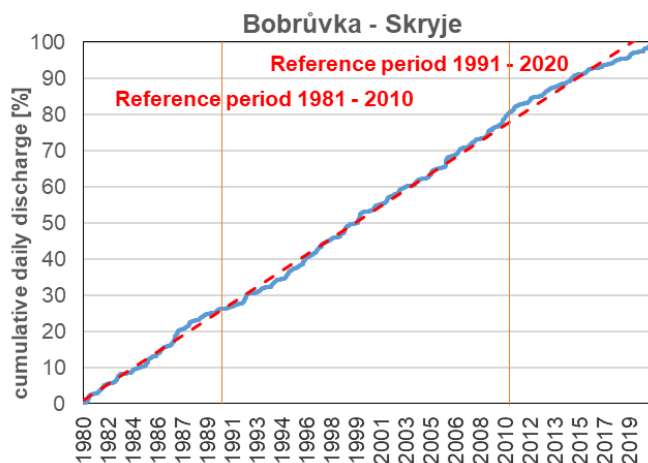


Fig. 8. Mass curve of mean daily discharges in the water gauging station Podhradí nad Dyjí (Dyje) for the period from November 1980 to October 2020 with indication of reference periods. Source of used data: CHMI.

Table 4. Comparison of series of M-day discharges for the current and proposed reference period in the water gauging station Skryje (Bobruvka)

	M-day discharges [ $\text{m}^3 \text{s}^{-1}$ ]		Difference [%]
	1981–2010	1991–2020	
$Q_a$	1.45	1.32	-9
$Q_{30d}$	3.50	3.20	-8
$Q_{60d}$	2.20	2.02	-8
$Q_{90d}$	1.60	1.49	-7
$Q_{120d}$	1.24	1.17	-6
$Q_{150d}$	0.985	0.943	-4
$Q_{180d}$	0.809	0.782	-3
$Q_{210d}$	0.686	0.660	-4
$Q_{240d}$	0.575	0.540	-6
$Q_{270d}$	0.480	0.432	-10
$Q_{300d}$	0.391	0.347	-11
$Q_{330d}$	0.300	0.262	-13
$Q_{355d}$	0.203	0.156	-23
$Q_{364d}$	0.118	0.072	-39

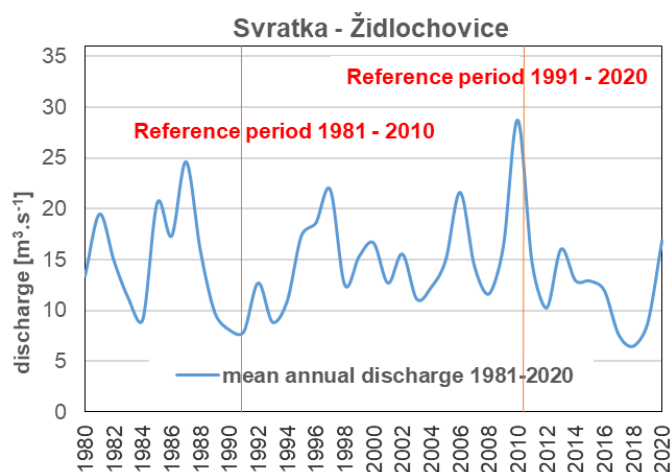


Fig. 9. Mean annual discharges in the water gauging station Židlochovice (Svratka) for the period from November 1980 to October 2020 with indication of reference periods. Source of used data: CHMI.

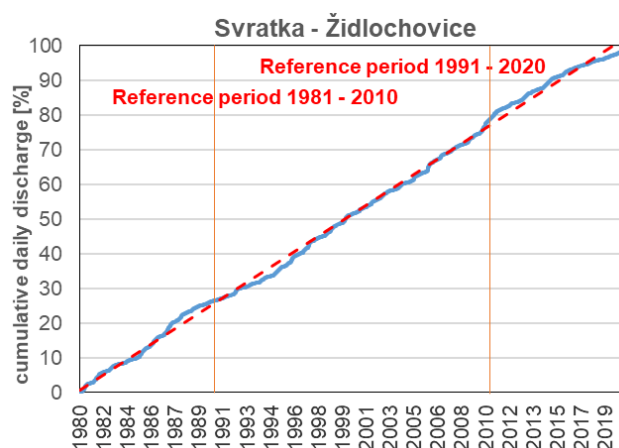


Fig. 10. Mass curve of mean daily discharges in the water gauging station Židlochovice (Svratka) for the period from November 1980 to October 2020 with indication of reference periods. Source of used data: CHMI.

**Table 5.** Comparison of series of M-day discharges for the current and proposed reference period in the water gauging station Židlochovice (Svratka)

	M-day discharges [ $\text{m}^3 \text{s}^{-1}$ ]		Difference [%]
	1981–2010	1991–2020	
$Q_a$	15.1	14.0	-7
$Q_{30d}$	30.7	27.9	-9
$Q_{60d}$	21.5	19.5	-9
$Q_{90d}$	17.0	15.6	-8
$Q_{120d}$	13.9	13.0	-6
$Q_{150d}$	11.9	11.4	-4
$Q_{180d}$	10.5	10.1	-4
$Q_{210d}$	9.37	9.15	-2
$Q_{240d}$	8.38	8.23	-2
$Q_{270d}$	7.50	7.42	-1
$Q_{300d}$	6.72	6.62	-1
$Q_{330d}$	5.85	5.70	-3
$Q_{355d}$	4.45	4.32	-3
$Q_{364d}$	3.68	3.06	-17

### Moravian Karst

The hydrological regime in the Moravian Karst is very specific and that is why it was included in the evaluation of differences in flow frequencies between the two reference periods.

For the purpose of evaluating flow frequency over 40 years, the Skalní Mlýn water gauging station on the Punkva watercourse was selected, which is located below an extensive cave system. Data from this station can provide us with a partial overview of how the cave systems of the Moravian Karst affect the runoff of rainwater in surface waters. According to the graphical expression of annual discharges over 40 years (see Fig. 11), it is clear that, similarly to the Svratka river basin, the years 1980 to 1987 are evident here, which were more favorable to higher discharges, and only then decrease of annual discharges up to  $0.5 \text{ m}^3 \text{ s}^{-1}$ . The years 2010 to 2019 in the newly proposed reference period

were below normal in terms of flow frequency, the long-term normal was exceeded only in 2013. In 2017 and 2018, the mean annual discharge decreased to  $0.3 \text{ m}^3 \text{ s}^{-1}$ , which was the lowest decrease in 40 years. In the mean daily discharges in the station, the minimum values appeared from 28 to 31 August 2018, when there was a decrease to only  $75 \text{ l s}^{-1}$  (below the level of 364-day discharge), which was also confirmed by hydrometric measurements. During this hydrometric measurement on August 29, 2018,  $75 \text{ l s}^{-1}$  was measured at the lowest value since 1928. It is also interesting to delay the occurrence of historical minimum discharges in this station for the period from 28 to 31 August 2018 compared to all mentioned stations where minimal discharges occurred most often from 12 to 24 August 2018, which could be caused by the influence of the cave system of the Moravian Karst. The above-mentioned facts were subsequently reflected in a decrease in the long-term mean discharge ( $Q_a$ ) between periods

by 11%. In minimal discharges in the reference period 1991–2010, this is a decrease of up to 21% (see Table 6). The analysis of the trend in the time series by the mass curve method shows smaller declines around the years

1984–1985. Compared to other stations, there is a much smaller trend to lower discharges in the 1990s. The most significant is clearly the declining trend since 2015 (see Fig. 12).

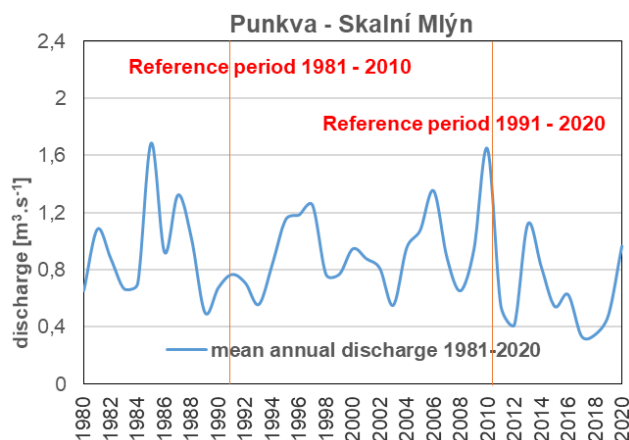


Fig. 11. Mean annual discharges in the water gauging station Skalní Mlýn (Punkva) for the period from November 1980 to October 2020 with indication of reference periods. Source of used data: CHMI.

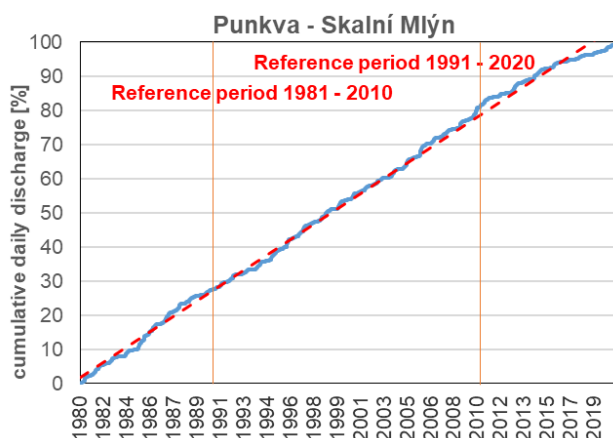


Fig. 12. Mass curve of mean daily discharges in the water gauging station Skalní Mlýn (Punkva) for the period from November 1980 to October 2020 with indication of reference periods. Source of used data: CHMI.

**Table 6. Comparison of series of M-day discharges for the current and proposed reference period in the water gauging station Skalní Mlýn (Punkva)**

	M-day discharges [ $\text{m}^3 \text{s}^{-1}$ ]		Difference [%]
	1981–2010	1991–2020	
$Q_a$	0.933	0.827	-11
$Q_{30d}$	2.28	2.00	-12
$Q_{60d}$	1.40	1.25	-11
$Q_{90d}$	0.990	0.884	-11
$Q_{120d}$	0.733	0.649	-12
$Q_{150d}$	0.557	0.503	-10
$Q_{180d}$	0.456	0.398	-13
$Q_{210d}$	0.366	0.321	-12
$Q_{240d}$	0.306	0.259	-15
$Q_{270d}$	0.252	0.210	-17
$Q_{300d}$	0.200	0.175	-13
$Q_{330d}$	0.165	0.146	-11
$Q_{355d}$	0.129	0.114	-12
$Q_{364d}$	0.105	0.083	-21

### Jihlava River Basin

The Ivančice water gauging station was chosen to assess the flow frequency of the Jihlava river basin. The Ivančice station is located below a very important confluence junction of the Jihlava, Oslava and Rokytná watercourses. In this station, which already has an area of 2680 km<sup>2</sup>, a water flowing practically from half of the Vysočina Region flows.

A significant influence on the river Jihlava is the system of reservoirs Dalešice – Mohelno in close proximity to the nuclear power plant Dukovany. The outflow from these reservoirs stabilizes the fluctuations and fall of the flow frequency to the minimum discharges, which is clearly evident from the table (Tab. 7), where there was a significant decrease in long-term mean discharge  $Q_a$  between periods by 12%, but the difference in 364-day discharge remained unchanged. The decrease in the long-term mean discharges and other data between the periods in Table 6 is due, as in the previous case, to the period

1980–1989 with the occurrence of higher discharges (e.g. floods in May 1985), which does not occur within the reference period 1991–2020. Instead, it is significantly below normal in the newly proposed period, only in 2013 and 2020 are annual discharges at least at the level of normal. Other years are below normal, the largest decreases are recorded in 2017 and 2018 (see Fig. 13).

From the analysis of the trend in the time series by the mass curve method, it was found that the daily discharges around 1988–1989 and 2010–2014 have an upward trend. Between 1992 and 1996, there were decreases to minimum flows. Since 2016, the trend is declining (see Fig. 14).

### Kyjovka River Basin

Kyjovka (referred to in the older maps as Stupava) is an example of a watercourse, where the occurrence of hydrological drought in the period 2016–2018 caused

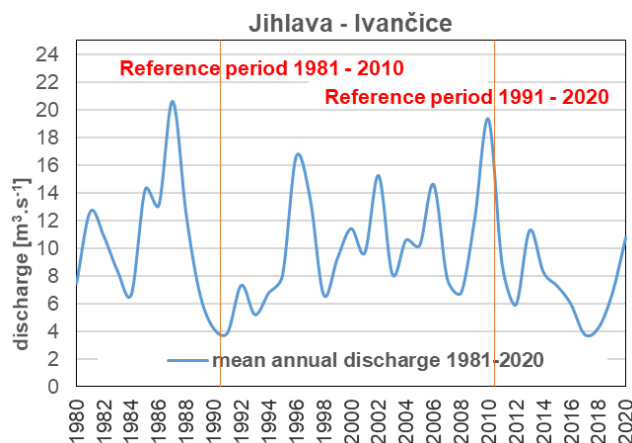


Fig. 13. Mean annual discharges in the water gauging station Ivančice (Jihlava) for the period from November 1980 to October 2020 with indication of reference periods. Source of used data: CHMI.

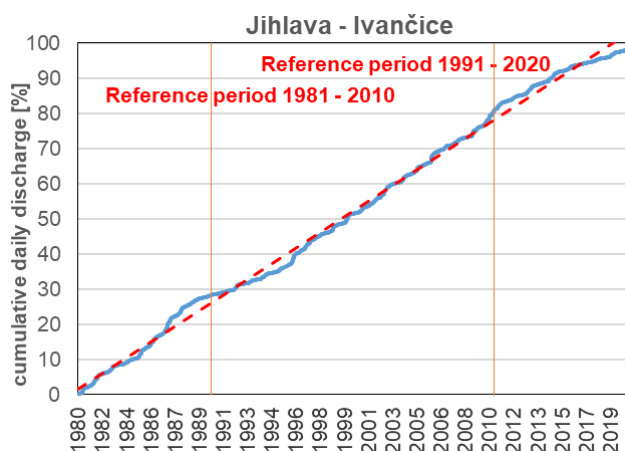


Fig. 14. Mass curve of mean daily discharges in the water gauging station Ivančice (Jihlava) for the period from November 1980 to October 2020 with indication of reference periods. Source of used data: CHMI.

significant differences in minimum flows between reference periods. The Kyjov water gauging station was chosen for the evaluation of flow frequencies. The Koryčany water reservoir is located in the upper part of the Kyjovka catchment area, but with the growing area of the catchment area, its influence on the water stability in Kyjovka is weakening. In addition, in the last 5 years, the dam of the reservoir has been undergoing reconstruction, so it operated for most of the year in the inflow-outflow regime, which means that the Koryčany reservoir could not sufficiently improve

the flow frequency in Kyjovka. As can be seen from the graphical and tabular expression of flow frequencies at the Kyjov station, the difference in long-term mean discharge between periods by 6%, but in the minimal discharges (364-day discharge) is over 60 (see Fig. 15 and Tab. 8).

Significant increases in the period 1980–1984, 1987–1990 and 2009–2014 can be identified from the graphical expression of daily discharges trends. Significant downward trends are in the period 1991–1997 and since 2016 (see Fig. 16).

**Table 7. Comparison of series of M-day discharges for the current and proposed reference period in the water gauging station Ivančice (Jihlava)**

	M-day discharges [ $\text{m}^3 \text{s}^{-1}$ ]		Difference [%]
	1981–2010	1991–2020	
$Q_a$	10.4	9.15	-12
$Q_{30d}$	24.6	19.9	-19
$Q_{60d}$	14.6	13.1	-10
$Q_{90d}$	11.1	10.2	-8
$Q_{120d}$	9.25	8.45	-9
$Q_{150d}$	7.98	7.18	-10
$Q_{180d}$	7.00	6.10	-13
$Q_{210d}$	6.13	5.17	-16
$Q_{240d}$	5.34	4.49	-16
$Q_{270d}$	4.52	3.84	-15
$Q_{300d}$	3.78	3.28	-13
$Q_{330d}$	3.09	2.90	-6
$Q_{355d}$	2.50	2.39	-4
$Q_{364d}$	1.60	1.60	0

**Table 8. Comparison of series of M-day discharges for the current and proposed reference period in the water gauging station Kyjov (Kyjovka)**

	M-day discharges [ $\text{m}^3 \text{s}^{-1}$ ]		Difference [%]
	1981–2010	1991–2020	
$Q_a$	0.255	0.240	-6
$Q_{30d}$	0.493	0.479	-3
$Q_{60d}$	0.329	0.321	-2
$Q_{90d}$	0.262	0.254	-3
$Q_{120d}$	0.220	0.209	-5
$Q_{150d}$	0.190	0.176	-7
$Q_{180d}$	0.170	0.156	-8
$Q_{210d}$	0.151	0.139	-8
$Q_{240d}$	0.137	0.121	-12
$Q_{270d}$	0.120	0.103	-14
$Q_{300d}$	0.105	0.086	-18
$Q_{330d}$	0.088	0.068	-23
$Q_{355d}$	0.065	0.039	-40
$Q_{364d}$	0.040	0.015	-62

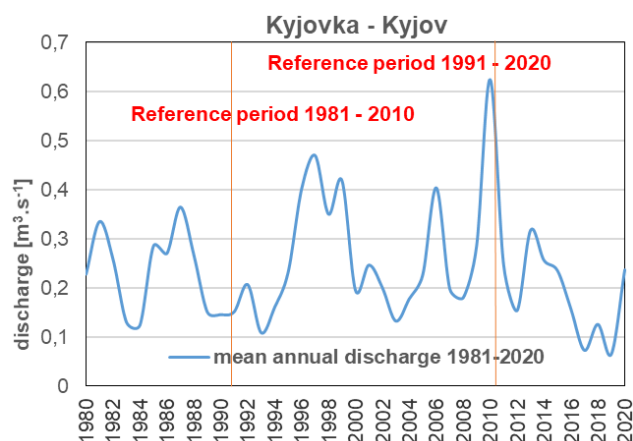


Fig. 15. Mean annual discharges in the water gauging station Kyjov (Kyjovka) for the period from November 1980 to October 2020 with indication of reference periods. Source of used data: CHMI.

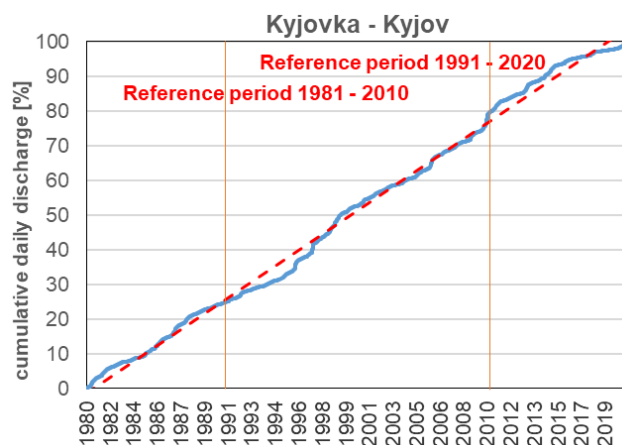


Fig. 16. Mass curve of mean daily discharges in the water gauging station Kyjov (Kyjovka) for the period from November 1980 to October 2020 with indication of reference periods. Source of used data: CHMI.

## Conclusion

Based on the above results, it is clear that the dry period 2015 to 2020 had a significant role in the flow frequencies of watercourses in the South Moravian Region than the dry period in the 1990s. The average flow frequencies for the period 1981–1991, which are included in the still valid reference period 1981–2010, were more favorable than the average flow frequencies in the period 2011–2020, which are included in the newly proposed reference period 1991–2020. This difference affects the decrease in long-term mean discharge ( $Q_a$ ) and other data within M-day discharges. The effect of the dry season is noticeable in all selected water gauging stations, e.g. in the Strážnice station (Morava) there is a noticeable decrease in the long-term mean discharge between periods by 8%. The most significant decrease is evident in the quantiles around the 300-day to 364-day discharge, which represent the minimum flows in a given watercourse (up to 15%).

The most significant decrease in the long-term mean discharge in the newly proposed reference period from the evaluated water gauging stations will be evident in the Ivančice station (Jihlava) by 12%, as the more watery 80s will fall out of the 1991–2020 reference period (e.g. floods in May 1985). On the contrary, the smallest decrease from the evaluated stations will be evident in the station Kyjov (Kyjovka) by 6%. In minimal flows, however, the situation is exactly the opposite. The value of the 364-day flow in the new period will be unchanged in Ivančice (this is most likely due to the stabilization of fluctuations and the prevention of water drop to minimum flows due to manipulations at the outflow from the Dalešice – Mohelno reservoir system). In Kyjov, however, there will be a noticeable decrease of up to 62%, which is the largest difference between the periods of all evaluated stations. On average, of all evaluated stations, this is a decrease in the long-term average flow by 9%, in the minima it is a decrease of 28% in the period 1991–2020.

Furthermore, from the data of water gauging stations, e.g. from the Svatka river basin, it is clear that the occurrence of historically significant minimum flows also affected the supply of large water reservoirs, which kept runoff at the necessary minimums so that they themselves had enough water for their own management. The Skalní Mlýn water gauging station (Punkva) in the Moravian Karst was also evaluated for interest. There is a noticeable decrease between periods in the long-term mean discharge (by 11%). In addition, a hydrometric measurement was performed in the station profile (August 2018), where, according to available data, the historically lowest flow since 1928 was measured, where minimal flows occurred most often from 12 to 24 August 2018, which could be caused by the influence of the cave system of the Moravian Karst.

The above-mentioned analyzes of the trend of mean daily discharges confirmed the above. The results support the conclusions describing the differences between the two reference periods. Above all, there is a significant dry period in all stations since 2015–16, where a significant declining trend in daily discharges is evident. These conclusions are evident from various other outputs of the author of this paper. For example, the Evaluation of Minimum Discharges on Watercourses in the South Moravian Region for the period 2015–2018 (Coufal, 2019) or the same for the last 10 years

(Coufal, 2020) can be mentioned. The problem with the dry season is also evident in other parts of the Czech Republic, for example in the Vysočina Region (Coufal et al., 2018).

The results and conclusions will serve for practical use in applied hydrology, e.g. as a basis for determining the minimum residual flows in water management and other other purposes in providing standard hydrological data of surface waters according to ČSN 75 1400.

## References

- Coufal, P., Bárta, B., Boráková, J., Černá, I., Koštek, J., Matulová, J. (2018): Hydrologie. Vyhodnocení sucha na území Kraje Vysočina za období 2015–2018. ČHMÚ: Brno. 21–46.
- Coufal, P. (2019): Vyhodnocení minimálních průtoků na vodních tocích v Jihomoravském kraji v období 2015–2018. Cyklus odborných seminářů ČHMÚ: Brno.
- Coufal, P. (2020): Minimální průtoky v povodí Dyje a Moravy za období posledních 10-ti let, Cyklus odborných seminářů ČHMÚ: Brno.
- ČSN 75 1400. Hydrologické údaje povrchových vod. Praha: Úřad pro technickou normalizaci, metrologii a státní zkušebnictví, 2014, 16 s.
- Kaňok, J. (1999): Antropogenní ovlivnění velikosti průtoků řek povodí Odry pro profil Kožle. Spisy prací Přírodovědecké Fakulty Ostravské Univerzity: Ostrava.
- Němec, J. (1964): Inženýrská hydrologie, SNTL: Praha.

Mgr. Pavel Coufal (\*corresponding author, e-mail: pavel.coufal@chmi.cz)  
Czech Hydrometeorological Institute  
Hydrology Department  
Kroftova 2578/43  
616 00 Brno  
Czech Republic

## Extreme low flow change analysis on the Tysa River within Ukraine

Liudmyla GORBACHOVA\*, Borys KHRYSYTIUK

In the current conditions of a changing climate, which directly affects the variability of river runoff, it is very important to have the knowledge about the trends of its extreme flow. Extreme low flows, just like floods are causing a significant material damage. The Tysa River has the two periods with the low flow during year. In addition, some years are dry and such years can be observed for several years in a row. This research used the Indicators of Hydrologic Alteration method (IHA) for investigation of extreme low flow characteristics and their changes along the Tysa River within Ukraine. The research was carried out based on the observations of 4 gauging stations that are located along the Tysa River within Ukraine. The mean daily discharges were used from the beginning of observations until 2018 inclusive. It turned out that at the Tysa River – Vylok Village gauging station the low flow trends differ from the trends at other gauging stations that are located in the upper part of the Tysa River.

KEY WORDS: extreme low flow, IHA, Tysa River, statistical analysis

### Introduction

Knowledge of low flow trends is important for practice, especially for design, construction and operation of hydraulic structures on rivers, as well as for shipping, agriculture, etc. Extreme low flows, just like floods are causing a significant material damage. It should also be borne in mind that many scientists predict that in the warmer climate the droughts will become more common in the future. Longer periods of low flow and a decrease of discharge values, and for some rivers their complete disappearance are expected (Wimmer et al., 2015; Loboda and Bozhok, 2016; Chang et al., 2017; Ionita and Nagavciuc, 2020).

Usually, the assessment of trends and changes in river runoff is carried out on the basis of statistical approaches that allow to determine some quantitative indicators. So, to estimate the spatial and temporal homogeneity, stationarity of hydrological observation series, statistical tests are most often used (Kundzewicz and Robson, 2004; Blöschl et al., 2019). Also, the method of frequency analysis of time series is in great demand (Caruso, 2000; Onoz et al., 2019; Pekárová and Miklánek, 2019; Bačová Mitková and Halmová, 2020). Such approaches allow to operate with a certain set of information (statistical criteria, discharges of different probability, average value, variation and asymmetry coefficients). In the late 20th century, the method of Indicators of Hydrologic Alteration (IHA), which was developed in the United States, became widely used in the world (Richter et al., 1997; Gao et al., 2009; Halmová

et al., 2011; Yu et al., 2017; Zhou et al., 2020). This approach allows to calculate quantitative statistical characteristics for runoff estimating of rivers, lakes and reservoirs and the degree of changes in their hydrological regime.

The research of low flow is an actual task for the Tysa River, which is characterized by low flow twice a year, namely in winter and summer-autumn. In the dry years that have been observed in the last few years, there are some problems with water supply to consumers in the region (Pochaievets and Obodovskiy, 2018). It should be noted that the study of the low flow of the Tysa river, as well as the Ukrainian Carpathians region, does not receive due attention due to the fact that, first of all, this area is the dangerous floods zone. For the upper part of the Tysa River the recent research of the low flow has been carried out in the papers by Gorbachova (2017) and Pochaievets (2020). However, this research focused on the study of long-term fluctuations and the definition of design characteristics.

The purpose of this research is to use the Indicators of Hydrologic Alteration approach to investigate extreme low flow characteristics and their changes along the Tysa River within Ukraine.

### Material and methods

#### *The study area*

The Tysa River Basin is the largest sub-basin in the Danube River Basin with an area of 157 186 km<sup>2</sup>.

The Tysa River also is the longest tributary of the Danube and the second largest by flow after the Sava River, its length is 966 km (Halmová et al., 2011). Five countries are sharing the Tysa Basin, namely Ukraine, Romania, Hungary, Slovakia and Serbia. In north-western Ukraine in the Carpathian Mountains the Tysa River rises. It is formed from the confluence of the Bila Tysa and Chorna Tysa Rivers (Fig. 1). At the same time, the source of the Tysa is taken to be the source of its longer tributary – the Chorna Tysa River. In Ukraine the Tysa River Basin area is 12 732 km<sup>2</sup>, that is 2.1% of its territory. Moreover, share of the Tysa River Basin area in Ukraine is 8.1% (Makovinska, 2018). In the territory of Ukraine, there is the mountainous Upper part of the Tysa River Basin, namely mostly the right bank. The left tributaries of Upper part are located in Romania. The river at the upper part is a typical mountain river with a narrow valley, and it sometimes looks like a gorge with relatively steep slopes. The right bank tributaries of the Tysa River are located the southern slope of the Ukrainian Carpathians. The average altitudes of mountainous catchments are 800–1 200 m, and the average slopes are 200–400 m/km (Borsos and Sendzimir, 2018; Zabolotnia et al., 2019). In the Upper part river shows a high flow rate and low

turbidity. Near Vylok village the multi-annual mean discharge is 202 m<sup>3</sup> s<sup>-1</sup> (1954–2018). The climate of the Upper Tysa in the Ukrainian Carpathians is reasonably continental. There are mild winters with thaws, a long, though unstable spring, a mild summer and warm autumn. The annual precipitation is between 1 750 mm in the mountains and 700 mm in the lowlands. The variability of the mean annual temperature is in the range of 3.0–8.5°C (Makovinska, 2018; Pochaievets, 2020).

The Tysa River Basin belongs to two hydrological regions, namely the Uzh-Borzhava and Carpathian regions according to hydrological regionalisation by the intra-annual distribution of the flow within Ukraine (Gorbachova, 2015).

Carpathian region covers the upper reaches of the Tysa River to the Rika River. There the snow-rain flood period lasts from March to July, the autumn period is characterised by floods, and winter is characterised by the smallest discharges in the year.

For the rivers of the Uzh-Borzhava region the lowest discharges are observed from August to October. Winters are characterised by intense floods in the cold period of the year.

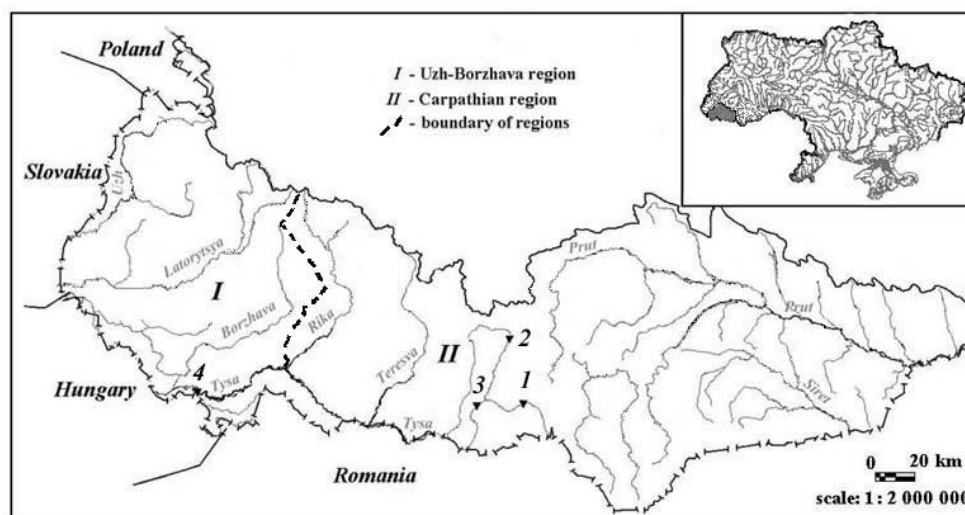


Fig. 1. Scheme of the Tysa River Basin within Ukraine and location of the main gauging stations on its channel (numbering of posts corresponds to Table 1).

Table 1. List of the gauging stations on the Tysa River within Ukraine

№	Name of gauging station	Distance from the mouth [km]	Catchment area [km <sup>2</sup> ]	Latitude	Longitude	Altitude [m.a.s.l.]	Daily data [years]	$Q_a$ [m <sup>3</sup> s <sup>-1</sup> ]
1	Bila Tysa River – Luhy village	15*	189	48° 04' N	24° 56' E	652	1955–2018	5.13
2	Chorna Tysa River – Yasynay village	28*	194	48° 16' N	24° 21' E	650	1956–2018	4.78
3	Tysa River – Rakhiv town	962	1070	48° 03' N	24° 12' E	430	1947–2018	25.4
4	Tysa River – Vylok village	808	9140	48° 06' N	22° 50' E	117	1954–2018	202

Note: \* – to the confluence of the rivers Chorna Tysa and Bila Tysa;  $Q_a$  – multi-annual mean discharge.

### Input data

The research was carried out based on observations of 4 gauging stations that are located along the Tysa River within Ukraine (Table 1). In the upper Tysa River the low flow analysis was carried out by the observation series at the rivers Chorna Tysa and Bila Tysa. The mean daily discharges from the beginning of observations until 2018 inclusive were used. Observations series have almost the same duration, which makes a comparative analysis of the calculated statistical indicators more reliable.

### Methodology

Indicators of Hydrologic Alteration was used to study the low flow of the Tysa River. In the IHA the daily levels and discharges of rivers, lakes and groundwater are used that allows to determine the statistic parameters of natural and disturbed hydrological regime of water bodies. According to this methodology, the river runoff is conditionally divided into five components:

- "Extreme low flows" – low flow, which is observed on rivers during droughts;
- "Low flows" – flow on river in the periods after spring floods, snow and rain floods, when the river is fed only by groundwater;
- "High-flow pulses" – flow on river during rainfalls in summer or thaw in winter, as well as for other reasons (reservoir releases, etc.); at the same time, the river does not overflow;
- "Small floods" – same as "High-flow pulses", but with the outflow of the river to the floodplain without catastrophic consequences;
- "Large floods" – extremely high floods, which are rare and cause catastrophic consequences.

To divide the arrays of daily discharges on 5 components, the values of the parameters recommended by the IHA

were used, which were developed by The Nature Conservancy (2009). To calculate the river flow parameters of the Tysa River we used the IHA software, version 7.1.0.10.

This made it possible to separate from the total flow the extreme low flows, for which the IHA statistics were calculated.

The study calculated the following statistics:

- discharge thresholds for 5 flow components, [ $\text{m}^3 \text{s}^{-1}$ ];
- mean values of the extreme low discharges (peaks) for each year, [ $\text{m}^3 \text{s}^{-1}$ ];
- mean duration of the extreme low flows, [days];
- mean frequency of the extreme low flows, [number of cases/year];
- mean Julian dates of the extreme low discharges (peaks) for each year, [days].

Changes of extreme low flow characteristics along the river and over time were also analysed.

### Results and discussion

At each gauging station the river flow was divided into five components: "Extreme low flows", "Low flows", "High-flow pulses", "Small floods", "Large floods" according to the discharge thresholds and the results are presented in Table 2. An example of such a distribution for the hydrological post of the Tysa River – Vylok village is shown in Fig. 2.

In the Upper part of the Tysa River all 5 flow components of the multi-annual mean and discharge thresholds are increasing in the direction from the headwaters to the Tysa River - Vylok village gauging station (Table 1, 2, 3; Fig. 3 a, b, c), that fully corresponds to the physical and geographical conditions of its formation. Further, the analysis of the calculated statistical parameters by IHA for the "Extreme low flows" component was carried out (Table 3).

**Table 2. Discharge thresholds at the gauging stations in the upper part of the Tysa River, [ $\text{m}^3 \text{s}^{-1}$ ]**

№	Name of gauging station	Large floods	Small floods	High-flow pulses	Low flows	Extreme low flows
1	Bila Tysa River – Luhy village	39.5	24.2	6.43	3.68	1.54
2	Chorna Tysa River – Yasynay village	58.2	32.8	5.96	3.19	1.15
3	Tysa River – Rakhiv town	351	174	31.3	17.4	7.0
4	Tysa River – Vylok village	2480	1370	244	133	56

**Table 3. Statistical parameters of IHA for the "Extreme low flows" at the gauging stations in the upper part of the Tysa River**

№	Name of gauging station	Mean values of peak discharge [ $\text{m}^3 \text{s}^{-1}$ ]	Mean duration [days]	Mean frequency [number of cases/year]	Mean Julian dates peaks [days]
1	Bila Tysa River – Luhy village	1.18	14	3.70	19
2	Chorna Tysa River – Yasynay village	0.89	12	3.57	29
3	Tysa River – Rakhiv town	5.66	9	4.82	30
4	Tysa River – Vylok village	46.4	11	3.65	302

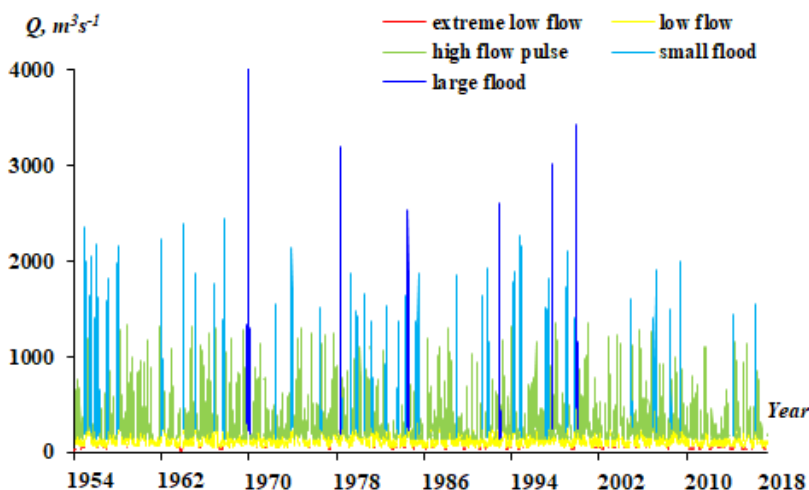


Fig. 2. Separation of hydrographs into different flow types for gauging station of the Tysa River – Vylok village.

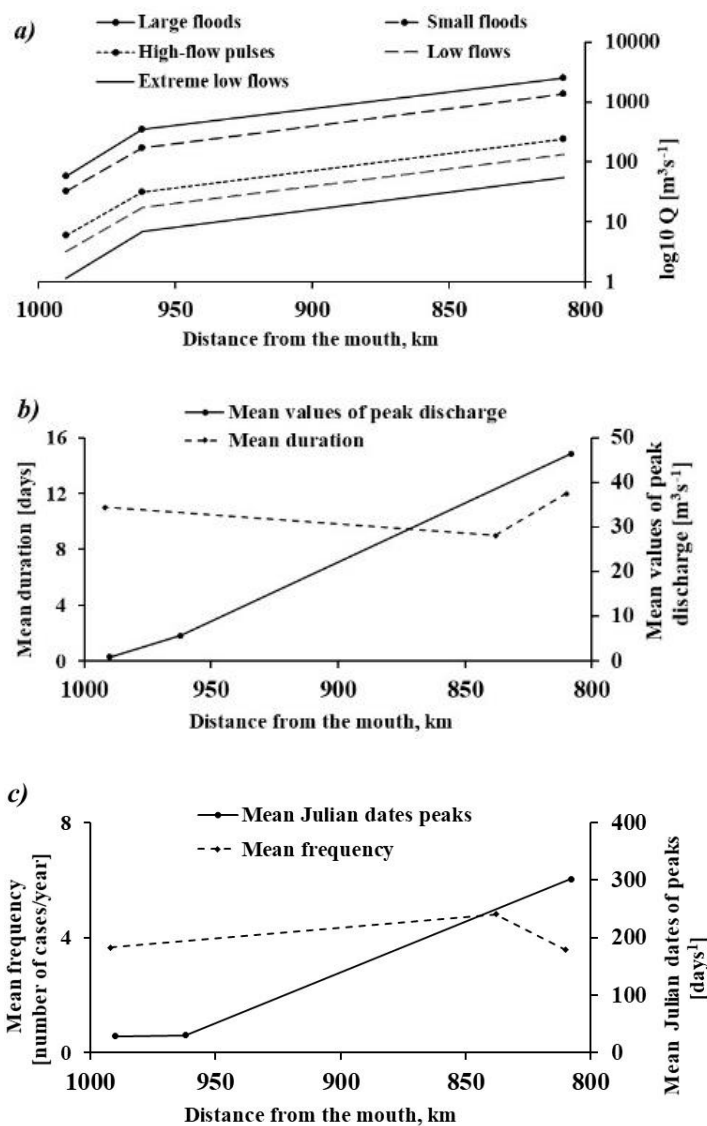


Fig. 3. Discharge thresholds (a) and mean values of the peak discharges during for each year, mean duration (b) and mean frequency, mean Julian dates of peaks (c) of the extreme low flows at gauging stations in the upper part of the Tysa River.

Mean duration of extreme low flows is in the range of 9 to 14 days. Gauging stations that are located on the headwaters have the greatest mean duration of the extreme low flows. Extreme low flows are observed in the mean 4 times a year. According to the mean Julian dates, the extreme low flow peaks are observed in January in the upper part of the Tysa River and in October for the Tysa River – Vylok village gauging station.

During the observations period, the mean values of the extreme low discharges (peaks) for each year have the tendency to increase in the upper part of the Tysa River and to decrease in the Tysa River – Vylok village

gauging station (Fig. 4). However, only the Chorna Tysa River – Yasynay village gauging station has the significant trend. Mean duration and mean Julian dates of the extreme low discharges (peaks) for each year did not undergo significant changes for all gauging stations studied. At the same time, such a characteristic as the mean frequency of the extreme low flows has undergone significant changes over time. Wherein, on the Tysa River – Vylok village gauging station the mean frequency of the extreme low flows has the trends to increase. In all other gauging stations, this characteristic has the opposite tendency, i.e. it decreases.

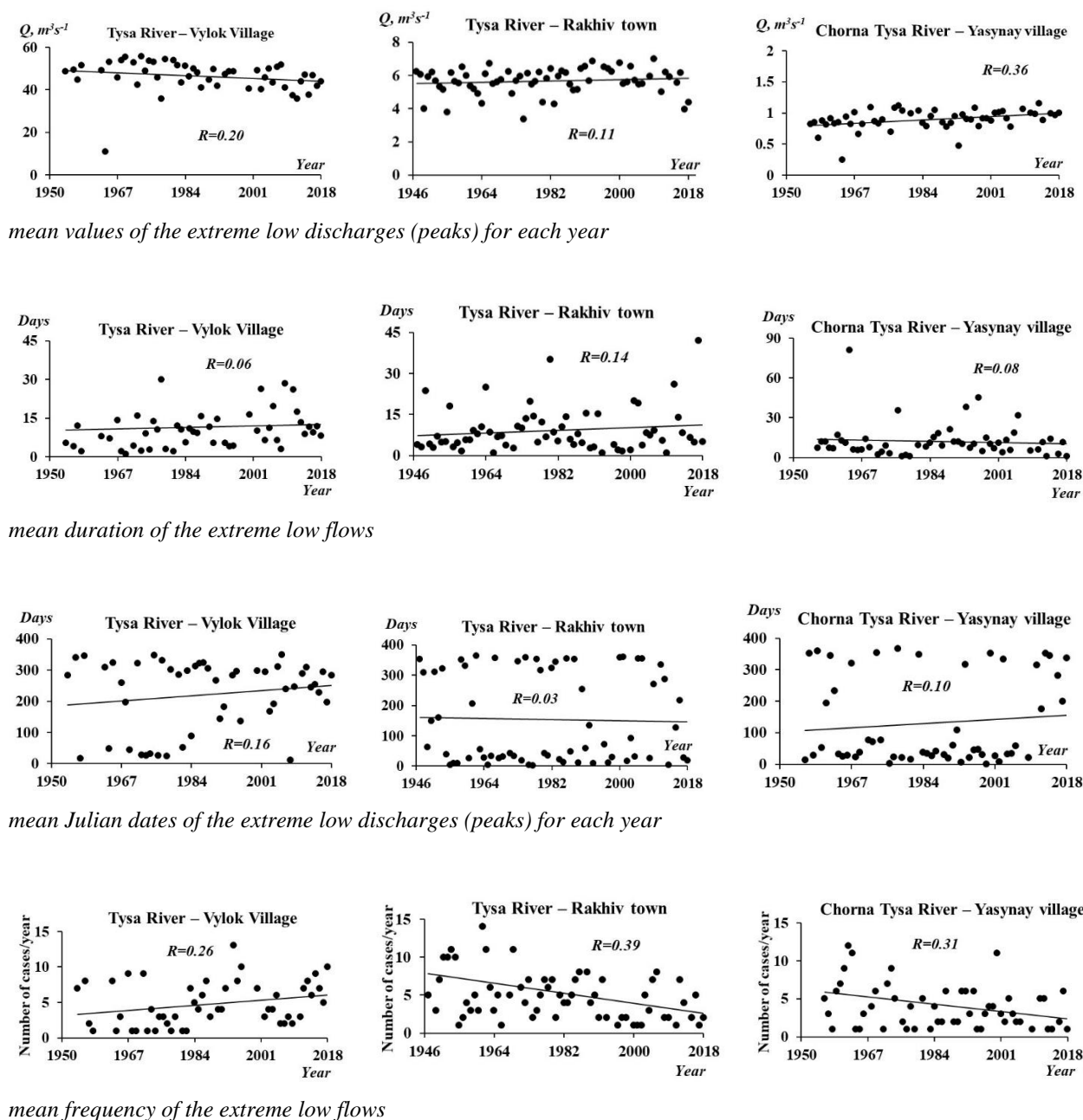


Fig. 4. Identification of trends in the characteristics of the extreme low flows in the upper part of the Tysa River.

The Tysa River - Vylok village gauging station has the trends of extreme low flows which differ from the trends at other gauging stations that are located in the upper part of the Tysa River. This gauging station is the closing post in the upper part of the Tysa River. Its flow is formed under the influence of left and right tributaries, which are located both on the territory of Ukraine and on the territory of Romania. These are the mountain basins with the features of the surface watershed and climatic factors that are manifested in the uneven distribution of rainfall, temperature and evaporation. This is reflected in different runoff trends at such catchments (Gorbachova, 2017; Pochaievets, 2020). It is clear that the explanation of trends in extreme low flows on the Tysa River - Vylok village gauging station requires further research with additional observation data as along the river channel and its main tributaries.

### Conclusion

The application of the IHA method for the study of extreme low flows allows to obtain a new knowledge and expand the understanding about its statistical indicators. Dividing of hydrographs according to the calculated discharge thresholds into five components allowed to obtain the characteristics and periods of the extreme low flows in the upper part of the Tysa River. Analysis of extreme low flow characteristics showed that its mean duration is in the range of 9 to 14 days. Extreme low flow is observed in mean 4 times a year. Extreme low flow peaks are observed in January in the upper part of the Tysa River and in October for the Tysa River – Vylok village gauging station.

Analysis of the fluctuations of the extreme low flow characteristics showed that its mean peak values have the tend to increase over time in the upper part of the Tysa River except the Tysa River – Vylok village gauging station. At the same time, on this gauging station the mean frequency of the extreme low flows has the trends to increase. It is clear that in the future the continuation of such trends will cause the negative consequences for the population and the economy in the river basin. It should be noted that deeper understanding of the features of extreme low flows requires further research with using observation data along the river channel and its tributaries.

### References

- Bačová Mitková, V., Halmová, D. (2020): Analysis of the runoff volumes of the wave belongs to maximum annual discharges. *Acta Hydrologica Slovaca*, Vol. 21, no. 2, 188–196. DOI: 10.31577/ahs-2020-0021.02.0023
- Blöschl, G., Hall, J., Viglione, A., Perdigão, R. A. P., Parajka, J., Merz, B., Lun, D., Arheimer, B., Aronica, G. T., Bilibashi, A., Boháč, M., Bonacci, O., Borga, M., Čanjevac, I., Castellarin, A., Chirico, G. B., Claps, P., Frolova, N., Ganora, D., Gorbachova, L., Gül, A., Hannaford, J., Harrigan, Sh., Kireeva, M., Kiss, A., Kjeldsen, T. R., Kohnová, S., Koskela, J. J., Ledvinka, O., Macdonald, N., Mavrova-Guirguinova, M., Mediero, L., Merz, R., Molnar, P., Montanari, A., Murphy, C., Osuch, M., Ovcharuk, V., Radevski, I., Salinas, J. L., Sauquet, E., Šraj, M., Szolgay, J., Volpi, E., Wilson, D., Zaimi, K., Živković, N. (2019): Changing climate both increases and decreases European river floods. *Nature*, Vol. 573, no. 7772, 1–4. <https://doi.org/10.1038/s41586-019-1495-6>
- Borsos, B., Sendzimir, J. (2018): The Tisza River: Managing a Lowland River in the Carpathian Basin. In: Schmutz, S., Sendzimir, J. (eds.) *Riverine Ecosystem Management. Science for Governing Towards a Sustainable Future*. Springer, Cham, 541–560. <https://doi.org/10.1007/978-3-319-73250-3>
- Caruso, B. S. (2000): Evaluation of low-flow frequency analysis methods. *Journal of Hydrology (New Zealand)*, Vol. 39, no. 1, 19–47. <https://www.jstor.org/stable/43944831>
- Chang, J., Zhang, H., Wang, Y., Zhang, L. (2017): Impact of climate change on runoff and uncertainty analysis. *Natural Hazards*, Vol. 88, no. 2, 1113–1131. DOI: 10.1007/s11069-017-2909-0
- Gao, Y., Vogel, R. M., Kroll, C. N., Poff, N. L. R., Olden, J. D. (2009): Development of Representative Indicators of Hydrologic Alteration. *Journal of Hydrology*, Vol. 374, no. 1, 136–147. <https://doi.org/10.1016/j.jhydrol.2009.06.009>
- Gorbachova, L. (2015): Modern intra-annual distribution of water runoff in Ukraine's river. *Ukrainian Geographical Journal*, no. 3, 16–23. [doi.org/10.15407/ugz2015.03.016](https://doi.org/10.15407/ugz2015.03.016) (In Ukrainian with English summary).
- Gorbachova, L. (2017): Spatio-temporal fluctuations of minimum flow in the Danube basin within Ukraine. Book of abstract of the XXVII Conference of the Danubian countries on Hydrological Forecasting and Hydrological Bases of Water Management, 26–28 September 2017, Golden Sands, Bulgaria, 26.
- Halmová, D., Pekárová, P., Mészároš, I. (2011): Low flow change analysis in selected gauging stations on the Danube River. *Acta Hydrologica Slovaca*. Vol. 12, no. 2, 286–295. (In Slovak)
- Ionita, M., Nagavciuc, V. (2020): Forecasting low flow conditions months in advance through teleconnection patterns, with a special focus on summer 2018. *Scientific Reports*, no. 10, 13258. <https://doi.org/10.1038/s41598-020-70060-8>
- Kundzewicz, Z. W., Robson, A. J. (2004): Change detection in hydrological records – a review of the methodology. *Hydrological Sciences Journal*, Vol. 49, no. 1, 7–19. <https://doi.org/10.1623/hysj.49.1.7.53993>
- Loboda, N. S., Bozhok, Y. V. (2016): Water resources of Ukraine in the XXI century under climate change scenarios (RCP4. 5 AND RCP8. 5). *Ukrainian hydrometeorological journal*, no. 17, 114–122. <https://doi.org/10.31481/uhmj.17.2016.13>
- The Nature Conservancy Indicators of Hydrologic Alteration (2009): Version 7. User's Manual, 75 p. <https://www.conservationgateway.org/Documents/IHAV7.pdf>
- Makovinska, J. (Ed.) (2018): Tisza River Basin Characterization Report on Surface Water. Interreg – Danube Transnational Programme, 30 p. <http://www.interreg-danube.eu/approved-projects/jointisza>
- Onoz, B., Cetin, M., Yuce, M. I., Selek, B., Aksu, H., Burgan, H. I., Esit, M., Yildirim, I. and Karakus, E. U. (2019): Frequency analysis of low flows in intermittent and non-intermittent rivers from hydrological basins in Turkey. *Water Supply*, Vol. 19, no. 1, 30–39. <https://doi.org/10.2166/ws.2018.051>
- Pekárová, P., Miklánek, P. (Eds.) (2019): Flood regime of rivers in the Danube River basin. Followup volume IX of the Regional Cooperation of the Danube Countries in IHP

- UNESCO. IH SAS, Bratislava, 215 p. <https://doi.org/10.31577/2019.9788089139460>
- Pochaievets, O., Obodovskiy, O. (2018): Assessment of the influence of the main hydrographic characteristics of the water catchments of the rivers of the Tisza basin (within Ukraine) on the formation of the minimum flow. *Hydrology, hydrochemistry and hydroecology*, no. 2(49), 6–15. (in Ukrainian with English abstract)
- Pochaievets, O. (2020): Spatio-temporal dynamics of the minimum flow of the Tisza River basins within Ukraine. PhD thesis. The Taras Shevchenko National University of Kyiv, 139 p. (In Ukrainian with English summary)
- Richter, B., Baumgartner, J., Wigington, R., Brau, D. (1997): How Much Water Does a River Need? *Freshwater Biology*, Vol. 37, no. 1, 231–249. <https://doi.org/10.1046/j.1365-2427.1997.00153.x>
- Wimmer, F., Audsley, E., Malsy, M., Savin, C., Dunford, R., Harrison, Rüdi P. A., Schaldach, R., Flörke, M. (2015): Modelling the effects of cross-sectoral water allocation schemes in Europe. *Climatic Change*, Vol. 128, no. 3–4, 229–244. DOI: 10.1007/s10584-014-1161-9
- Yu, C., Yin, X., Yang, Z., Dang, Z. (2017): Assessment of the degree of hydrological indicators alteration under climate change. In *Proceedings of the 6th International Conference on Energy and Environmental Protection (ICEEP 2017)*. *Advances in Engineering Research (AER)*, vol. 143, 210–216.
- Zabolotnia, T., Gorbachova, L., Khrystyuk, B. (2019): Estimation of the long-term cyclical fluctuations of snow-rain floods in the Danube basin within Ukraine. *Meteorology Hydrology and Water Management. Research and Operational Applications*, Vol. 7, no. 2, 3–11. <https://doi.org/10.26491/mhwm/99752>
- Zhou, X., Huang, X., Zhao, H., Ma, K. (2020): Development of a revised method for indicators of hydrologic alteration for analyzing the cumulative impacts of cascading reservoirs on flow regime. *Hydrol. Earth Syst. Sci.*, Vol. 24, no. 8, 4091–4107. <https://doi.org/10.5194/hess-24-4091-2020>

Mgr. Liudmyla Gorbachova, Dr.Sc. (\*corresponding author e-mail: [gorbachova@uhmi.org.ua](mailto:gorbachova@uhmi.org.ua))  
Ing. Borys Khrystiuk, PhD  
Ukrainian Hydrometeorological Institute  
37, Prospekt Nauky  
03028, Kyiv  
Ukraine

**Trend changes analysis of the minimum and average annual discharges  
in selected Slovak rivers during the two periods 1961–2000 and 1961–2015**

Viliam ŠIMOR\*, Ľudovít LUPTÁK

This paper deals with the development of trends of minimum and average annual discharges for the period 1961–2015 and their comparison with the trends for the period 1961–2000, which have been used by the Slovak Hydrometeorological Institute (SHMI) since 2006 as a reference period.

In assessing both periods, we have dealt with their comparison with each other and subsequent analysis of any change. In general, time series trends can become an important indicator of whether there is a change in selected hydrological characteristics. In this paper, discharge series were processed and statistically analysed using a simple linear trend and the non-parametric Mann-Kendall test.

KEY WORDS: Mann-Kendall test, Sen's slope, Average annual discharge, Minimum annual discharge

### Introduction

At the present time of global climate change, the occurrence of periods of extreme weather phenomena is significantly increasing, warm weather without rain for a long time is alternating with local storm activity, the intensity of which creates flood situations in various parts of Slovakia. The impact of a prolonged drought can cause considerable damage not only to property and human life but also to the country's economy. The effects of a long-term drought are dangerous because, unlike a flood situation, the outward signs of a long-term drought are not noticeable for a long time.

In Slovakia and abroad, several authors have dealt with the trend analysis of various hydrological characteristics, as an example we can mention the works of Zeleňáková *et al.* (2011), in which an analysis of drought in terms of the significance of trends in flow characteristics was carried out. The authors applied their research on the occurrence of the significance of trends and subsequent spatial analysis in a GIS environment in the regions of eastern Slovakia. Bačová Mitková and Halmová (2021) in their work deals with the trend analysis of the extreme flows regime at gauging station Váh –Liptovský Mikuláš. The identification of trends in hydrological data also deals Malik *et al.* (2020), who identify the long-term trend and magnitude in monthly, seasonal, and annual streamflow by employing three non-parametric approaches conventional Mann-Kendall, Innovative-Sen trend, and Sen-slope at 5% level of significance in the upper Ramganga river catchment in

India. A more detailed study of this type of tests is discussed by Dabanlı *et al.* (2016), the authors also identify the weakness of the Mann Kendall test and explain the principles of the innovative-Sen method, that is based on cluster.

In the present paper, we evaluate by trend analysis the minimum and average annual discharges at selected gauging stations, and we are interested only in those where occurs a change in significance, as determined by the Mann-Kendall test.

### Material and methods

The minimum discharge is the lowest immediate discharge in a given profile for the selected period. On natural streams, the minimum discharge is generally the lowest average daily discharge, expressed in  $\text{m}^3 \text{s}^{-1}$  or  $\text{l s}^{-1}$ .

The average discharge is the arithmetic mean of all the discharges in a given profile over the period considered (e.g. day, month, season, year, etc.). It is generally determined by the arithmetic mean of the average daily discharges (average daily, arithmetic mean hourly discharges) or by the ratio of the total amount (volume) of water discharged and the number of seconds over the period considered. It shall be expressed in  $\text{m}^3 \text{s}^{-1}$  or  $\text{l s}^{-1}$ . According to the above definition, the minimum annual discharge is the smallest average daily discharge in a given hydrological year and the average annual discharge represents in the average daily discharge in a given hydrological year (Hydrology. Terminological glossary, 2002).

The discharge data for the period 1961–2015 were taken from the hydrological service database, which allows direct reporting of minimum and average annual discharges. Trends were evaluated in a selection of 65 gauging stations (GS) with long-term observations, which we consider as unaffected 1 in the Bodva basin, 8 in the Bodrog basin, 2 in the Danube basin, 4 in the Hornád basin, 4 in the Ipel basin, 2 in the Morava basin, 7 in the Nitra basin, 3 in the Dunajec and Poprad basins, 7 in the Hron basin, 4 in the Slaná basin and 23 in the Váh basin.

The hydrological datasets were processed and statistically analysed using two methods, the simple linear trend and the non-parametric Mann-Kendall test, which is used to detect significant trends in time series. The advantage of the Mann-Kendall test is that, it is not affected by the actual distribution of the data and it is less sensitive to outliers in the time series (Adámyová, 1989). The test is suitable for larger scale statistical datasets with more than 40 data points (WMO, 2008).

The Mann-Kendall test is based on the statistical value "S", which is calculated by comparing every two values  $x_i, x_j, (i > j)$  in a time series, where the statistical value "S" is given by the relationship:

$$S = \sum_{i=2}^n \sum_{j=1}^{i-1} \text{sign}(x_i - x_j) \quad (1)$$

where:

$n$  – is the number of values in the time series,  
 $x_i$  and  $x_j$  – are the compared values (discharges).

$\text{sign}(x_i - x_j)$  is:

$$\begin{cases} +1 & \text{if } x_i - x_j > 0 \\ 0 & \text{if } x_i - x_j = 0 \\ -1 & \text{if } x_i - x_j < 0 \end{cases}$$

The Mann-Kendall statistic ( $Z$ ) is based on the standard normal distribution and is given by the following relationship:

$$Z = \begin{cases} \frac{S-1}{\sqrt{\sigma_s}} & \text{if } S > 0 \\ 0 & \text{if } S = 0 \\ \frac{S+1}{\sqrt{\sigma_s}} & \text{if } S < 0 \end{cases} \quad (2)$$

where:

$\sigma_s$  – represents the variance and is defined as:

$$\sigma_s = \frac{1}{18} [n(n-1)(2n+5) - \sum_t f_t(f_t-1)(f_t+5)] \quad (3)$$

where:

$n$  – is the number of values in the time series.

$t$  – varies over the set of tied ranks

$f_t$  – is the number of times (i.e. frequency) that the rank  $t$  appears.

The sign of the statistic "Z" indicates whether the trend is

increasing ( $Z > 0$ ) or decreasing ( $Z < 0$ ), and we cannot obtain an estimate of the magnitude of the trends by this test (Santos and Portela, 2007).

#### Estimating the magnitude of significant trends (Sen's slope):

The magnitude of statistically significant trends of discharges at the gauge stations were calculated using by the slope estimator of Sen (1968). The method is based on a simple non-parametric procedure developed by the mentioned author as follows:

If there is a linear trend in the time series, we can express its real slope using a linear equation:

$$f(t) = Qt + B \quad (4)$$

where:

$Q$  – is a slope,

$B$  – is a constant,

$f(t)$  – is a linear model.

The slope estimate "Q" for all pairs in the time series is calculated as:

$$Q_i = \frac{x_j - x_k}{j - k}, i = 1, 2, \dots, N, j > k \quad (5)$$

where:

$x$  – are the values in the time series,

$N$  – is the number of estimated slopes while:

$$N = n \cdot (n - 1) / 2 \quad (6)$$

where:

$n$  – is the number of values in the original time series.

The resulting estimated slope is the median of these  $N$  values of the estimated slopes  $Q_i$  (Drápela and Drápelová, 2011). In determining the individual significance of a trend, its increase and decrease, we only evaluate significance at the 95% level (if it has been observed in gauge station, we consider the trend as significant), which is used in most statistical tasks.

We consider trends that occurred at a lower significance level (90%, 85% and below) to be non-significant. When comparing the two periods 1961–2000 and 1961–2015 to each other, we look for those gauge stations at which this significance level has changed. If there is a change in a significance, we also evaluate the size of the trends in the appropriate gauge stations using by a simple linear trend and the Sen's slope as well. All the trend calculations were processed in MS Excel.

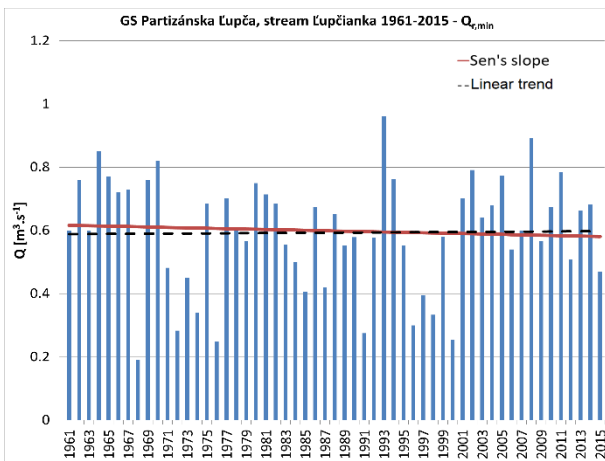
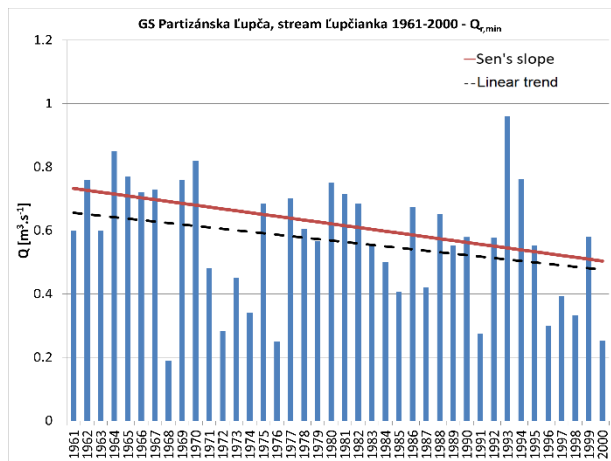
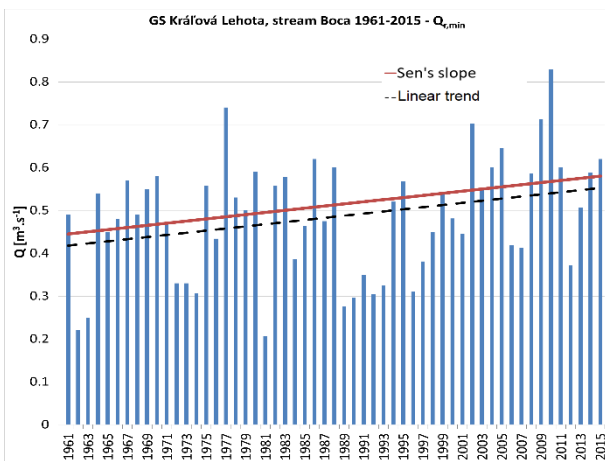
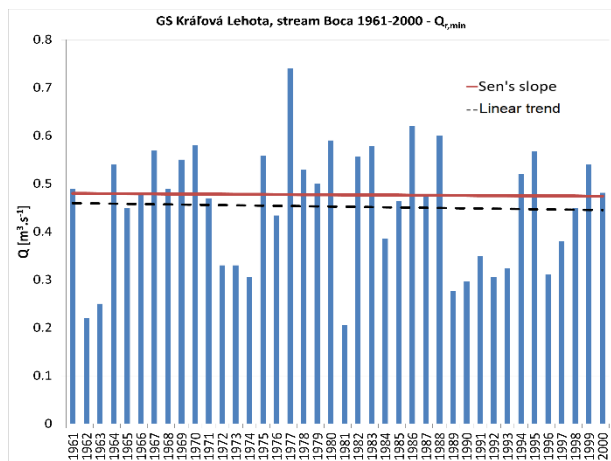
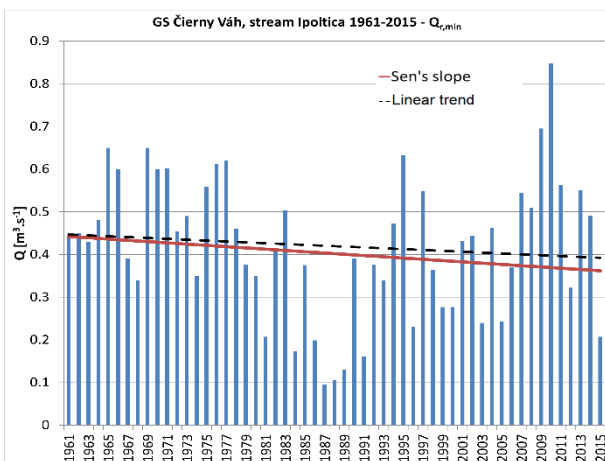
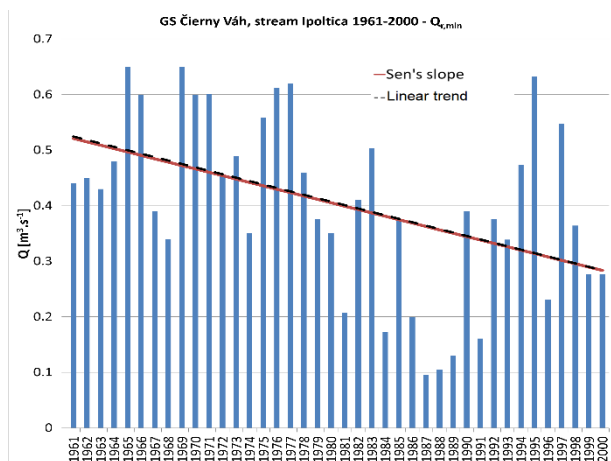
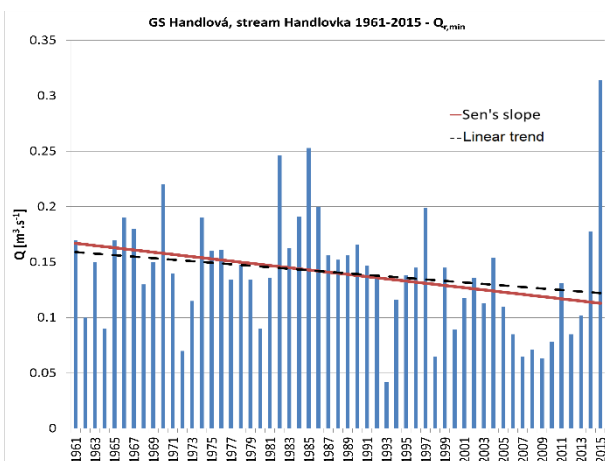
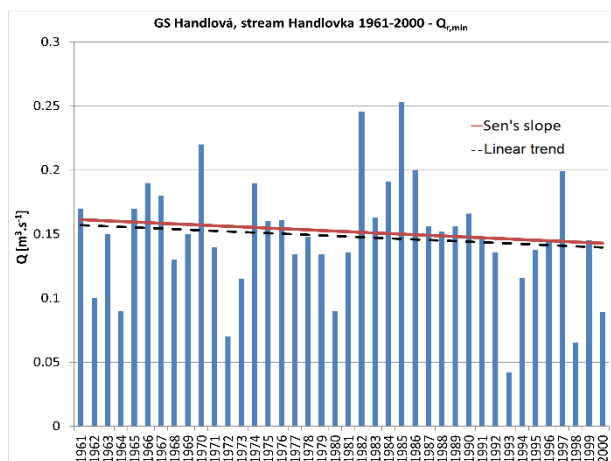
## Results

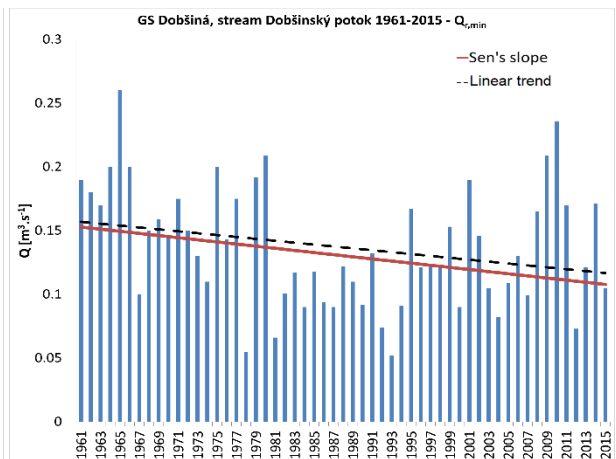
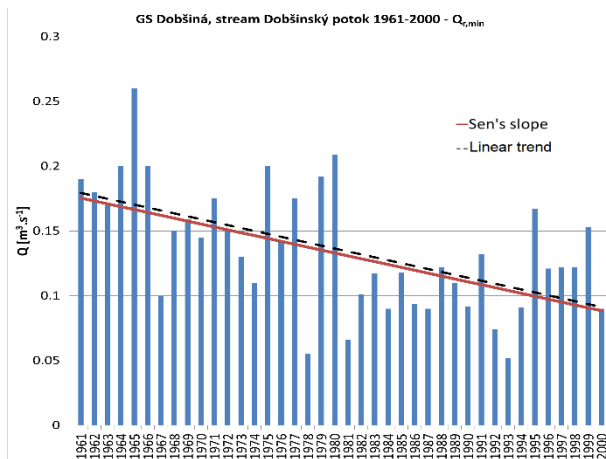
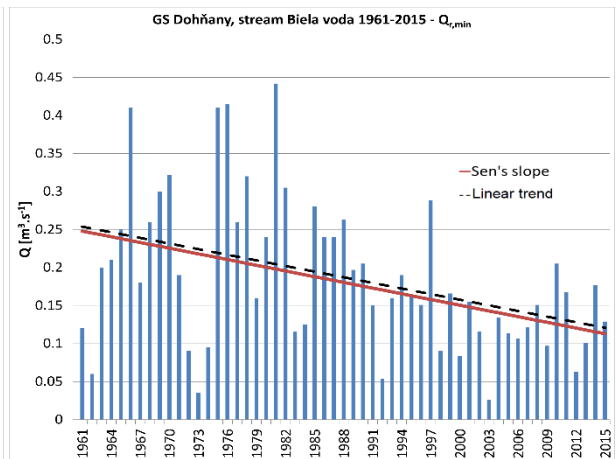
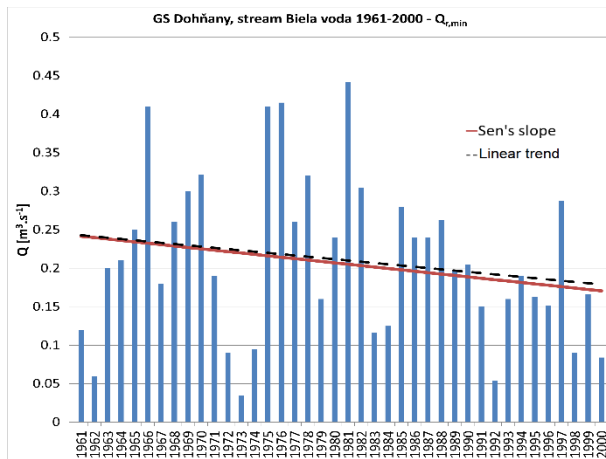
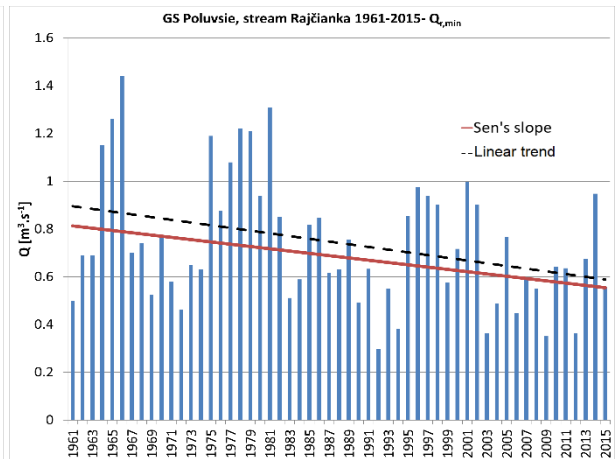
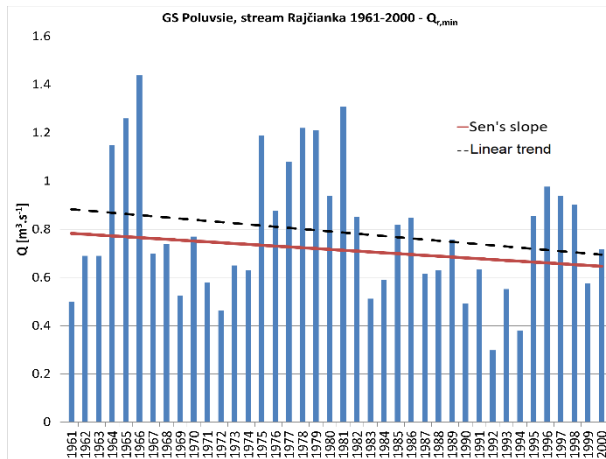
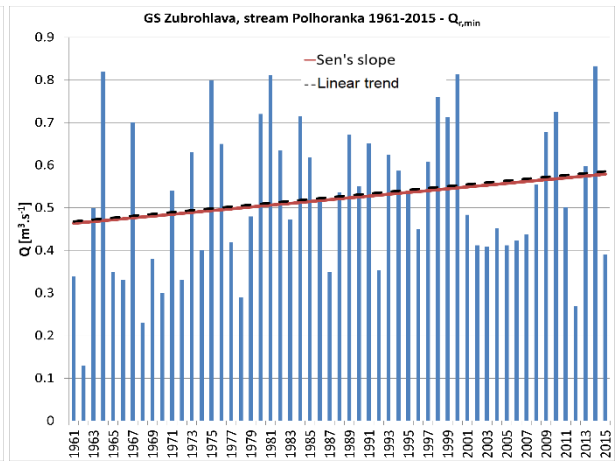
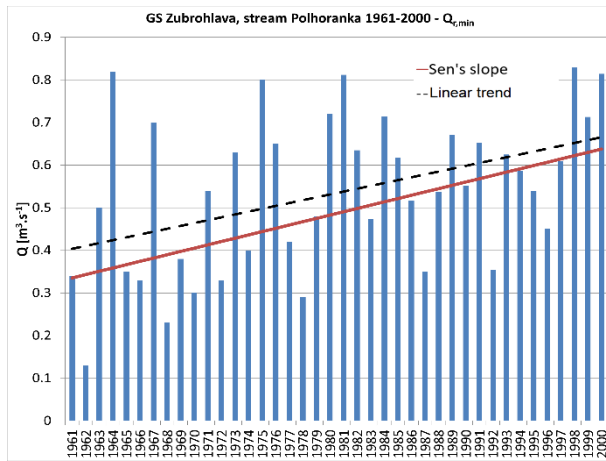
### Minimum annual discharges ( $Q_{r,min}$ )

In the period 1961–2000 were at the 95% significance level 7 gauge stations with increasing trends, 13 gauge stations with decreasing trends, and 45 gauge stations (Table 1). In the period 1961–2000 were at the 95%

**Table 1.** Change in the significance of minimum annual discharges ( $Q_{r,min}$ ) at individual gauging stations

gauge station	stream	catchment area	significance at level 95 %		change of significance
			period for 1961-2000	period for 1961-2015	
Moravský Ján	Morava	Morava	decreasing trend	decreasing trend	no
Láb	Močiarka	Morava	decreasing trend	decreasing trend	no
Spariská	Vydrica	Dunaj	non-significant or no trend	non-significant or no trend	no
Bratislava	Dunaj	Dunaj	non-significant or no trend	non-significant or no trend	no
Pezinok	Blatina	Malý Dunaj	non-significant or no trend	non-significant or no trend	no
Bernolákovo	Čierna voda	Malý Dunaj	non-significant or no trend	non-significant or no trend	no
Horné Orešany	Parná	Malý Dunaj	decreasing trend	decreasing trend	no
Píla	Gidra	Malý Dunaj	non-significant or no trend	non-significant or no trend	no
Nedožery	Nitra	Nitra	decreasing trend	decreasing trend	no
Handlová	Handlovka	Nitra	non-significant or no trend	decreasing trend	yes
Chalmová	Nitra	Nitra	non-significant or no trend	non-significant or no trend	no
Liešťany	Nitrica	Nitra	non-significant or no trend	non-significant or no trend	no
Nadice	Bebrava	Nitra	decreasing trend	decreasing trend	no
Nitrianska Sreda	Nitra	Nitra	non-significant or no trend	non-significant or no trend	no
Vieska n. Žitavou	Žitava	Nitra	non-significant or no trend	non-significant or no trend	no
Čierny Váh	Ipoltica	Váh	decreasing trend	non-significant or no trend	yes
Východná	Biely Váh	Váh	non-significant or no trend	non-significant or no trend	no
Kráľová Lehota	Boca	Váh	non-significant or no trend	increasing trend	yes
Podbanské	Belá	Váh	non-significant or no trend	non-significant or no trend	no
Liptovský Mikuláš	Váh	Váh	non-significant or no trend	non-significant or no trend	no
Partizánska Lupča	Lupčianka	Váh	decreasing trend	non-significant or no trend	yes
Podsúchá	Revúca	Váh	non-significant or no trend	non-significant or no trend	no
Lubochňa	Lubochňanka	Váh	increasing trend	increasing trend	no
Lokca	Biela Orava	Váh	non-significant or no trend	non-significant or no trend	no
Oravská Jasenica	Veselianka	Váh	decreasing trend	decreasing trend	no
Zubrohlava	Polhoranka	Váh	increasing trend	non-significant or no trend	yes
Trstená	Oravica	Váh	non-significant or no trend	non-significant or no trend	no
Martin	Turiec	Váh	non-significant or no trend	non-significant or no trend	no
Čadca	Kysuca	Váh	non-significant or no trend	non-significant or no trend	no
Poluvsie	Rajčianka	Váh	non-significant or no trend	decreasing trend	yes
Bytča	Petrovička	Váh	increasing trend	increasing trend	no
Vydrná	Petrinovec	Váh	decreasing trend	decreasing trend	no
Dohňany	Biela voda	Váh	non-significant or no trend	decreasing trend	yes
Horné Šnie	Vlára	Váh	non-significant or no trend	non-significant or no trend	no
Zlatno	Hron	Hron	non-significant or no trend	non-significant or no trend	no
Brezno	Hron	Hron	non-significant or no trend	non-significant or no trend	no
Hronec	Čierny Hron	Hron	decreasing trend	decreasing trend	no
Bystrá	Bystrianka	Hron	non-significant or no trend	non-significant or no trend	no
Mýto p. Ďumbierom	Štiavnička	Hron	non-significant or no trend	non-significant or no trend	no
Dolná Lehota	Vajskovský potok	Hron	non-significant or no trend	non-significant or no trend	no
Brehy	Hron	Hron	decreasing trend	decreasing trend	no
Holiša	Ipeľ	Ipeľ	non-significant or no trend	non-significant or no trend	no
Plášťovce	Krupinica	Ipeľ	non-significant or no trend	non-significant or no trend	no
Plášťovce	Litava	Ipeľ	non-significant or no trend	non-significant or no trend	no
Lučenec	Krivánsky p.	Ipeľ	non-significant or no trend	non-significant or no trend	no
Dobšiná	Dobšinský potok	Slaná	decreasing trend	non-significant or no trend	yes
Štítnik	Štítnik	Slaná	non-significant or no trend	non-significant or no trend	no
Lenartovce	Slaná	Slaná	non-significant or no trend	non-significant or no trend	no
Lehota nad Rimavicou	Rimavica	Slaná	non-significant or no trend	decreasing trend	yes
Nížny Medzev	Bodva	Bodva	decreasing trend	decreasing trend	no
Stratená	Hnilec	Hornád	non-significant or no trend	non-significant or no trend	no
Jaklovce	Hnilec	Hornád	non-significant or no trend	non-significant or no trend	no
Košické Oľšany	Torysa	Hornád	increasing trend	increasing trend	no
Ždaňa	Hornád	Hornád	non-significant or no trend	non-significant or no trend	no
Koškovce	Laborec	Bodrog	non-significant or no trend	non-significant or no trend	no
Lekárovce	Uh	Bodrog	increasing trend	non-significant or no trend	yes
Remetské Háme	Okna	Bodrog	non-significant or no trend	non-significant or no trend	no
Veľké Kapušany	Latorica	Bodrog	non-significant or no trend	non-significant or no trend	no
Hanušovce nad Topľou	Topľa	Bodrog	non-significant or no trend	non-significant or no trend	no
Svidník	Ondava	Bodrog	non-significant or no trend	non-significant or no trend	no
Jasenovce	Olka	Bodrog	non-significant or no trend	non-significant or no trend	no
Streda nad Bodrogom	Bodrog	Bodrog	increasing trend	increasing trend	no
Ždiar, Podspády	Javorinka	Poprad	non-significant or no trend	non-significant or no trend	no
Poprad, Matejovce	Slavkovský potok	Poprad	increasing trend	increasing trend	no
Chmelnica	Poprad	Poprad	non-significant or no trend	increasing trend	yes





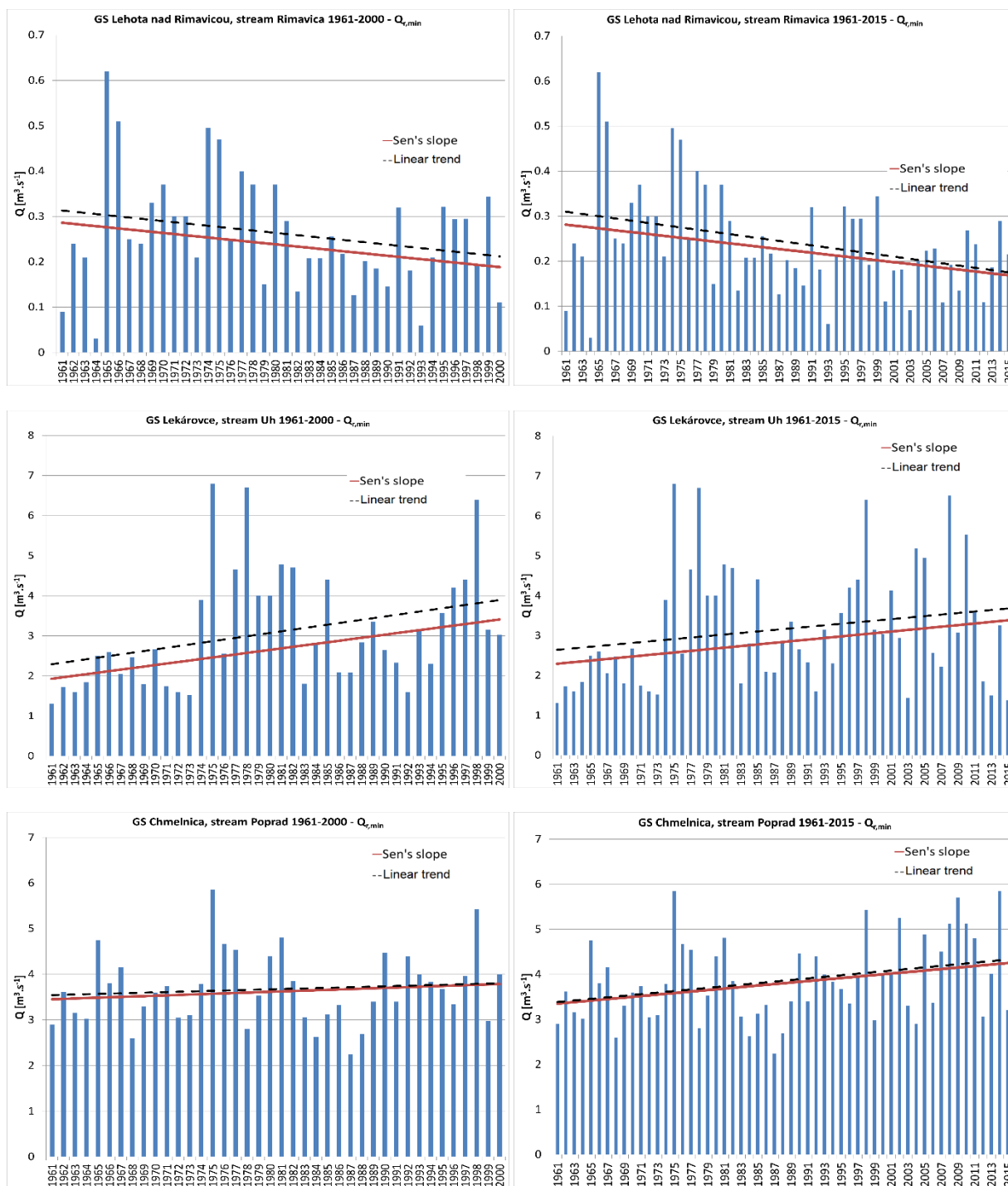


Fig. 1. Magnitude of trends in minimum annual discharges ( $Q_{r,min}$ ) at selected gauging stations (GS) for the period 1961–2000 and 1961–2015.

significance level 7 gauge stations with increasing trends, 14 gauge stations with decreasing trends and 44 gauge stations with insignificant or no trends (Table 1). The change in trend significance after adding 15 years occurred in 11 gauge stations. The most significant and most cases of changes in the trends of minimum discharges in the compared periods were calculated for the Váh river basin (Table 1).

Figure 1 shows the magnitudes of the trends (both Sen's slope and linear trend) at the gauging stations where occurred the change in significance. More significant differences in slopes occurred only at the gauge station Partizánska Ľupča, Ľupčianka stream in period 1961–2000. The trend in this period is significantly decreasing, but both trends has a different magnitude. The linear trend has a smaller slope than Sen's slope, the change is

**Table 2.** Change in the significance of average annual discharges ( $Q_r$ ) at individual gauging stations

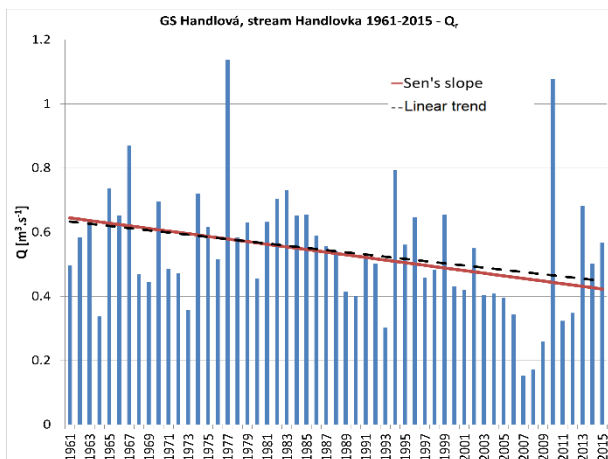
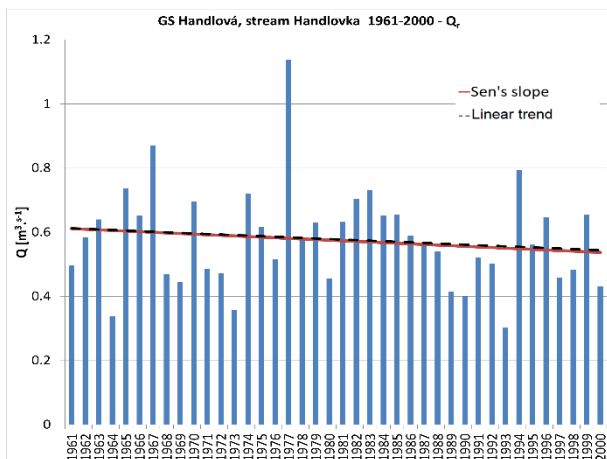
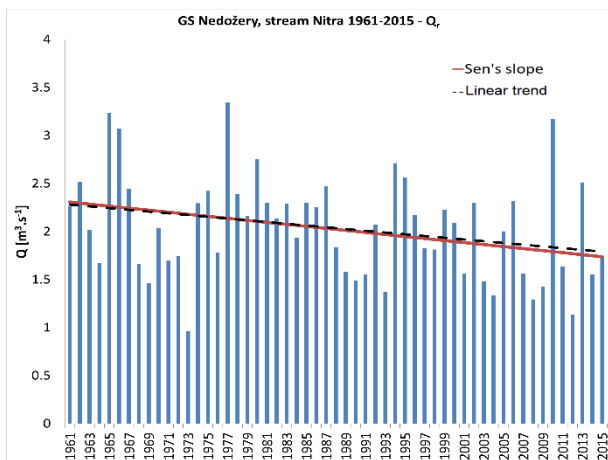
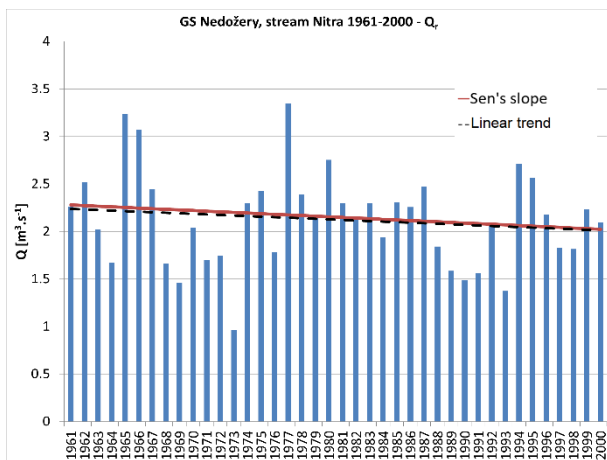
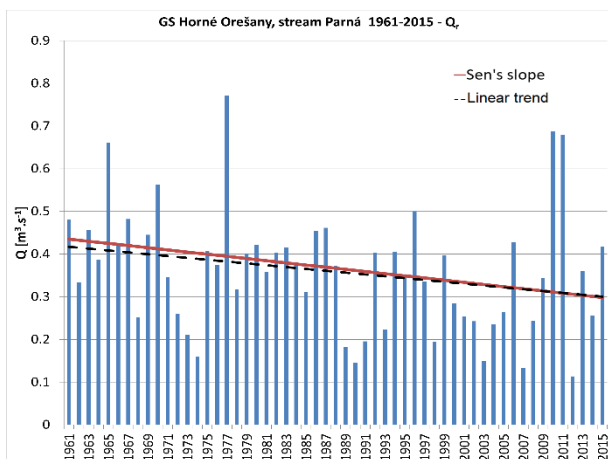
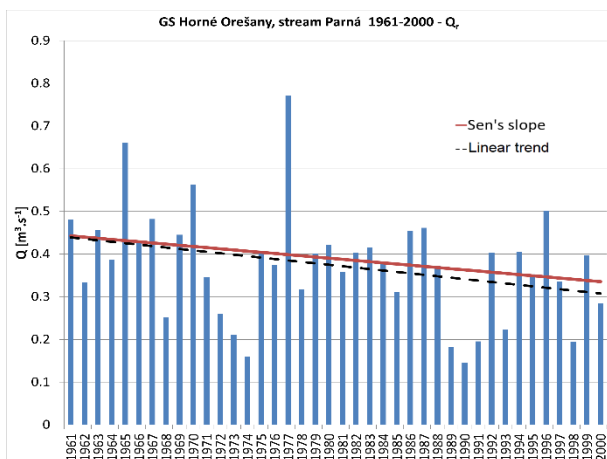
gauge station	stream	catchment area	significance at level 95 %		change of significance
			period for 1961-2000	period for 1961-2015	
Moravský Ján	Morava	Morava	non-significant or no trend	non-significant or no trend	no
Láb	Močiarka	Morava	decreasing trend	decreasing trend	no
Spariská	Vydrica	Dunaj	non-significant or no trend	non-significant or no trend	no
Bratislava	Dunaj	Dunaj	non-significant or no trend	non-significant or no trend	no
Pezinok	Blatina	Malý Dunaj	non-significant or no trend	non-significant or no trend	no
Bernolákovo	Čierna voda	Malý Dunaj	decreasing trend	decreasing trend	no
Horné Orešany	Parná	Malý Dunaj	non-significant or no trend	decreasing trend	yes
Pila	Cídra	Malý Dunaj	non-significant or no trend	non-significant or no trend	no
Nedožery	Nitra	Nitra	non-significant or no trend	decreasing trend	yes
Handlová	Handlovka	Nitra	non-significant or no trend	decreasing trend	yes
Chalmová	Nitra	Nitra	non-significant or no trend	decreasing trend	yes
Liešťany	Nitrica	Nitra	non-significant or no trend	decreasing trend	yes
Nadlice	Bebrava	Nitra	non-significant or no trend	non-significant or no trend	no
Nitrianska Streda	Nitra	Nitra	non-significant or no trend	non-significant or no trend	no
Vieska n. Žitavou	Žitava	Nitra	non-significant or no trend	non-significant or no trend	no
Čierny Váh	Ipoltica	Váh	non-significant or no trend	non-significant or no trend	no
Východná	Biely Váh	Váh	non-significant or no trend	non-significant or no trend	no
Kráľová Lehota	Boca	Váh	decreasing trend	non-significant or no trend	yes
Podbanské	Belá	Váh	non-significant or no trend	non-significant or no trend	no
Liptovský Mikuláš	Váh	Váh	non-significant or no trend	non-significant or no trend	no
Partizánska Ľupča	Ľupčianka	Váh	non-significant or no trend	decreasing trend	yes
Podsúchá	Revúca	Váh	non-significant or no trend	non-significant or no trend	no
Lubochňa	Lubochňanka	Váh	non-significant or no trend	non-significant or no trend	no
Lokca	Biela Orava	Váh	non-significant or no trend	non-significant or no trend	no
Oravská Jasenica	Veselianka	Váh	non-significant or no trend	non-significant or no trend	no
Zubrohlava	Polhoranka	Váh	non-significant or no trend	non-significant or no trend	no
Trstená	Oravica	Váh	non-significant or no trend	non-significant or no trend	no
Martin	Turiec	Váh	non-significant or no trend	non-significant or no trend	no
Čadca	Kysuca	Váh	non-significant or no trend	non-significant or no trend	no
Poluvsie	Rajčianka	Váh	non-significant or no trend	non-significant or no trend	no
Bytča	Petrovička	Váh	non-significant or no trend	increasing trend	yes
Výdrná	Petrinovec	Váh	non-significant or no trend	non-significant or no trend	no
Dohňany	Biela voda	Váh	non-significant or no trend	decreasing trend	yes
Horné Slnie	Vlára	Váh	non-significant or no trend	non-significant or no trend	no
Zlatno	Hron	Hron	non-significant or no trend	non-significant or no trend	no
Brezno	Hron	Hron	non-significant or no trend	non-significant or no trend	no
Hronec	Čierny Hron	Hron	decreasing trend	decreasing trend	no
Bystrá	Bystrianka	Hron	decreasing trend	decreasing trend	no
Mýto p. Ďumbierom	Štiavnička	Hron	decreasing trend	non-significant or no trend	yes
Dolná Lehota	Vajskovský potok	Hron	non-significant or no trend	non-significant or no trend	no
Brehy	Hron	Hron	decreasing trend	non-significant or no trend	yes
Holiša	Ipeľ	Ipeľ	decreasing trend	non-significant or no trend	yes
Plášťovce	Krupinica	Ipeľ	non-significant or no trend	non-significant or no trend	no
Plášťovce	Litava	Ipeľ	non-significant or no trend	non-significant or no trend	no
Lučenec	Krivánsky p.	Ipeľ	decreasing trend	decreasing trend	no
Dobšiná	Dobšinský potok	Slaná	non-significant or no trend	non-significant or no trend	no
Štítnik	Štítnik	Slaná	decreasing trend	non-significant or no trend	yes
Lenartovce	Slaná	Slaná	nevýznamný alebo žiadny trend	non-significant or no trend	no
Lehota nad Rimavicou	Rimavica	Slaná	decreasing trend	decreasing trend	no
Nížny Medzev	Bodva	Bodva	non-significant or no trend	non-significant or no trend	no
Stratená	Hnilec	Hornád	decreasing trend	non-significant or no trend	yes
Jaklovce	Hnilec	Hornád	non-significant or no trend	non-significant or no trend	no
Košické Oľšany	Torysa	Hornád	non-significant or no trend	non-significant or no trend	no
Ždaňa	Hornád	Hornád	non-significant or no trend	non-significant or no trend	no
Koškovce	Laborec	Bodrog	non-significant or no trend	non-significant or no trend	no
Lekárovice	Uh	Bodrog	non-significant or no trend	non-significant or no trend	no
Remetské Hámre	Okna	Bodrog	non-significant or no trend	non-significant or no trend	no
Veľké Kapušany	Latorica	Bodrog	non-significant or no trend	non-significant or no trend	no
Hanušovce nad Topľou	Topľa	Bodrog	non-significant or no trend	non-significant or no trend	no
Svidník	Ondava	Bodrog	non-significant or no trend	non-significant or no trend	no
Jasenovce	Olka	Bodrog	increasing trend	increasing trend	no
Streda nad Bodrogom	Bodrog	Bodrog	non-significant or no trend	non-significant or no trend	no
Ždiar, Podspády	Javorinka	Poprad	non-significant or no trend	non-significant or no trend	no
Poprad, Matejovce	Slavkovský potok	Poprad	non-significant or no trend	non-significant or no trend	no
Chmelnica	Poprad	Poprad	non-significant or no trend	non-significant or no trend	no

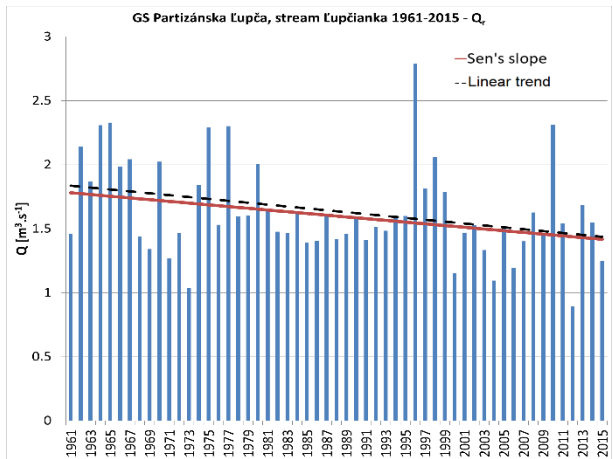
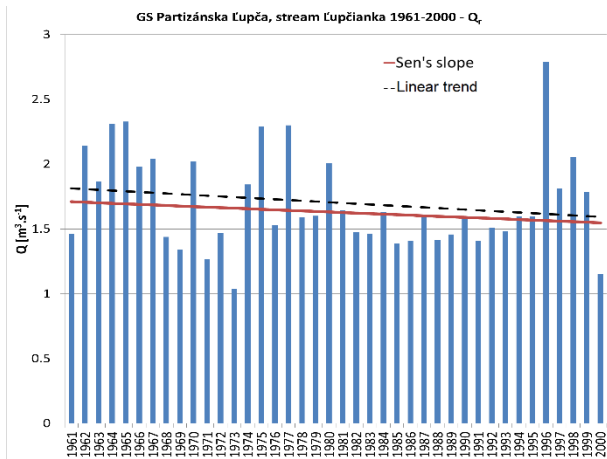
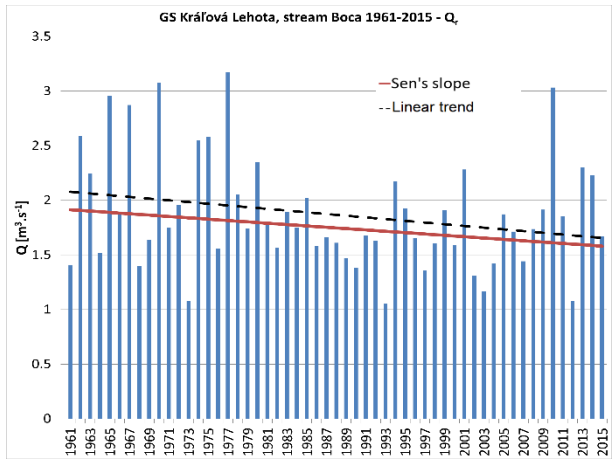
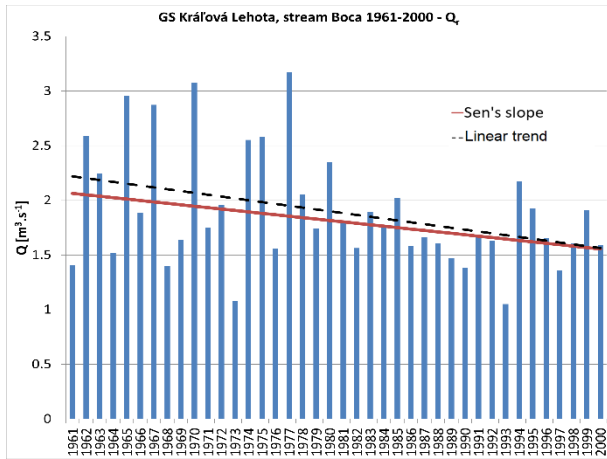
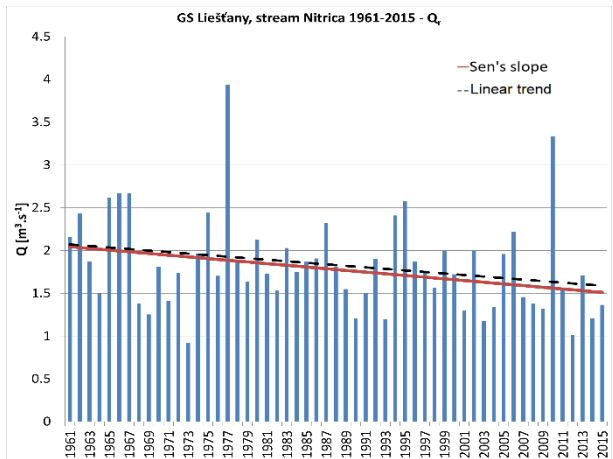
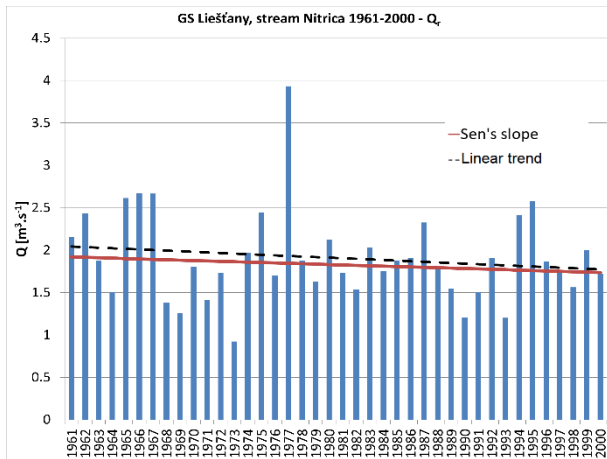
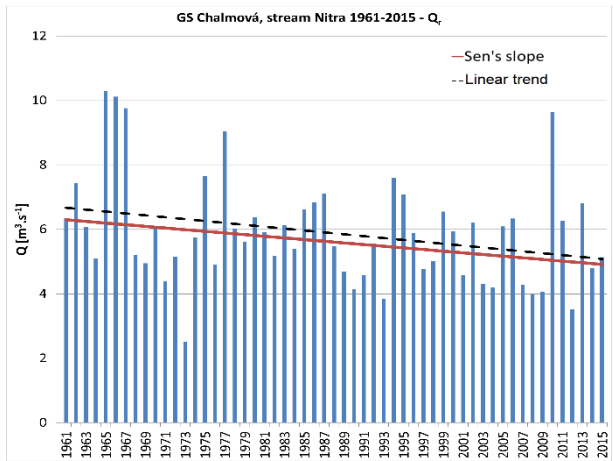
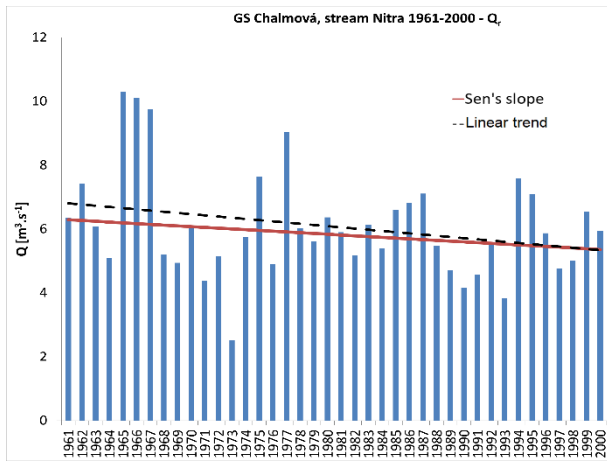
due to the occurrence of an extremely low discharge in 1968, to which the linear trend responds. In gauge station Zubrohlava, Polhoranka stream in period 1961–2000 is a similar case as in gauge station Partizánska Ľupča, however, the difference in slopes is due to the occurrence of an extremely high discharge in 1964. In gauge station Poluvsie, Rajčianka stream, the decreasing insignificant trend of the period 1961–2000 changed to decreasing significant trend after adding 15 years. We can see in both periods the variation in the magnitude of the slopes. This

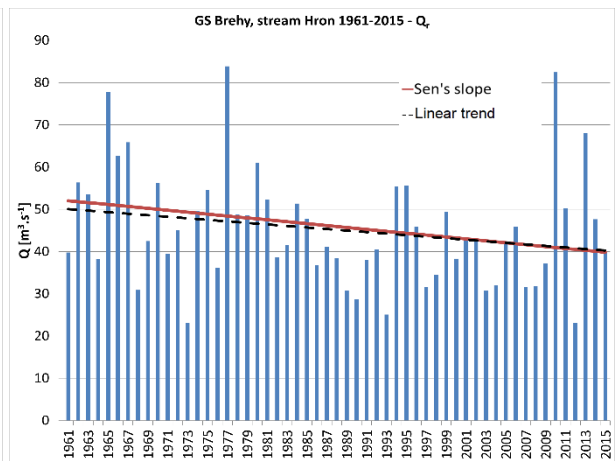
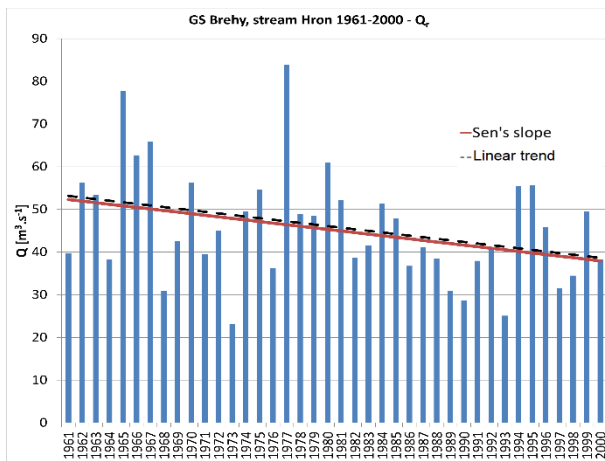
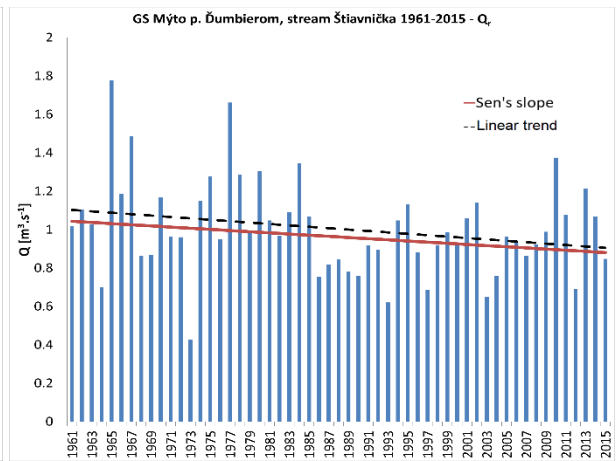
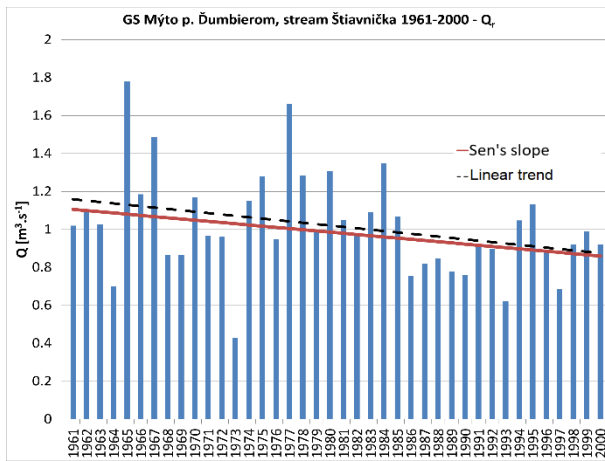
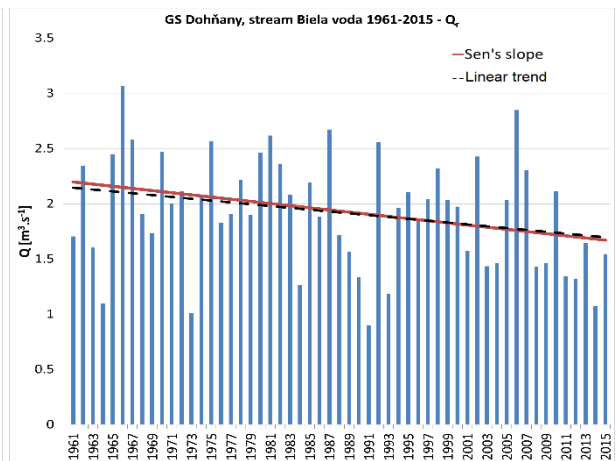
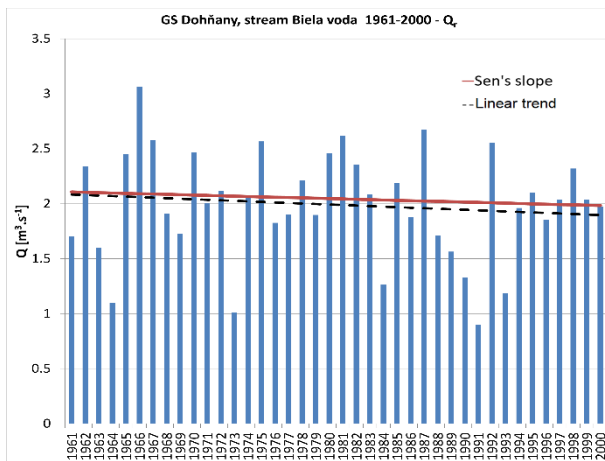
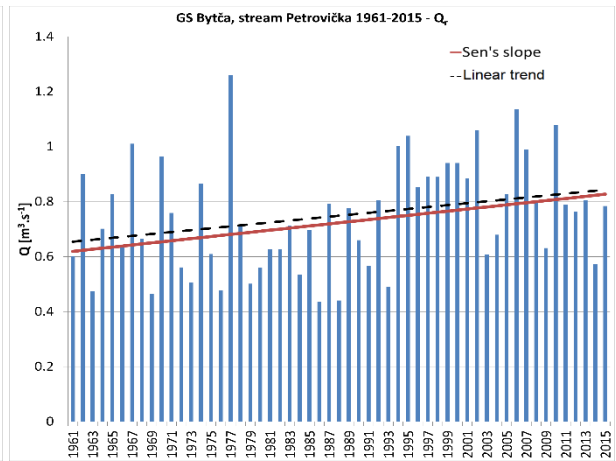
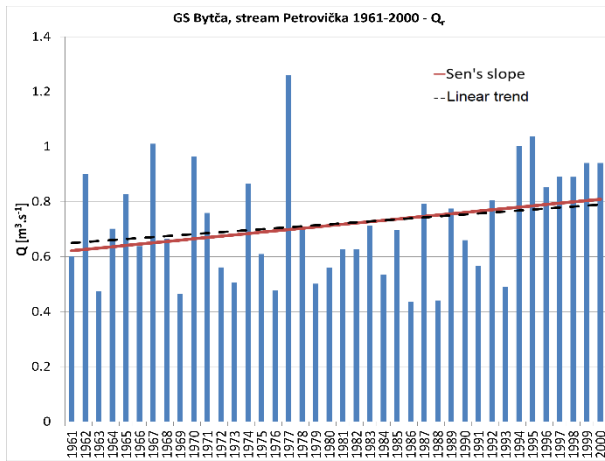
is due to the occurrence of extremely high discharge in 1966.

**Average annual discharges ( $Q_r$ )**

For the period 1961–2000 there was at the 95% significance level 1 gauge station with increasing trend, 12 gauge stations with decreasing trends, and 52 gauge stations with non-significant trends. In the 1961–2015 period there were at the 95% significance level 2 gauge







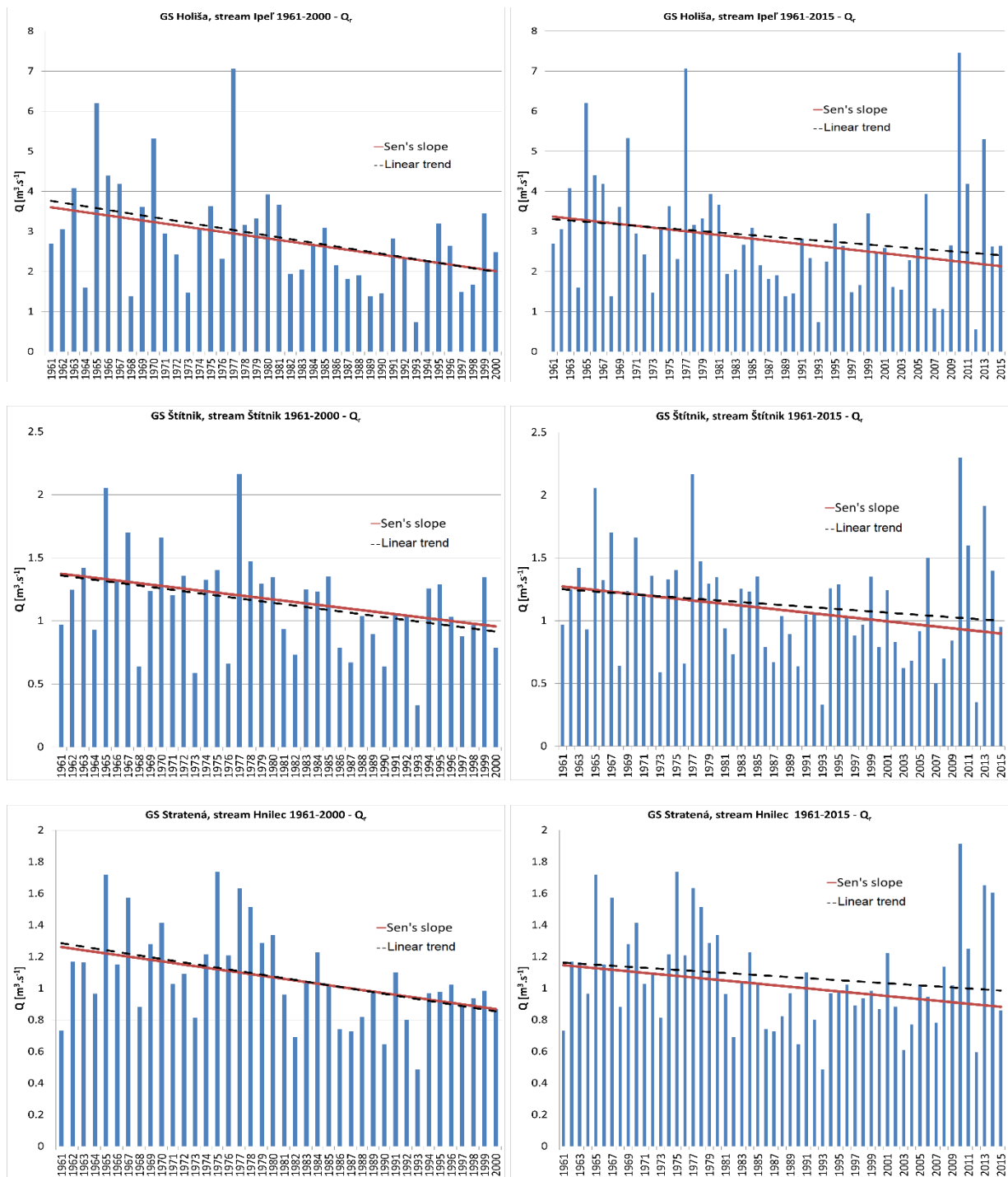


Fig. 2. Magnitude of trends in average annual discharges ( $Q_r$ ) at selected gauging stations (GS) for the period 1961–2000 and 1961–2015.

stations with increasing trends, 13 gauge stations with decreasing trends, and 50 gauge stations with non-significant trends or no trends (Table 2).

The change in trend significance after adding 15 years occurred in 14 gauge stations. The most significant and most cases of changes in the trends of average discharges in the compared periods were calculated for the Nitra and Váh river basin (table 2).

More significant variation in the magnitude of the slopes was observed in gauge station Chalmová, Nitra River in period 1961–2000, the linear trend has more steepness compared to Sen's slope, this is due to the occurrence of extremely high discharges in 1965 and 1966.

In gauge station Kráľová Lehota, Boca stream, the difference in trend magnitude occurred in both periods, the difference is due to the occurrence of high

discharges in 1965 and 1967.

Gauge station Stratena, Hnilec stream recorded more significant differences in slopes in the period 1961–2015. These are due to the occurrence of high discharges in 2013 and 2014 (Fig. 2).

## Discussion

In this paper, we used a non-parametric method to assess the significance of trends and used the chosen significance to determine the trends, in which the magnitude of the slopes were later analysed using the Sen's slope method and the common linear trend method.

The initial significance analysis of the individual trends for the period 1960–2000 determined the number of water gauging stations of interest in which we founded a trend that satisfies the condition of 95% significance level, the remaining trends that occurred at a lower level we consider as insignificant. After adding 15 years to the time series, we again determined the significance of the trends at the same water gauging stations (GS). The change in significance that occurred at the gauging stations indicates to us the occurrence of discharges (low or high) that affect the trend at a given gauging station only at these selected gauging stations we observed the change in trend magnitude using the Sen's slope and linear trend.

In this way, we attempted to speed up the trend analysis, we did not analyse the magnitudes of all trends (using Sen's slope and linear trend) that are located in each water gauging station (which can be a time consuming task with a larger number of GS), but only in those GS where a change in significance occurred. Finally, we included 11 GS at minimum annual flows and 14 GS at average annual flows in the final trend analysis from a total of 65 water gauging stations.

For the individual charts (Fig. 1 and Fig. 2), we were interested in the difference in the magnitude of the Sen's slope and linear trend. This difference was not very pronounced at most gauging stations, however, we recommend using the Sen's slope in addition to the simple linear trend because it is less sensitive to the occurrence of outliers that occur at the end or beginning of the time series. If there are these two trends magnitudes different, we know that an outlier discharge has occurred at the gauging station.

## Conclusion

The aim of the present work was to evaluate the trends for the period 1961–2000 in terms of significance and magnitude at selected water gauging stations and their possible change after the addition of 15 years. In both periods, non-significant trends prevail over significant trends in both minimum and average annual discharges, despite the occurrence of two extreme years. The year 2010, which is considered to be an abnormally wet year, and the year 2012, which is considered to be an abnormally dry year in the added period 2001–2015. In the sub-basins, the change in significance in the mini-

um annual discharges was mainly in the Váh river basin. In the upper part of the basin, the trends change from significantly decreasing to insignificant, which is due to the higher occurrence of higher minimum discharges in the added period 2001–2015, and conversely in the middle part of the basin, the trends change mainly from insignificant to significantly decreasing, which is due to the higher occurrence of low minimum discharges. In the other basins, the significance of trends did not change at most stations after the 15-year period was added.

In the sub-basins, the change in significance of the mean annual discharges was most pronounced in the upper Nitra basin. Trends change from non-significant to significant decreasing, indicating a greater occurrence of lower flows in the period 2001–2015. In the other basins, the significance of the trends did not change at most stations after the addition of 15 years.

The significance of the trends did not change significantly in either minimum or average annual flows over the entire country with the addition of 15 years, indicating that a large number of low or high annual discharges did not occur in most of the selected gauge stations. The magnitude of the trend slope, both linear and Sen's slope, are also very similar at most stations (where there has been a change in significance), indicating that there are not such extreme low or high discharges in the added time series 2001–2015 that would cause them to be potentially different. In general, the trends in both minimum and average annual flows over the assessment periods can be considered to be balanced to slightly decreasing across the whole of the country.

To assess and better understand the evolution of water bearing is in addition to hydrological characteristic necessary assessment climatological characteristics, in particular air temperature and evaporation.

## References

- Adámyová, S. (1989): Dlhodobé ročné prietoky, ich územná a časové premenlivosť. Zborník SHMÚ 29/II, s. 30.
- Báčová Mitková, V., Halmová, D. (2021): Statistical Analysis and Trend Detection of the Hydrological Extremes in the Váh River at Liptovský Mikuláš. In *Acta Horticulturae et Regiotechnicae: The Scientific Journal for Horticulture, Landscape Engineering and Architecture*, 2021, vol. 24, issue s1: Special Issue, 80–89. ISSN 1338-5259.
- Dabanlı, İ., Şen, Z., Yeleğen, M. Ö. et al. (2016): Trend Assessment by the Innovative-Şen Method. *Water Resour Manage* 30, 5193–5203.
- Drápela, K., Drápelová, I. (2011): Application of Mann-Kendall test and the Sen's slope estimates for trend detection in deposition data from Bílý Kříž (Beskydy Mts., the Czech Republic) 1997–2010. *Beskydy*, 2011, 4 (2): 133–146. Mendelova univerzita v Brně. ISSN: 1803-2451.
- Hydrology. Terminological glossary. (2002): Bratislava: MŽP SR, 2002. 157 s. ISSN 1335-1564.
- Malik, A., Kumar, A., Ahmed, A. N., Fai, Ch. M., Afan, H. A., Sefelnasr, A., Sherif, M., El-Shafie, A. (2020): Application of non-parametric approaches to identify trend in streamflow during 1976–2007 (Naula watershed),

- Alexandria Engineering Journal, Volume 59, Issue 3, 2020, 1595–1606, ISSN 1110-0168.
- Santos, J., Portela, M. (2007): Monitoring of monthly and annual series of precipitation (in Portugal), Portugal: Department of Engineering, 1–11.
- Sen, P. K. (1968): Estimates of the regression coefficient based on Kendall's tau. *Journal of the American Statistical Association*, 63: 1379–1389.
- World Meteorological Organization (WMO) (2008). Guide to Hydrological Practices No 1211/168 on hydrology – from measurement to hydrological information. Volume I., Switzerland. 9–10.
- Zeleňáková, M., Soľáková, T., Purcz, P., Kuzevičová, Ž. Demeterová, B. (2011): Hydrologické sucho na východnom Slovensku. In: Konferencia „Manažment povodí a povodňových rizík“, Častá-Papiernička. 8s.

Ing. Viliam Šimor, PhD. (\*corresponding author, e-mail: viliam.simor@shmu.sk)  
Ing. Ľudovít Ľupták  
Slovak Hydrometeorological Institute  
Jeséniova 17  
833 15 Bratislava  
Slovak Republic

## Hydrological analysis of the Danube regime on the section through the Republic of Croatia and the Republic of Serbia

Marija ŠPERAC\*, Ivan DJEDOVIĆ

The flow regime of the Danube in the area of the middle part of the basin, on the section of the Danube through Croatia and Serbia, was analyzed. This paper contains a hydrological analysis of the Danube regime using measured flow data at four regression stations; Batina in the Republic of Croatia, and the regression stations Bezdán, Bogojevo and Smederevo in the Republic of Serbia for the period 1992–2018. On this section, two large rivers, the Drava and the Sava, flow into the Danube, which significantly affect the Danube regime. Parde's method of modular coefficients was used to classify the flow regime. Comparing the curves of mean monthly flows expressed through modular coefficients for the Danube, Drava and Sava, it can be concluded that the Danube has an alpine snow regime at the top of the analyzed section, just like the Drava that flows into the Danube. At the regression station Smederevo, the curve of mean monthly flows expressed in modular coefficients is similar to the curve for the Sava, which flows into the Danube upstream from Smederevo, and the Danube has a combined flow regime like the Sava.

KEY WORDS: flow regime, modular coefficients, „central Danube region”

### Introduction

The Danube is the second longest and water richest river in Europe, with a length of 2 857 km and a catchment area of 817 000 km<sup>2</sup>. (Fig. 1.) The Central Danube Region is an imposing and unique geographical entity in Europe. It is bounded by Carpathian sand, part of the Balkan Mountains in the north and east, near the Alps in the west and the Dinarides in the south. This closed circle of mountains includes the "Pannonian Basin

System", which consists of the south-eastern and Slovak lands, the Lesser and Great Hungarian Plain, the Transylvanian Basin, the Slavonian Middle Range, the Sava Basin and part of the Great Morava Basin. (Schiller et al., 2010).

With its middle part, the Danube flows through Croatia and Serbia and represents the border between these countries. In this part of the Danube basin, the Danube flows along the Kopački rit swamp, and two large rivers, the Drava and the Sava, flow into it, which significantly



Fig. 1. Danube River basin.

affects the Danube flow regime itself. The surface area of the Danube basin in Croatia is 35 101 km<sup>2</sup>, which represents 62% of the Croatian mainland. (Croatian River Basin Management, CRBM 2016–2021).

When analyzing the flow regimes of rivers, including the Danube, special attention should be paid to hydrological extremes: floods (Prohaska and Iličić, 2009; Hattermann et al., 2018) and droughts (Koleva, 1995;

Stojanovic et al., 2017). analysis of the Danube flow regime (in Slovakia) through the period from 1840 to 2015 was presented by Pekarova et al. (2019). Romanova et al. (2019). investigated natural and anthropogenic impacts on the course of the Danube in the area from Reni to Izmail. Changes in the flow regimes of rivers due to changes in climatic elements in Europe are primarily related to the way rivers are supplied, ie the type of their recharge. (Čanjevac, 2012) At the national level (and level of large regions of Croatia), certain climatic changes have already been recorded, and their influence on changes in the water balance observed (Bonacci and Gereš, 2001; Pandžić et al., 2009) or their influence on changes of the discharge regime (Gajić-Čapka and Cesarec, 2010; Čanjevac, 2012; Barbalić and Kuspilić, 2014; Čanjevac and Orešić, 2015; 2018). Changes to discharge on the Sava River were examined by Bonacci and Ljubenkov (2004), Šegota and Filipčić (2007), Trninić and Bošnjak (2009), Bonacci and Oskoruš (2011) and Orešić et al. (2017), while changes on the Drava River by Bonacci and Oskoruš (2010) and Gajić-Čapka and Cesarec (2010).

This paper contains a hydrological analysis of the Danube regime using measured flow data at four regression stations; regression station Batina in the Republic of Croatia, and the regression stations Bezdan, Bogojevo and Smederevo in the Republic of Serbia for the period 1992–2018.

## Material and methods

The paper analyzes databases on measured flows at regression stations Batina, Bezdan, Bogojevo and Smederevo. Due to the insufficient length of the series of available data for the regression station Batina, it was performed correlation analysis between that regression station and the closest one in the Republic of Serbia – regression station Bezdan. How is it analysis determined extremely strong correlation ratio (correlation coefficient is 0.998), flow analysis was performed for the regression station Bezdan, the results of which can be considered representative for the regression station Batina as well Republic of Croatia. Based on the data on mean daily flows, the minimum, mean and maximum annual flows were obtained. Statistical processing of data constructed flow duration curves and frequency histograms for the average daily flows of the Danube River for the regression stations Bezdan (Batina), Bogojevo and Smederevo, and additionally singled out characteristic curves for the dry, normal and wet years recorded for the given series 1992–2018. The flow regime classification is defined according to Parde's modulus coefficients. The flows expressed in modular coefficients

are suitable for comparing individual hydrological features at different hydrological stations. The hydrological analysis of the seasons was performed, ie the flow tendencies for the warm and cold seasons for the observed period were shown.

## Results

By processing the database on mean daily flows, the following results were obtained: for the regression stations Bezdan (Batina) the lowest mean daily flow of 742 m<sup>3</sup> s<sup>-1</sup> was recorded in October 1992, and the largest of 8 380 m<sup>3</sup> s<sup>-1</sup> in June 2013. A slight upward trend is visible minimum and medium annual flows, while for maximum the trend is negative. (Fig. 2)

For the regression station Bogojevo, the lowest mean daily flow of 926 m<sup>3</sup> s<sup>-1</sup> was recorded in September 2003, and the largest of 8700 m<sup>3</sup> s<sup>-1</sup> in June 2013. There is a considerable upward trend in the minimum and mean annual flows, while for maximum annual flows the upward trend is slightly negative. (Fig. 3)

For the regression station Smederevo, the lowest mean daily flow of 1400 m<sup>3</sup> s<sup>-1</sup> was recorded in September 2003, and the highest of 14800 m<sup>3</sup> s<sup>-1</sup> in April 2006. At the minimum annual flows for this regression station, a strong positive trend is visible. A very slight upward trend is visible for medium annual flows, and a slight decrease for maximum annual flows. (Fig. 4)

Correlation analysis of mean flows (Table 1) confirmed the strong dependence between regression stations Batina and Bezdan (located opposite each other), and Bezdan and Bogojevo, which means that on the section Batina – Bogojevo flow regime does not change, while the results of correlation analysis for regression stations Bogojevo and Smederevo showed that there is almost no correlation between them – which indicates the fact that the flow regime changes significantly.

## Flow duration curves expressed by Parde modular coefficients

Various methods are used in the literature to classify the flow regime of fluids. One of the better known classifications is the classification made by the French geographer hydrologist Maurice Pardé. Pardé introduced a modular coefficient that represents the ratio between two quantities of a given period and the corresponding average (Pardé, 1933). In practice, the values of mean monthly and annual flows are most often used in these comparisons.

It is obtained by dividing the mean flow of each month by the mean annual flow. Pardé's simple formula makes it possible to compare the flow regimes of rivers of different flows.

Modular coefficient ( *Mk* ) formula:

$$Mk = \frac{MQ - \text{The average flow of an individual month}}{MQ - \text{mean annual flow}} \quad (1)$$

On the basis of modular coefficients, ie flow regimes obtained by such an approach, Pardé divided all fluids

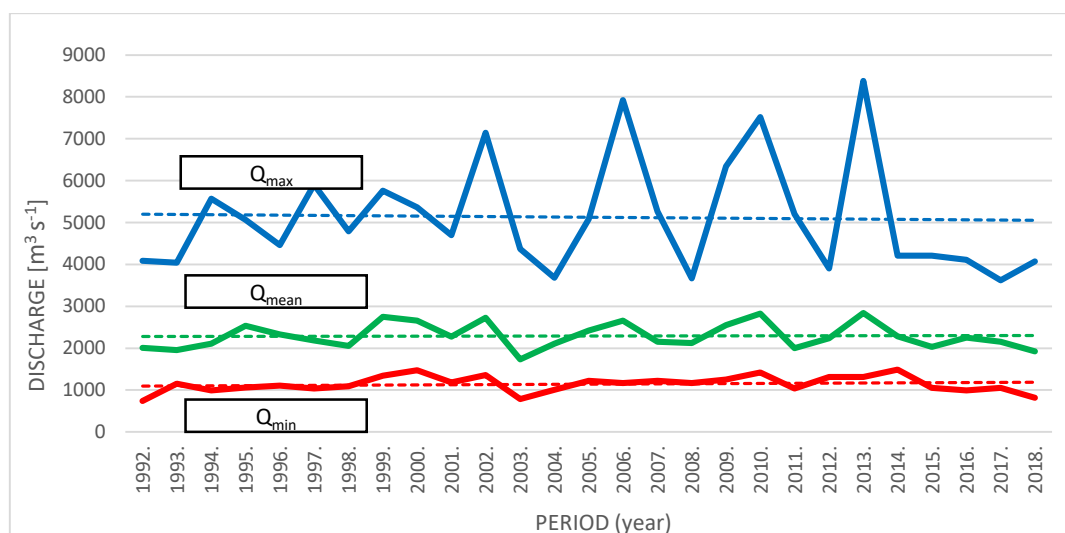


Fig. 2. Annual mean minimum, mean and maximum flows for the period 1992–2018 (regression stations Batina/Bezdan).

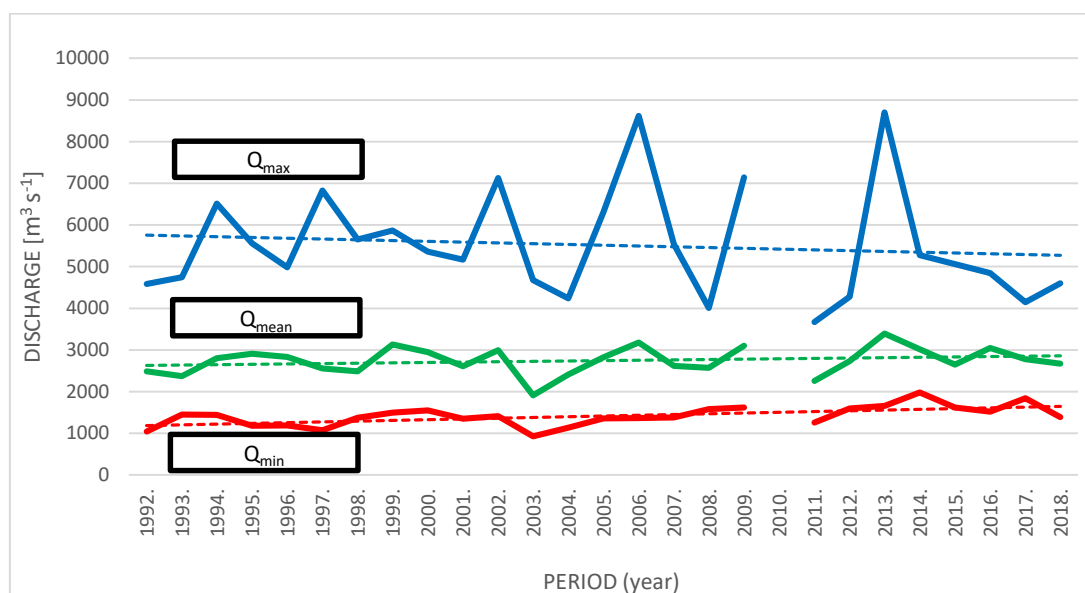


Fig. 3. Annual mean minimum, mean and maximum flows for the period 1992–2018 (regression station Bogojevo).

Table 1. Flow correlation coefficients between measuring stations

Regression Statistics	Batina – Bezdan	Bezdan – Bogojevo	Bogojevo – Smederevo
Multiple R	<b>0.997983378</b>	<b>0.968586032</b>	<b>0.118338021</b>
R Square	0.995970822	0.938158902	0.014003887
Adjusted R Square	0.995913263	0.937959415	0.010240543
Standard Error	57.94458563	216.1527741	1458.720637
Observations	72	312	264

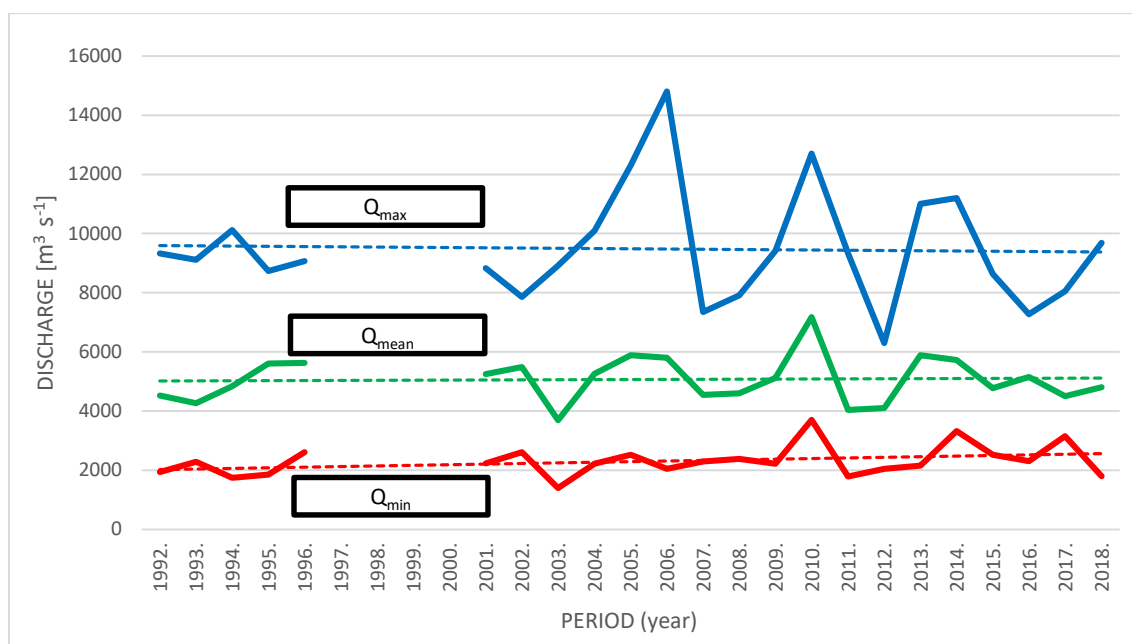


Fig. 4. Annual mean minimum, mean and maximum flows for the period 1992–2018 (regression station Smederevo).

into those with simple and those with complex regimes. "S. Ilešić (1947) used Pardé's coefficients for the sixteen-year period 1923–1938 when researching and determining the typology of Yugoslav fluids and determined the existence of the following types in Croatia:

- snow regime
  - mild (Drava)
  - transitional (Mura)
- rain-snow regime
  - transitional Central European or Posavina variant (Sutla, Sava downstream from Zagreb)
  - moderately Mediterranean variant (Kupa)
  - Mediterranean variant (Neretva, Cetina, Krka, Zrmanja and Rječina)
- clean or almost clean rain regime (Čazma and Istrian rivers)
- combined-complex regime (Danube)." (Čanjevac 2012)

Their importance comes to the fore when it comes to comparing a certain hydrological quantity on the same river, in the same time period, but in different profiles, or when comparing these same quantities, but for different watercourses.

If a certain similarity is established in the forms of flow duration curves in modular coefficients for individual watercourses, it is possible to define the flow duration curve by interpolation between two profiles with similar duration curves.

In the further part of this chapter, the flow duration curves for the regression stations Bezdan (Batina) (Fig. 5), Bogojevo (Fig. 6) and Smederevo (Fig. 7) for the period 1992–2018 are attached year, with the proviso that when grouping their data, the flow class interval was

250 m<sup>3</sup> s<sup>-1</sup>. The characteristic curves for the dry, normal and wet years recorded for the given series 1992–2018 are separated.

The analysis of mean monthly flows expressed in Parde's modular coefficients shows that the Danube at the regression stations Batina (Bezdan) and Bogojevo has an alpine snow regime. The primary maximum occurs in May and June, when the values of modular coefficients are from 1.25 to 1.45, while the much less pronounced second maximum occurs in October and November with values of modular coefficients slightly higher than 1. At the regression station Smederevo Danube has a combined complex mode. It is characterized by a complex regime with two annual highs and lows. The first maximum occurs in March or April, when the values of the modular coefficients range from 1.14 to 1.66. The second, mostly more pronounced maximum occurs in December (exceptionally in November), when the modular coefficients range from 1.37 to 2.04. The primary minimum occurs in August and only at a few stations in July, when the values of the modular coefficients range between 0.31 and 0.74. The second, less pronounced minimum occurs regularly in February with coefficient values from 0.78 to 1.31. Insight into the graphs of mean monthly flows expressed in modular coefficients for the Danube (Fig. 8) and the Drava (regression station Terezino polje) and Sava (regression station Županja stepenica) (Fig. 9) (Čanjevac and Orešić, 2018), rivers flowing into the Danube, a similar shape of curves is visible for the Drava and Danube at the stations Batina and Bogojevo, while similar graphs for the Sava and Smederevo. These similarities indicate the strong influences of the Drava and Sava rivers on the changes in the flow regime of the Danube.

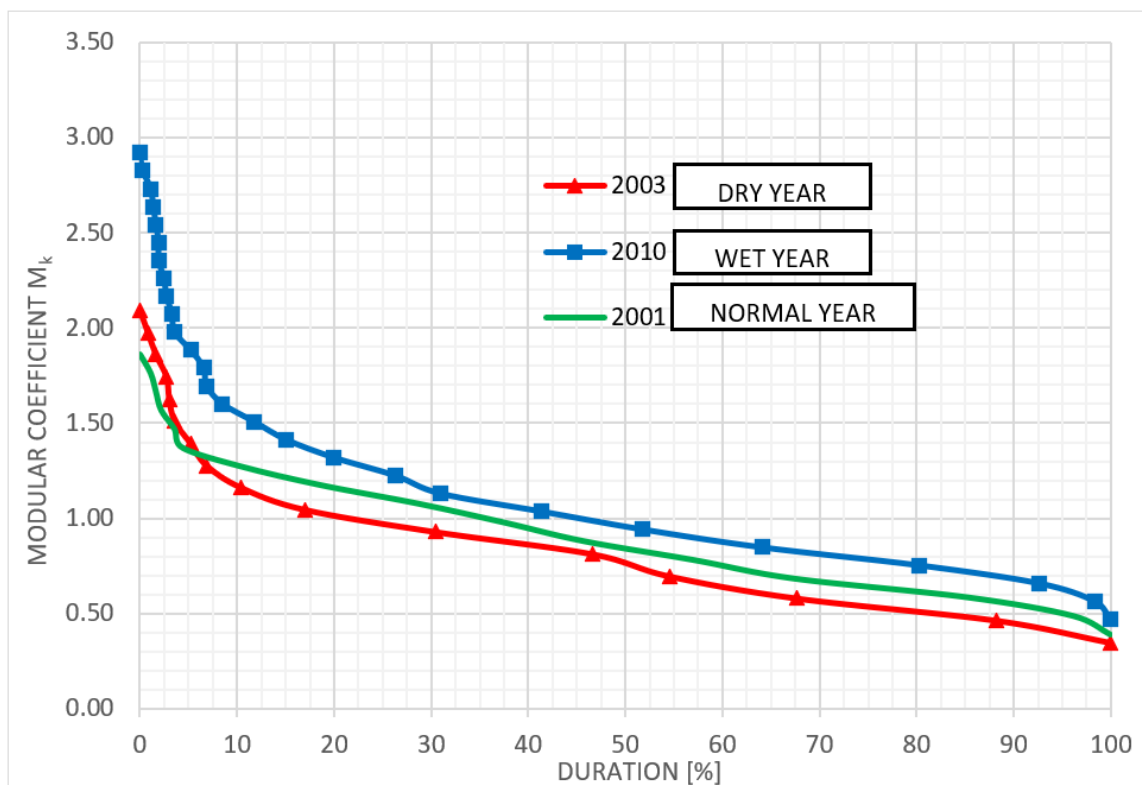


Fig. 5. Characteristic flow duration curves for the Danube River represented in modular coefficients (regression stations Batina/Bezdan).

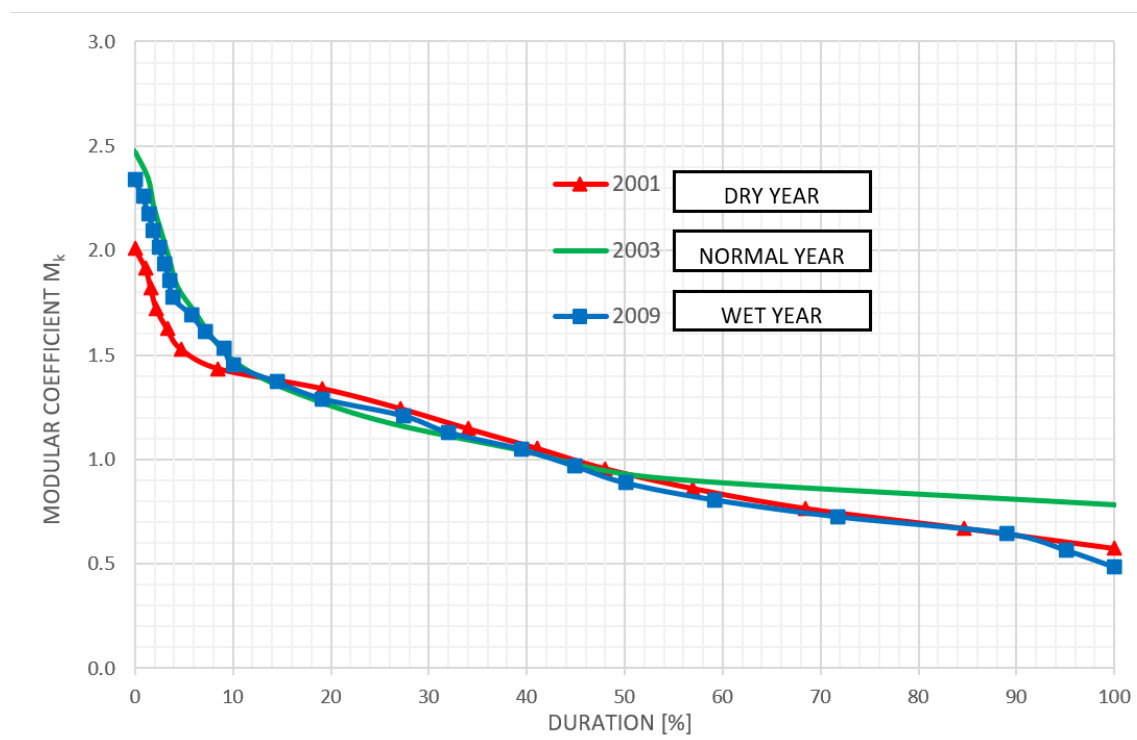


Fig. 6. Characteristic flow duration curves for the Danube River represented in modular coefficients (regression station Bogojevo).

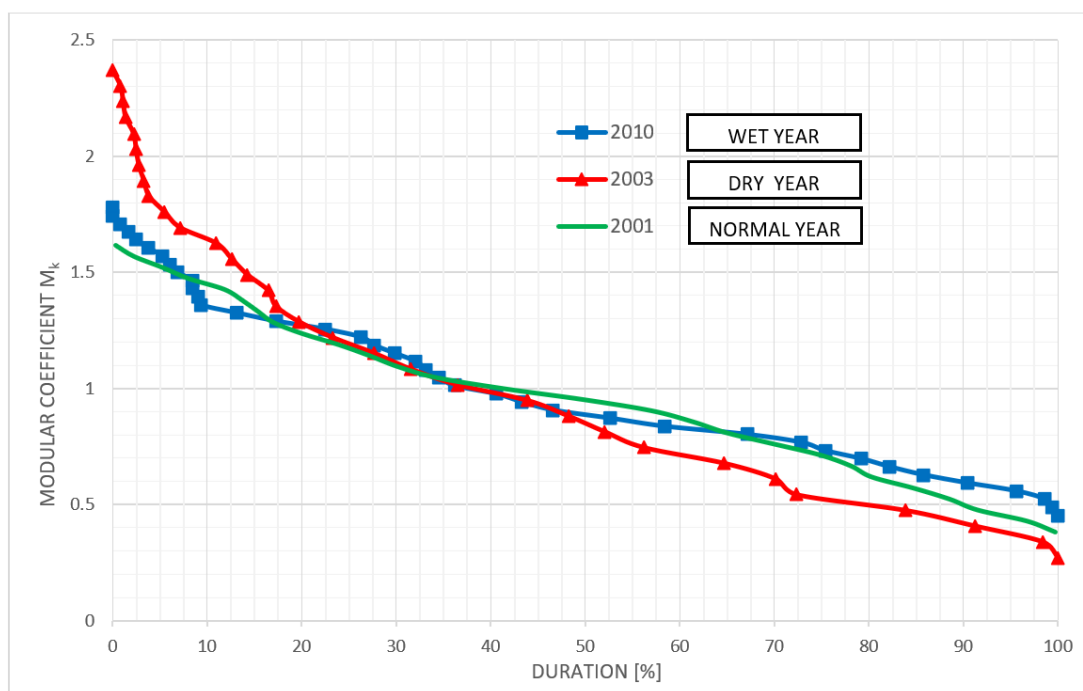


Fig. 7. Characteristic flow duration curves for the Danube River represented in modular coefficients (regression station Smederevo).

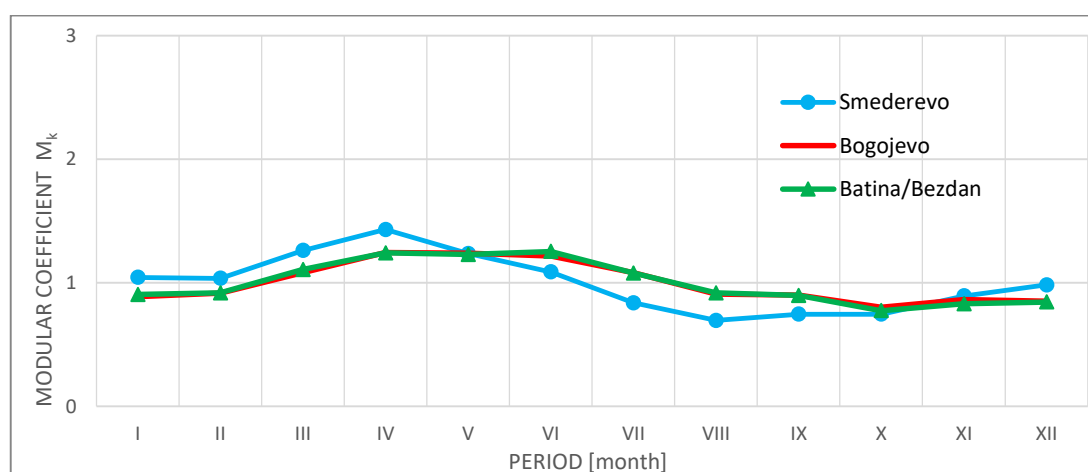


Fig. 8. Mean monthly flows represented in modular coefficients for the Danube River (regression stations Batina/Bezdan, Bogojevo and Smederevo).

#### Analysis of hydrological seasons

In order to better manage water resources, it is necessary to find such a solution that they are used rationally, conscientiously, environmentally and ultimately – economically. Analysis of hydrological seasons is an important basis for water resources management. The analysis of multi-year mean monthly flows on the observed section revealed two hydrological seasons: the warm season from April to September with higher flows and the cold season from October to March with a negative flow trend. The analysis of the obtained results

for the regression stations Bezdan (Batina) (Fig. 10) shows a slight tendency of increase of mean monthly flows in the cold season as well as a slight trend of decrease of mean monthly flows in the warm season during the observed period. The lowest mean monthly flow of the warm season of  $1562 \text{ m}^3 \text{ s}^{-1}$  was recorded in 2003, and the cold one of  $1700 \text{ m}^3 \text{ s}^{-1}$  was recorded in 1997. The mean monthly flow of the warm season is  $3016 \text{ m}^3 \text{ s}^{-1}$ , and the cold season is  $2471 \text{ m}^3 \text{ s}^{-1}$ . The highest mean monthly flow of the warm season was  $4250 \text{ m}^3 \text{ s}^{-1}$  recorded in 2006, and in the cold season  $3137 \text{ m}^3 \text{ s}^{-1}$  was recorded in 2002.

For the regression station Bogojevo, a significant positive trend of mean monthly flows for the warm and cold seasons during the observed period is observed. (Fig. 11.) The lowest mean monthly flow of the warm season of  $1701 \text{ m}^3 \text{ s}^{-1}$  was recorded in 2003, and the cold season  $2014 \text{ m}^3 \text{ s}^{-1}$  recorded in 1997. The mean monthly flow of the warm season is  $3016 \text{ m}^3 \text{ s}^{-1}$ , and the cold season  $2471 \text{ m}^3 \text{ s}^{-1}$ . The highest mean monthly flow of the warm season was  $4250 \text{ m}^3 \text{ s}^{-1}$  recorded in 2006, and in the cold season  $3137 \text{ m}^3 \text{ s}^{-1}$  recorded in 2002.

For the regression station Smederevo (Fig. 12), the results show a slight increase in mean monthly flows

for both season with the proviso that it should be noted that for the observed series from 1992 to 2018 one is missing data period from 1997 to 2000 so the results for this station should be taken with less dose of reliability. The lowest mean monthly flow of the warm season of  $2893 \text{ m}^3 \text{ s}^{-1}$  was recorded in 2003, and the cold season one of  $3898 \text{ m}^3 \text{ s}^{-1}$  was recorded in 2012. The mean monthly flow of the warm season is  $5103 \text{ m}^3 \text{ s}^{-1}$ , and the cold season  $5041 \text{ m}^3 \text{ s}^{-1}$ . The highest mean monthly flow of the warm season was  $7368 \text{ m}^3 \text{ s}^{-1}$  recorded in 2006, and in the cold season  $7018 \text{ m}^3 \text{ s}^{-1}$  recorded in 2010 (Djedović, 2020).

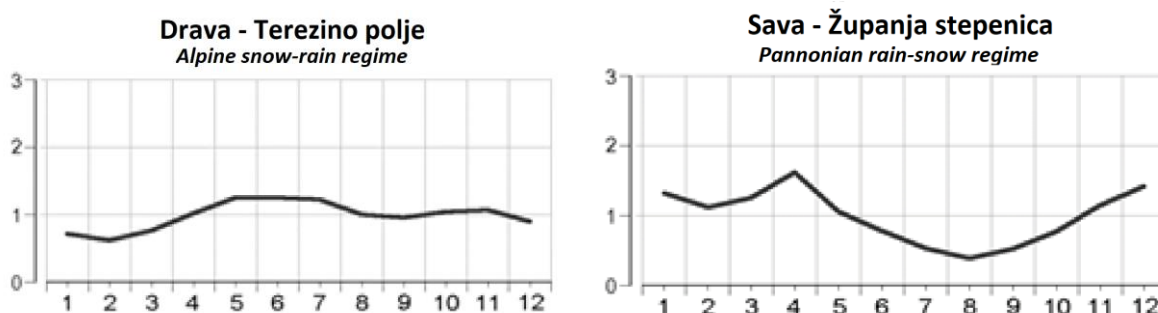


Fig. 9. Mean monthly flows represented in modular coefficients for the Sava River (regression station Županja stepenica) and Drava River (regression station Terezino polje).

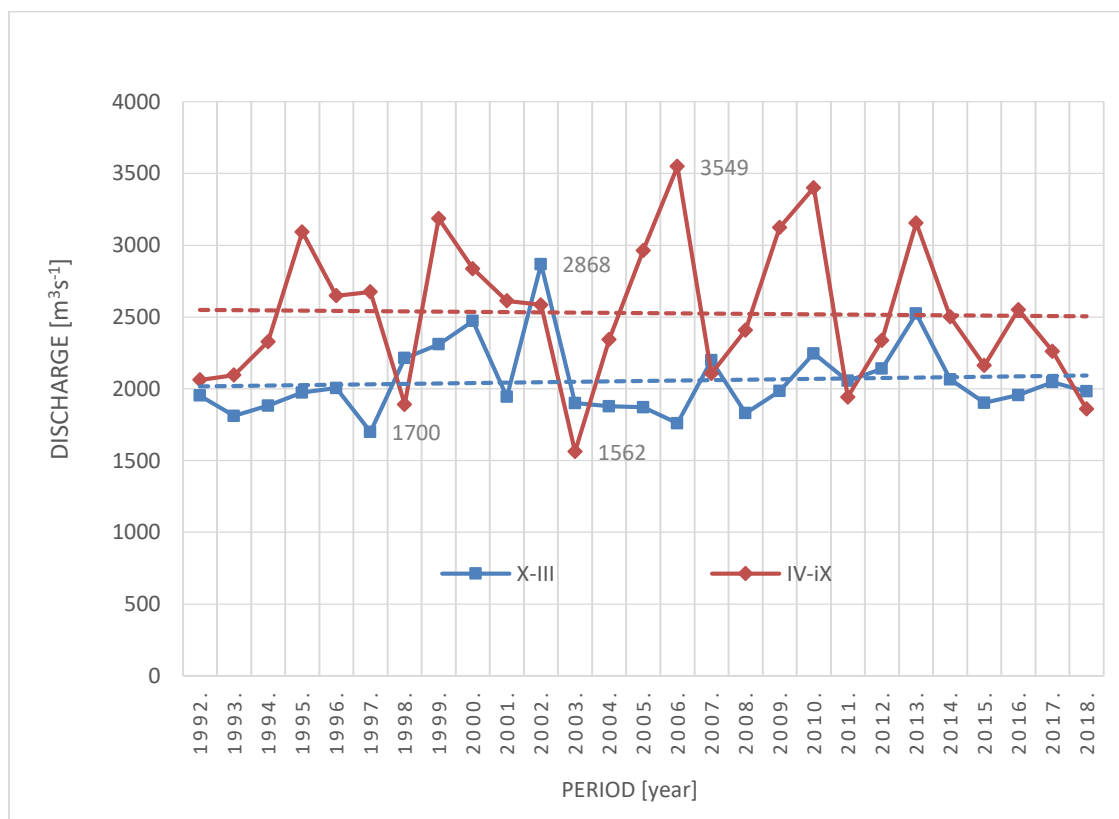


Fig. 10. Mean annual flows during warm (April–September) and cold (October–March) season for the period 1992–2018 ( regression stations Batina/Bezdan).

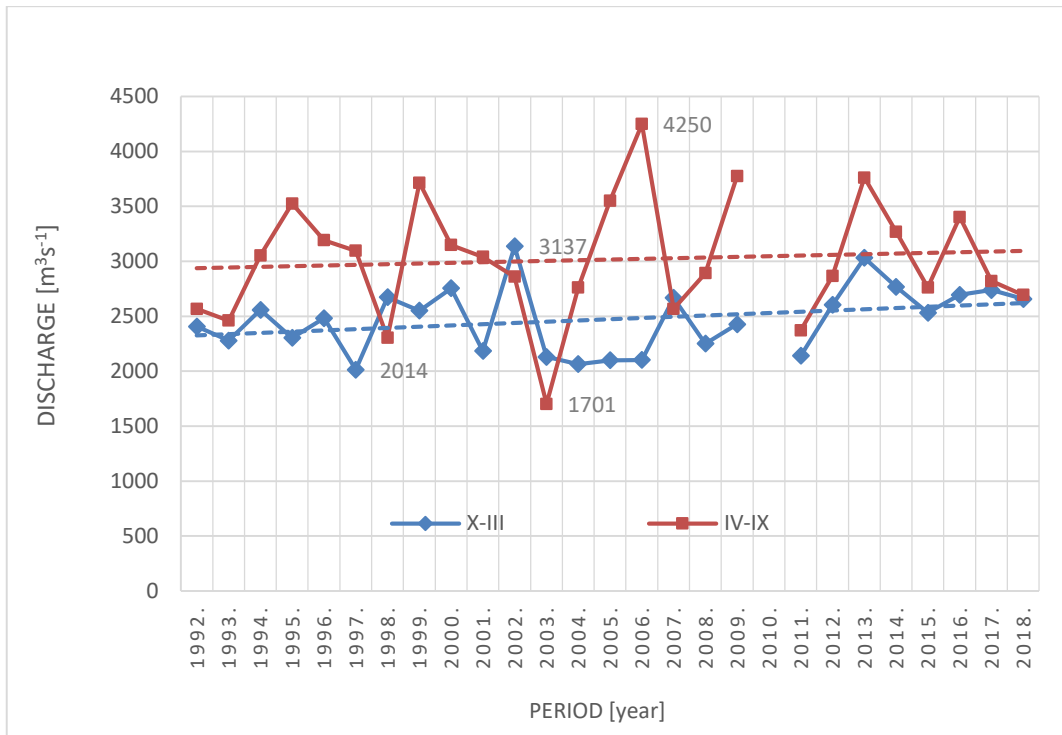


Fig. 11. Mean annual flows during warm (April–September) and cold (October–March) season for the period 1992–2018 (regression station Bogojevo).

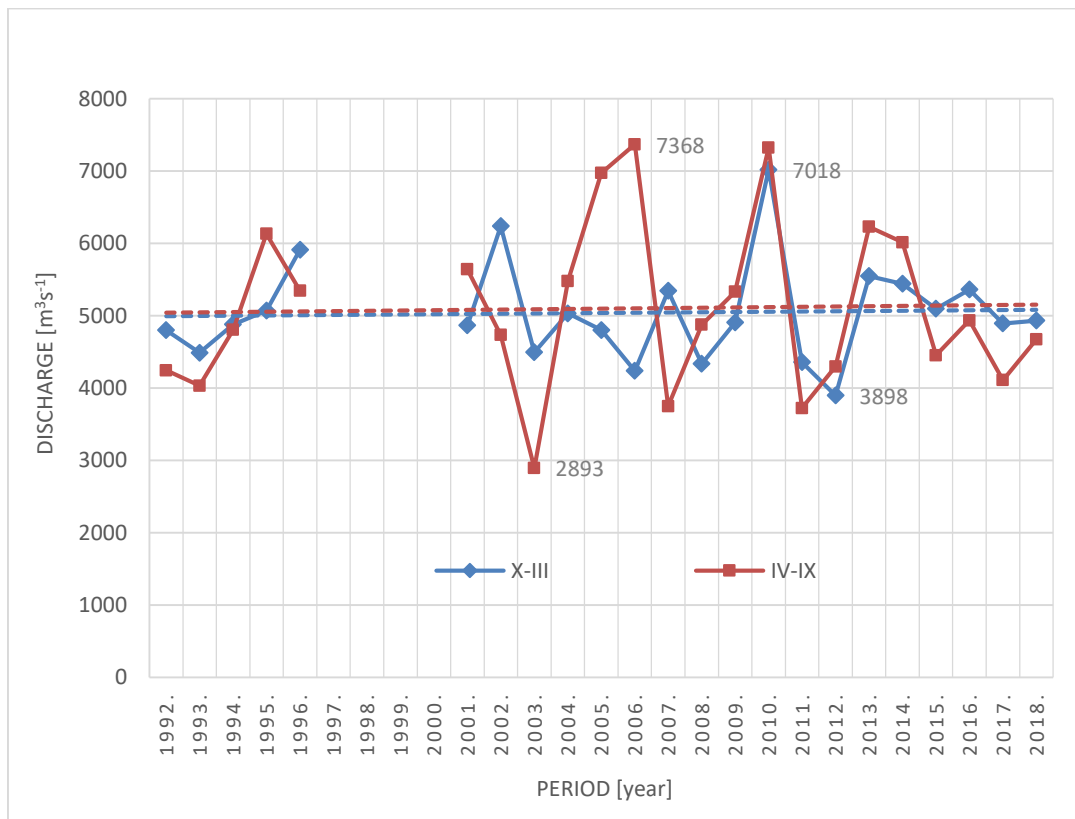


Fig. 12. Mean annual flows during warm (April–September) and cold (October–March) season for period 1992–2018 (regression station Smederevo).

## Conclusion

The regime of the Danube along its entire course is variable, which is a consequence of natural and anthropogenic influences. Analysis of the flow regime of a watercourse, including the Danube, can be analyzed with regard to different parameters and time intervals. Given that the Danube is an international river with a large catchment area, consisting of a large number of countries, and a large number of different tributaries, it is advisable to analyze the flow regimes on certain sections with specific parameters of sections.

On the section of flow through Croatia and Serbia, the Danube River has two flow regimes (according to the Croatian classification of characteristic flow regimes): alpine rain-snow regime (regression stations Batina, Bezdan and Bogojevo) and combined-complex regime at regression station Smederevo. The change in the flow regime of the Danube is a consequence of the confluence of the Sava River with the Danube, which has a Pannonian rain-snow regime.

## References

- Barbalić, D., Kuspilić, N. (2014): Trends of indicators of hydrological alterations. *Građevinar* 66 (7), 613–624.
- Bonacci, O., Gereš, D. (2001): Utjecaj i prilagodba klimatskim promjenama: Hidrologija i vodni resursi. Prvo nacionalno izvješće RH prema Okvirnoj konvenciji UN o promjeni klime (UNFCCC) (ur. Jelavić, V.), RH, Ministarstvo zaštite okoliša i prostornog uređenja, Zagreb, 175–189.
- Bonacci, O., Ljubenkov, I. (2004): Statistička analiza maksimalnih godišnjih protoka Save kod Zagreba u razdoblju 1926–2000. *Hrvatske vode* 12 (48), 243–252.
- Bonacci, O., Oskoruš, D. (2010): The changes of the lower Drava River water level, discharge and suspended sediment regime. *Environmental Earth Sciences* 59 (8), 1661–1670.
- Bonacci, O., Oskoruš, D. (2011): Hidrološka analiza sigurnosti Zagreba od poplave vodama rijeke Save u novim uvjetima. *Hrvatske vode* 19 (75), 13–24.
- Croatian River Basin Management, 2016–2021 (accessed on February 15, 2018, March 10, 2018, April 3, 2018) [http://www.voda.hr/sites/default/files/plan\\_upravljanja\\_vodnim\\_podrucjima\\_2016.\\_-2021.pdf](http://www.voda.hr/sites/default/files/plan_upravljanja_vodnim_podrucjima_2016._-2021.pdf)
- Čanjevac, I. (2012): Changes in Discharge Regimes of Rivers in the Croatian Part of the Danube River Basin, *Hrvatski Geografski Glasnik* 74/1, 61–74.
- Čanjevac, I., Orešić, D. (2015): Contemporary changes of mean annual and seasonal river discharges in Croatia. *Hrvatski geografski glasnik* 77 (1), 7–27.
- Čanjevac, I., Orešić, D. (2018): Changes in discharge regimes of rivers in Croatia. *Acta Geographica Slovenica* 58 (2), 7–18.
- Djedović, I. (2020): Analysis of the Danube river runoff regime through the Republic of Croatia and the Republic of Serbia, J. J. Strossmayer University of Osijek Faculty of Civil Engineering and Architecture Osijek, Croatia, graduate thesis.
- Gajić-Čapka, M., Cesarec, K. (2010): Trend i varijabilnost protoka i klimatskih veličina u slivu rijeke Drave. *Hrvatske vode* 18 (71), 19–30.
- Hattermann, F. F., Wortmann, M., Liersch, S., Toumi, R., Sparks, N., Genillard, C., Schröter, K., Steinhausen, M., Gyalai-Korpos, M., Máté, K., Hayes, B., del Rocio Rivas López, M., Rácz, T., Nielsen, M. R., Kaspersen, P. S., Drews, M. (2018): Simulation of flood hazard and risk in the Danube basin with the Future Danube Model. – *Climate Services*, 12, 14–26
- Koleva, E. (1995): Drought in the Lower Danube. *Drought Network News (1994–2001)*. 21. <https://digitalcommons.unl.edu/droughtnetnews/21>
- Orešić, D., Čanjevac, I., Maradin, M. (2017): Changes in discharge regimes in the middle course of the Sava River in the 1931–2010 period, *Prace Geograficne* 151, 93–119.
- Pandžić, K., Trninić, D., Likso, T., Bošnjak, T. (2009): Long-term variations in water balance components for Croatia. *Theoretical and Applied Climatology* 95 (1–2), 39–51.
- Pardé, M. (1933): *Fleuves et Rivières*. Paris: Armand Colin. 224 p.
- Pekarova, P., Gorbachova, L., Bacová, V., Pekar, J., Miklanek, P. (2019): Statistical Analysis of Hydrological Regime of the Danube River at Ceatal Izmail Station IOP Conf. Ser.: Earth Environ. Sci. 221 012035
- Prohaska, S., Ilić, A. (2009): Coincidence of Flood Flow of the Danube River and Its Tributaries Hydrological Process of Danube River, pages 175–226
- Romanova, Y., Shakirzanova, Z., Ovcharuk, V., Todorova, O., Medvedieva, I., Ivanchenko, A. (2019): Temporal variation of water discharges in the lower course of the Danube River across the area from Reni to Izmail under the influence of natural and anthropogenic factors *ENERGETIKA*. 2019. T. 65. Nr. 2–3. P. 144–160 © Lietuvos mokslų akademija.
- Schiller, H., Miklós, D., Sass, J. (2010): The Danube River and its Basin Physical Characteristics, Water Regime and Water Balance, Hydrological Process of Danube River, pages 25–77.
- Stojanovic, M., Drumond, A., Nieto, R.; Gimeno, L. (2017): Transport Anomalies over the Danube River Basin during Two Drought Events: A Lagrangian Analysis. *Atmosphere* 2017, 8, 193. <https://doi.org/10.3390/atmos8100193>
- Šegota, T., Filipčić, A. (2007): Suvremene promjene klime I smanjenje protoka Save u Zagrebu. *Geoadria* 12 (1), 47–58.
- Trninić, D., Bošnjak, T. (2009): Karakteristični protoci Save kod Zagreba. *Hrvatske vode* 17 (69/70), 257–268.

Associate Professor Marija Šperac, Ph.D.in Civ. Eng.; (\*corresponding author, e-mail: msperac@gfos.hr)  
J. J. Strossmayer University of Osijek  
Faculty of Civil Engineering and Architecture Osijek  
Vladimira Preloga 3  
31000 Osijek  
Croatia

Ivan Djedović, M.CE  
Institut IGH d.d. Regional Centar Osijek  
Drinska 18  
31000 Osijek  
Croatia

## Hydrological situation on Slovak rivers from the point of view of hydrological drought assessment in the period 2011–2020

Zuzana DANÁČOVÁ, Katarína JENEIOVÁ\*, Lotta BLAŠKOVIČOVÁ

In this paper, the occurrence of the area-wide droughts during the years 2011 to 2020 in Slovakia is assessed on the data from 164 water gauging station displayed online on the drought monitoring webpage of Slovak Hydrometeorological Institute and further analysed on 43 selected water-gauging stations. The mean monthly discharges are compared with the long-term mean monthly discharges for the reference period 1961–2000. Trend detection analysis of the mean monthly discharges in period 1961–2020 was concluded by Mann-Kendall trend test. The months of April, June, July, August and October were detected as the months with the highest occurrence of mean monthly discharges below 40% long – term mean monthly discharges for the reference period. The trend analysis of the mean monthly discharges confirmed significant decreasing trend in April, May, June, July and August. These results reinforce the need of continuous monitoring of the mean monthly discharges. Results of the monitoring available online in form of simple graphical output can present a tool for the timely detection of the incoming long-term drought periods with possibility of implementation of appropriate measures.

KEY WORDS: hydrological drought, mean monthly discharge, online monitoring, Mann-Kendal trend test

### Introduction

Due to climate change, the topic of drought and water scarcity is an important issue in water management, including for example water resources for agriculture, various industries and surface water utilization in navigation, fishing, etc.

The runoff regime in Slovak streams is generally characterized by increased runoff in the spring months and minimal flows in the summer-autumn season or in winter for mountain streams. Trend analysis of total annual precipitation at 48 stations in Slovakia for time period from 33 to 119 years (end year 2019) showed no significant changes (Repel et al., 2021). A study for the time period 1981–2013 points to a change in the distribution of precipitation during the year in Slovakia. Observed was an increasing trend of precipitation in June, July and January and a decreasing trend of precipitation in December, April, May and August (Zeľeňáková et al., 2017). In recent years several hydrological droughts occurred in Slovakia in 2003, 2011–2012, 2015 (Fendeková et al., 2017) and 2018 (Jeneiová et al., 2019). By analysis of precipitation records from 1981 to 2013 at 491 stations in Slovakia. Fendeková et al. (2018) analysed drought events in 21<sup>st</sup> century in Slovakia, among the results the water balance components analysis for the time period 1931–2016 revealed decreased runoff in Slovakia, mainly due to

increased air temperature and balance evapotranspiration. According to Blaškovičová (2020), changes in long-term discharges in the years 2001–2015 compared to the reference period 1961–2000 coincide relatively well with the hydrological drought vulnerability map of Slovakia, which was created based on analyses of changes in long-term discharges for the reference period 1961–2000 compared to 1931–1980 time period. In this analysis, there was a decrease in the values of mean annual discharges in the areas originally designated as areas with low vulnerability: Orava and Kysuce region (both located in the north Slovakia) and tributaries of the Váh River from the Carpathians. The evaluation of mean monthly discharges in the period 2001–2015 compared to the reference period 1961–2000 in this study showed a significant increase in discharges in January for almost the entire territory of Slovakia and a decrease in April and October. A study on long-term fluctuations of low flows based on analysis of daily flow and precipitation series from 1980 to 2019 on the Laborec River (eastern Slovakia) by Kubiak-Wojcika et al. (2021) identified August and September as the months with the greatest culmination of flows below 95% quantile.

Monitoring and studying long-term droughts gives the valuable inputs for setting up the measures to improve the hydrological situation in surface waters. Since 2017 the Slovak Hydrometeorological Institute

(SHMI), online on its website, is presenting the Drought monitoring and evaluation based on operational data from selected water-gauging stations, with little or no human impact on the hydrological regime (SHMI, 2021). This enables a daily assessment of the current situation on Slovak streams during the year, with an emphasis on the assessment of hydrological drought on surface waters.

The presented paper deals with the evaluation of the occurrence of the area-wide droughts during the years 2011 to 2020 in Slovakia by the analysis of mean monthly discharges during a time period between 2011 and 2020 in comparison with long-term mean monthly discharges for the reference period 1961–2000. Trend analysis of the mean monthly discharges in period 1961–2020 was concluded to assess the potential change in the hydrological regime of Slovak rivers. This evaluation shows the potential of the real time data use for continuous hydrological drought assessment available online on the SHMI web page (SHMI, 2021), which is important for planning and proposals of appropriate measures for timely drought mitigation measures.

## Data and methods

The assessment is based on hydrological data from selected 164 water-gauging stations of the Slovakian hydrological network. The operational data (not verified) from these stations are used for the online evaluation and presentation of hydrological drought situation on the SHMI website. The criterion for selection the stations for hydrological drought monitoring was minimal or no human impact on the hydrological regime. Water-gauging stations affected, for example by abstractions could appear to be significantly dry due to the abstractions and not due to the hydrological situation. On the SHMI website, the current hydrological situation is displayed on a simple map of Slovakia, with the possibility of zooming onto a specific region, as well as with the possibility of selecting a water gauging station for a detailed view of the discharges (SHMI, 2021). Currently the website is only available in Slovak language, an example of output is shown in Fig. 1. In this paper, we focus on the assessment of the mean monthly discharges ( $Q_m$ ), during time period between 2011 and

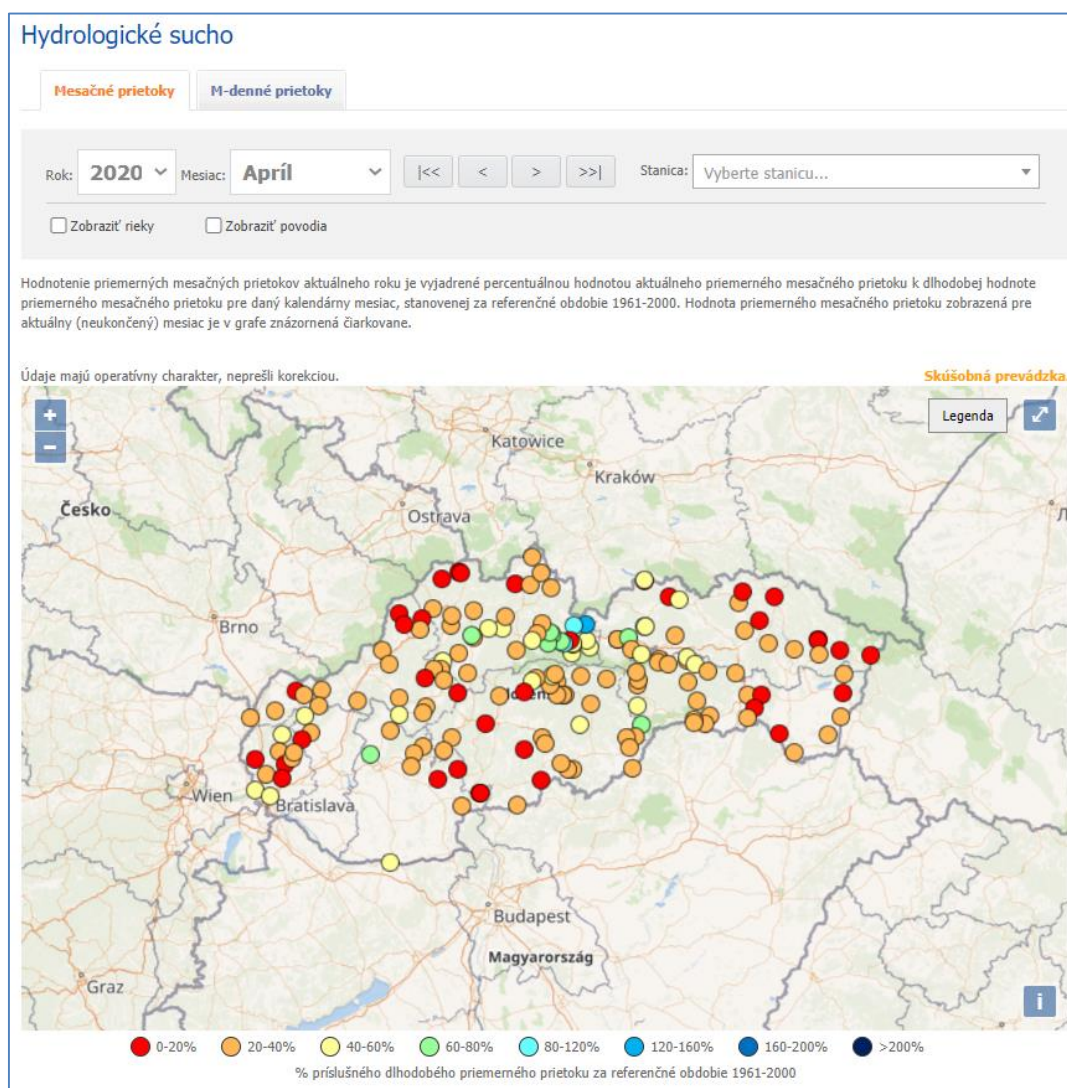


Fig. 1. Example of the online data from hydrological drought monitoring on the SHMI webpage (SHMI, 2021).

2020 in comparison with long-term mean monthly discharges ( $Q_{ma}$ ) for the reference period 1961–2000.

In this article the  $Q_m$  for selected year in the range of 80–120%  $Q_{ma, 1961-2000}$  are considered to be the values close to the relevant long-term values and months with  $Q_m$  higher than 120%  $Q_{ma, 1961-2000}$  to be above normal to extreme (more than 200%). As subnormal are rated the months with  $Q_m$  in the range from 60–80%  $Q_{ma, 1961-2000}$  and significantly below normal from 40 to 60%  $Q_{ma, 1961-2000}$ . The  $Q_m$  lower than 40%  $Q_{ma, 1961-2000}$  is considered to be a manifestation of the dry month and months with  $Q_m$  lower than 20%  $Q_{ma, 1961-2000}$  are considered to be extremely dry.

As the first step in assessment of the occurrence of the hydrological drought we used graphical outputs from the online version of the drought monitoring, where we

visually selected periods and areas with a predominant occurrence of  $Q_m$  below 40% of the relevant  $Q_{ma, 1961-2000}$  for the hydrological years 2011 to 2020. These were further analysed with verified discharge data from 43 representative water-gauging stations (Fig. 2), with long-term observations at least since 1961 and with the minimally affected hydrological regime. The basic characteristics (average elevation, catchment area range) for the main river basins in Slovakia based on 43 selected stations are displayed in table 1.

The mean monthly discharge data from the 43 selected gauging stations for the period 1961–2020 were further tested for the occurrence of the trend in the  $Q_m$ . The rank based non-parametric Mann-Kendall trend test (Mann, 1945; Kendall, 1975), which is widely used trend detection test in hydrology, was used for the analysis.

**Table 1.** Catchment characteristics of analysed water gauging stations

Catchment	Number of water gauging stations	Catchment area [km <sup>2</sup> ]	Average elevation [m a.s.l.]
Morava	1	47.1	144.3
Dunaj	2	7.25–131331.1	224.8
Nitra	2	136.08–181.57	310.7
Váh	17	8.4–1107.21	528.7
Malý Dunaj	3	19.09–37.86	247.8
Hron	6	36.01–582.08	565
Ipeľ	1	214.27	142
Slaná	3	31.97–148.95	334
Hornád	3	68.23–1298.3	434.1
Bodrog	3	173.94–2915.46	110.8
Poprad	2	34.89–44.64	781.7

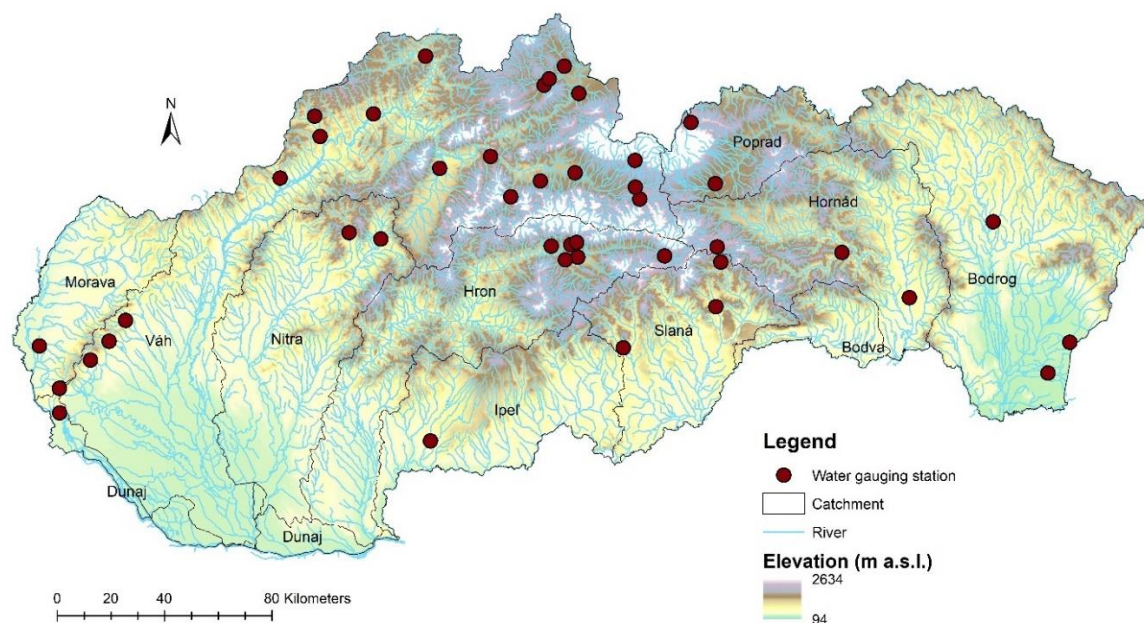


**Fig. 2.** Water gauging stations selected for the analysis.

The test statistic  $S$  equals to:

$$S = \sum_{k=1}^{n-1} \sum_{j=k+1}^n \text{sign}(x_j - x_k) \tag{1}$$

Where

$x_j$  – are the values of the data;  
 $n$  – is the length of the time series and

$$\text{Sign}(x_j - x_k) = \begin{cases} 1; & \text{if } x_j - x_k > 0; \\ 0; & \text{if } x_j - x_k = 0; \\ -1; & \text{if } x_j - x_k < 0. \end{cases} \tag{2}$$

In case the time series has  $n \geq 8$ , the statistic  $S$  has and almost normal distribution, and its variance is computed as:

$$\text{VAR}(S) = \frac{1}{18} [n(n-1)(2n+5) - \sum_{p=1}^g t_p(t_p-1)(2t_p+5)] \tag{3}$$

where

$g$  – is the number of tied groups,  
 $t_p$  – the amount of data with the same value in the group  
 $p=1 \dots g$ .

The normalised test statistic  $Z$ :

$$Z = \begin{cases} \frac{S-1}{\sqrt{\text{Var}(S)}} & \text{for } S > 0 \\ 0 & \text{for } S = 0 \\ \frac{S+1}{\sqrt{\text{Var}(S)}} & \text{for } S < 0 \end{cases} \tag{4}$$

If the Mann-Kendall test statistic  $Z$  equals to zero, it is expected that the data are normally distributed and there is no trend present in the time series. Positive values of the  $Z$  statistic point to increasing trend and negative ones to decreasing trend in the time series. The detected trend was evaluated on the significance level of  $p=0.05$ .

## Results and discussion

Online monitoring of hydrological drought offers simple map overview of the  $Q_m$  during time period 2011–2020 in comparison with  $Q_{ma, 1961-2000}$ . By the visual analysis of the maps in selected time period we have identified the periods from October 2011 to September 2012 and from April 2018 to January 2019 as the periods with the highest occurrence of respective  $Q_m$  below 40%  $Q_{ma, 1961-2000}$ . During these time periods the mean monthly discharges were continuously below 40%  $Q_{ma, 1961-2000}$  also in areas of Slovakia, which are usually not particularly prone to low flow occurrence, for example the north-west part of Slovakia.

Table 2 contains the percentage of 43 analysed water-gauging stations with  $Q_m$  lower than 40%  $Q_{ma}$ . The results of the analysis of the data shows that between 2011–2020 the years with the highest occurrence (more than 40% of evaluated stations) of  $Q_m$  lower than 40%  $Q_{ma}$  were the years 2012, 2015, 2018, 2019 and 2020. In addition, it confirms the results of the visual analysis of the longest time events of respective  $Q_m$  below 40%  $Q_{ma, 1961-2000}$  from October 2011 to September 2012 and from April 2018 to January 2019.

Months of April, June, July, August and October were the months with the highest occurrence of  $Q_m$  below 40%  $Q_{ma, 1961-2000}$  (more than 20% of analysed water gauging stations, Table 2.). The percentage of mean monthly discharges in April in time period 2011–2020 in comparison with  $Q_{ma, 1961-2000}$  is shown in the Table 3. The increasing occurrence of drier months in last years is clearly visible. The highest country-wide (all areas except of High Tatras mountains region) occurrence of  $Q_m$  below 40%  $Q_{ma, 1961-2000}$  was in April 2020 at 70% of analysed stations (Fig. 3). These results confirm the study of Blaškovičová (2020). Especially the higher occurrence of values under the average in April signifies the change

**Table 2.** The percentage of analysed water gauging stations with  $Q_m$  lower than 40% of  $Q_{ma, 1961-2000}$  (yellow 20%–40% of stations, red 40% and more of the stations)

Month/Year	2011	2012	2013	2014	2015	2016	2017	2018	2019	2020
11	0%	67%	7%	5%	7%	5%	2%	7%	51%	5%
12	0%	47%	16%	19%	7%	9%	5%	2%	40%	5%
1	0%	14%	0%	5%	0%	2%	21%	0%	23%	16%
2	0%	33%	0%	0%	0%	0%	2%	0%	2%	2%
3	12%	16%	0%	21%	2%	5%	12%	7%	12%	2%
4	23%	35%	0%	47%	2%	28%	26%	23%	53%	70%
5	37%	44%	0%	2%	5%	2%	9%	47%	0%	58%
6	19%	21%	0%	23%	28%	23%	30%	26%	12%	0%
7	0%	30%	23%	12%	40%	7%	28%	33%	42%	12%
8	0%	42%	33%	2%	44%	7%	26%	35%	16%	14%
9	19%	53%	7%	0%	35%	7%	2%	23%	9%	5%
10	37%	9%	30%	2%	26%	5%	2%	47%	23%	0%

of the yearly hydrological regime. If a snow cover is not formed in the winter season (December–February), or sudden increase of temperatures happens (years 2011 to 2020 are the warmest decade on record according to 2020 WMO provisional report) then the condition for spring season, usually typical for higher runoffs in Slovakia (March–May) are not met. This, in combination with the changing climatological regime influence the hydrological regime and its distribution during the year.

In the next step we analyzed the long term trends in

the selected 43 stations to further assess the potential of the change in the hydrological regime. Significant trend was detected by the Mann-Kendall trend test at the 95% confidence level. The highest occurrence of significant decreasing trend in the period 1961–2020 was in April in 47% of the evaluated stations (Fig. 4). Significant decreasing trend was also detected in May (28% of stations), June (40% of stations), July (23% of stations) and August (19% of stations). On the other hand significant rising trend was detected mostly in January (9% of stations) and February (19% of stations).

**Table 3.** The percentage of mean monthly discharges in April in period 2011–2020 in comparison with  $Q_{ma, 1961-2000}$

Station ID	Station	River	2011	2012	2013	2014	2015	2016	2017	2018	2019	2020
5100	Láb	Močiarka	53	26	116	25	41	53	36	27	43	26
5130	Spariská	Vydrica	112	56	153	26	61	47	31	51	32	16
5140	Bratislava	Dunaj	60	87	102	55	92	72	72	87	85	56
5160	Pezinok	Blatina	61	33	145	31	70	45	22	40	15	19
5250	Horné Orešany	Parná	104	23	133	43	76	69	20	46	20	19
5260	Píla	Gidra	78	31	163	41	67	41	18	39	25	30
6540	Nedožery	Nitra	33	42	163	38	106	43	81	45	37	36
6620	Liešťany	Nitrica	29	43	123	27	85	37	70	30	31	20
5310	Čierny Váh	Ipolitica	46	76	185	63	94	91	117	188	73	42
5330	Východná	Biely Váh	62	73	131	60	86	60	92	95	58	53
5400	Podbanské	Belá	95	123	136	122	102	149	142	249	177	134
5550	Liptovský Mikuláš	Váh	57	86	145	74	95	93	119	158	105	63
5730	Partizánska Lupča	Lupčianka	46	65	169	54	80	79	96	120	66	53
5740	Podsouchá	Revúca	35	81	138	44	95	57	78	92	75	40
5790	Lubochňa	Lubochňanka	50	91	120	44	99	62	79	77	79	42
5800	Lokca	Biela Orava	49	154	106	36	88	35	126	42	82	24
5810	Oravská Jasenica	Veselianka	37	100	100	35	81	29	164	37	64	20
5820	Zubrohlava	Polhoranka	41	142	97	34	89	42	127	37	67	27
5840	Trstená	Oravica	55	88	121	72	94	47	149	54	66	34
6130	Martin	Turiec	40	88	149	48	118	53	82	75	55	36
6180	Čadca	Kysuca	51	70	140	26	86	38	133	17	24	12
6360	Bytča	Petrovička	41	66	169	29	102	48	181	25	32	17
6390	Vydrná	Petrinovec	41	26	177	24	92	17	73	27	17	26
6400	Dohňany	Biela voda	28	39	130	34	103	34	131	25	19	21
6450	Horné Srnie	Vlára	42	39	135	29	101	45	115	27	20	23
6950	Zlatno	Hron	42	41	199	43	77	75	60	138	36	36
7015	Brezno	Hron	42	42	182	43	81	54	58	135	41	34
7045	Hronec	Čierny Hron	40	24	223	29	63	28	38	111	22	30
7060	Bystrá	Bystrianka	60	78	160	61	91	98	107	164	71	54
7065	Mýto p. Ďumbierom	Štiavnička	40	70	171	46	83	70	81	128	58	34
7070	Dolná Lehota	Vajskovský potok	52	69	168	60	84	89	76	131	58	51
7600	Plášťovce	Litava	27	19	344	16	80	17	21	81	10	15
7660	Dobšiná	Dobšinský potok	49	31	239	55	67	85	47	166	25	36
7730	Štítnik	Štítnik	58	22	228	52	63	56	46	135	28	44
7860	Lehota nad Rimavicou	Rimavica	52	14	288	33	80	39	26	122	22	42
8530	Stratená	Hnilec	44	33	167	43	68	78	45	173	29	31
8560	Jaklovce	Hnilec	39	25	208	28	45	38	39	112	18	27
8870	Košické Olšany	Torysa	47	39	178	42	53	48	64	99	31	33
9320	Lekárovce	Uh	42	99	160	27	53	29	37	98	40	22
9410	Veľké Kapušany	Latorica	39	72	168	27	49	29	38	121	27	28
9620	Jasenovce	Ofka	49	56	185	37	34	45	72	147	13	29
7930	Ždiar, Podspády	Javorinka	84	114	140	110	102	120	168	175	152	68
8070	Poprad, Matejovce	Slavkovský potok	69	72	108	116	89	77	134	97	68	48

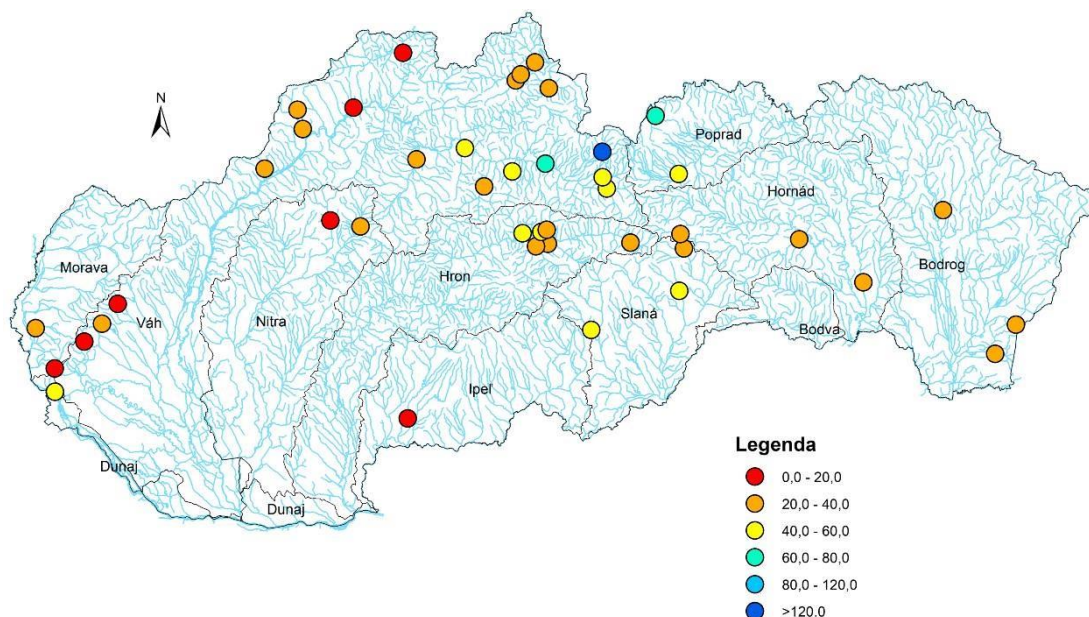


Fig. 3. April 2020, highest occurrence of  $Q_m$  below 40%  $Q_{ma, 1961-2000}$ .

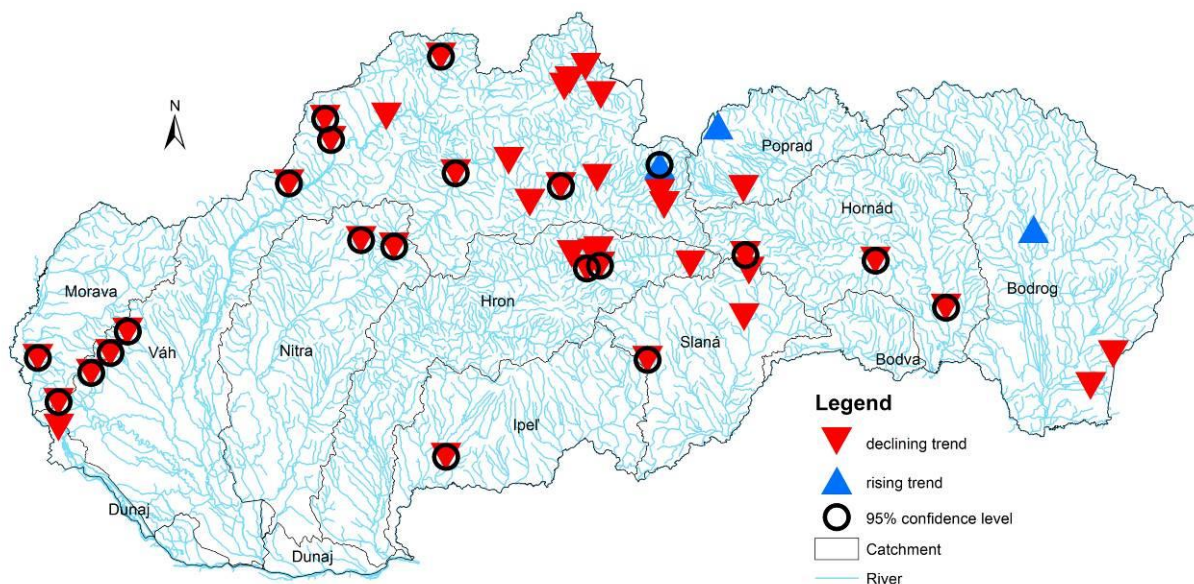


Fig. 4. The results of the Mann – Kendall trend test for the mean monthly discharges in April in the 1961–2020 time period, detected significant trend at 95% confidence level is marked according to the legend.

### Conclusion

The potential of the use of the real-time data for continuous hydrological drought assessment online on the SHMI web page (SHMI, 2021) was evaluated. The analyses show the change in the hydrological regime of the Slovak rivers and increase of the low flows occurrence in previously not prone areas. Therefore a further analysis of the occurrence of the area-wide droughts during the years 2011 to 2020 in Slovakia was concluded by the analysis of  $Q_m$  during this time period

in comparison with long-term values for reference period  $Q_{ma, 1961-2000}$  for selected 43 gauging stations. The results show, that the months of April, June, July, August and October were detected as the months with the highest occurrence of  $Q_m$  below 40%  $Q_{ma, 1961-2000}$  in the 2011–2020 time period. The trend analysis of the mean monthly discharges in the period 1961–2020 by the Mann-Kendall trend test assessed the potential change in the hydrological regime of Slovak rivers and confirmed significant decreasing trend in April, May, June, July and August for the 1961–2020 time period.

These results reinforce the need of continuous online monitoring of the mean monthly flows. The lower discharges in months where historically the highest runoff of the year is manifested are not so visible on the first sight – there are no close-to-dry riverbeds minimum discharges occurring. However, the situation with decreasing spring runoff (March, April, May) together with changing climatic conditions can introduce a critical start of a serious dry period later in summer (June, July, August) or even for a longer period. Therefore, there is a need to carefully monitor mean monthly flows in comparison with long-term mean monthly discharges (especially under 40% and 20%). Results of the monitoring available on the SHMI webpage can present a tool for the timely detection of the incoming long-term drought periods with possibility of timely implementation of appropriate measures.

## References

- Blašková, L. (Ed.) (2020): Hodnotenie hydrologického sucha, časť 2: Hodnotenie zmien a trendov mesačných a ročných prietokov, čiastková správa. 64 s. SHMÚ, 2019. 978-80-99929-14-3
- Jeneiová, K., Škoda, P., Blaškovičová, L. (2019): Výskyt hydrologického sucha v lete 2018 na Slovensku, Vodohospodársky spravodajca, vol.1–2, 16–20
- Fendeková, M., Danáčová, Z., Gauster, T., Labudová, L., Fendek, M., Horvát, O. (2017): Analysis of hydrological drought parameters in selected catchments of the southern and eastern Slovakia in the years 2003, 2012 and 2015, Acta hydrologica slovaca, vol. 18, no.2, 35–144
- Fendeková, M., Gauster, T., Labudová, L., Vrblíková, D., Danáčová, Z., Fendek, M., Pekárová, P. (2018): Analysing 21st century meteorological and hydrological drought events in Slovakia, Journal of Hydrology and Hydromechanics, vol. 66, no. 4, 393–403.
- Kendall, M. G. (1975): Rank Correlation Methods. London, Griffin. 1975.
- Kubiak-Wójcicka, K., Zelenáková, M., Blišťan, P., Simonová, D., Pilarska, A. (2021): Influence of climate change on low flow conditions. case study: Laborec river, eastern Slovakia. Ecohydrology and Hydrobiology, doi:10.1016/j.ecohyd.2021.04.001
- Mann, H. B. (1945): Nonparametric tests against trend. Econometrica 13, 245–259. doi: 10.2307/1907187
- SHMI (2021): Monitoring hydrologického sucha, online: <[http://www.shmu.sk/sk/?page=1&id=hydro\\_sucho](http://www.shmu.sk/sk/?page=1&id=hydro_sucho)>; cited on: 25.2.2021
- WMO (2020): WMO Provisional Report on the State of the Global Climate 2020, online: <[https://library.wmo.int/index.php?lvl=notice\\_display&id=21804#.X9n5bdhKhpZ](https://library.wmo.int/index.php?lvl=notice_display&id=21804#.X9n5bdhKhpZ)>, citované: 25.2.2021
- Repel, A., Zelenáková, M., Jothiprakash, V., Hlavatá, H., Blišťan, P., Gargar, I., Purcz, P. (2021): Long-Term Analysis of Precipitation in Slovakia, Water 2021, 13, 952
- Zelenáková, M., Vido, J., Portela, M.M., Purcz, P., Blišťan, P., Hlavatá, H., Hlušík, P. (2017): Precipitation trends over Slovakia in the period 1981–2013. In: Water, Vol. 9, Iss. 12, 922

Ing. Zuzana Danáčová, PhD.

Ing. Katarína Jeneiová, PhD. (\*corresponding author, e-mail: [katarina.jeneiova@shmu.sk](mailto:katarina.jeneiova@shmu.sk))

Ing. Lotta Blaškovičová, PhD.

Slovak Hydrometeorological Institute

Jeséniová 17

833 15 Bratislava

Slovak Republic

**Identification of the historical drought occurrence on the Danube River and its tributaries**Dana HALMOVÁ\*, Pavla PEKÁROVÁ, Ján PEKÁR, Pavol MIKLÁNEK,  
Veronika BAČOVÁ MITKOVÁ

In the presented paper, the changes in the minimum flows at five stations along the length of the Danube River and at its 5 selected significant tributaries were analyzed. Average daily flows with the longest possible series of observations (since 1901 or since 1921) were used as input data. In the first part, low water content, hydrological drought were statistically analyzed and long-term trends of 1- to 90-day minimum flows were identified. The second part presents changes in  $T$ - year minimum daily flows in selected stations. The most extreme drought at Hofkirchen occurred in 1921. Drought at Orsova occurred around 1862/63, 1882/83, 1900, 1920/21, 1946/47, 1961/62, 1971, 1991/92 and 2017 / 19. The analyzes show that there is a more or less regular alternation of water and low-water periods along the entire length of the Danube. Multi-annual dry periods along the length of the Danube occur in the same periods. In contrast, on the Danube tributaries, the dry seasons are time-shifted.

KEY WORDS: the Danube River basin, low flow and failure characteristics, hydrological drought, IHA model

**Introduction**

In the last decade after 2010, several dry years occurred in the entire Danube basin. E.g. Kukla et al. (2019) cites, that in the Czech Republic the year 2018 was the culmination of a number of few water years since 2014. The hydrological drought in 2018 affected practically the entire territory of the Czech Republic. In most rivers, their levels fell down to the level of hydrological drought (355 daily flow) for several weeks. In the Slovak part of the Morava river basin, 2017 and 2018 were also extremely dry. Mészáros (2018) cites, that in 2017, below-average flow was recorded in all stations in the Morava river basin, the most stations had more than 10-day periods with a flow below  $Q_{355}$  and eleven stations were more than one day below  $Q_{364}$ . In four water gauging stations there were days during which the riverbeds were dried and in two stations there were days with a flow rate of less than  $0.001 \text{ m}^3 \text{ s}^{-1}$ . The lowest flows occurred from June to September, but also in January, which was extremely cold. In the water gauging station with the longest series of measured flows, Moravský Svätý Ján: Morava, the year 2017 was evaluated as the third driest since the beginning of measurements. The water shortage situation was repeated in 2018.

Drought is a natural hazard. However, it differs in several ways. Most natural hazard (floods, earthquakes) arise very quickly (sometimes without any warning) and have

a rapid course (Pekárová et al., 2008). Drought is characterized by a slow onset and development that lasts for months. It can sometimes occur throughout a season, year, and even a decade. Determining the beginning and end of a drought is quite complex and requires the analysis of several meteorological as well as hydrological characteristics. The effects of drought are cumulative, the magnitude of the drought intensity increasing with each passing day. We encounter the effects of extreme drought for several years after the occurrence of average rains.

In Europe, drought occurred in the Mediterranean, in Spain, Italy or Greece. But also in the Danube basin in the past there were several extremely dry periods, e.g. in 1921, 1947, 1992–93, 2003, 2015. In the studies of Slovak and foreign authors, eg: Dracup et al. (1980), Wilhite and Glantz (1985), Bonacci (1993), Fendeková and Némethy (1994), Lešková, (1997), Tallaksen et al. (1997), Byun and Wilhite (1999), Tate and Gustard (2000), Smakhtin and Hughes (2007), Brilly (2010), Klementová and Litschmann (2001), Stahl (2001), Hisdal et al. (2001), Smakhtin (2001), Blinka (2004, 2005), Hrvoř and Tomlain (2008), Halmová et al. (2011), Fendeková et al. (2017), Hanel et al. (2019), Hološ and Šurda (2021) we can find a number of drought definitions.

Wilhite and Glantz (1985) define the following four types of drought:

- Meteorological drought: usually assessed on the basis

of the deviation of precipitation from normal for a certain period of time. It thus expresses one of the primary causes of drought.

- Hydrological drought: expressed in terms of deficits in surface and subsurface water supplies.
- Agricultural (soil) drought: usually refers to the soil moisture needs of specific crops at a given time.
- Socio-economic drought: a definition linking drought with economic theory of supply and demand.

An overview of older works concerning the processing of low water characteristics in Slovakia can be found in Szolgay (1977), Drako and Majerčáková (1989), Balco (1990), Majerčáková (1995), Majerčáková et al. (1995, 1997), Burger (2005), Demeterová and Škoda (2004, 2005, 2009), or Kohnová et al. (2021). A detailed elaboration of the characteristics of low water content of Slovak streams can be found recently in Fendeková et al. (2017).

The aim of this paper is to identify the occurrence of hydrological drought in rivers in a uniform manner in selected stations on streams in the Danube river basin for the longest possible time periods. Therefore, in the statistical analysis, rivers were selected where there have been evaluated daily discharges at least since 1921.

**Data**

At statistical evaluation of minimum discharges and to identify the occurrence of extreme hydrological droughts, we used a database of average daily discharges, processed within the international project IHP UNESCO WATSIM.

We selected 5 stations on important Danube tributaries (Lech: Landsberg (1901–2019), Morava: Moravský sv. Ján (1901–2019, except 1917–1919), Váh: Liptovský Mikuláš (1921–2019), Tisza: Senta (1921–2019), Sava:

Litija (1895–2019). The following stations were selected on the Danube: Hofkirchen (1901–2019), Achleiten (1901–2019), Bratislava (1876–2019), Orsova (1840–2005) and Reni (1921–2019) (Fig. 1).

The basic hydrological characteristics of the flows for the observation period are shown in Table 1. The example of average daily flow rates for Morava: Moravský sv. Ján is rendered on Fig. 2. From the course of 4-year moving averages of daily values it is obvious, that multi-annual dry periods occur more less regularly on the Morava River.

To evaluate the hydrological drought, it is evaluated:

- flow characteristics (minimum average daily flow rate (monthly and annual step, for the entire period), M-daily flow (curve of exceeding average daily flow), minimum monthly and annual flow rates, N-year minimum flow);
- failure characteristics: Time occurrence of dry periods (occurrence date, number of days of low flow period, longest dry season) and insufficient volumes.

Multiple time courses were assessed from average daily flow rates that represent a hydrological river regime (with an emphasis on hydrological drought):

- time series of average annual flow;
- time series of 1-, 3-, 7-, 30-, and 90-day minimum flow by calendar year;
- the time range of the annual minimum flow (the occurrence day of the extreme from 1 – to 365/366, 1 means the 1st January; 355/356 means 31. December);
- BFI (BASIC FLOW INDEX) – Basic drain index, calculated as a 7-day minimum flow / average flow rate per year.

An example of created rows for Morava River in Moravský sv. Ján is presented in Fig. 2 and 3.

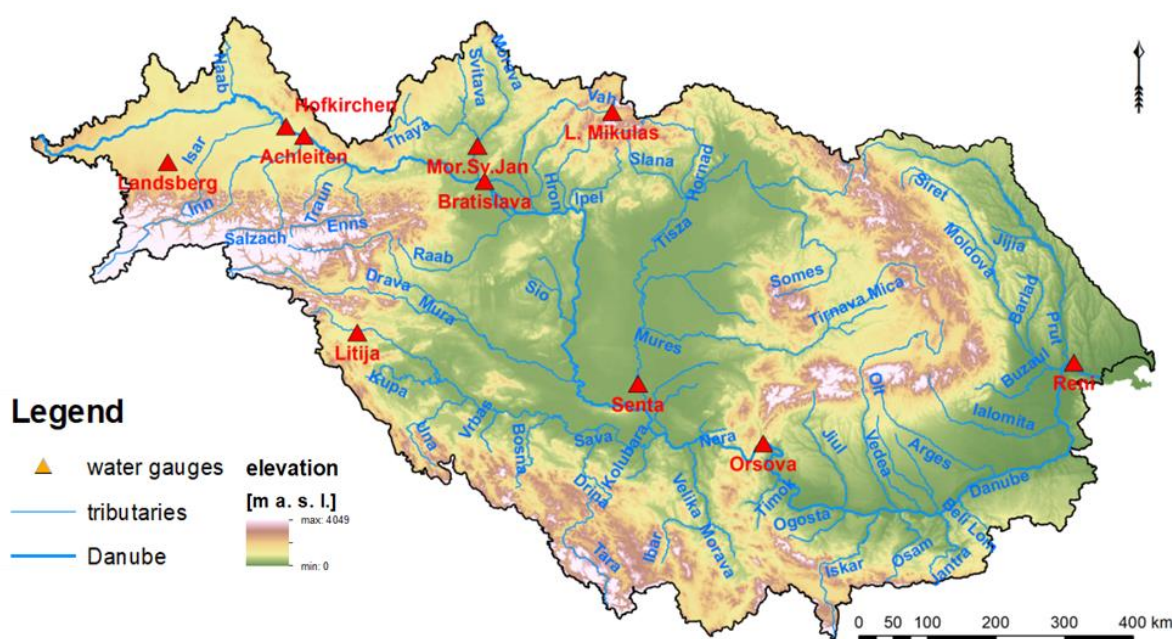


Fig. 1. Localization of used stations in the Danube Basin.

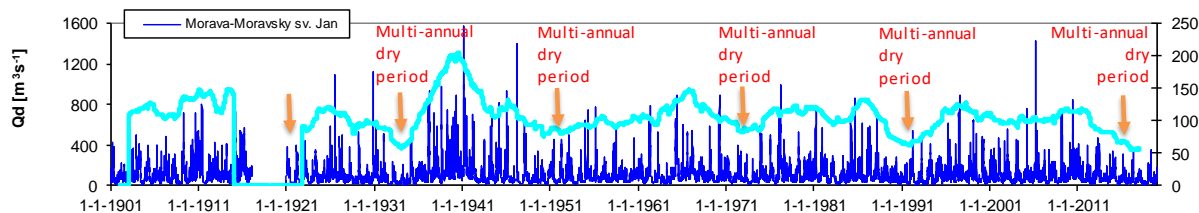


Fig. 2. The course of average daily flow on Morava: Moravský sv. Ján for the period 1901–2019 (dark blue line). The course of the 4-year-moving average (light blue line).

Table 1. Basic discharge ( $Q$ ) characteristics and average long-term specific runoff ( $q_a$ )

	Area [km <sup>2</sup> ]	$Q_{mean}$ [m <sup>3</sup> s <sup>-1</sup> ]	$Q_{min}$ [m <sup>3</sup> s <sup>-1</sup> ]	$Q_{max}$ [m <sup>3</sup> s <sup>-1</sup> ]	$Q_{330-day}$ [m <sup>3</sup> s <sup>-1</sup> ]	$Q_{30-day}$ [m <sup>3</sup> s <sup>-1</sup> ]	$q_a$ [l s <sup>-1</sup> km <sup>-2</sup> ]
Lech: Landsberg	2295	82	14.30	989	34	157	35.8
Morava: M. sv. Ján	24129	107	9.40	1573	29	247	4.5
Váh: L. Mikuláš	1107	21	4.20	300	7	44	18.5
Tisza: Senta	141715	782	79.0	3730	219	1739	5.5
Sava: Litija	4821	176	23	1992	59	373	36.4
Danube: Hofkirchen	47496	635	165	3450	337	1070	13.4
Danube: Achleiten	76653	1414	349	9300	740	2350	18.4
Danube: Bratislava	131338	2049	580	10810	1042	3420	15.6
Danube: Orsova	576232	5565	1060	15092	2760	9020	9.7
Danube: Reni	805700	6539	1280	15900	3260	10800	8.1

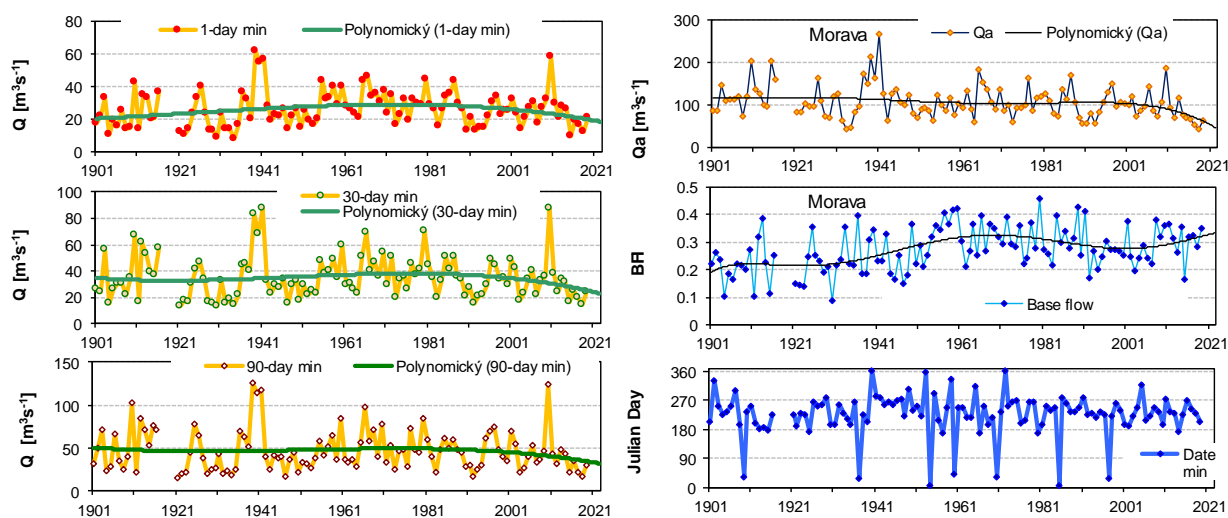


Fig. 3. Various minimum flow characteristics, Morava: Moravský sv. Ján, 7-day (7-day) minimum, date of minimum daily flow rate in year, 30-day (30-day) minimum, 90-day (90-day) minimum. Period 1901–2017 (1917–1919 missing data). Polynomial trend.

## Methods

### Statistical analyses

Statistical methods were used for data processing (time series, trend and frequency analysis) using special hydrological data processing software, e.g. AnClim (Štěpánek, 2004), IHA (Indicators of Hydrologic Alteration) Software (The Nature Conservancy, 2007, 2009, Mathews and Richter (2007), Gao et al. (2009)), PeakFQ Software (Flynn et al., 2006) and STATGRAPHICS Plus.

### Analysis of the frequency and duration of dry periods.

In the next step, the frequency of dry periods was evaluated. Hydrogram of average daily flow rates were separated into 5 types of flow:

1. low flows,
2. extreme low flows,
3. high flow pulses,
4. small floods,
5. large floods.

Periods of low flows are the dominant phenomenon in most rivers. In the natural riverbeds, after a period of rains or after melting the snow cover, the total (surface and subsurface) runoff from the catchment gradually decreases, while the runoff returns to its original flow state. These low flow rates are maintained by groundwater inflows into the streams. Extreme Low Flow periods occur during very long dry periods, when the river flows decrease and get into very low values.

The following criteria were used for hydrogram separation:

1. Extremely low flow rates - below 10% low flow rates.
2. Pulses / Periods of increased flow rates are all flow events with a flow over 25% (a flow wave begins if more than 25% per day will rise and ends if the decrease is less than 10% per day, while the flow does not fall below 50% value).
3. Small floods are defined as pulses / period of increased flow rates at least once in 2 years.
4. Large floods are defined as pulses / period of increased flow times with a recurrence time at least once every 10 years.

An example of separation of average daily flow for large floods, small floods, periods of increased flow, low flow and extremely low flow periods in the Morava: Moravský sv. Ján is shown in Fig. 4. Long-term changes in separated flow were identified by trend analysis.

Hydrological software IHA (Indicators of hydrological alterations) version 7 was used to identify changes in daily flow regime. The software IHA has been developed by The Nature Conservancy (TNC) as an easy-to-use tool for calculating the characteristics of natural and altered hydrologic regimes. The method and software will work on any type of daily hydrologic data and the power of the IHA method is that it can be used to summarize long periods of daily hydrologic data into a much more

manageable series of ecologically relevant hydrologic parameters.

## Results

### Statistical analyses

To characterize the periods of low water levels, which are the most significant manifestation of hydrological drought, parameters belonging to statistical, positional and probabilistic characteristics using time series of average daily flows are generally used. In addition to these characteristics, the volume and time characteristics of the drought are also determined. Methodically, the flow parameters of extreme flows in the region of the extreme minimum were assessed.

Rows of 4-year moving average daily specific runoff were calculated from the average daily discharges of selected five rivers in the Danube basin and from gauging stations on the Danube (Fig. 5a). The multi-annual small-water and water periods alternate more or less regularly cyclically along the entire length of the Danube in the same periods. Dry seasons occurred around 1862, 1882/83, 1900, 1920/21, 1946/47, 1961/62, 1971, 1991/92 and 2017/19. An extremely dry multi-year period occurred on the Danube at the Orsova station around 1863 and then around 1991. The cyclic repetition of dry periods on the Danube flow is shown by the red arrows in Figs. 5a, 5b. It is obvious that there is no significant shortening or lengthening of cycles.

From Fig. 5b on the example of the Morava River, it is evident that in the period 1921–1923, extreme 90-day dry periods occurred in three successive years. It was similar in 1932–1935; in 1947; in 1990–1994. Since 2013, an extremely dry period started again. The situation is similar on the Tisza River. The example of the Danube tributary Lech shows that extreme drought occurred at the turn of the 20th and 21st centuries, a more pronounced drought also occurred around 1960.

The results of the trend analysis are documented in Table 2. The analysis of selected characteristics of low water content of selected streams in the Danube basin shows that the period 1920–1921 was an extremely dry period, that the series of minimum discharges (1-, 3-, 7-, 30- and 90-day minimum discharges) in water gauging stations on the Danube River and selected tributaries are generally growing.

However, from the analysis of flows in the Danube: Orsova and Sava: Litija water gauging stations, it is clear that all evaluated minimum flows have a decreasing trend. For the Morava River, while the 7- day minimum flows are rising slightly, in the case of the 90-day minimums, the trend is slightly decreasing.

Regarding the occurrence of the minimum flow during the year, the differences are evident. In some water gauging stations their occurrence is evident at one time of the year (eg. Danube: Bratislava, Danube: Orsova, Lech: Landsberg, Morava: Moravský sv. Ján, Váh: Liptovský Mikuláš) and in others the minimum flow occurred throughout the year, whether in summer or winter (Danube: Hofkirchen, Sava: Litija).

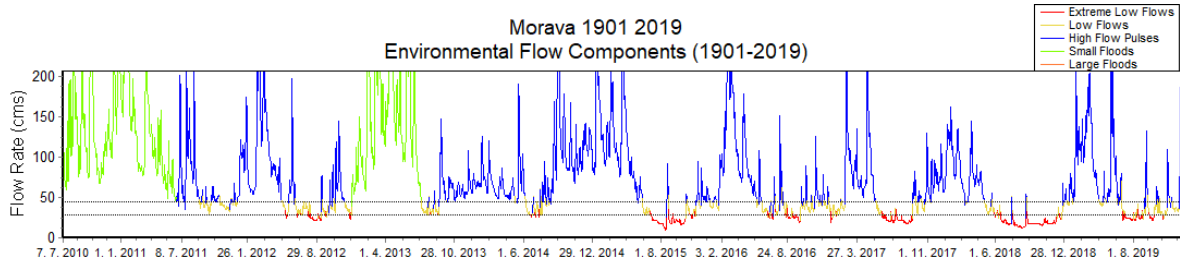


Fig. 4. Separation of daily flows into large floods, small floods, periods of increased flows, low and extremely low flows; at Morava: Moravský sv. Ján gauging station, detail from July 2010 to December 2019. The horizontal lines represent the flow boundaries for the separation of the hydrogram.

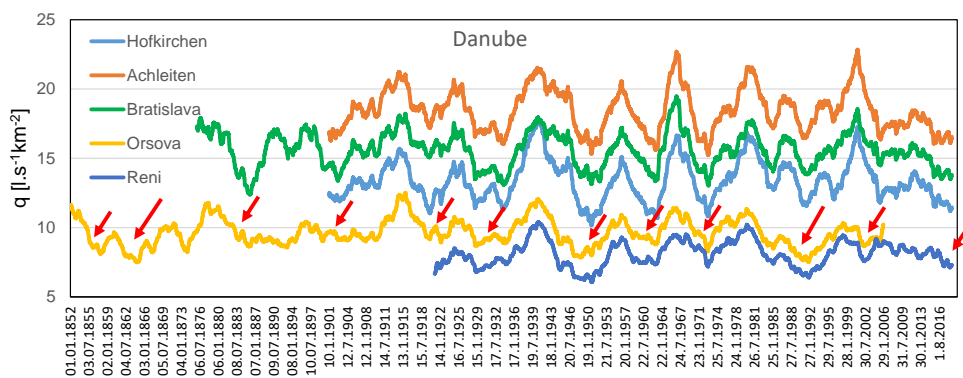


Fig. 5a. The course of 4-year moving average daily specific runoff of five selected gauging stations on the Danube River.

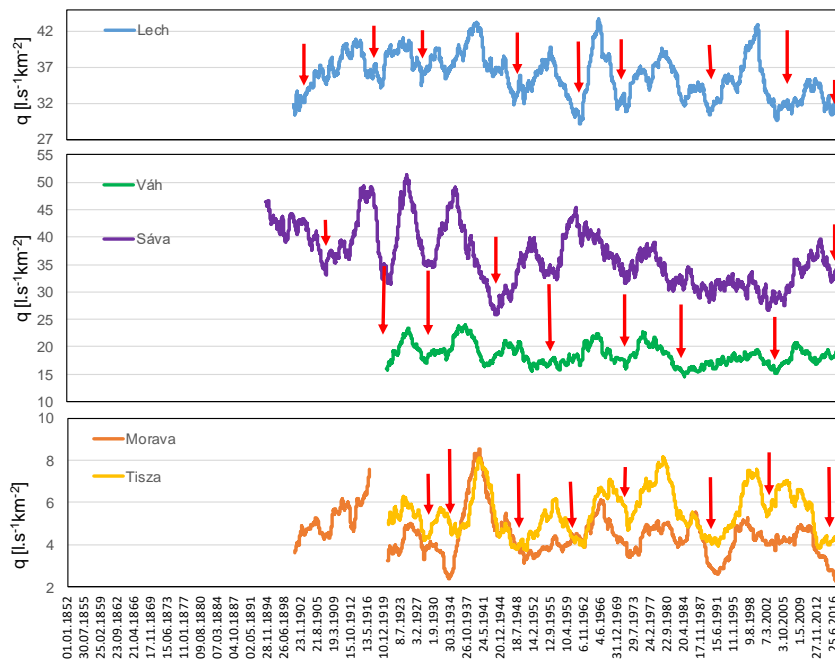


Fig. 5b. The course of 4-year moving averages of average daily specific runoff from water gauging stations of selected five tributaries of the Danube for the observed periods. The red arrows highlight the dry season.

**Identification of historical droughts on the Danube and selected tributaries.**

In the second part of the study, the duration of low and extremely low flow rates was evaluated. As mentioned in the Methods, we used IHA software to separate the hydrogram of average daily flows.

In order for the results of IHA outputs to be objective, it is necessary to have inputs from sufficiently long series of hydrological observations, which is fulfilled in our case. Examples of hydrogram separation for three stations on the Danube: Achleiten since 1901, Bratislava since 1876 and Reni since 1921 are depicted in Figs. 6. Extreme floods are better seen in the graphs. While floods occur in the Upper Danube region in the same years, the situation in the Lower Danube region is different. The wet period in the Lower Danube region was in the years 1939–1941. On the contrary, an exceptionally dry period in the Danube basin occurred in 1921, while low flows were recorded as early as November and December 1920, which is also evident from Fig. 7, where hydrograms of daily flows from 1920 and 1921 are plotted (graphs on the left) and from the dry

years of 1947 and 2003, from selected water gauging stations on the Danube: Bratislava, Orsova (Turnu Severin) and Reni.

The IHA software methodology allows to evaluate selected characteristics of minimum flows (average of extremely low wave flows per year, day of occurrence, average duration of waves, number of waves per year) and subsequently present changes of extremely low flow events of the Danube (Fig. 8a). The trends of the extremely low flow event averages correspond to the trends of the average annual minimum flows. The time of occurrence of droughts and the duration of the drought at Hofkirchen station are interesting. The greatest drought occurred at this station in 1921. After 1970, changes in the date of the occurrence of extreme drought can be seen. The average duration decreased at all selected water gauging stations. At the same time, the number of these events has increased during the year, only at the Reni station it is slightly decreasing. This means that although droughts last for a shorter time, they occur more often a year. This results from the setting of input parameters in the IHA model. The annual averages of extremely low flows have almost

**Table 2. Trend line slope coefficient of 1-, 3-, 7-, 30- and 90-day minimum flows at water gauging stations on the Danube River (Danube: Hofkirchen, Danube: Achleiten, Danube: Bratislava, Danube: Orsova, Danube: Reni) and water gauging stations on selected tributaries (Lech: Landsberg, Morava: Moravský sv. Ján, Váh: Liptovský Mikuláš, Tisza: Senta, Sáva: Litija). The negative slope coefficients are underlined.**

Danube: Hofkirchen		Lech: Landsberg	
1-day minimum	0.2837	1- day minimum	0.0727
3- day minimum	0.2974	3- day minimum	0.0834
7- day minimum	0.2953	7- day minimum	0.0914
30- day minimum	0.2145	30- day minimum	0.0967
<u>90- day minimum</u>	<u>-0.0027</u>	90- day minimum	0.0980
Danube: Achleiten		Morava: Moravský sv. Ján	
1- day minimum	0.975	1- day minimum	0.0217
3- day minimum	1.050	3- day minimum	0.0271
7- day minimum	1.098	7- day minimum	0.0275
30- day minimum	1.062	<u>30- day minimum</u>	<u>-0.0055</u>
90- day minimum	0.765	<u>90- day minimum</u>	<u>-0.0455</u>
Danube: Bratislava		Váh: Liptovský Mikuláš	
1- day minimum	0.5138	1- day minimum	0.0108
3- day minimum	0.6531	3- day minimum	0.0095
7- day minimum	0.7763	7- day minimum	0.0080
30- day minimum	0.6962	30- day minimum	0.0031
90- day minimum	0.3950	<u>90- day minimum</u>	<u>-0.0071</u>
Danube: Orsova		Tisza: Senta	
<u>1- day minimum</u>	<u>-0.7407</u>	1- day minimum	0.934
<u>3- day minimum</u>	<u>-0.2196</u>	3- day minimum	1.075
<u>7- day minimum</u>	<u>-0.1628</u>	7- day minimum	1.145
<u>30- day minimum</u>	<u>-0.6802</u>	30- day minimum	1.294
<u>90- day minimum</u>	<u>-2.0360</u>	90- day minimum	0.799
Danube: Reni		Sava: Litija	
1- day minimum	7.094	<u>1- day minimum</u>	<u>-0.0738</u>
3- day minimum	7.098	<u>3- day minimum</u>	<u>-0.0773</u>
7- day minimum	6.896	<u>7- day minimum</u>	<u>-0.0768</u>
30- day minimum	6.564	<u>30- day minimum</u>	<u>-0.1280</u>
90- day minimum	4.778	<u>90- day minimum</u>	<u>-0.2686</u>

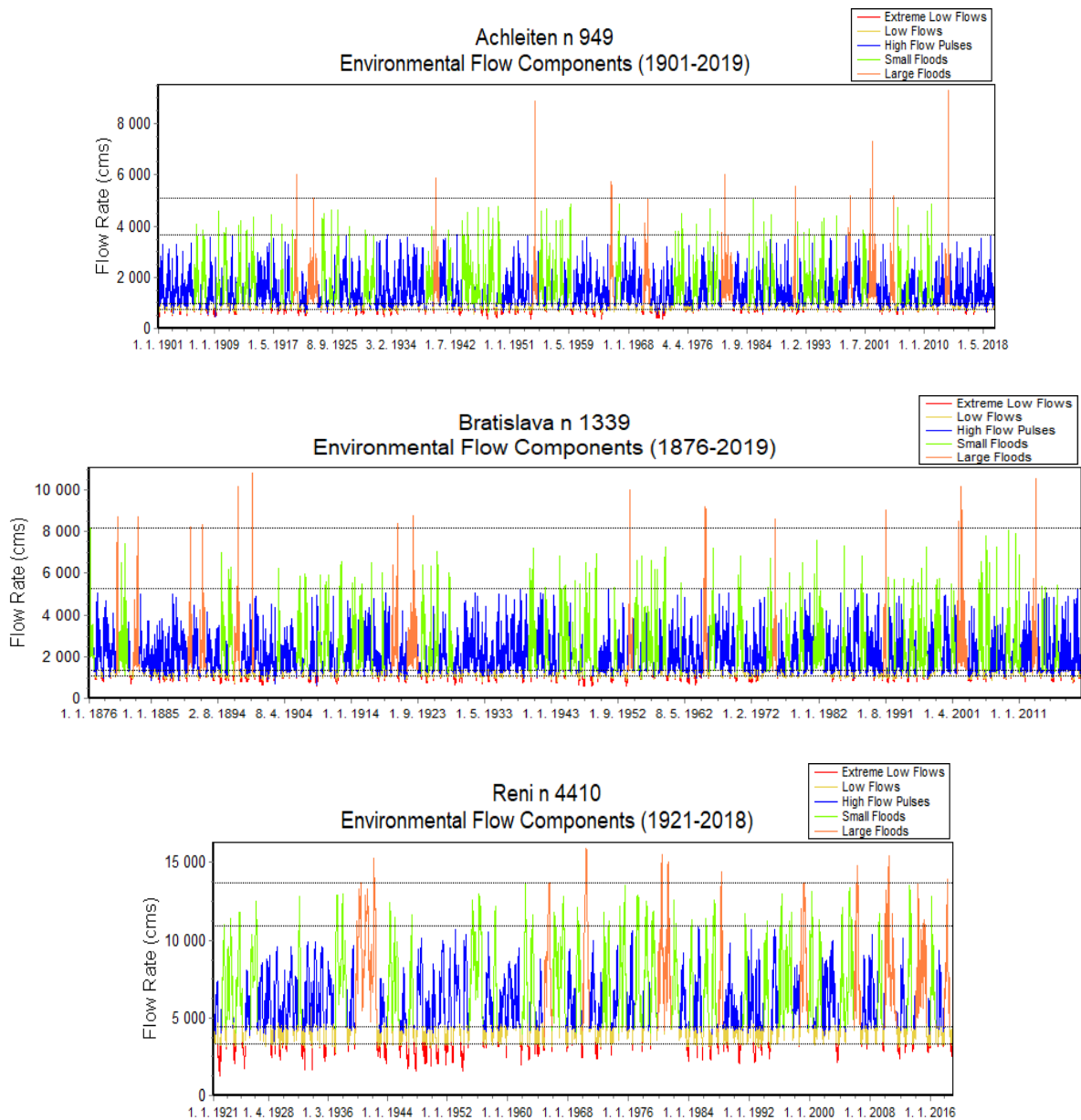


Fig. 6. Separation of daily flows into large floods, small floods, periods of increased flows, low flows and extremely low flow periods in selected water gauging stations on the Danube: Achleiten, Bratislava, Reni. The horizontal lines represent the individual flow limits for the separation of the hydrogram.

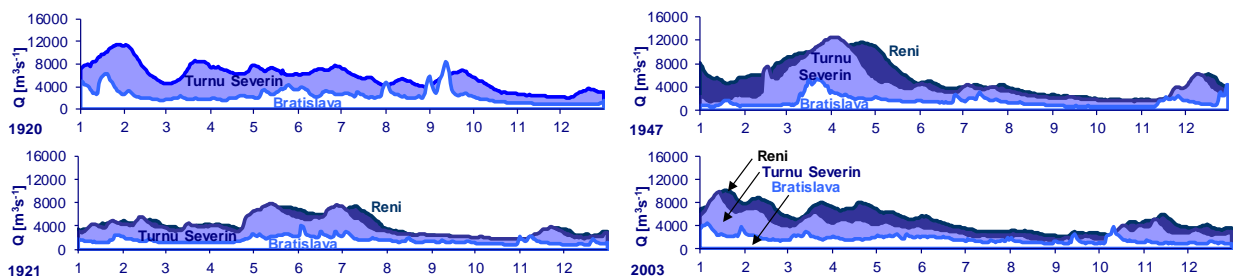
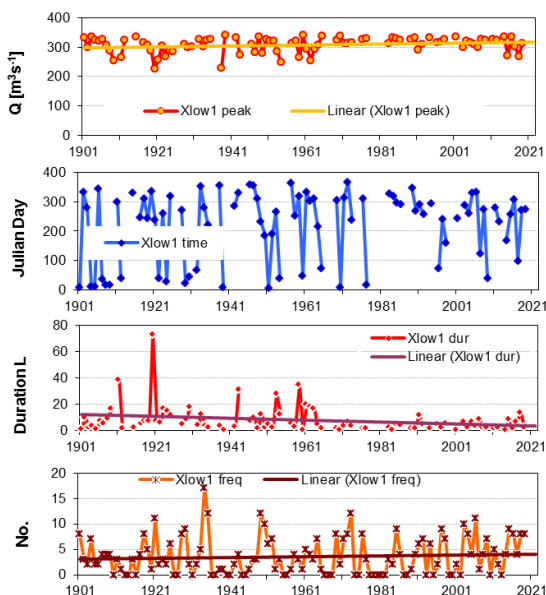


Fig. 7. Hydrograms of daily discharges from 1920 and 1921 (left) and from the dry years 1947 and 2003, from selected water gauging stations on the Danube: Bratislava, Orsova (Turnu Severin) and Reni.

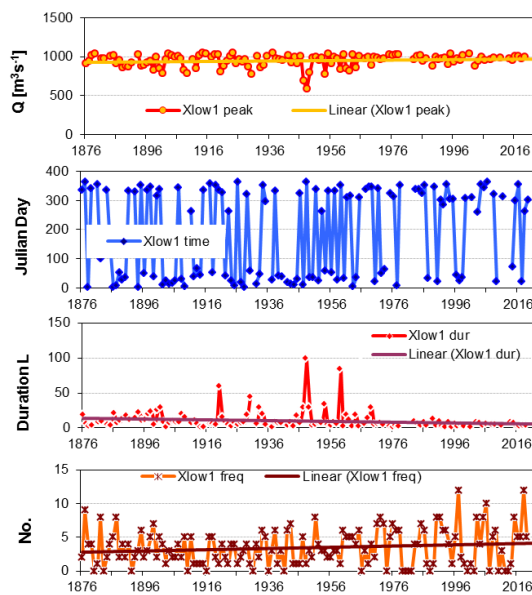
zero, resp. slightly increasing trend. They rise most significantly at the station Danube: Reni.

The same analysis we performed after processing the daily flows of selected tributaries of the Danube River (Lech, Moravia, Váh, Sava). Changes in the extremely low flow events of selected tributaries of

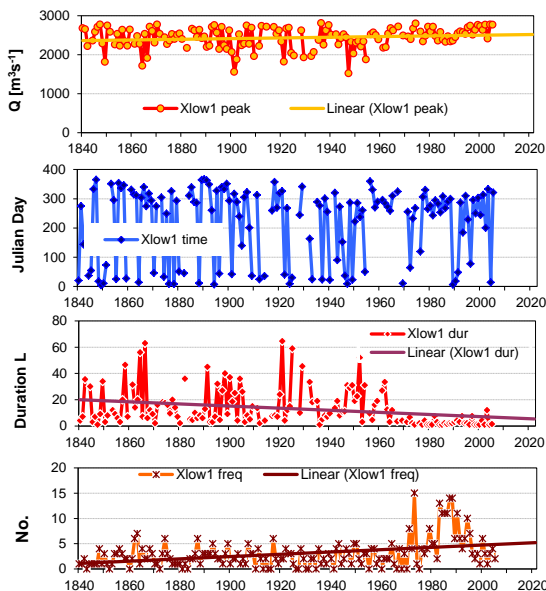
the Danube River are shown in Figs. 8b. The annual averages of extremely low flows have almost zero, resp. slightly increasing trend (tributaries Váh and Morava). The average duration decreases in all selected water gauging stations except the Váh station: Liptovský Mikuláš.



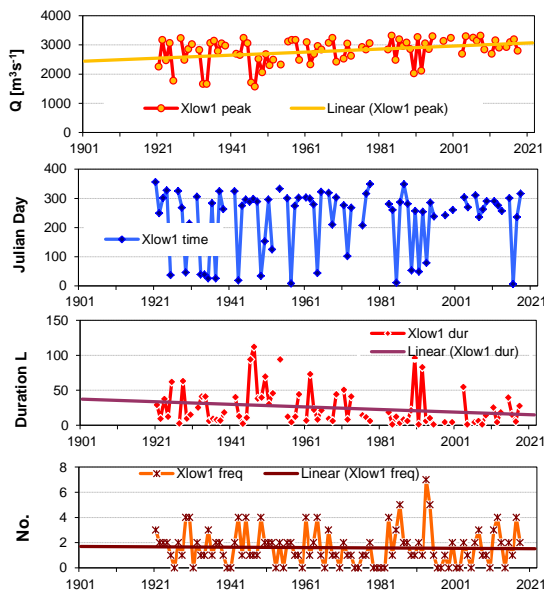
Danube: Hofkirchen



Danube: Bratislava

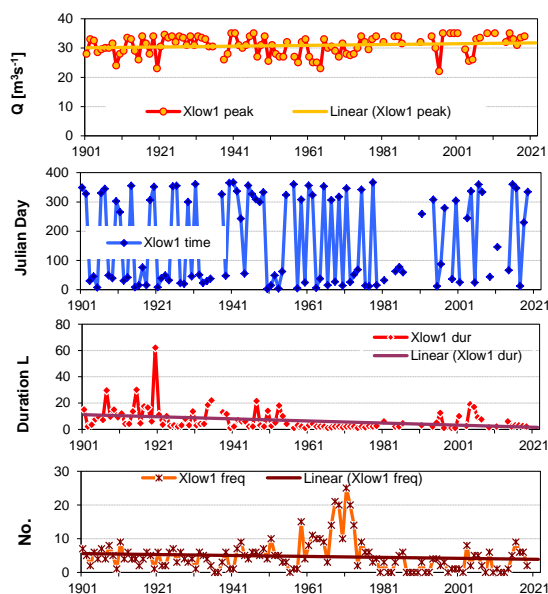


Danube: Orsova

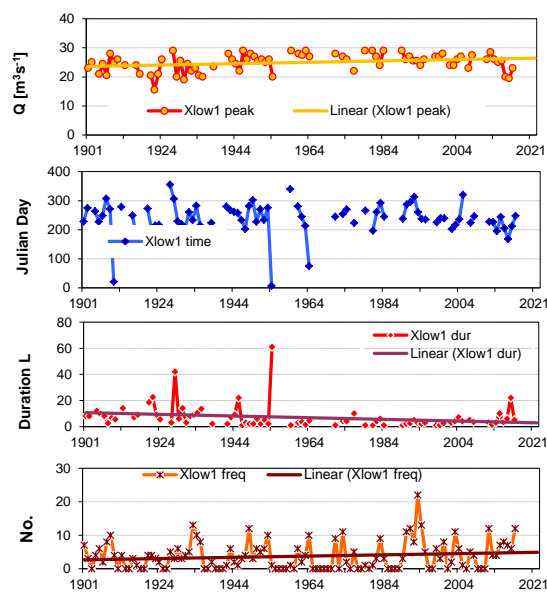


Danube: Reni

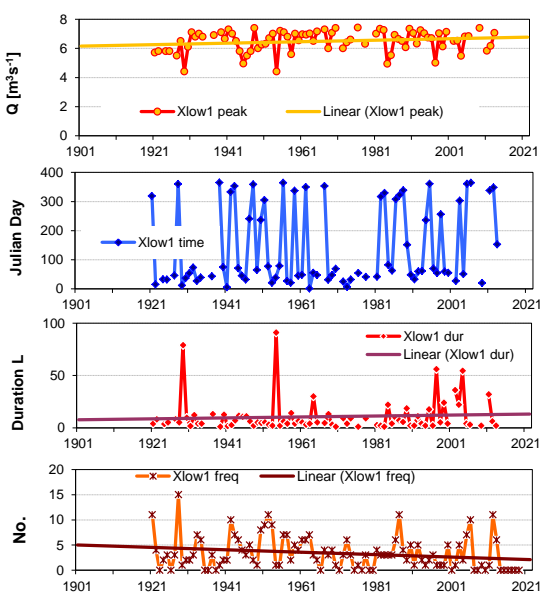
Fig. 8a. Evaluation of selected minimum flows characteristics (average of extremely low wave flows per year, day of occurrence, average duration of waves, number of waves per year). Danube: Hofkirchen, Bratislava, Orsova. and Reni, a linear trend.



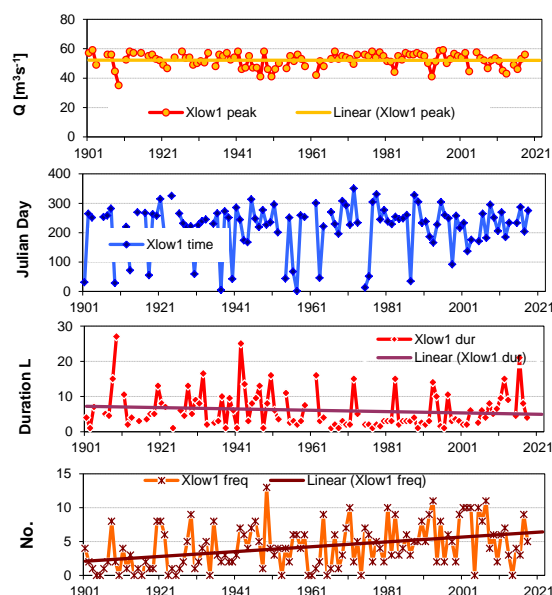
Lech: Landsberg



Morava: Moravský sv. Ján



Váh: Liptovský Mikuláš



Sava: Litija

Fig. 8b. Evaluation of selected minimum flows characteristics (average of extremely low wave flows per year, day of occurrence, average duration of waves, number of waves per year), selected Danube tributaries: Lech, Morava, Váh and Sava, linear trend.

## Conclusion

The presented contribution focused on a uniform evaluation of the occurrence of dry periods in terms of minimum flows of selected rivers in the Danube river basin. Water gauging stations in which observations have existed since at least 1921 were selected. The analysis shows that high and low-flow periods alternate along the entire length of the Danube (Fig. 5a). On the Danube,

minimal discharges occur in the same periods. In contrast, in the significant tributaries of the Danube Tisza and Sava rivers, droughts occur with a time shift – we could say that when dry years predominate in the Tisza, the Sava period is dominated by periods with higher flows (Fig. 5b). This is also true on a larger scale: in the years when extremely humid years prevailed in the Danube basin, more than 70% of US territory was affected by the longest drought. (Between 1933 and

1940, a known drought occurred in the United States under the name Dust Bowl, Andreadis et al., (2005); Ganguli and Ganguly (2016)).

The most extreme drought in the Hofkirchen water gauging station occurred in 1921. The time of occurrence of the droughts in the Orsova station is interesting. Dry seasons occurred around 1862/63, 1882/83, 1900, 1920/21, 1946/47, 1961/62, 1971, 1991/92 and 2017/19.

An extremely dry multi-year period occurred on the Danube at the Orsova station around 1863 and then around 1991. We do not consider these results to be final, further detailed analysis is needed. The results suggest that dry seasons occur more or less regularly. Dry periods occur at both lower and higher air temperatures. However, a higher air temperature increases the evaporation and there is less water in the streams – e.g. in Slovakia, despite higher precipitation, flows have been declining in recent years.

The evaluation of minimum flows and basic low flow characteristics is one of the basic bases for the design, construction and operation of water management facilities and facilities on streams for the purpose of economic management of water resources, therefore it is necessary to pay attention to these issues.

### Acknowledgement

*This study was supported by projects MVTs “Low flow and hydrological drought in Danube basin”, and APVV-20-0473 “Regional detection, attribution and projection of impacts of climate variability and climate change on runoff regimes in Slovakia”.*

### References

- Andreadis, K. M., Clark, E. A., Wood, A. W., Hamlet, A. F., Lettermaier, D. P. (2005): Twentieth century drought in the conterminous United States. *Journals Online, American Meteorological Society*, <http://journals.ametsoc.org/doi/abs/10.1175/JHM450.1>
- Balco, M. (1990): Malá vodnosť slovenských tokov. Veda, Bratislava, 260 s.
- Blinka, P. (2004): Klimatologické hodnocení sucha a suchých období na území ČR v letech 1876–2003. (Climatological evaluation of drought and dry periods in Czechia in the period 1876–2003). Rožnovský, J., Litschmann, T. (ed): Seminář „Extrémny počasí a podnebí“, Brno.
- Blinka, P. (2005): Klimatologické hodnocení sucha a suchých období na území České republiky v letech 1876–2002. (Climatological evaluation of drought and dry periods on the territory of Czech Republic in the years 1876–2002). Meteorologické zprávy, 58, 10–18.
- Bonacci, O. (1993): Hydrological identification of drought. *Hydrological Processes*, 7, 249–262.
- Brilly, M. (2010): Hydrological Processes of the Danube River Basin, Springer, 328 pp.
- Burger, F. (2005): Koncept a identifikácia hydrologického sucha - deficitu podzemnej vody. (The concept and identification of hydrological drought – groundwater drought). *Acta Hydrologica Slovaca*, 6, 1, 3–10.
- Byun, H.R., Wilhite, D.A. (1999): Objective Quantification of Drought Severity and Duration, *Journal of Climate*, 12, 2747–2756.
- Demeterová, B., Škoda, P. (2004): Porovnanie vybraných M-denných prietokov v období 1961–2000 a 1931–1980 na území Slovenska. (Comparison of M-day discharges in 1961–2000 and 1931–1980 at the territory of Slovakia). *Met. Čas.*, 7, 3, 137–142.
- Demeterová, B., Škoda, P. (2005): Režim minimálnych prietokov na slovenských tokoch v období 1961–2000 na staniách Národného Klimatického Programu. (Minimal discharges at the Slovak rivers in the period 1961–2000 at the stations of National Climate Programme). *Met. Čas.*, 8, 3, 155–163.
- Demeterová, B., Škoda, P. (2009): Malá vodnosť vybraných vodných tokov Slovenska. (Low flow in selected streams of Slovakia). *J. Hydrol. Hydromech.*, 57, 2009, 1, 55–69. DOI: 10.2478/v10098-009-0006-0.
- Dracup, J. A., Lee, K. S., Paulson, E. G. Jr. (1980): On the definition of droughts, *Water Resource Research*, 16, 297–302.
- Drako, J., Majerčáková, O. (1989): N-ročné minimálne prietoky. Zborník prác SHMÚ, 29/1, ALFA Bratislava, 307–380.
- Fendeková, M., Némethy, P. (1994): Low flows of Starohorsky Potok brook and their affecting factors. FRIEND: Flow regimes from International Experimental and Network Data, IAHS Publ. 221, 163–169.
- Fendeková, M., Poárová, J., Slivová, V., Eds. (2017): Hydrologické sucho na Slovensku a prognóza jeho vývoja (Drought and prognosis of its development in Slovakia) 1. vydanie. Bratislava, Univerzita Komenského, 2017. ISBN 978-80-223-4398-5, 300 s.
- Flynn, K. M., Kirby, W. H., Hummel, P. R. (2006): User's manual for program PeakFQ, Annual Flood Frequency Analysis Using Bulletin 17B Guidelines: U.S. Geological Survey Techniques and Methods Book 4, Chap. B4, 42 pp.
- Gao, Y., Vogel, R. M., Kroll, Ch. N., Poff, N. L., Olden, J. D. (2009): Development of representative indicators of hydrologic alteration. *Journal of Hydrology*, 374, 136–147. Doi: 10.1016/j.hydrol.2009.06.009.
- Ganguli, P., Ganguly, A. R. (2016): Space-time trends in U.S. meteorological droughts. *Journal of Hydrology: Regional Studies*, 8, 235–259.
- Halmová, D., Pekárová, P., Mészáros, I. (2011): Identifikácia zmien minimálnych denných prietokov vo vybraných staniách rieky Dunaj (Low flow change analysis in selected gauging stations on the Danube River). In: *Acta Hydrologica Slovaca*, Vol. 12, No. 2, 2011, 286–295.
- Hanel, M., Rakovec, O., Markonis, Y., Moravec, V., Máca, P., Kyselý, J., Samaniego, L., Kumar, R. (2019): Vyhodnocení změn výskytu sucha v dlouhodobé perspektive. In: Zborník abstraktov Sucho 2014–2018, jún 2019, ČHMÚ a VÚV TGM, Praha, 11–13. ([https://www.chmi.cz/files/portal/docs/ruzne/Sbornik\\_Sucho\\_komplet\\_web.pdf](https://www.chmi.cz/files/portal/docs/ruzne/Sbornik_Sucho_komplet_web.pdf))
- Hološ, S., Šurda, P. (2021): Evaluation of drought – review of drought indices and their application in the recent studies from Slovakia. *Acta Horticulturae et Regiotecturae – Special Issue/2021*, 97–108.
- Hisdal, H., Stahl, K., Tallaksen, L. M., Demuth, S. (2001): Have streamflow droughts in Europe become more severe or frequent? *Int. J. Climatol.*, 21, 317–333.
- Hrvol, J., Tomlain, J. (2008): Dlhodobý chod indexu sucha na vybraných staniách Slovenska za obdobie 1951–2007. In: 16. Medzinárodný posterový deň. ÚH SAV. Bratislava. 225–231.
- Klementová, E., Litschmann, T. (2001): Výsledky hodnotenia sucha v oblasti Hurbanova. Rožnovský, J., Janouš, D. (ed): Sucho, hodnocení a predikce. Pracovní seminář, Brno 2001.
- Kohnová, S., Poárová, J., Blaškovičová, L., Danáčová, M. (2021): Detection of changes in the mean monthly discharges on the Váh river basin in Slovakia. Public

- Recreation and Landscape Protection – With Sense Hand in Hand! Conference Proceedings, 146–149.
- Kukla, P., Boháč, M., Kourková, H., Šercl, P. (2019): Zhodnocení vývoje povrchových vod v roce 2018. (https://www.chmi.cz/files/portal/docs/ruzne/Sbornik\_Sucho\_komplet\_web.pdf) In: Zborník abstraktov Sucho 2014–2018, jún 2019, ČHMÚ a VÚV TGM, Praha, 3–7.
- Lešková, D. (1997): Selected statistical and probability characteristics of low flow. SVH, SHMÚ Bratislava, 57 s.
- Majerčáková, O. (1995): Niektoré problémy posudzovania malej vodnosti a minimálnych prietokov. Práce a štúdie 50, SHMÚ, Bratislava, 14–18.
- Majerčáková, O., Lešková, D., Šedík, P. (1995): Selected characteristics of low flows of Slovak rivers. *J Hydrol. Hydromech.*, 43, 4–5, 331–353.
- Majerčáková, O., Fendeková, M., Lešková, D. (1997): The variability of the hydrological series due to extreme climate conditions and the possible change of the hydrological characteristics with respect to potential climate change. IAHS Publ. 246, 59–66.
- Mathews, R., Richter, B.D. (2007): Application of the indicators of hydrologic alteration software in environmental flow setting. *Journal of the American Water Resources Association*, 43, 1400–1413.
- Mészáros, J. (2018): Rok 2017 v slovenskej časti povodia Moravy so zameraním na sucho (Year 2017 in the Slovak part of the Morava river basin with a focus on drought). In Zborník príspevkov: 30. konferencia mladých hydroológov [el. zdroj]. – Bratislava : Slovenský hydrometeorologický ústav, 2018, 1–12. ISBN 978-80-88907-98-5.
- Pekárová, P., Onderka, M., Pekár, J., Miklánek, P., Halmová, D., Škoda, P., Bačová Mitková, V. (2008): Hydrologic scenarios for the Danube river at Bratislava. Key Publishing Ostrava, 159 s.
- Smakhtin, V. U. (2001): Low flow hydrology, a review. *J. of Hydrol.*, 240, 147–186.
- Smakhtin, V. U., Hughes, D. A. (2007): Automated estimation and analyses of meteorological drought characteristics from monthly rainfall data. *Environmental Modelling & Software*, 22/6, 880–890.
- Stahl, K. (2001): Hydrological drought – a study across Europe. PhD. Thesis.
- Szolgay, J. (1977): On the study of monthly low flows. *J. Hydrol. Hydromech.* 25, 2, 135–144.
- Štěpánek, P. (2004): Homogenization of air temperature series in the Czech Republic during a period of instrumental measurements. In: Fourth seminar for homogenization and quality control in climatological databases (Budapest, Hungary, 6–10 October 2003), WCDMP-No. 56. WMO, Genova. 117–133.
- Tallaksen, L. M., Madsen, H., Clausen, B. (1997): On the definition and modeling of streamflow drought duration and deficit volume. *Hydrol. Sci. J.* 42, 1, 15–33.
- Tate, E. L., Gustard, A. (2000): Drought definition: a hydrological perspective, In: Drought and Drought Mitigation in Europe (ed. by J. V. Vogt and F. Somma), Kluwer Academic Publishers, the Netherlands, 23–48
- The Nature Conservancy (2007): Indicators of Hydrologic Alteration Version 7 User's Manual.
- The Nature Conservancy (2009): Indicators of Hydrologic Alteration, Version 7.1, User's Manual, 81 pp.
- Wilhite, D. A., Glantz, M. H. (1985): Understanding the drought phenomenon: The role of definitions, *Water International* 10, 111–120.

Ing. Dana Halmová, PhD. (\*corresponding author, e-mail: halmova@uh.savba.sk)

RNDr. Pavla Pekárová, DrSc.

RNDr. Pavol Miklánek, PhD.

Ing. Veronika Bačová Mitková, PhD.

Slovak Academy of Sciences

Institute of Hydrology

Dúbravská cesta 9

841 04 Bratislava

doc. RNDr. Ján Pekár, CSc.

Comenius University in Bratislava

Faculty of Mathematics, Physics, and Informatics

Department of Applied Mathematics and Statistics

Mlynská dolina,

842 48 Bratislava

## Groundwater response to extreme flows in the Danube River

Zinaw D. SHENGA\*, Andrej ŠOLTÉSZ, Danica LEŠKOVÁ

The presented paper deals with the numerical modeling of groundwater response to the extreme hydrological situations in the Danube River. A 3-D numerical groundwater modeling is carried out using MODFLOW (McDonald and Harbaugh, 1998) and Groundwater Modeling System (AQUAVEO, 2021) simulation packages for available hydrological, geological, and hydro-geological parameters to study how the groundwater responded to the flood event in the Danube River that occurred in June 2013.

KEY WORDS: Danube River, groundwater head, groundwater-surface water interaction, GMS MODFLOW package

### Introduction

The Danube River is the main hydrological factor that controls the formation and hydrodynamics of groundwater along its course in Bratislava and downstream. There is a continuous dynamic interaction between the groundwater and the Danube River. The water level in the river is located above the groundwater table throughout the whole year, and it permanently replenishes the groundwater reservoir. After the construction of the Gabčíkovo hydropower plant, the effect of the backwater of the reservoir is extended upstream up to Bratislava, i.e., the water level in the Danube is increased so as the groundwater at the vicinity of the river (Mucha et al., 1999). In addition, the groundwater regime became more stable after the implementation of the structure (Jarabíková et al., 2014). The process of this interaction is mostly very complex to solve. The seepage between the river and the adjacent aquifer system occurs along their entire intersection and it depends on the river stage, hydraulic head in the groundwater system, and the riverbed conductance (Winter et al., 1998).

The presented paper deals with the numerical modeling of groundwater response to the extreme hydrological situations in the Danube River. A 3-D numerical groundwater modeling is carried out for saturated flow conditions using MODFLOW (McDonald and Harbaugh, 1998) and Groundwater Modeling System (GMS) (AQUAVEO, 2021) simulation packages for available hydrological, geological, and hydro-geological parameters to study how the groundwater responded to the flood event in the Danube River that occurred in June 2013. Since the portion of the subsurface above the water

table is mainly composed of manmade ground, building constructions, and roads, saturated groundwater flow systems were considered for this specific work.

To calibrate the model parameters for both steady-state and transient flow including hydraulic conductivity and river conductance, observed groundwater heads in several boreholes of Slovak Hydrometeorological Institute (SHMI) were used (19 boreholes for steady state and 17 boreholes for transient flow). The results of the model are in good agreement with the observed data and therefore, the model can be used for studying and analyzing the changes and movements of the groundwater level in the aquifer in response to the extreme flow conditions in the Danube River. It could also be used as a base for further studies on pollutant movement from industrial and/or urban areas towards Rye Island along the Danube River. Specifically, the movements of pollutants from bombarded Apollo refinery could be the one that needs more attention as this region is currently accommodating construction of several high-rise buildings, where deep excavation takes place.

### Methodology

#### *Mathematical background*

MODFLOW, which was developed by the United States Geological Survey (USGS), can be used to simulate both steady and transient flow systems in confined, unconfined, or a combination of a confined and unconfined aquifer. McDonald and Harbaugh (1998), who developed the MODFLOW program, used a finite difference version of Eq. (1) to describe three-dimensional incompressible groundwater flow in

a heterogeneous and anisotropic medium, provided that the principal axes of the hydraulic conductivity are aligned with the coordinate directions.

$$\frac{\partial}{\partial x} \left( K_{xx} \frac{\partial h}{\partial x} \right) + \frac{\partial}{\partial y} \left( K_{yy} \frac{\partial h}{\partial y} \right) + \frac{\partial}{\partial z} \left( K_{zz} \frac{\partial h}{\partial z} \right) + W = S_s \frac{\partial h}{\partial t} \quad (1)$$

where

$K_{xx}$ ,  $K_{yy}$ ,  $K_{zz}$  – are values of hydraulic conductivity along the  $x$ ,  $y$  and  $z$  coordinate axes, which are assumed to be parallel to the major axes of hydraulic conductivity [ $L T^{-1}$ ],

$h$  – is the potentiometric aquifer head [ $L$ ],

$W$  – is a volumetric flux per unit volume and represents sources and/or sinks of water,  $W < 0.0$  for flow out of the groundwater system and  $W > 0.0$  for flow into the groundwater system [ $T^{-1}$ ],

$S_s$  – is the specific storage of the porous medium [ $L^{-1}$ ],

$t$  – is time [ $T$ ].

The river conductance ( $C$ ), which is a function of riverbed hydraulic conductivity and riverbed geometry, is calculated roughly based on Eq. 2. Below (Cousquer et al., 2017; Harbaugh, 2005). The concept of riverbed conductance was introduced in 1971 by Prickett and Lonquist and it is well described in MODFLOW as a river package (Cousquer et al., 2017).

$$C = \frac{KLW}{M} \quad (2)$$

where

$C$  – is riverbed conductance [ $L^2 T^{-1} L^{-1}$ ],

$K$  – is hydraulic conductivity of the riverbed material [ $L T^{-1}$ ],

$L$  – is the length of the river reach within the grid cell [ $L$ ],

$W$  – is the river width [ $L$ ],

$M$  – is the riverbed thickness [ $L$ ].

### Study area

The study region is a part of the Danubian Plain (Hreško et al., 2014) and it is located between the Danube River and the Little Carpathians. It includes different parts of Bratislava – bordered from the North by Little Carpathian, on Southwest by Danube River, on the Southeast by Little Danube, and on the Eastern side by Vajnory. The Danubian Plain is mainly known by a flat elevation which is created due to tectonic instability.

### Hydrology and Meteorology

The Danube River is the main hydrological factor that controls the hydrodynamics of groundwater in the major parts of the study area. There is a continuous dynamic interaction between the groundwater and the Danube River. Historic data about the water level of the Danube River at Bratislava gage is obtained from SHMI for the periods between 2002 and 2016. A minimum water level of 130.54 m a.s.l. was observed on 26.9.2004 at the Bratislava gauging station. However, a maximum water level of 138.65 m a.s.l. was observed on 6.6.2013. It is a historic record for the Bratislava gauging station. On the other hand, the average water level for the specified periods, 2002–2016, is 131.87 m a.s.l. as shown in Table 1 below.

On the other hand, mean annual precipitation of 720 mm is estimated by SHMI at Bratislava-Kolibá and 580 mm at Bratislava-Airport for 2002–2016. More than 60%

**Table 1. The minimum, maximum, and average water stage in the Danube River for the hydrologic year between 2003 and 2017 at Bratislava gage**

Hydrologic year	Minimum [m a.s.l.]	Maximum [m a.s.l.]	Average [m a.s.l.]
2003	130.84	134.54	131.82
2004	130.93	133.87	131.72
2005	130.54	135.55	131.89
2006	130.68	136.63	132.01
2007	130.87	136.17	131.66
2008	131.08	134.08	131.91
2009	130.92	136.85	132.04
2010	131.18	136.70	131.98
2011	131.01	135.95	131.68
2012	130.77	134.61	131.89
2013	131.07	138.65	132.26
2014	131.07	134.90	131.79
2015	131.07	134.57	131.77
2016	130.82	135.04	131.91
2017	130.88	134.25	131.73

of the precipitation falls between April and September.

### Geology and Hydrogeology

From the geological point of view, the study region is generally classified under Danube Plain. The subsoil is formed from Paleozoic, Neogene, and Quaternary sediments. The topmost layer is predominantly covered by made ground, which is mainly created due to anthropogenic activities. It is then followed by quaternary sediments, which appear to be chaotically arranged, and their composition changes horizontally over a very short distance.

The thickness of gravel-shaped fluvial sediments in the area ranges from 8 to 18 m. This part of the aquifer has high hydraulic conductivity ( $10^{-4}$  to  $2 \times 10^{-2} \text{ m s}^{-1}$ ). Based on data about groundwater head from SHMI, the water table is located from 3 to 8 m below the terrain. There is no significant fluctuation in the groundwater level throughout the year. The groundwater in the study area has a free surface, and it is connected directly to the surface water. A large amount of groundwater reservoir in the study area is found in Quaternary Sediment, which is located a few meters below the terrain.

There is a clear hydraulic connection between groundwater and the Danube River. The groundwater level increases or decreases based on the water level in the Danube River. However, a study conducted by (Mucha et al., 1999) indicated that the level of groundwater increased in the study region since Gabčíkovo's water work was put into operation. Water from the river always (throughout the year) infiltrates to the groundwater reservoir which is bound to

the Quaternary Sediment. The groundwater heads in selected SHMI observation wells which are located along the Danube River (the locations of each well can be seen in Fig. 3) for the 2013 flood events are shown in Fig. 1 below.

### Conceptual Model

The GMS MODFLOW package, which is used to solve the finite-difference equation of groundwater flow, requires many spatial and non-spatial data inputs. Therefore, input data collection, creation, and analysis will be an important component in this study. Most of the spatial data will be created from terrain analysis of the Digital Elevation Model (DEM) which is processed using different approaches. Then the stream networks and hillslopes are created from terrain analysis of the processed DEM. Archive data about groundwater hydrology for the period of 2002 to 2019 is obtained from the Slovak Hydrometeorological Institute. Based on the request, the SHMI institute also provided precipitation data from Bratislava-airport and Bratislava-Koliba stations. Specifically, weekly precipitation data is obtained from 2002 to 2016 to estimate the effective recharge rate. The thickness and values of horizontal hydraulic conductivities of the aquifer were collected from archive data of State Geological Institute of Dionýz Štúr (SGIDŠ).

### Model setup and Boundary Conditions

Construction of groundwater model consists of series of steps and requires several input data. For setting up a quality numerical model, the first and the most

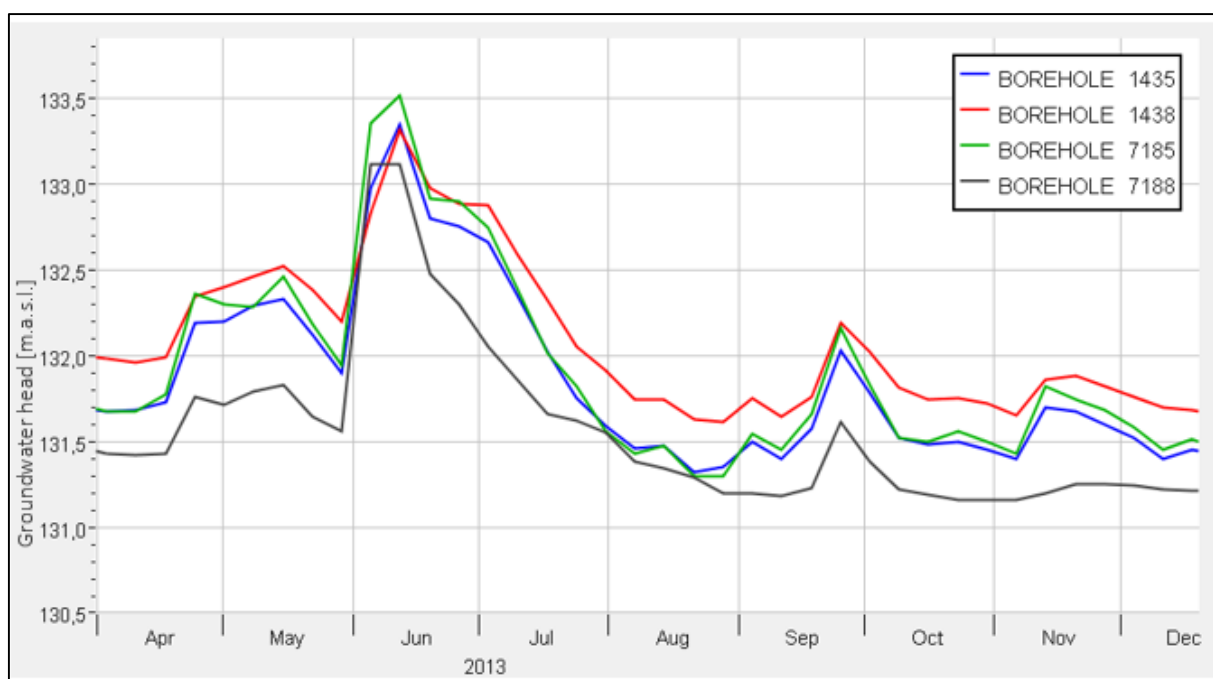


Fig. 1. Groundwater head in selected SHMI observation wells for the 2013 flood events in m a.s.l.

important step is developing a conceptual model that physically describes the natural groundwater water system. On the other hand, the mathematical model is used to describe the system using numerical procedures or mathematical algorithms.

The boundary of the model is created by considering surface water divides and the physical topography of the study area. The processed input data were used to create a conceptual model which is associated with calculation grids. Horizontally, finite-difference computation networks of 236 columns by 374 rows were discretized. Four model layers were created to divide the aquifer in the vertical direction.

The assigned boundary conditions for the steady state simulation include specified head for the Danube River on the western side, the artificial boundary condition of general head on the eastern side, general head in the Little Danube on the southern side, and flux to the boundary on the northern side of the boundary. As there is no significant change on the Danube River stage due to water exchange with the aquifer, the river is used as a specified head boundary. The specified heads at the nodes are determined by both interpolation and extrapolation of measured average stages (Devin and Bratislava stations) in the Danube River. There is no barrier to flow as the aquifer is directly connected to the river channel. The boundary condition along the Little Danube is assumed to be a general head that acts as an infinite sink for water to leave the boundary of the model. The flux to the boundary accounts for specified flow from Little Carpathian Mountain to the model area.

The transient simulations were carried out by considering the flood event in the Danube River at the Bratislava gauging station which occurred in June 2013. The water level in the Danube River was started to rise at the end of May and reached a peak level of 138.65 m a.s.l. with

a culminated discharge of  $10\,641\text{ m}^3\text{ s}^{-1}$  on June 6 (Pekárová et al., 2013). It was recognized as one of the historic records and the water level was above the 3<sup>rd</sup> level flood stage for a couple of days, see Fig. 2 below.

## Results

### Steady state flow

For study state flow, different input parameters were manually (trial-and-error method) calibrated to match the simulated and observed groundwater heads. Great attention is given to horizontal hydraulic conductivities, river conductance, and flux to the model. During calibration, the hydraulic head data of 16 SHMI observation wells were used. The horizontal hydraulic conductivities, which were obtained from SGIDŠ, were adjusted by trial-and-error method. The calibrated results were in the order of  $10^1$  to  $10^2\text{ m day}^{-1}$ . Trial-and-error methods were chosen due to the fact that the hydraulic conductivities in the study area changes in a very short distance because of the complexity of the aquifer. Thus, it was difficult to use the common zonation method for automated parameter estimation. On the other hand, due to a lack of data about riverbed thickness and its hydraulic conductivity, the river conductance ( $C$ ) was calculated roughly using Eq. 2. Then, the calculated riverbed conductance was adjusted by trial-and-error during the calibration process, as well.

In GMS MODFLOW, the quality of the calibration can be evaluated using some statistical indices like mean error, mean absolute error or mean root square error. The results after calibration show that there is good agreement between the simulated and observed groundwater head ( $\pm 0.50\text{ m}$ ), thus, the model can be used for further study as shown in Fig. 3 and Table 2 below.

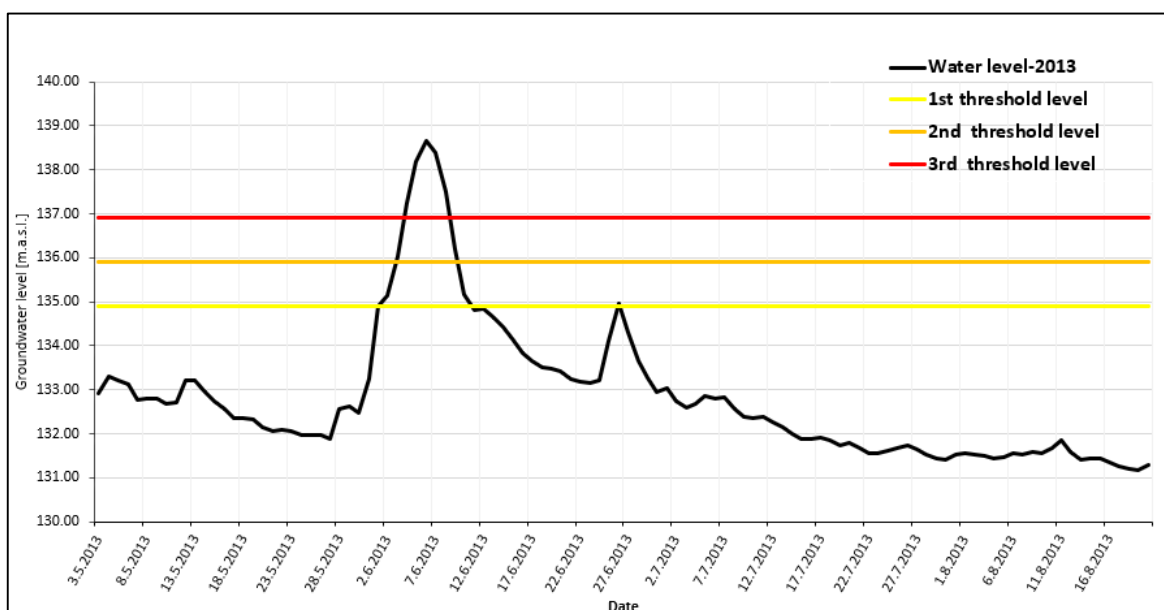


Fig. 2. The water level in the Danube River at Bratislava gauging station during a flood event in 2013 and proposed flood threshold levels by SHMI.

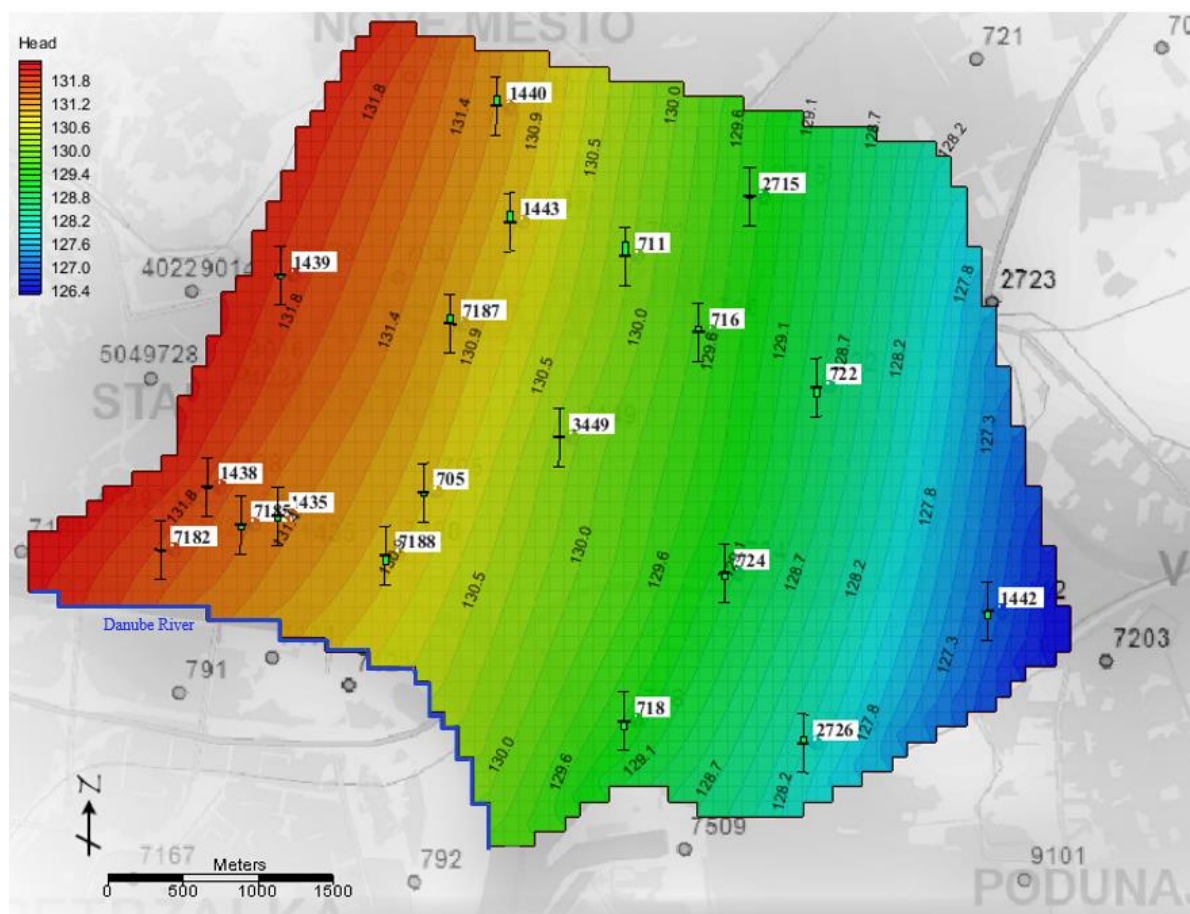


Fig. 3. Simulation result that shows calibrated groundwater head as a contour map [m a.s.l.] and location of SHMI observation wells.

Table 2. Comparison between observed and calculated groundwater heads for the steady state flow condition

Borehole ID	Observed head [m.a.s.l.]	Simulated Head [m.a.s.l.]	Differences [m]
705	130.95	130.86	0.10
711	129.62	130.11	-0.49
716	129.41	129.59	-0.18
718	129.61	129.31	0.30
722	129.07	128.75	0.32
724	129.30	129.09	0.21
1435	131.56	131.38	0.18
1438	131.77	131.72	0.05
1439	131.95	131.87	0.08
1440	130.74	131.11	-0.37
1442	127.24	126.98	0.26
1443	130.50	130.86	-0.36
2715	129.44	129.39	0.05
2726	127.92	128.13	-0.21
3449	130.15	130.19	-0.04
7182	131.80	131.73	0.07
7185	131.65	131.49	0.16
7187	130.69	131.01	-0.32
7188	131.23	130.91	0.32

As it can be seen from Fig. 3 above and Table 2 below, the calibrated groundwater in the boreholes has shown a good match except borehole ID 711, where the difference between simulated and observed groundwater head was about -0.49 m. The negative sign indicates the computed groundwater head is greater than the observed groundwater head.

### Transient flow

The transient simulation was carried out based on the hydrological situation in the Danube River. Specifically, the flood event which occurred in 2013 was the main period where detailed attention was given. The calibrated steady state, which was based on the average water level in the Danube River, was used as an initial condition or as starting head for the transient simulation. The transient calibration was carried out to adjust aquifer storage, specific yield, riverbed conductance, and hydraulic conductivities of the aquifers. The calibration was also carried out by the trial-and-error method. The calibrated values were as follows: specific yield = 0.22, specific storage = 0.00067. The increase in water level in the Danube River caused a significant change in groundwater level in the narrow adjacent area. However, the change in water level was insignificant (almost negligible) in the areas far from

the banks of the river as shown in Fig. 4 and 5. This might indicate that there is a parallel flow of groundwater along the river during the transient state.

The simulation results also showed that the flow of the groundwater is towards the southwest of Slovakia, where Rye Island (Žitný Ostrov) is located. Rye Island, which is one of the biggest river islands in Europe, is located between the Danube, Little Danube, and Vah Rivers. The island is the biggest source of drinking water reservoirs and agricultural products in Slovakia (Michalko et al., 2015). The rise in the water table and groundwater flow towards this area could have positive and negative impacts. As a positive impact, groundwater around Rye Island could be recharged. As a negative impact, there might be movement of toxic contaminants from bombed Appolo refinery, which is in Bratislava at the banks of the Danube River, along with groundwater flow during peak hydrological situations. This is because of the fact, that the groundwater in the region of Danubian Lowland is mainly recharged from the Danube River and the increase in the water level facilitates high movement of polluted groundwater. Additionally, the undergoing construction of several high-rise buildings around the bombed Appolo refinery could disturb the accumulated refinery and facilitates pollutant movements along with the Danube River towards the Rye Islands.

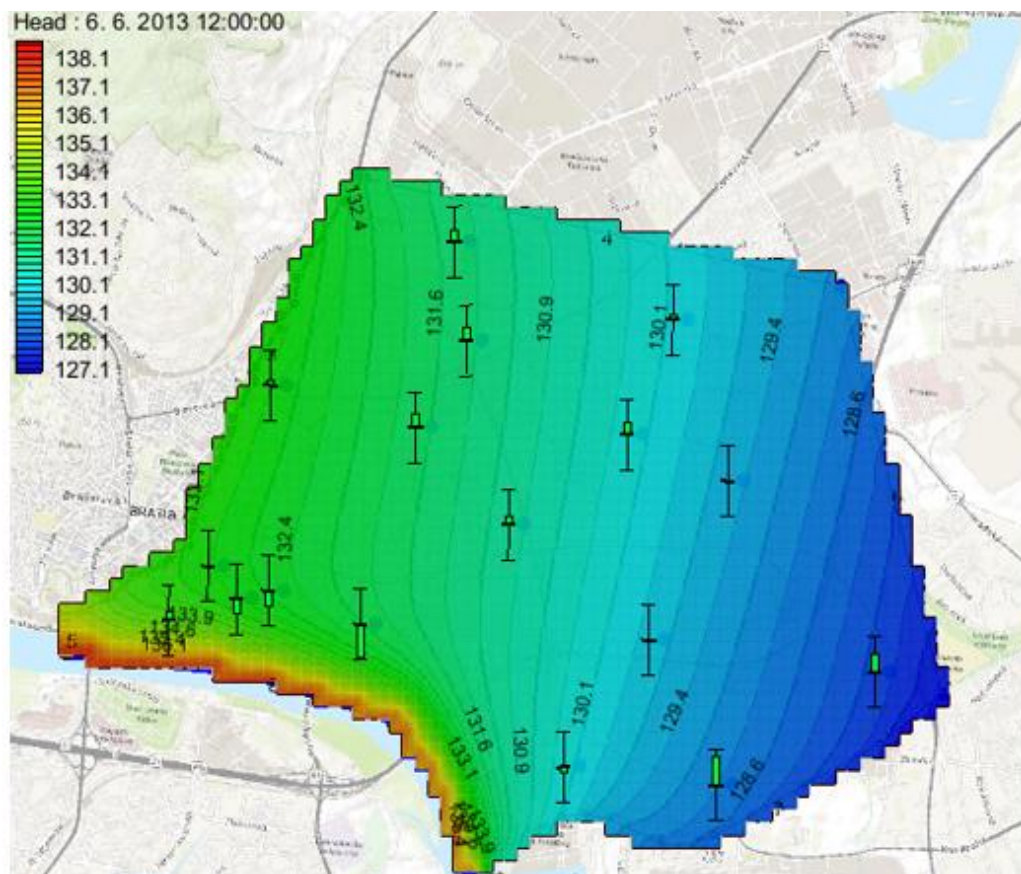


Fig. 4. Course of simulated and observed groundwater head in borehole-7188, which is located close to Danube River, Appolo bridge (the weekly observed groundwater head is converted to daily observed head).

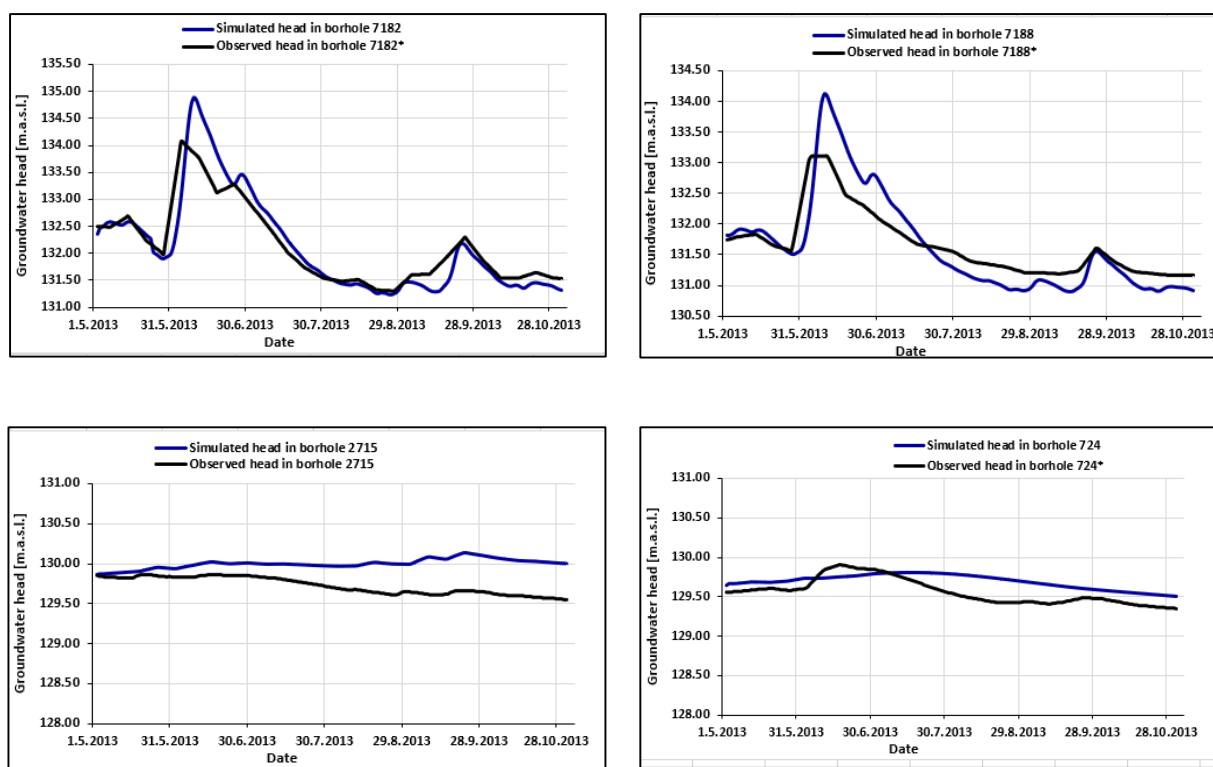


Fig. 5. The course of simulated and observed groundwater head in selected boreholes (boreholes 7182 and 7188 are located very close to the Danube River and the others are relatively far). \*Observed weekly data, which is obtained from SHMI is converted to daily data.

## Conclusion

A 3-D groundwater flow was modeled to investigate the interaction between aquifer and river. The main analysis was focused on a transient flow for specific flood events that occurred in 2013. Even though most of the simulated transient heads matched the observed head in boreholes of SHMI during the flood events, certain lag time differences were observed in some of them (i.e., short lag time between observed and simulated peak heads). The obtained results could be used as relevant information for water resources planning and management. It could also be used as a base for further study on contaminant movement from Bratislava towards Rye Island along the Danube River. Specifically, the movements of pollutants from bombed Apollo refinery could be the one that needs more attention as this region is currently accommodating construction of several high-rise buildings. Most of such construction requires deep excavation work (below groundwater level) and pumping of groundwater during and after construction. These activities may facilitate the movements of pollutants during peak flows in the adjacent river. Therefore, certain technical measures should be considered in this region to avoid or minimize movements of pollutants during flood events in the Danube River.

## Acknowledgments

This work was supported by the Slovak Research and Development Agency under Contract no. APVV-19-0340 and APVV-19-383.

## References

- AQUAVEO website (2021): URL: <https://www.aquaveo.com/software/gms-groundwater-modeling-system-introduction>, Groundwater Modeling System (GMS), [Accessed during March].
- Cousquer, Y., Pryet, A., Flipo, N., Delbart, C., Dupuy, A. (2017): Estimating River Conductance from Prior Information to Improve Surface-Subsurface Model Calibration, National Ground Water Association, 11 pp.
- Harbaugh, A., W. (2005) MODFLOW-2005 The U.S. Geological Survey Modular Ground-Water Model—the Groundwater Flow Process. U.S. Geological Survey Techniques and Methods 6–A16, 253.
- Hreško, J., Petrovič, F., Hrozenská, S., Mišovičová, R., Rybanský, L., Petluš, P. (2014): Archetypes of Lowland Fluvial Landscape of Slovakia. *Životné prostredie*, 48, 1, 33 – 37 (in Slovak language).
- Jarabicová, M., Pásztorová, M., Vitková, J., Minarič, P. (2014): Diagnosis of the impact of the Gabčíkovo Water Project on soil water regime in the surroundings, *Acta horticulturae et regioteuriae* 2, 48–51.
- McDonald, M. G., Harbough, A. W. (1998): A Modular

- Three-Dimensional Finite-Difference Ground-Water Flow Model. Geological Survey, Open File Report 83– 875; US Geological Survey: Reston, VA, USA.
- Michalko, J., Bodiš, D., Ženišová, Z., Malík, P., Kordík, J., Čech, P., Grolmusová, Z., Luptáková, A., Bottlik, F., Švasta, J., Káša, Š. (2015): Groundwater and surface water interactions in the Podunajská Nížina Lowland and Trnavská Pahorkatina hills. Slovak Association of hydrologists, *Podzemná voda*, 21(1), 2015, 24–39.
- Mucha, P., Rodak, D., Hlavaty, Z., Banský, L., Kucarova, K. (1999): Development of groundwater regime in the area of the Gabčíkovo Hydroelectric Power Project, Slovak Geological Magazine, 5, 151–167.
- Pekárová, P., Halmová, D., Bačová, M., Miklánek, P., Pekár, J., Škoda, P., (2013): Historic flood marks and flood frequency analysis of the Danube River at Bratislava, Slovakia. *Journal of Hydrology and Hydromechanics*, 61(10.2478/johh-2013-0041), 326–333.
- Winter, T. C., Harvey, J. W., Franke, O. L., Alley, W. M. (1998): *Ground Water and Surface Water A Single Resource*. Denver (Colorado): U.S. Department of the Interior Bruce Babbitt, Secretary.

Ing. Zinaw D. Shenga (\*corresponding author, e-mail: zinaw.shenga@shmu.sk)

Ing. Danica Lešková, PhD.

Slovak Hydrometeorological Institute

Jeséniova 17

833 15 Bratislava

Slovak Republic

prof. Ing. Andrej Šoltész, PhD.

Slovak University of Technology in Bratislava

Vazovova 5

812 43 Bratislava

Slovak Republic

**Comparison of winter design floods between Austrian and Ukrainian  
Danube River tributaries**Tetiana ZABOLOTNIA\*, Borbala SZELES, Liudmyla GORBACHOVA,  
Juraj PARAJKA, Rui TONG

The consequences of large-scale floods in several regions have drawn attention to prevention and protection of territories from such natural phenomena. Therefore, it is important to determine the expected magnitudes of floods, their differences, as well as to understand the factors controlling the magnitude of snowmelt design floods. This paper compares snowmelt design floods in 24 catchments situated in two regions in Austria (the upper Steyr River Basin) and Ukraine (the upper Rika River Basin). The two regions are similar in terms of catchment sizes and elevation but differ in climate characteristics, because the Ukrainian catchments are influenced by increased continentality. The aim of this paper is thus to compare the magnitude of design floods with 2-, 5-, 10-, 50-, and 100-year return periods occurring during the cold periods of the year (November–April). The objective is to estimate design values of winter floods and to explore factors controlling their differences. The results show that the design floods scaled with catchment area are larger in the upper Rika River Basin (Ukraine) than in upper Steyr River Basin (Austria) for all examined periods. The winters in Ukrainian catchments tend to be warmer and occur earlier. The magnitude of scaled floods in Ukrainian catchments is larger, even the mean annual maximum snow depth ( $D_{mam}$ ) is approximately 40% lower than in the Austrian catchments. The results of this initial analysis can improve the understanding and hence management of water resources in catchments with similar hydrological characteristics, but slightly different climate characteristics.

KEY WORDS: flood frequency analysis, design floods, winter floods, climate zones

**Introduction**

Floods are one of the most pressing societal issues catchment hydrology has to face. Flood frequency hydrology is based on the extreme river flow data analysis to obtain the probability distribution of floods (Merz and Blöschl, 2008). The previous flood frequency studies showed that one of the statistical approaches mostly used to model design flood data (Zelenhasic, 1970; Mujere, 2011; Bertola et al., 2020) and often provided the best fit is the Gumbel distribution (Onen and Bagatur, 2017). However, it is still not well understood which factors are causing the differences in design flood magnitude in different regions (Blöschl et al., 2019).

The seasonality assessment of floods in the Alp-Carpathians region (Jeneiova et al., 2016; Parajka et al., 2010) indicates that while summer floods are dominant in the Alps, winter floods occur mainly in the northern upper Danube River tributaries. The timing of winter floods there is very diverse (Jeneiova et al., 2016), which impacts the flood magnitude.

This study presents a comparison the magnitude of design winter floods in two regions (Ukraine and Austria) situated in the Danube River catchment. The increased

continentality of Ukrainian catchments is hypothesized to explain the difference in design flood magnitudes in selected study regions.

**Material and methods****Study area**

This study is carried out for small and medium size Ukrainian and Austrian, unaffected mountainous catchments of the Danube River Basin (Fig. 1). The Austrian part consists of ten catchments (6 small and 4 medium) located in the upper Steyr River basin, which belongs to the Upper Danube River Basin (Table 1). The 14 Ukrainian catchments (12 small and 2 medium) are situated in the upper Rika River basin, which belongs to the Central Danube River Basin (Table 2). The mean catchment elevation for the Austrian catchments is slightly higher (ranging between 951 and 1506 m a.s.l.) than for the Ukrainian catchments (ranging between 747 and 1000 m a.s.l.) (Table 1 and 2). The catchment areas in the upper Steyr River range from 18 to 545 km<sup>2</sup>, while they range from 3.2 to 550 km<sup>2</sup> in the upper Rika River. The study river basins have different forest cover, from

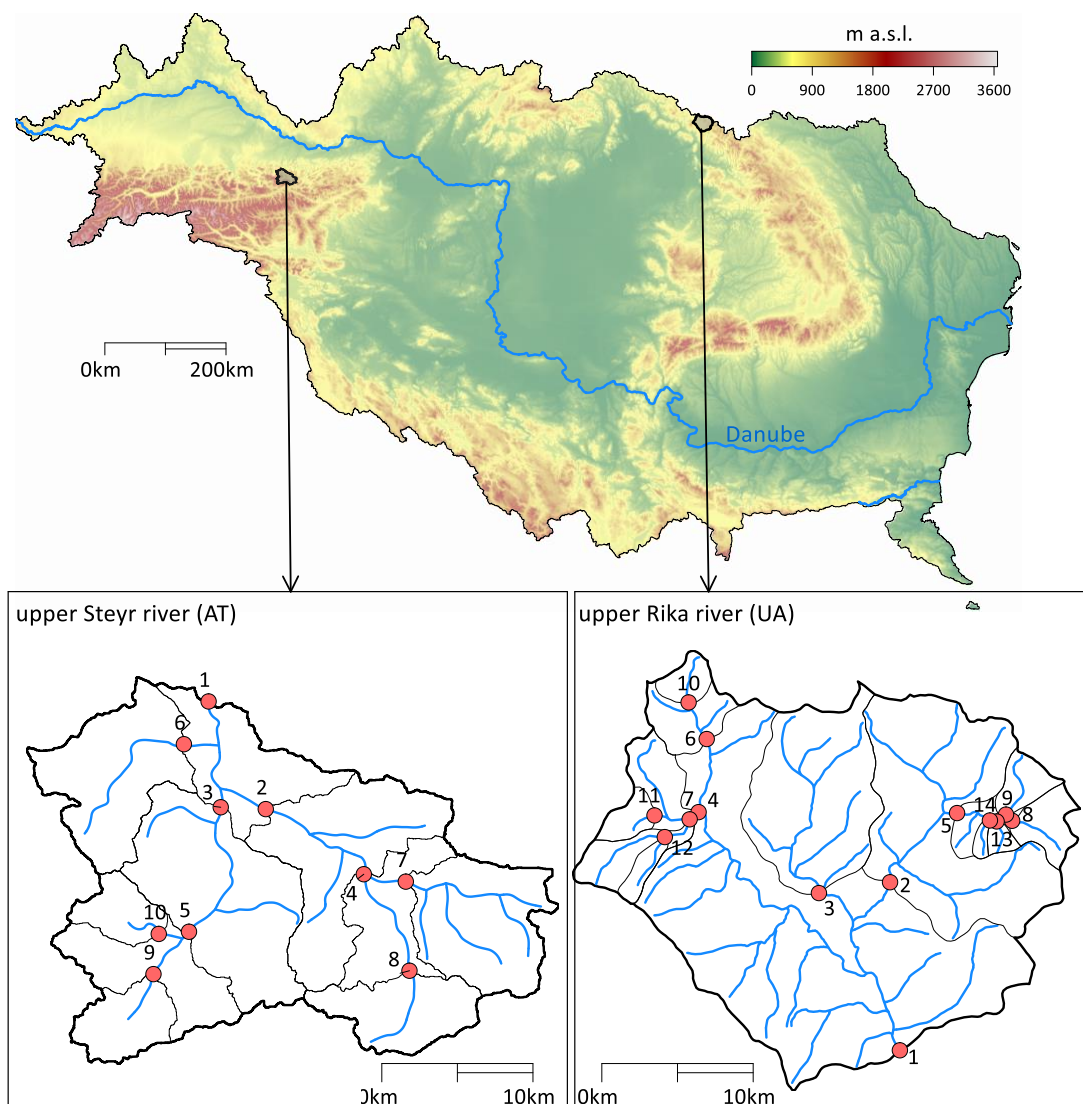


Fig. 1. Study area: location of Austrian (bottom left panel) and Ukrainian (bottom right panel) catchments in the Danube River basin. Labels of symbols refer to ID number in Table 1 (upper Steyr river, Austria) and Table 2 (upper Rika River, Ukraine).

**Table 1. Characteristics of the Austrian catchments (area, forest cover) and the corresponding gauging station (mean elevation) and the length of the study period**

ID	Gauge	Area [km <sup>2</sup> ]	Mean elevation [m a.s.l.]	Forest cover [%]	Study period
1	Steyr River – Klaus an der Pyhrnbahn	542	1059	65	1952–2016
2	Teichl River – St. Pankraz	233	1009	63	1976–2016
3	Steyr River – Kniewas	185	1213	58	1952–2016
4	Teichl River – Teichlbrücke	149	1015	61	1952–2016
5	Steyr River – Hinterstoder	82	1358	46	1977–2016
6	Steyrling River – Steyrling	72	951	85	1957–2016
7	Dambach River – Windischgarsten	67	1016	63	1972–2016
8	Teichl River – Spital am Pyhrn	40	1205	71	1967–2016
9	Steyr River – Dietlgut	25	1375	46	1952–2016
10	Krumme Steyr River – Polsterlucke	16	1506	38	1977–2016

**Table 2. Characteristics of the Ukrainian catchments (area, forest cover) and the corresponding gauging station (mean elevation) and the length of the study period**

ID	Gauge	Area	Mean elevation	Forest cover	Study period
		[km <sup>2</sup> ]	[m a.s.l.]	[%]	
1	Rika R. – Mizhhiria v.	550	800	41	1958–2016
2	Rika R. – Verkhniy Bystryi v.	165	920	64	1958–2016
3	Holiatynka R. – Maidan v.	86	790	40	1958–2016
4	Pylypets R. – Pylypets v.	44	854	19	1958–2016
5	Lopushna R. – Lopushne v. (nyzhn.)	37	897	78	1958–2016
6	Studenyi R. – Nyzhniy Studenyi v.	25	800	18	1958–2016
7	Ploshanka S. – Pylypets v. (nyzhn.)	20	983	29	1958–2016
8	Lopushna R. – Lopushne v. (verkh.)	13	925	93	1960–2016
9	Branyshe S. – Lopushne v.	10	916	72	1958–2016
10	Studenyi R. – Verkhniy Studenyi v.	8	809	20	1959–2016
11	Pylypets R. – Podobovets v.	7.4	747	12	1958–2016
12	Pylypetskyi S. – Pylypets v.	5.7	1000	37	1958–2016
13	Ziubrovets S. – Lopushne v.	3.2	871	91	1958–2016
14	Seredniy Zvir S. – Lopushne v.	2.2	984	95	1958–2016

*R. – River; S. – Stream; v. – village*

38% (Krumme Steyr River – Polsterlucke) to 85% (Steyrling River – Steyrling) in the Austrian basins, and from 12% (Pylypets River – Podobovets village) to 95% (Seredniy Zvir Stream – Lopushne village) in the Ukrainian basins (Table 1 and 2).

According to the Köppen-Geiger climate classifications system (Kottke et al., 2006) the entire Ukrainian study area is located in the warm summer continental climatic zone, while most of the analyzed Austrian catchments belong to the temperate oceanic climatic zone. This means that the Ukrainian catchments experience an increased continentality effect, which can translate to the difference in snow accumulation and melt processes and mechanisms of flood generation in the cold period of the year.

### Data

The discharge data for this study are obtained from the Hydrographic Service of Austria (<https://ehyd.gv.at/>) and from the archive of the Central Geophysical Observatory of Ukraine. The analysis is based on mean daily discharges ( $Q_{mean}$ ). The winter flood maxima ( $Q_{max}$ ) are selected from the winter half-year (November–April). The length of the series is various. The longest series are in four Austrian gauges: Steyr River – Klaus an der Pyhrnbahn, Steyr River – Kniewas, Teichl River – Teichlbrücke and Steyr River – Dietlgut (1952–2016); while the shortest series are collected in two Austrian catchments: Krumme Steyr River – Polsterlucke and Steyr River – Hinterstoder (1977–2016) (Table 1). The study period for most Ukrainian gauges is 1958–2016 (Table 2).

Snow depth data are obtained from one Austrian and one Ukrainian station, which are located approximately at the same elevation. Daily snow depth data (D) for the Austrian catchments, for the period 1970–2016, is obtained from a station at Spital am Pyhrn located at 630 m a.s.l. Five daily snow depth data for the Ukrainian

catchments, for the period 1935–2016, is obtained from a station at Nyzhniy Studenyi located at 629 m a.s.l. (from 1952 located at 615 m a.s.l.).

### Methods

The basic assumptions for the application of the flood frequency analysis are the following:

- the observations are identically distributed, statistically independent and random,
- the annual maximum daily discharges ( $Q_{max}$ ) measurements are stationary with respect to time (data series homogeneity). This requires that the river has not been regulated within the duration of the time series, i.e. not affected by human modifications such as reservoir, urbanization, etc.,
- observed daily discharge data are available for more than 10 years with good quality. Only such data are deemed sufficient for the estimation of design flood values associated to low return periods.

### Hydro-genetic analysis

The assessment of the homogeneity and stationarity of winter floods is based on hydro-genetic analysis proposed by Gorbachova (2014). The method uses the mass curve, the residual mass curve and the combined graph to identify long-term fluctuations and cycles of winter floods. Homogeneity is defined as the absence of unidirectional changes of the flood time series against the backdrop of their variability due to long-term cyclical fluctuations (Gorbachova et al., 2018). The stationarity of winter floods time series is characterized by the persistence of average floods over time if the time series have at least one full closed cycle (dry and wet phase) of long-period fluctuations. More details about assumptions and applications of the methodology are presented in Gorbachova (2016) and Zabolotnia et al. (2019).

### Flood frequency analysis

In order to estimate the design floods with 2, 5, 10, 20 and 100 year return periods, a direct, at site frequency analysis is chosen. First, a sample of annual daily flood maxima is compiled for each gauge. For each year, the maximum daily discharge value in winter period (November–April) is selected. Second, the plotting positions, i.e. the empirical return periods  $T_s$  are estimated according to (1)

$$T_s = \frac{1}{1-F_s} \quad (1)$$

where

$F_s$  – is the return probability or cumulative frequency, which can be calculated according to (2)

$$F_s = \frac{k}{1+N} \quad (2)$$

where

$k$  – rank of each flood peak, ranging between 1 and  $N$ ,  
 $N$  – total number of observed peaks.

Third, a distribution function is fitted to the data. In this study, the Gumbel distribution is chosen (Gumbel, 1954). The cumulative distribution function  $F(x)$  of the Gumbel distribution is as follows (3)

$$F(x) = \exp \left[ -\exp \left( -\frac{x-c}{d} \right) \right] \quad (3)$$

where

$x$  – random variable, in this case daily flood maximum,  
 $c, d$  – parameters of the distribution, which are estimated from the flood data.

As a final step, the design flood with a specific return period  $x_T$  is calculated, according to (4)

$$x_T = c - d \cdot \ln \left[ -\ln \left( 1 - \frac{1}{T} \right) \right] \quad (4)$$

where

$T$  – return period (in years) and the parameters can be estimated based on the method of moments according to (5)

$$d = \frac{\sqrt{6}}{\pi} \cdot \sigma \quad \text{and} \quad c = \mu - 0.5772 \cdot d \quad (5)$$

where

$\mu$  – mean,  
 $\sigma$  – standard deviation,  
 0.5772 – Euler-Mascheroni constant.

The calculations are performed in R (R Core Team, 2016) that is an open-source programming language and software environment for statistical computing (linear and nonlinear modelling, classical statistical tests, time-series analysis, classification, clustering, etc.) and graphics. It includes an effective data handling and storage facility, a suite of operators for calculations on

arrays, in particular matrices, a large, coherent, integrated collection of intermediate tools for data analysis and others.

### Seasonality of winter floods

The mean seasonality and the variability of the winter floods is assessed for the two largest catchments, i.e. Steyr River – Klaus an der Pyhrnbahn and Rika River – Mizhhiria village, using the Burn index (Burn, 1997; Parajka et al., 2009). First the day of the year is calculated for each peak. Then the day of the year values are transformed into angles, i.e. each peak is treated as a unitary vector in the direction of the calculated angle; and the average of the vectors is calculated in order to obtain the mean seasonality. The variability of the seasonality is expressed as the length of the mean seasonality vector, which can range between zero (uniform distribution) and one (all extremes occur on the same day).

## Results and discussion

### Hydro-genetic analysis

The assessment of the homogeneity and stationarity of the winter floods in the upper Rika River basin and its tributaries according to Gorbachova's methodology shows that the series of observations for all 14 study gauges are homogeneous and stationary (Bauzha and Gorbachova, 2013; Gorbachova et al., 2018; Zabolotnia et al., 2019; 2021).

The mass curves of the winter and spring floods in the upper Steyr river basin are not characterized by "jumping", "emissions" or unidirectional deviation and do not break the general trend of the curve, which indicates that the climatic conditions and flood generation processes in the study area are homogeneous (Fig. 2). Therefore, the series of observations in the Austrian catchments are also homogeneous and stationary in accordance with the hydrological genetic (graphical) methods. Fig. 2 shows only 3 out of 10 gauges, as the other 7 have similar trends in discharge fluctuations.

### Flood frequency analysis

The estimated flood design values ( $Q_T$ ) and observed minimum ( $Q_{min}$ ) and maximum ( $Q_{max}$ ) winter floods for Austrian and Ukrainian catchments are presented in Tables 3 and 4. The flood frequency analysis shows that the largest flood (with maximum instantaneous flow of  $246 \text{ m}^3 \text{ s}^{-1}$ ) in the upper Steyr River is the event of 1962, which corresponds to an empirical return period of 66 years, while the lowest flood flow of  $2.7 \text{ m}^3 \text{ s}^{-1}$  was recorded in 1953. For the upper Rika River the maximum flow of  $471 \text{ m}^3 \text{ s}^{-1}$  was observed in 1958, which has an empirical return period of 60 years, while the lowest flood flow of  $55.1 \text{ m}^3 \text{ s}^{-1}$  was observed in 2015.

The estimated flood frequency curves for Austrian and Ukrainian catchments are presented in Fig. 3. The shapes of the curves look very similar.

The estimated design floods with 2yrs, 5yrs, 10yrs, 50yrs and 100yrs return periods are listed in Table 3 for Austria, and in Table 4 for Ukraine. The results show that the estimated design floods with 100-yr return period scaled with the catchment area are larger for the Ukrainian catchments compared to Austrian catchments (Fig. 4). The results are similar for the other return periods as well. One outlier Austrian catchment is Polsterlucke on the Krumme Steyr River (ID 10), where the logarithm of the 100-yr return period specific discharge is  $0.05 \text{ m}^3 \text{ s}^{-1} \text{ km}^{-2}$ , which is the smallest as well as highest catchment among the Austrian catchments.

The comparative assessment of selected physiographic characteristics shows that topography or vegetation do not differ significantly between the selected regions. The proportion of catchment area covered by forest shows a large variety between catchments (Table 1 and 2), and therefore does not explain the difference between Austrian and Ukrainian catchments. The mean catchment elevation is slightly higher for Austrian than Ukrainian catchments (Table 1 and 2), but the difference is not large. More noticeable difference is expressed by the increased continentality of Ukrainian catchments. Fig. 5 compares the seasonality of winter floods.

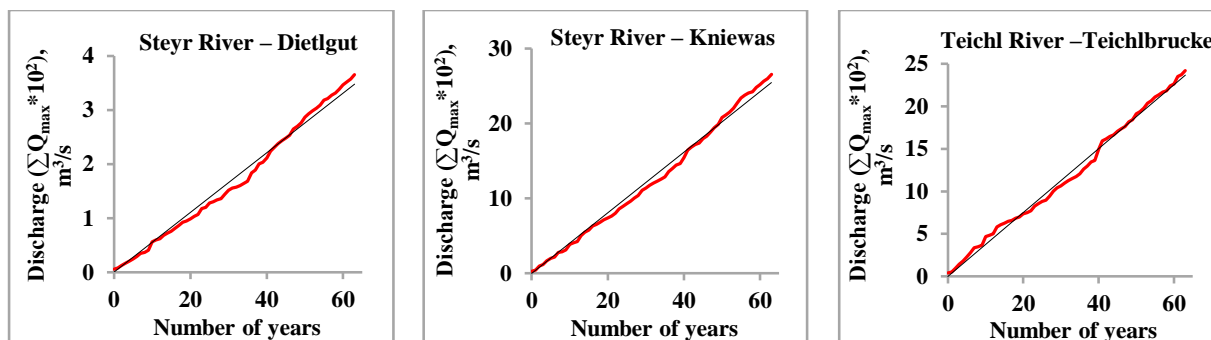


Fig. 2. Mass curves of the winter floods in the upper Steyr river basin.

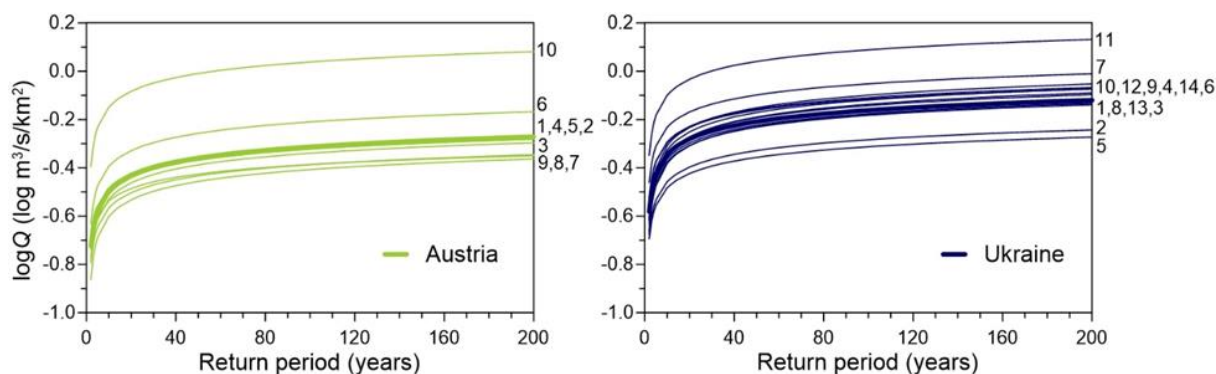


Fig. 3. Flood frequency curves of the Austrian (left) and Ukrainian (right) catchments (catchment IDs listed on the right sides of the plots correspond to the IDs listed in Table 1 and 2; bold lines show the largest Austrian and Ukrainian catchments).

**Table 3. Estimated design floods with 2, 5, 10, 50 and 100 years return periods [ $\text{m}^3 \text{ s}^{-1}$ ], largest ( $Q_{max}$ ,  $\text{m}^3 \text{ s}^{-1}$ ) and lowest ( $Q_{min}$ ,  $\text{m}^3 \text{ s}^{-1}$ ) observed winter flood discharges for all Austrian study catchments**

Gauge / $Q_T$ -year	$Q_2$	$Q_5$	$Q_{10}$	$Q_{50}$	$Q_{100}$	$Q_{min}$ [year]	$Q_{max}$ [year]
Steyr River – Klaus an der Pyhrnbahn	102.3	145.5	174.1	237.1	263.7	42.7 (1953)	246.0(1962)
Teichl River – St. Pankraz	44.4	62.1	73.8	99.6	110.5	19.6 (1991)	109.0(1993)
Steyr River – Kniewas	30.6	45.1	54.7	75.7	84.7	10.1 (1960)	80 (1965)
Teichl River – Teichlbrücke	25.2	37.7	46.0	64.3	72.0	10.8 (1969)	74.0 (1965)
Steyr River – Hinterstoder	15.1	21.5	25.8	35.1	39.0	6.1 (1984)	41.9 (1993)
Steyrling River – Steyrling	16.8	24.2	29.1	39.8	44.4	5.6 (1963)	45.4 (1965)
Dambach River – Windischgarsten	9.2	13.7	16.8	23.4	26.2	3.8(1991)	27.0 (1993)
Teichl River – Spital am Pyhrn	7.7	10.1	11.6	15.0	16.4	4.2(1991)	18.2 (1993)
Steyr River – Dietlgut	4.0	5.7	6.8	9.2	10.3	1.6 (1984)	10.7 (1975)
Krumme Steyr River – Polsterlucke	6.4	9.4	11.3	15.7	17.5	2.2 (1984)	15.7 (1993)

**Table 4.** Estimated design floods with 2, 5, 10, 50 and 100 years return periods [ $\text{m}^3 \text{s}^{-1}$ ], largest ( $Q_{max}$ ,  $\text{m}^3 \text{s}^{-1}$ ) and lowest ( $Q_{min}$ ,  $\text{m}^3 \text{s}^{-1}$ ) observed winter flood discharges for all Ukrainian study catchments

Gauge / $Q_T$ -year	$Q_2$	$Q_5$	$Q_{10}$	$Q_{50}$	$Q_{100}$	$Q_{min}[\text{year}]$	$Q_{max}[\text{year}]$
Rika River – Mizhhiria village	144.4	207.2	248.7	340.2	378.9	55.1 (2015)	471.0 (1958)
Rika River –Verkhniy Bystryi village	34.7	48.4	57.5	77.4	85.9	9.5 (2015)	93.8 (1999)
Holiatynka River – Maidan village	20.0	29.8	36.2	50.5	56.5	7.58 (2015)	74.1 (1958)
Pylypets River – Pylypets village	13.2	18.8	22.4	30.5	33.9	3.86 (2003)	27.3 (1973)
Lopushna River – Lopushne village (nyzhn.)	7.5	10.4	12.3	16.4	18.2	2.9 (2003)	25.6 (1958)
Studenyi River – Nyzhnii Studeniyi village	6.1	9.4	11.5	16.3	18.3	2.4 (2015)	26.0 (1999)
Ploshanka Stream – Pylypets village (nyzhn.)	6.9	9.8	11.7	15.9	17.6	1.00 (2015)	14.4 (1985)
Lopushna River – Lopushne village (verkh.)	2.8	4.4	5.5	7.8	8.8	1.2 (1960)	11.0 (1999)
Branyshche Stream – Lopushne village	2.5	3.9	4.9	6.9	7.8	0.6 (2015)	11.2 (1958)
Studenyi River – Verkhniy Studeniyi village	2.0	3.2	3.9	5.6	6.4	1.0 (1973)	8.0 (1999)
Pylypets River – Podobovets village	3.3	4.9	5.9	8.2	9.1	0.76 (2015)	7.6 (1986)
Pylypetskyi Stream – Pylypets village	1.7	2.4	2.9	4.0	4.4	0.42 (2015)	5.1 (1985)
Ziubrovets Stream – Lopushne village	0.8	1.1	1.4	1.9	2.1	0.2 (2003)	2.9 (1958)
Serednii Zvir Stream – Lopushne village	0.5	0.8	1.0	1.4	1.6	0.1 (2003)	2.4 (1999)

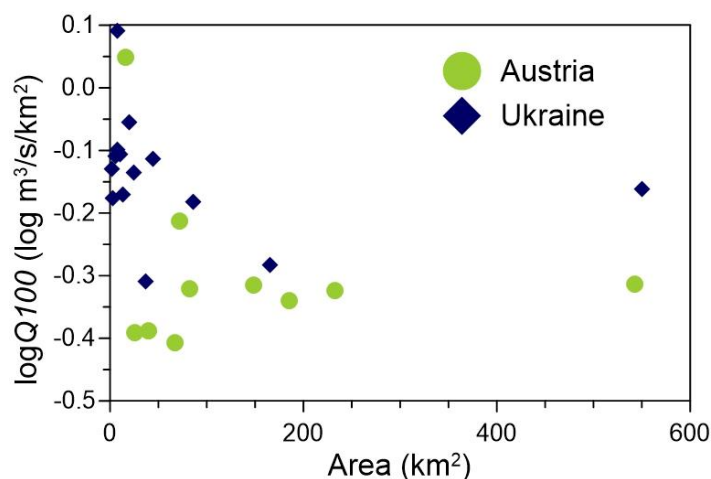
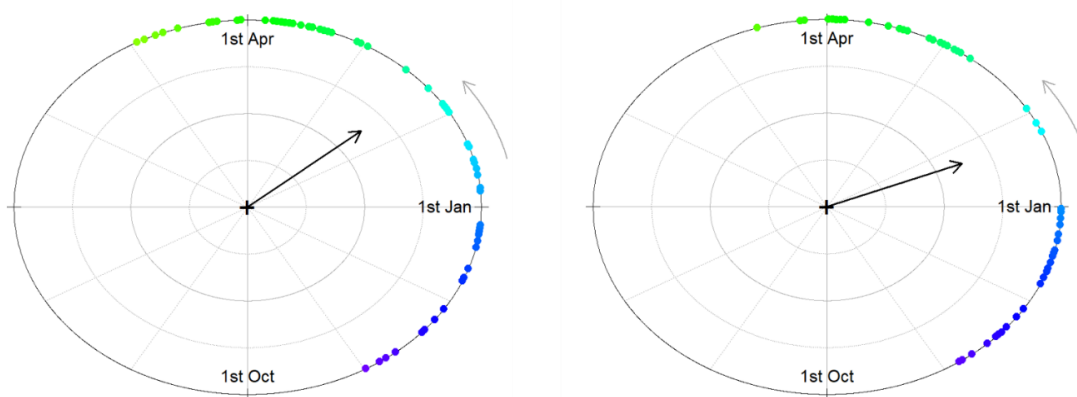


Fig. 4. Logarithm of 100-year floods scaled with catchments area as a function of catchment area in the upper Steyr River (Austria, green points) and upper Rika (Ukraine, blue points) basins.



a Steyr R. - Klaus an der Pyhrnbahn (Austria)

b Rika R. - Mizhhiria v. (Ukraine)

Fig. 5. Mean seasonality of the outlet of the Austrian catchments, Steyr River – Klaus an der Pyhrnbahn (a) and of the outlet of the Ukrainian catchments, Rika River – Mizhhiria village (b).

As it is evident from Fig. 5, the floods in upper Rika catchment tend to occur earlier. The comparative assessment of observed snow depth at climate stations shows that the average annual maximum snow depth ( $D_{aam}$ ) is 38 cm at the Ukrainian station, and 68 cm at the Austrian station. The approximately 40% smaller average annual maximum snow depth ( $D_{aam}$ ) again proves the increased effect of continental climate on the Ukrainian study catchments.

## Conclusion

In this study we explore the impact of increased continentality on the magnitude of snowmelt design floods in hydrologically homogeneous Ukrainian and Austrian basins of Danube River regions. The study catchments are similar in terms of catchments size and elevation, but slightly differ climate characteristics, i.e. the Ukrainian catchments experience the effect of larger continentality. The main results of the present study can be summarized in the following points:

- Winter floods with 2 yrs, 5 yrs, 10 yrs, 50 yrs and 100 yrs return periods are estimated for all the study catchments, which may be useful for various management purposes (for designing bridges and dams, floodplain management, barrages etc.).
- It is found that the design floods scaled with the catchment areas are larger in the upper Rika River Basin in Ukraine than in the upper Steyr River Basin in Austria.
- We explain the found difference by the effect of increased continentality in the Ukrainian catchments.
- The mean seasonality of winter floods in Ukrainian catchments tend to occur 2–3 weeks earlier compared to the Austrian catchments.

## References

- Bauzha, T., Gorbachova, L. (2013): Features of maximum discharges change of mountain rivers in the Carpathian region: a case study of the water courses in the upper part of the Rika River Basin [Electronic resource] Conference proceeding 10th annual International Conference of Young Scientists on Energy Issues, Cyseni-2013, May 29–31, Kaunas, Lithuania. – C. IX 590-600. – Access to the article: [www.cyseni.com](http://www.cyseni.com)
- Bertola, M., Viglione, A., Lun, D., Hall, J., Blöschl, G. (2020): Flood trends in Europe: are changes in small and big floods different? *Hydrology and Earth System Sciences*, 24, 1805–1822, <https://doi.org/10.5194/hess-24-1805-2020>.
- Blöschl, G., Hall, J., Viglione, A. et al. (2019): Changing climate both increases and decreases European river floods. *Nature*, 573, 108–111. <https://doi.org/10.1038/s41586-019-1495-6>.
- Burn, D. H. (1997): Catchment similarity for regional flood frequency analysis using seasonality measures. *Journal of Hydrology*, 202, 212–230.
- Gorbachova, L. (2014): Methodical approaches the assessment of the homogeneity and stationarity of hydrological observation series. *Hydrology, Hydrochemistry and Hydroecology*, vol. 5, no. 32, 22–31. (in Ukrainian).
- Gorbachova, L. O. (2016): Place and role of hydro-genetic analysis among modern research methods runoff. *Proceedings of Ukrainian Hydrometeorological Institute*, vol. 268, 73–81. (in Ukrainian).
- Gorbachova, L., Zabolotnia, T., Khrystyuk, B. (2018): Homogeneity and stationarity analysis of the snow-rain floods in the Danube Basin within Ukraine. *Acta hydrologica Slovaca*, vol. 19, n. 1, 35–41.
- Gumbel, E. J. (1954): *Statistical Theory of Extreme Values and Some Practical Applications*; Applied Mathematics Series. US Government Printing Office: Washington, DC, USA, 60p.
- Jeneiova, K., Kohnova, S., Hall, J., Parajka, J. (2016): Variability of seasonal floods in the Upper Danube River basin. *Journal of Hydrology and Hydromechanics*, vol. 64, n. 4., 357–366.
- Kottek, M., Grieser, J., Beck, C., Rudolf, B., Rubel, F. (2006): World Map of the Köppen-Geiger climate classification updated. *Meteorol. Z.*, vol. 15, 259–263. DOI: 10.1127/0941-2948/2006/0130.
- Merz, R., Blöschl, G. (2008): Flood frequency hydrology: 1. Temporal, spatial, and causal expansion of information. *Water Resources Research*, vol. 44, 8, article number W08432, 17 pp.
- Mujere, N. (2011): Flood Frequency Analysis Using the Gumbel Distribution. *International Journal on Computer Science and Engineering*, vol. 3, 2774–78.
- Onen, F., Bagatur, T. (2017): Prediction of Flood Frequency Factor for Gumbel Distribution Using Regression and GEP Model. *Arabian Journal for Science and Engineering*, 42, 3895–3906.
- Parajka, J., Kohnová, S., Bálint, G., Barbuc, M., Borga, M., Claps, P., Cheval, S., Dumitrescu, A., Gaume, E., Hlavcová, K., Merz, R., Pfaundler, M., Stancalie, G., Szolgay, J., Blöschl, G. (2010): Seasonal characteristics of flood regimes across the Alpine–Carpathian range. *Journal of Hydrology*, vol. 394, 78–9.
- Parajka, J., Kohnova, S., Merz, R., Szolgay, J., Hlavcova, K., Blöschl, G. (2009): Comparative analysis of the seasonality of hydrological characteristics in Slovakia and Austria. *Hydrological Sciences Journal*, 54(3), 456–473.
- R Core Team (2016): R: A language and environment for statistical computing. R Foundation for Statistical Computing, Vienna, Austria. URL <http://www.R-project.org/>.
- Zabolotnia, T., Gorbachova, L., Khrystyuk, B. (2019): Estimation of the long-term cyclical fluctuations of snow-rain floods in the Danube basin within Ukraine. *Meteorology, Hydrology and Water Management*, vol.7, n. 2, 3–11. doi:10.26491/mhwm/99752.
- Zabolotnia, T., Parajka, J., Gorbachova, L., Szeles, B., Blöschl, G., Aksiuk, O., Tong, R., Komma, J. (2021): Fluctuations of winter floods in small Austrian and Ukrainian rivers. *Hydrology* (Submitted).
- Zelenhasic, E. (1970): *Theoretical Probability Distributions for Flood Peaks*. Colorado University Press, Colorado.

Tetiana Zabolotnia, PhD. (\* corresponding author, e-mail: tzabolotnia@gmail.com)  
Mgr. Liudmyla Gorbachova, Dr.Sc.  
Ukrainian Hydrometeorological Institute  
Nauky Prospect 37  
03028 Kyiv  
Ukraine

Dr. Borbala Szeles  
Assoc. Prof. Juraj Parajka  
Dr. Rui Tong  
Institute of Hydraulic Engineering and Water Resources Management  
Faculty of Civil Engineering  
Vienna University of Technology  
Karlsplatz 13  
A-1040 Vienna  
Austria

## Improvement of the operational HEC-HMS hydrological model embedded in the Flood Forecasting and Warning System of the Sava River Basin

Mirza SARAC<sup>\*</sup>, Maja KOPRIVŠEK, Oliver RAJKOVIĆ, Azra BABIĆ, Merima TRAKO,  
Saša MARIĆ, Adnan TOPALOVIĆ, Srđan MARJANOVIĆ, Dejan PETKOVIĆ,  
Marija IVKOVIĆ, Ervin KALAČ, Danijela BUBANJA

In 2017 the HEC-HMS model for the Sava River Basin was embedded under the Flood Forecasting and Warning System in the Sava River Basin (Sava FFWS) and coupled with many hydraulic models. Since the model was initially calibrated as the event-based model, a lack of accuracy has been recognized during the continuous simulations within the Sava FFWS operational use. Therefore, the Sava FFWS users organizations: ten forecasting organizations from five Sava countries, agreed to upgrade and improve this hydrological model. The activities of the model improvement were performed in period January 2019 till June 2020. It was implemented by the national experts from the Sava FFWS users' organizations as a true joint action and coordinated by the Secretariat of the International Sava River Basin Commission. This paper presents the results of the Sava HEC-HMS model improvements and updated parameters, including a comparison of results of initial and improved models within the operational forecasting system. The paper also discusses the potentials of the remote sensing and radar- and satellite-based data that will be used for the future model improvements.

KEY WORDS: forecasting, modelling, calibration, Sava River Basin

### Introduction

The Sava River is the third longest and the largest by discharge tributary of the Danube River. The length of the Sava River from its main source in western Slovenian mountains to its mouth to Danube in Belgrade is about 945 km. The Sava River runs through four countries (Slovenia, Croatia, Bosnia and Herzegovina, and Serbia). The Sava River Basin has a surface area of about 97700 km<sup>2</sup> and covers considerable parts of Bosnia and Herzegovina, Croatia, Montenegro, Serbia, Slovenia and a small part of the Albanian territory. The objectives of transboundary flood risk management in the Sava River Basin are regulated with the Framework Agreement on the Sava River Basin (FASRB) and the accompanying Protocol on Flood Protection to FASRB (Protocol). With respect to an efficient flood awareness and preparedness, the Protocol has committed all Sava countries to establish a joint flood forecasting system for the entire Sava River Basin under the coordination of the International Sava River Basin Commission (ISRBC). The Flood Forecasting and Warning System in the Sava River Basin (Sava FFWS) was established in October 2018 and represents a comprehensive and versatile system that combines data and models of individual countries, as well as common models, making it a unique example of

cross-border cooperation in flood forecasting even globally. Sava FFWS currently has ten users, i.e. national organizations responsible for the flood forecasting and it is hosted at five locations: primary and three backup server modules that are installed in the four Sava countries, while archive and web server in ISRBC.

One of hydrological models integrated in Sava FFWS is the HEC-HMS model for the Sava River Basin (Sava HEC-HMS) which represents the backbone of system. The model was initially calibrated as event-based hydrological model on several selected periods, up to a six-month long. Calibration periods were mainly from the winter seasons characterized by average to high flow conditions while dry and low flow periods were not included. In the operational mode within Sava FFWS the lower reliability of Sava HEC-HMS was recognized during the continuous simulations. It was suspected that the way of the initial calibration was one of the reasons for less accurate simulations of the state of the model and forecasts. Given that Sava FFWS currently collects real-time data from many meteorological stations that were not included into the initial Sava HEC-HMS model it was reasonable to expect that the improved density of the meteorological stations would result with the improved hydrological model. Sava HEC-HMS calibration, as the process of estimating model

parameters by comparing model outputs for a given set of assumed conditions with observed data for the same conditions, was performed. Validation involved running a model using input parameters measured or determined during the calibration process. According to Refsgaard (1997), model validation is the process of demonstrating that a given site-specific model is capable of making “sufficiently accurate” simulations, although “sufficiently accurate” can vary based on project goals (Moriassi et al., 2007). A number of publications have addressed model evaluation statistics (Willmott, 1981; ASCE, 1993; Legates and McCabe, 1999) as well as some recently developed statistics that were used within the study.

In this study the Sava HEC-HMS model was updated without interventions on the hydrological modelling processes while the number of the measuring locations was significantly increased and the model parameters were assigned in the process of the calibration suitable for the continuous models. The process was jointly performed by the users of the Sava FFWS under coordination of ISRBC.

### Flood Forecasting and Warning System in the Sava River Basin

Sava FFWS is operating as an open shell platform for

managing the data handling and forecasting processes through the integration of the wide range of external data and models (Deltares, 2018). This concept is particularly important for the cooperating countries, taking into account that the Sava River basin is shared by five countries where each country is using its own models, monitoring systems, forecasting systems, water authorities and interests.

Sava FFWS integrates the Hydrological Informational System for Sava River Basin (Sava HIS) – data hub for the collection of real-time observed hydrological and meteorological data (precipitation, air temperature, snow, water levels, discharges); various Numerical Weather Prediction (NWP) models; available weather radar and satellite imagery; outputs of existing national forecasting systems and different hydrological and hydraulic models (Fig. 1), including the Sava HEC-HMS model as the backbone of system.

The system is in use simultaneously by several organizationally independent forecasting teams (Table 1). Given the open nature of the Sava FFWS environment, responsibilities for the output and the forecast dissemination within each country are very clearly defined in accordance with the national legislation.

An effective Sava FFWS has aim to bridge differences and supports collaboration in the field of hydrological

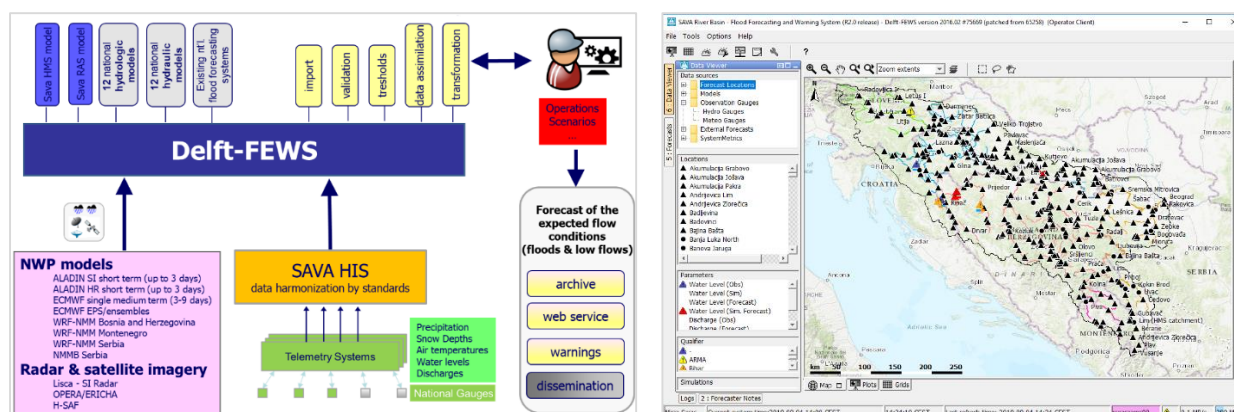


Fig. 1. Schematic overview of the Sava FFWS and screen of the operator client (forecasting locations).

Table 1. List of the Sava FFWS users and hosting organizations

Country	Institution	Note
Slovenia (SI)	Slovenian Environment Agency	Central server and User
Croatia (HR)	Croatian Meteorological and Hydrological Service	User
	Croatian Waters	3 <sup>rd</sup> backup and User
Bosnia and Hercegovina (BA)	Federal Hydrometeorological Service	User
	Sava River Watershed Agency	2 <sup>nd</sup> backup and User
	Republika Srpska Hydro-Meteorological Service	User
Serbia (RS)	Public Institution “Vode Srpske”	User
	Republic Hydrometeorological Service of Serbia	1 <sup>st</sup> backup / test system and User
Montenegro (ME)	Public Water Management Company “Srbijavode”	User
	Institute of Hydrometeorology and Seismology	User
	International Sava River Basin Commission	Archive / web server and Coordinator

forecasting keeping the countries own autonomy in monitoring, modelling and forecasting and remain open to developing its own models and supplementary forecasting initiatives. The system is assessed as added value to existing or developing systems, expecting that a common forecasting platform with well trained staff should provide better preparedness and optimized mitigation measures to significantly help reduce adverse consequences from floods, in future from droughts, ice hazards.

### ***Models setup within the forecasting platform***

The setup of Sava FFWS is modular where the combination of a numerical weather prediction and observations of precipitation and temperature, a hydrological model converting precipitation and temperature to discharge and, in most cases, a hydraulic model routing discharge downstream and computing water levels, define a unique forecast workflows (Deltares, 2018). Due to the number of hydrological models, hydraulic models and numerical weather prediction models available for the Sava River basin, several forecast workflows are configured in Sava FFWS. In case there was no hydrological model connected to a hydraulic model, the Sava HEC-HMS model covering entire basin is connected to deliver lateral flows.

In this moment 13 hydrological models are included in Sava FFWS where some of them are integrated models including hydraulic component. Some cover complete basin or a large area, others just small local river basins. HEC-HMS for the Sava River Basin and WFlow (BA, ME, RS) are models representing hydrological processes on the complete or the major part of the Sava basin. While Mike-NAM Sava (HR), Mike-NAM Una (BA/HR), Mike-NAM Vrba (BA), HBV-light Bosna (BA), WFlow (ME), HEC-HMS Kolubara, HBV Kolubara and HBV Jadar (RS) are models with the local or national coverage.

Regarding hydrological modelling, the backbone of the Sava FFWS forecasting system represents the Sava HEC-HMS model, as the only hydrological model that covers the entire Sava River Basin. The model was developed by the U.S. Army Corps of Engineers (USACE), in close collaboration with ISRBC and national experts and initially calibrated as event-based model.

### **Development and update of the HEC-HMS model of the Sava River Basin (Sava HEC-HMS)**

#### ***Initial Sava HEC-HMS model (version 1.0)***

Sava HEC-HMS model consists of 235 subbasins, carefully selected to take the local hydrology into account, 174 junctions mainly located at the hydrological stations locations or locations of confluences and 158 river sections as well as 20 reservoirs. Sava HEC-HMS simulates hydrological processes through the meteorological and basin model working together to define the rainfall-runoff processes within the watershed. The meteorological model provides precipitation in

the form of rain or snow as input to the basin model, while the basin model uses input loss parameters to calculate precipitation lost to storage in the watershed, precipitation infiltrating into the soils, and the subsequent amount of excess runoff precipitation. Excess precipitation is routed to the subbasin outlet as overland flow using a unit hydrograph transform (Clark Unit Hydrograph) method. Precipitation infiltrating into the soil is routed to the subbasin outlet using the recession baseflow method. Overland flow and baseflow are combined at each subbasin outlet before entering the reach network. As the combined flow is routed down through the river reach network of the basin, flow is aggregated from additional subbasins and routing reaches in hydrological order (USACE and ISRBC, 2017).

Evapotranspiration rates are also defined within the meteorological model where the Monthly Average method was utilized to represent evapotranspiration rates in the basin but also considering that the evapotranspiration is not a critical component for short-term simulations.

Hourly precipitation and temperature data at all available meteorological stations in period of the initial model development were integrated, 74 meteorological stations in total (rainfall and air temperature).

In addition to the relatively modest number of meteorological stations, within the Sava River Basin existed areas where precipitation input was very sparse. In an attempt to rectify the lack of observed precipitation in these areas, the Inverse Distance Weighting precipitation method (IDW) was applied. The IDW method calculates subbasin average precipitation by applying and inverse distance squared weighting all available precipitation gages in the user-specified search radius (Feldman, 2000).

A dense coverage of stations exists in the headwaters of the Sava River Basin, mainly in Slovenia while there is a relative lack of stations in the middle and far downstream portions of the basin. Fig. 2 illustrates the areas of the Sava River Basin with less meteorological station coverage showing every station with a 25-km radius buffer overlaying the basin delineation, and 50-km radius that was at the end used as a necessity. This was one of the main gaps of the initial model but a result of the real precipitation stations network coverage in the period of the model development.

In addition to precipitation in the form of rainfall, the meteorological model is configured to compute the snowmelt and for that purpose the temperature index method was used. The meteorological model, at every time step, whether the precipitation falling is rainfall or snowfall based on the temperature data at nearby meteorological stations. The temperature index approach considers snowmelt as a mass-balanced process (Feldman, 2000).

Available snow-related data in the Sava River Basin are very limited, therefore the most parameters for the snowmelt method were established from the related studies and the consultation of the USACE snow experts.

Initial snow-water-equivalent (SWE) values and elevation band parameters were developed through GIS processes on available data. Daily Advanced Microwave Scanning Radiometer (AMSR-E)/Aqua Level 3 global snow water equivalent grids were compiled from the National Aeronautics and Space Administration's (NASA) National Snow and Ice Data Center (NSIDC) in Boulder, Colorado USA (Tedesco et al., 2004). Due to the large grid size of the SWE grids, the accuracy of this method is uncertain. However, the satellite-based SWE grids were the best available data at the time of model development.

Elevation bands, which are input into the meteorological model to account for the differences in snowfall and snowpack across the range of elevations in each subbasin, were developed as the elevation-area relationships using the SRTM DEM digital elevation map with 30 meter resolution (Rodriguez et al. 2005). These elevation-area relationships were segmented at natural breakpoints in the topography to define the elevation bands for each subbasin. For each defined elevation band, initial snowpack parameters were required to define any snowpack that may be present at the beginning of the hydrological model simulation. The aforementioned AMSR-E SWE grids were used to define the initial SWE for each elevation band within each

subbasin.

The Sava HEC-HMS basin model consists of 235 analytical units carefully selected to take the local hydrology into account (Fig. 3). A unique local characteristic in Sava River basin is the presence of karst which affects the subbasins boundaries and the parameterization of the subbasins. For some specific areas like karst geology, levees, and canals especially in the flatter areas of the basin SRTM DEM needed to be manually manipulated.

SRTM DEM and the GIS module of the HEC-HMS were also used to generate the physical parameters of the Sava River basin such as drainage area, stream lengths, basin slopes, etc. From these physical parameters, initial estimates of unit hydrograph parameters, time of concentration and storage coefficient were developed for each subbasin. Reach routing parameters, such as reach slope and length, were also extracted.

The Sava HEC-HMS implements various methods to represent the rainfall-runoff processes of the basin of interest. Various factors contributed to the decision for each of the modeling component methods Sava River Basin such as applicability of the method based on specific basin characteristics (such as terrain and urbanization) and availability of data supporting a specific method.

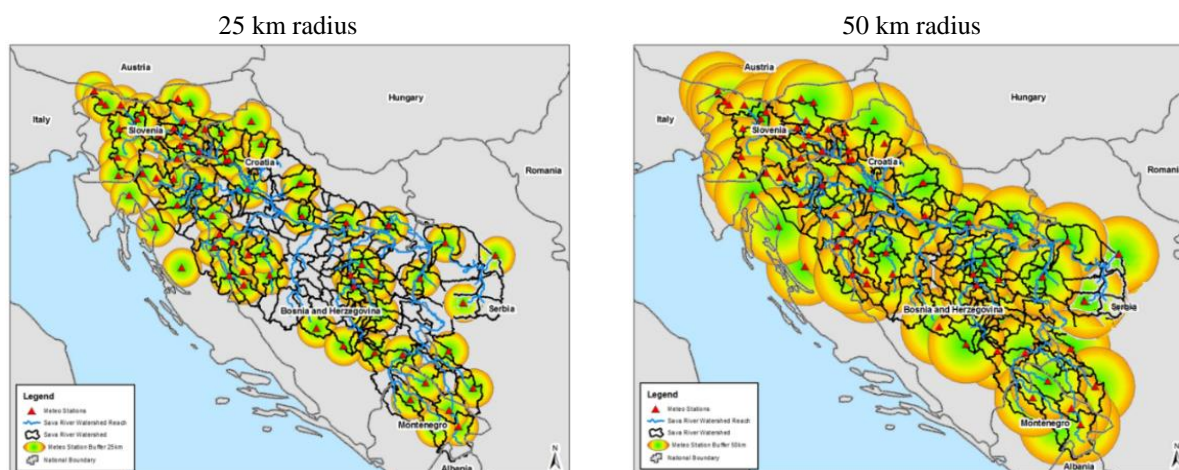


Fig. 2. Precipitation gauge coverage (Sava HEC-HMS v1.0).

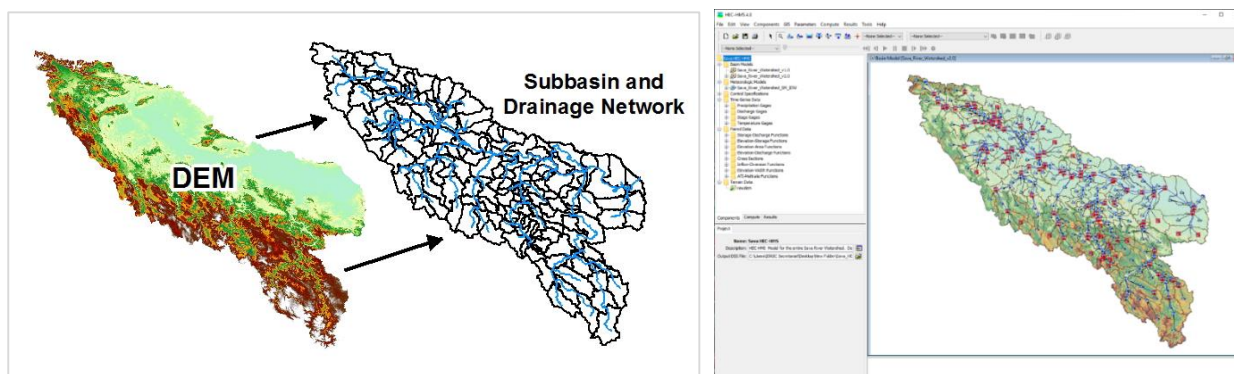


Fig. 3. Illustration of the SRTM DEM conversion to subbasin and river network and the final model structure.

The decision to use these methods were based on:

- Simple Canopy Method – chosen for its simplicity due to a lack of available data defining the canopy.
- Deficit-Constant Soil Loss Method – chosen based on the success of this method for large basin studies such as the Sava River Basin. The method provides the ability to simulate soil moisture characteristics throughout an event using easily derived and calibrated parameters. In addition, is the method used for most major flood forecasting models within USACE.
- Clark Unit Hydrograph Transformation Method – chosen based on its ability to be estimated using available terrain data and the successful implementation of this method across modeling studies within USACE. The parameters for this method are also fairly easy to calibrate especially in situations where discharge stations are relatively abundant such as in the Sava River Basin. In addition, this method has shown to be very effective in representing the timing and shape of flow hydrographs through varying magnitudes and volumes of floods.
- Recession Baseflow – chosen for its simplicity and its ease of application.
- Muskingum-Cunge Reach Routing Method – chosen because it primarily based on physical characteristics of the routing reaches which can be attained from the available information. This method has been widely used within USACE and provides the ability to represent the flow hydrograph translation and attenuation in situations with varying levels of floodplain storage.

The parameters used to define the hydrological model are described in more detail below and a summary of the various basin parameters is provided along with the basin modeling methods developed within the Sava HEC-HMS (Table 2). These parameters were the subject of the model calibration.

#### Updated Sava HEC-HMS (version 2.0)

Since the Sava HEC-HMS was initially calibrated as event-based model using hourly data values, the lower reliability was recognized during the continuous simulations in the operational mode within the Sava FFWS. Regularly performed simulations of the Sava HEC-HMS model coupled with NWP data in Sava FFWS shows that the model has a strong reaction to moderate

**Table 2. Number of stations with the hourly (real-time) data exchange available in the Sava HIS / Sava FFWS**

Modeling Method	Parameter	Description and representative values in the model v1.0
<b>Canopy Storage Soil Losses</b>	Canopy	Initial Storage 100 %
		Max Storage 2–50 mm
	Deficit	Initial Deficit 0–35 mm
	Constant	Maximum Deficit Maximum amount of water the soil layer can hold (30–75mm)
		Constant Loss Percolation rate of the soil layer 0.1–2.25 mm/hr
<b>Hydrograph transformation</b>	Clark Unit Hydrograph	Percent Impervious Area Percent of the subbasin that is covered by directly connected impenetrable surfaces such as concrete, rooftops, and urban development 0–53.8 %
		Time of Concentration Travel time from the most hydrologically remote point in the subbasin to the watershed outlet 0.2–50 hr
<b>Baseflow</b>	Recession Baseflow	Storage Coefficient Conceptual parameter representing basin's storage capacity 0.7–160 hr
		Initial Baseflow Baseflow at the beginning of the simulation 0.001–0.621 m <sup>3</sup> s <sup>-1</sup> km <sup>-2</sup>
		Recession Ratio Rate at which baseflow recedes between events 0.72–0.98
<b>Reach routing</b>	Muskingum-Cunge Routing	Threshold Ratio Flow at which the baseflow is reset ratio to the peak
		Length Length of reach 0.22–106.16 km
		Slope Slope of reach 0.00001–0.0196 m m <sup>-1</sup>
		Manning's n-Values Roughness coefficient for the channel, left overbank, and right overbank 0.02–0.05
	Shape Shape of the routing reach cross section 8-point or trapezoidal	

amounts of rain and produce untimely and overestimated forecasts. Reasons for a such behavior of the model are the modelling methods initially selected (Table 2) e.g., soil loss method which is not capable of long-term soil moisture accounting, but also due to meteorological data availability and coverage, snow data availability as well as the reservoirs regulation at various dam.

Any intervention on the robust and complex model like Sava HEC-HMS, which is in use by many experts per different institutions and countries, has to be done in well organized and coordinated way. After a joint agreement of the expert team that the initial model needs to be updated with the new information, the action plan has been made to upgrade the model with new measuring locations and to perform the recalibration of the model parameters. The expected goal was that the new precipitation and air temperature data would complement the existing spatial and temporal accuracy of the meteorological component of the model.

Meteorological inputs are typically the greatest limitation in any hydrological model because meteorology is such a random and natural phenomenon. The IDW method, used to model precipitation in the Sava HEC-HMS, relies heavily on the location and density of stations because the precipitation applied at any given subbasin is computed by interpolating between measured precipitation values at these stations. If the spacing between stations is too great, a storm could pass between two stations and not be recorded at either station, which means that the Sava HEC-HMS would not register this event and apply the improper precipitation to the subbasins between the stations. In addition, if a rainfall event does not pass over enough stations to capture the shape and volume of the rainfall, the model will not accurately apply precipitation to the adjacent subbasins (Feldman, 2000). These inherent limitations exist for all meteorological models relying on point stations, which is why acquiring the best available data and quality controlling this data is critical to the performance of the Sava HEC-HMS model as well.

The two immediate solutions are increasing the density of stations in areas with limited or insufficient coverage and/or incorporating radar-based gridded precipitation data into the model. For a robust flood forecasting system such as Sava FFWS, incorporating both gauge- and radar-based precipitation is the best solution to create

redundant data sources and to protect against one of the source data feeds failing.

Radar-based precipitation has become a standard data source for hydrological models across the world because it solves the issue of spatial coverage of precipitation data that exists with readings at meteorological stations. As with any measurement, raw radar-based data possesses some level of uncertainty and must be verified and corrected to measurements made at standard single-point meteorological stations further emphasizing the need for ground stations. In spite of this uncertainty, radar-based data, when processed through proper quality controls, provides the spatial and temporal distribution of precipitation data necessary for large, complex hydrological models such as the Sava HEC-HMS. The European National Meteorological Services Network (EUMETNET), with members from the European Union and Balkans, collaborate and produce network-wide radar mosaics through the Operational Program for Exchange of Weather Radar Information (OPERA), which could provide a source of radar-based nowcasting information for the Sava River Basin. As mentioned in the Chapter 2, along with NWP data, Sava FFWS is prepared to extrapolate radar or satellite imagery in order to provide a very accurate short-term hydrological forecast (nowcasting) for several hours in advance based on measured values. Nowcasting products are currently not available within the Sava basin and the existing radars are currently still not able to produce accurate rainfall images. Considering the importance of providing a such input and raising the awareness of experts to this type of precipitation data, the Lisca radar data (Slovenia) are implemented Sava FFWS, next to Opera radar composite images and H-SAF satellite images (Fig. 4).

However, considering that radar- and satellite-based images are only displayed within the system but are not connected to any of hydrological models neither to Sava HEC-HMS, it was decided to update the model in this stage to include the new hydrological and meteorological inputs and recalibrate Sava HEC-HMS without changing the structure of the model. Challenging work resulted with an improved Sava HEC-HMS model more suitable for continuous hydrological simulations needed for accurate process of the flood forecasting in Sava FFWS. Important step, beside technical interventions on



Fig. 4. Available radar and satellite images in the Sava River Basin integrated under Sava FFWS.

the model, was managing and coordination of all activities and application of a consistent methodology since many Sava countries experts were involved in this process. The applied methodological approach consisted of the following steps: (1) preparation of the necessary technical documentation and time plan for the work of national experts; (2) inclusion of the new hydrological and meteorological stations to the model; (3) collection of historical hydrological and meteorological hourly data for the period from 2010 to 2018; (4) uploading of the collected data to Sava HIS/Sava FFWS Archive module; (5) enhance the model components; (6) calibration and validation the new model setup and (7) hindcast analysis and validation of the operability performances of the model through the Sava FFWS testing module including comparison of different model versions.

A first step of the model enhancement was related to increase of the number of precipitation and temperature data inputs at all available meteorological stations. In total 258 meteorological stations for precipitation and temperature data inputs are currently available in the Sava HEC-HMS v2.0 as well as 151 hydrological stations for the observed discharge data presentation and the purpose of comparison with the simulated runoff. However, from the total number of stations integrated in the model, data were collected for a part of stations that have regular and hourly measurements of precipitation, air temperature and discharge (Table 3), representing an increase of 125 meteorological and 41 hydrological stations compared to the initial setting of the model.

The greatest number of the new meteorological stations integrated under Sava HEC-HMS v2.0 are located in the central part of the basin while the number of the stations in the upper and lower parts was not changed significantly. Following the model configuration enhancements along with integration of the new measuring locations and their historical data the model was recalibrated. Different approach to the calibration was mainly dependent on the calibration skills of the expert team members. The calibration of the parameters in the initial Sava HEC-HMS v1.0 model was performed for the six short periods related to the flood events between 2009 and 2015. The updated v2.0 model has been calibrated and primarily validated using different periods per subbasins while additional two validations of the model were performed for period 01 Jan 2014–31 Dec 2014 and 01 Jan 2016–31 Dec 2016. Work performed on calibration and validation of the Sava HEC-HMS model v2.0 was jointly agreed and distributed among the team members considering responsibility of each organization but also the model structure, capacities

and expertise of individuals and a rule of equivalence as well, so activities were divided per subbasins and countries. Most of data and information used for model improvement was provided by the national organizations involved in the activity. Each organization has provided input time-series data for the stations in its responsibility despite the distribution of work related to calibration and validation of the model. A substantial amount of data was collected as part of the initial model development efforts. The period from 2010 to 2018 was divided into sub-periods where one was used for the calibration and others for the validation of the Sava HEC-HMS v2.0 model. In the end three validation procedures were performed given that the calibration and first validation were done per subbasins while additional two validations were performed for the entire model.

The model calibration was performed at 107 calibration points i.e., 32 more compared to the initial model.

For the determination of the model parameters two approaches were used: trial-and-error method and the built-in automatic calibration procedure of HEC-HMS software (Zhang et al., 2013). For both calibration approaches the hydrograph volume, peak discharge and timing of the peak were also monitored. In order to ensure the model's ability to represent these characteristics, three metrics were analyzed during the calibration simulations at various locations: Nash-Sutcliffe Coefficient (NSE), Root mean square error to Standard deviation of observations Ratio ( $RSR=RMSE/Std$ ), Coefficient of determination ( $R^2$ ). The goodness of fit for each model parameter was evaluated based on NSE, while other coefficients were continuously monitored. These metrics provided an overall measure of the numerical performance of the model's ability to capture all characteristics of the outflow discharge hydrographs, which incorporates peak, volume, timing, and shape.

In addition to these three metrics, calibration plots depicting the time series discharge hydrograph output versus the observed discharge hydrograph were also analyzed. The calibration plots provided an effective visual illustration of the performance of the model and were monitored using HEC-HMS, as well as the graphical user interfaces of Sava FFWS.

## Results and discussion

The main improvements of the Sava HEC-HMS calibration process included: (1) improvements of the meteorological inputs with higher spatial and temporal data coverage for precipitation and air temperature; (2) some corrections of the meteorological

**Table 3. Number of stations per countries available in Sava HEC-HMS v2.0**

Type of the station / parameter		BA	HR	ME	RS	SI	Totals
<b>Hydrological stations</b>	Discharge	54	35	9	17	19	<b>134</b>
<b>Meteorological stations</b>	Precipitation	41	49	3	10	96	<b>199</b>
	Air temperature	41	27	3	8	18	<b>97</b>

model of snow melting; (3) increased number of calibration points; (4) increased number of calibrated sub-basins, up to 98 from initial 66; (5) longer time series of discharge observations; (6) new version of the Sava HEC-HMS model integrated under the Sava FFWS testing module.

The model skill was evaluated using NSE on the period from 2010 to 2018 and about 50% of stations score a NSE greater than 0.55 (rates: good and very good), while a higher percentage of stations score a NSE greater than 0.40 (rate: satisfactory). The higher NSE scoring was achieved in the upstream parts of the basin and along the Sava river. The new model accuracy and NSE increased in comparison to the initial model.

During the calibration process, it was noticed that the change of the model parameters would not necessarily lead to the better performance of the updated model, therefore the parameters for some computation points and accompanying subbasins have not been changed. This was the case on the parts of basin where new input data have not been changed. The changes were needed on areas where new input data were available and mainly in the module for the direct runoff transformation to decelerate and attenuate the simulated hydrographs. In the baseflow module change has been made on the recession constant that needed to be increased together with the ratio to peak parameter. In the karstic area e.g., the upstream part of the Bosna River subbasins, it was necessary to increase the soil percolation rate and initial loss. All these changes were expected having in

mind a transition from the event-based to the continuous model. Statistical analysis of the performance metrics, from the initial and the updated model achieved on 87 locations, where two models were possible to compare, has been done using one and two-tailed t-test and Mann-Whitney test (Table 4). The test results are showing that there is no significant statistical difference between NSE values for the two models and that the NSE value for the updated value is greater than the initial model. In the case of root mean square error-observations standard deviation ratio ( $RSR=RMSE/Stdev$ ), the p-values are indicating that statistical difference between the two models exists and that the RSR for the updated model is lower than for the initial model.  $R^2$  is not showing a clear signal whether the updated model is better than the initial one.

Following the statistics, a comparison between the initial and updated model has been performed. The Nash-Sutcliffe efficiency coefficient values, used for evaluation of the numerical model performance were greater than 0.55 for more than 50% of locations classifying the model as good and very good in the calibration period. Most of the rest of NSE values are greater than 0.4 meaning that the model is in the class of the satisfactory models.

In this paper 11 selected location (Table 5) were used for an analysis of the numerical goodness of fit for two periods. For the basin parts where, new meteorological stations have been installed the model performance has increased while the other subbasins record the same or

**Table 4. Statistics for the performed one-tailed and two-tailed t-test and Mann-Whitney test based on simulations of the two models versions**

Model performance metrics	t-test ( $\alpha=0.050$ )		Mann-Whitney test ( $\alpha=0.050$ )	
	one tailed	two tailed	one tailed	two tailed
NSE	0.046	0.092	0.002	0.004
RSR	0.009	0.019	0.001	0.003
$R^2$	0.292	0.584	0.244	0.489

**Table 5. Performance metrics of the initial (v1.0) and updated (v2.0) Sava HEC-HMS model for two periods using the general performance ratings: Very Good; Good; Satisfactory; Unsatisfactory (Moriasi et al., 2007)**

Up to downstream	Computation point (hydrological station)	01 Jan 2014–31 Dec 2014				01 Jan 2016–31 Dec 2016			
		Model v1.0		Model v2.0		Model v1.0		Model v2.0	
		NSE	RSR	NSE	RSR	NSE	RSR	NSE	RSR
10	J_01_08_03_Laško	-0.03	1.01	0.57	0.65	-0.39	1.18	0.71	0.54
16	J_01_13_11_Jesenice	0.65	0.59	0.76	0.49	0.69	0.56	0.80	0.45
18	J_04_02_05_Kupljenovo	0.41	0.77	0.43	0.76	0.28	0.85	0.33	0.82
31	J_06_10_06_Farkašić	0.61	0.62	0.65	0.59	0.67	0.58	0.68	0.57
39	J_12_02_04_Kralje	0.45	0.74	0.55	0.67	0.68	0.56	0.79	0.46
48	J_14_01_02_Daljan	-1.02	1.42	-0.18	1.08	-3.38	2.09	-0.04	1.02
67	J_20_19_06_Maglaj	0.82	0.43	0.70	0.55	0.56	0.66	0.46	0.74
75	J_24_01_02_Bijelo Polje	-1.50	1.58	0.06	0.97	-0.22	1.10	0.67	0.57
82	J_27_01_04_Sr. Mitrovica	0.74	0.51	0.72	0.53	0.77	0.48	0.80	0.45
85	J_28_03_01_Beli Brod	0.59	0.64	0.59	0.64	0.28	0.85	0.15	0.92
87	J_28_03_05_Draževac	0.03	0.98	-0.58	1.26	0.39	0.78	0.51	0.70

lower values of NSE. In addition to analysis of the numerical model performance the calibration plots, as an effective visual illustration of the model performance, depicting the simulated discharge hydrograph versus the observed discharge hydrograph, were also monitored (Fig. 5). Analyzing results at the selected computation points an improvement in the matching of the simulated and observed hydrograph was obvious although parameters during the recalibration for some locations have not changed significantly (Farkašić). Also for some locations (Bijelo Polje) the initial model was not able to perform the simulated hydrograph at all, while the Sava HEC-HMS v2.0 compute it successfully. The overall hydrograph matching is also slightly better, as a result of the model inputs improvements and calibration that was carried out for a long-term period, unlike the initial

model. The added value in the updated model was recognized in the better fitting of timing of the peak and the peak value itself but also in the better fitting of low and mean flows. A good example of the peak fitting can be seen at the computation point: J\_20\_19\_06\_Maglaj (Fig. 6) and where peaks are better simulated in the updated model. Another good example of the peak but also low and mean flows fitting can be seen at the computation point: J\_01\_13\_11\_Jesenice (Fig. 7) showing that data are better simulated in the updated model. Due to the lack of in-situ measurements of stream discharges there is always a doubt whether the rating curve (discharge vs stage) of observed data is properly developed in the high flow range and the observed flow is over or underestimated and whether comparison of the simulated and observed values is reliable.

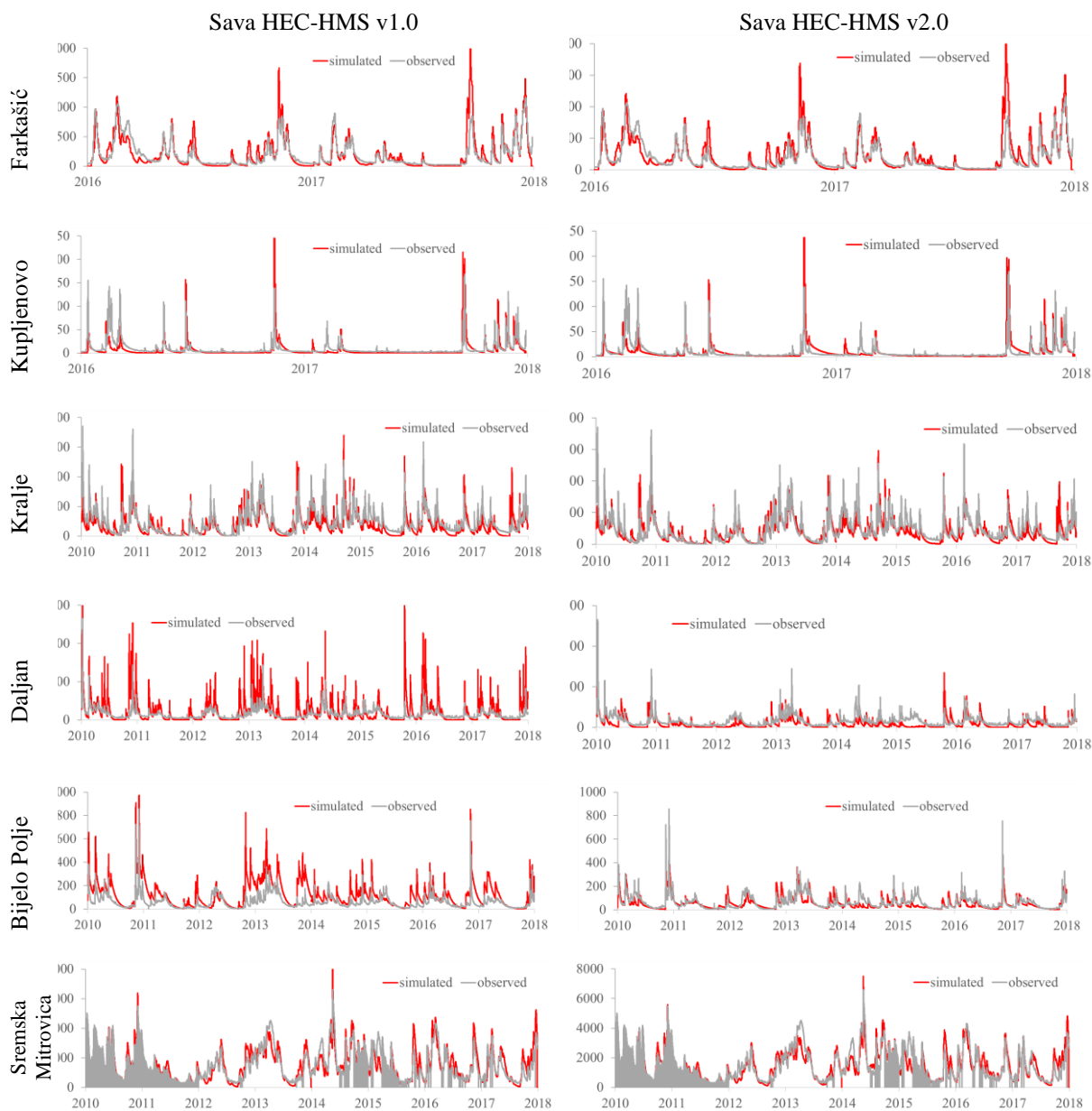


Fig. 5. Comparison of the simulated and observed flow at the selected locations.

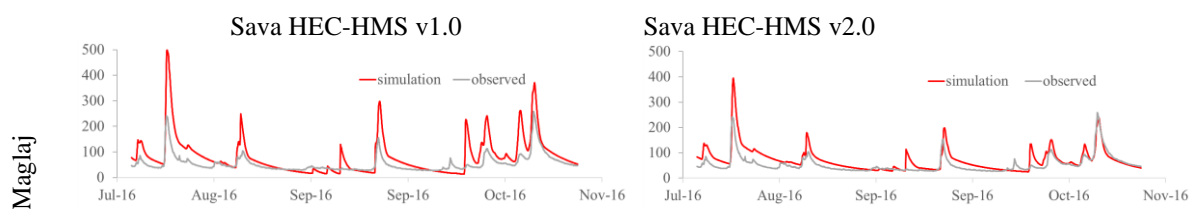


Fig. 6. Comparison of the simulated and observed flow at the location Maglaj.

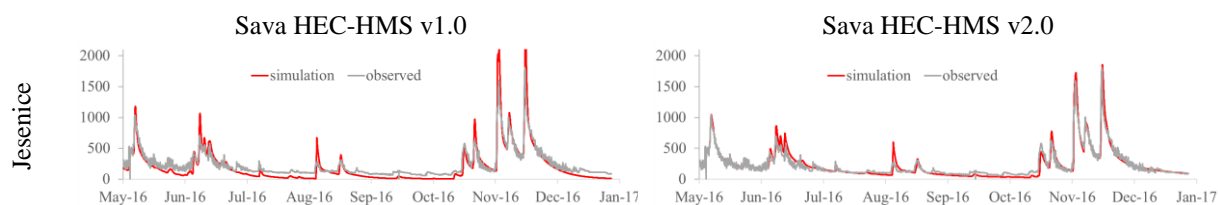


Fig. 7. Comparison of the simulated and observed flow at the location Jesenice na Dolenjskem.

## Conclusions and recommendations

The hydrological simulations were conducted for the period 2010–2018 including extreme May 2014 flood and several smaller floods, with evaluation of daily mean hydrological conditions and processes. The main findings are as follows: (i) performance and forecast accuracy of the existing Sava HEC-HMS model was significantly improved; (ii) the model was (re)calibrated for both high flows (for accuracy) and low flows (for stability and model performance); (iii) data sources for further developments were improved; (iv) a solid background for an international team of experts was established.

Considering that the Sava FFWS users have access to all data and workflows as well as managing the functioning and further developments of the system, it was very important that the national experts were fully involved in the study. Therefore, joint work and close cooperation of the national experts (duty forecasters) should be emphasized as an additional achievement, as follows: (i) experts deeply familiarized with the HEC-HMS software capabilities as well as with methods and techniques implemented into the Sava HEC-HMS model; (ii) upgraded own knowledge how to calibrate a such model; (iii) recognized all benefits of the model, its limitations and possible future applications; (iv) much more prepared for using this model under the Sava FFWS.

After performed activities and obtained results, the following recommendations are suggested: (i) development of a more complex soil loss method capable of long-term soil moisture accounting; (ii) a more detailed analysis of snowmelt within the model necessary (snow data availability); (iii) reservoir regulations at dams through the incorporation of a reservoir regulation model component (HEC-RESSIM). The future updates should utilize remote sensing data inputs for the soil

moisture accounting, snow melting, reservoir regulating as well as other specific applications in the Sava HEC-HMS. For future recommendations, the incorporation of high-resolution grid-based snow water equivalent and precipitation data, as well as the placement of additional meteorological stations in areas currently lacking observed data, will serve to improve performance of the model. Application of available products of missions like Sentinel, Landsat, AVHRR (Advanced Very High Resolution Radiometer), MODIS (Moderate Resolution Imaging Spectroradiometer), AMSR-E (Advanced Microwave Scanning Radiometer-Earth Observing System), DMS (Defense Meteorological Satellite Program) in the Sava HEC-HMS will be explored. The great potential of remote sensing data application is in general evident, both for the calibration of hydrological models and for operational hydrological forecasting, as well as for filling the data in catchments without observations or with an insufficient network of measuring stations and therefore will be used in the further Sava HEC-HMS model and Sava FFWS improvements including the related adaption of the modelling methods especially related to a rapid work of HEC and all latest developments of the software.

## Acknowledgement

This research is supported by the International Sava River Basin Commission and responsible authorities from the Sava River Basin: Sava River Watershed Agency, Federal Hydrometeorological Institute, Republic Hydrometeorological Service of the Republika Srpska, Public Institution "Vode Srpske", Croatian Meteorological and Hydrological Service, Institute of Hydrometeorology and Seismology, Republic Hydrometeorological Service of Serbia, Slovenian Environment Agency. The authors also thank Dragan

Zeljko, Secretary of the ISRBC, Brantley A. Thames, U.S. Army Corps of Engineers, Matthijs Lemans, Deltares and Damir Bekić, University of Zagreb for their constructive advice and immense help to improve this study.

## References

- ASCE (1993): Criteria for evaluation of watershed models. J. Irrigation Drainage Eng., vol. 119 no. 3, 429–442.
- Deltares (2018): Sava Flood Forecasting and Warning System, Technical Reference Manual, 106 p.
- Feldman, A. (2000): Hydrologic Modeling System Technical Reference Manual, Hydrologic Modeling System HEC-HMS Technical Reference Manual, 138 p.
- Legates, D. R., McCabe, G. J. (1999): Evaluating the use of “goodness-of-fit” measures in hydrologic and hydroclimatic model validation. Water Resources Res., vol. 35 no. 1, 233–241.
- Moriassi, D. N., Arnold, J. G., Liew, M. W. van Bingner, R. L., Harmel, R. D., Veith, T. L. (2007): Model Evaluation Guidelines for Systematic Quantification of Accuracy in Watershed Simulations. Transactions of the ASABE, vol. 50, 885–900.
- Refsgaard, J. C. (1997): Parameterization, Calibration, and Validation of Distributed Hydrological Models. Journal of Hydrology, vol. 198, 69–97.
- Rodriguez, E., Morris, C. S., Belz, J. E., Chapin, E. C., Martin, J. M., Daffer, W., Hensley, S. (2005): An assessment of the SRTM topographic products. Technical Report JPL D-31639, Jet Propulsion Laboratory, 143p.
- Tedesco, M., Kelly, R., Foster, J. L., Chang, A. T. C. (2004): AMSR-E/Aqua Daily L3 Global Snow Water Equivalent EASE-Grids. Version 2. Boulder, Colorado USA: NASA National Snow and Ice Data Center Distributed Active Archive Center.
- USACE and ISRBC (2017): Sava River Basin Flood Study - HEC-HMS Technical Documentation Report, 275 p.
- Willmott, C. J. (1981): On the validation of models. Physical Geography 2, 184–194.
- Willmott, C. J. (1984): On the evaluation of model performance in physical geography. In Spatial Statistics and Models, 443–460.
- Zhang, H. L., Wang, Y. J., Wang, Y. Q., Li, D. X., Wang, X. K. (2013): The effect of watershed scale on HEC-HMS calibrated parameters. Hydrology and Earth System Sciences, vol. 17, 2735–2745

Mirza Sarač, MSc. (\*corresponding author, e-mail: msarac@savacommission.org)  
International Sava River Basin Commission

Maja Koprivšek, BSc.  
Slovenian Environment Agency  
Slovenia

Oliver Rajković, MSc.  
Croatian Meteorological and Hydrological Service  
Croatia

Azra Babić, MSc.  
Merima Trako, BSc.  
Federal Hydrometeorological Service  
Bosnia and Herzegovina

Saša Marić, BSc.  
Republika Srpska Hydro-Meteorological Service  
Bosnia and Herzegovina

Adnan Topalović, MSc.  
Sava River Watershed Agency  
Bosnia and Herzegovina

Srđan Marjanović, MSc.  
Dejan Petković, MSc.  
Republic Hydrometeorological Service of Serbia  
Serbia

Marija Ivković, MSc.  
Public Water Management Company “Srbijavode”  
Serbia

Ervin Kalač, MSc.  
Danijela Bujanja, MSc.  
Institute of Hydrometeorology and Seismology  
Montenegro

## Statistical post-processing of short-term hydrological ensemble forecasts using the application of the dressing method

Tomáš VLASÁK\*, Jakub KREJČÍ

Probabilistic hydrological forecasts used in forecasting offices are often based only on different variants of precipitation forecast, which are the dominant source of forecast uncertainty during flood periods. The proposed method called dressing extends the uncertainty of meteorological forecast input by estimating the uncertainty of hydrological modeling using statistical analysis of deviations derived from simulated and observed flows. Adjustment of probabilistic flow forecasts is applied by post-processing without interfering with the hydrological model itself. The method is focused primarily on runoff phases, where heavy precipitation is not expected and the dispersion of the original ensemble is insufficient. A comparison of the success of short-term operative ensemble predictions of river discharge in the upper Vltava basin before and after adjusting by the dressing method showed a clear improvement in statistics.

KEY WORDS: hydrological forecast, ensemble forecast, dressing, post-processing

### Introduction

Simplification of reality in prediction models, inaccurate input data and other sources of uncertainty lead to predictions that always, more or less, differ from observation. Lack of accuracy of forecasts is the most important limitation in their use, and one solution is to quantify their uncertainty. Therefore, flow forecasts often include two basic products: 1.) **deterministic forecast**, single flow calculated from one selected set of causes (precipitation, saturation, etc.) and 2.) **ensemble (probabilistic) forecast**, model calculation is repeated for different scenarios of inputs and settings of the hydrological model. Ensemble forecast allows forecasters to estimate the risks (probabilities) of exceeding specific threshold. It also makes it possible to extend the time advance of forecasts and use them more effectively not only in flood protection but also at low flow rates.

In the case of hydrological river flow prediction, the ensemble forecasts are very often based solely on different variants of precipitation and temperature forecasting. The uncertainty of hydrological modelling (observed inputs, initial conditions, model parameters, etc.) is omitted. This simplification is acceptable in flood forecasting of upper basins when the effect of the uncertainty of the precipitation forecast is so dominant that the expression of uncertainty by the ensemble forecast calculated in this way is acceptable. However, hydrological forecasts are gradually being used for purposes

other than flood protection. Probability predictions are also important for dam manipulation planning, hydropower management or for river water use in times of drought, even in times of insignificant fluctuations or decrease inflows. In addition, a functional ensemble system in times of average flows is important for gaining confidence in probabilistic predictions as a whole. Probabilistic predictions should therefore contain quantified information on the uncertainty of the whole prediction system, not just precipitation forecast.

The presented method includes the uncertainty of hydrological modelling into the calculation of the ensemble hydrological forecast. It is primarily intended for the improvement of probabilistic forecasts based exclusively on precipitation variants. The method was inspired by the dressing method published by Pagano et al. (2012). It is based on the analysis of historical deviations of simulated and observed flows and the subsequent construction of error models. The method was tested in order to increase the success of operational ensemble predictions which serve as an irreplaceable source of information for river navigation in the Elbe and for the management of water reservoirs with regard to optimizing electricity production and minimizing the impact of drought. It is applied as a post-processing procedure, which means adjusting the hydrological forecast after its output from the hydrological model. The advantage of post-processing is easy implementation into operation without disrupting other established procedures.

### Hydrological forecast uncertainty

Understanding the reasons why hydrological forecasts deviate from observations is key step in developing the success of both deterministic and probabilistic forecasts. Krzysztofowicz (1999) decomposes the total uncertainty into input uncertainty and hydrological uncertainty.

The uncertainty of the inputs is solved by pre-processing methods, which precede the calculation itself in the prediction model. The observed elements (precipitation, temperatures, flows) are usually not subject to such a significant error. Their uncertainty is usually neglected, or they are reduced or quantified using some of the pre-processing methods, for example (Schaake et al., 2004). The dominant source of uncertainty in the period of heavy rainfall is the quantitative precipitation forecast from numerical weather forecasting models. Different precipitation variants are therefore fundamental and often also the only quantified uncertainty for the probabilistic hydrological forecast. Probabilistic hydrological forecasts based only on different precipitation variants suffer mainly from an insufficient variance of variants during the precipitation-poor period. In these cases, the more significant is hydrological uncertainty. The distinction between meteorological and hydrological uncertainty and independent work with them was used, among others, in the work of Demargne et al. (2013) and Verkade et al. (2017).

Hydrological uncertainty is usually adjusted by post-processing methods, which stand between the output of the forecast from the model and its final publication for users. Statistical post-processing is simply a model that uses the relationship between the prediction and the observed element (Fig. 1). There are a number of statistical post-processing methods, from a simple percentile method through more complex statistical procedures such as the Kalman filter or the Bayesian method to the application of neural networks. An overview of post-processing methods in hydrology was published for example, by Li (2017).

The dressing method combines the already created

hydrological ensemble forecast, which is based on the probabilistic prediction of precipitation, with the statistical distribution of deviations of hydrological modelling, and thus achieves a comprehensive description of the entire uncertainty of the hydrological forecast.

### Materials and Methods

Hydrological forecasting system AquaLog (Krejčí and Zezulák, 2009) was used for the calculation of forecasts needed for method design and assessment. This system is the main tool for real-time hydrological forecasting in the Czech Republic in the Labe basin. AquaLog model consists of continuous SAC-SMA (Burnash, 1995) precipitation-runoff component and its operation is largely automated, excepts for assimilation of simulated flow to the last measured discharge. The upper Vltava river basin (tributary of the Elbe) was selected for testing the method. The catchment with area of 12105 km<sup>2</sup> is divided into 45 sub-basin delimited by water gauging stations with the observed discharge (Fig. 2).

Three statistical methods commonly used in the field of ensemble predictions verification were used for evaluating the success of the dressing method. They focus on the reliability, the skill and the conditional verification of ensemble prediction. The rank histogram (sometimes called Talagrand diagram) was used for assessing the spread of the prediction ensemble in relation to real observational variability. The Brier score is a suitable criterion for verifying a categorical prediction from the point of view of the accuracy of a probabilistic prediction when we examine whether a defined phenomenon did/didn't occur. It answers the question of how big the probability prediction error is (0 if it does not happen and 1 if it does happen). The benefit of the last used ROC (relative operation characteristics) criteria lies in its ability to distinguish between the occurrence and non-occurrence of a particular event for a given condition. All the mention methods are in detail described in WMO (2021). Basic interpretation of rank histogram and ROC plot used in Results chapter is shown on the Fig. 3.

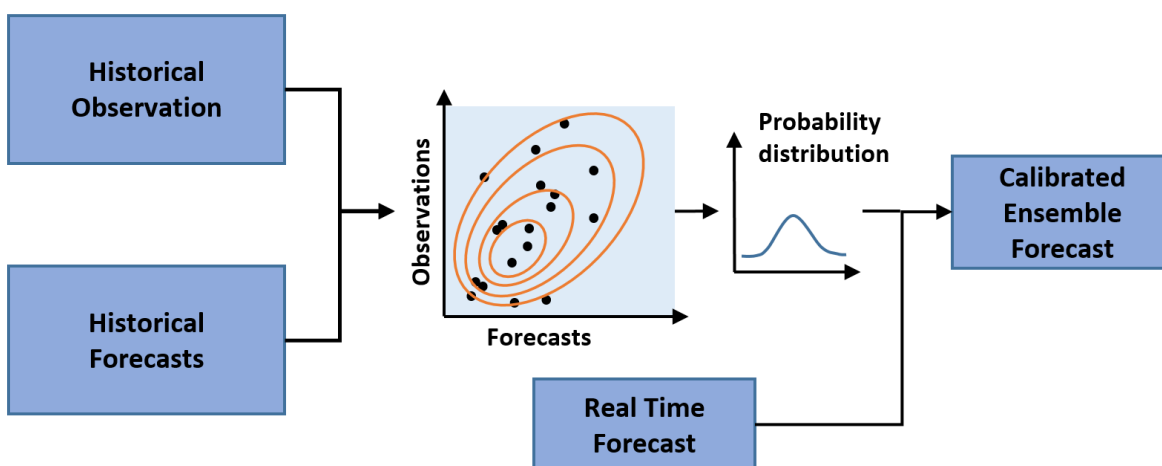


Fig. 1. Scheme of statistical post-processing of hydrological forecast (Li, 2017).

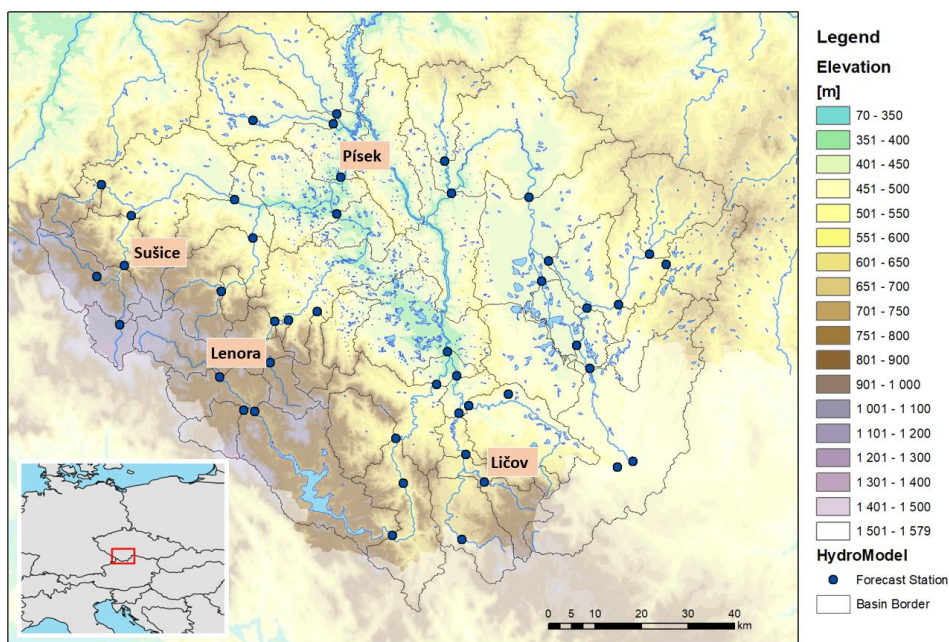


Fig. 2. The upper Vltava river basin with forecasted water gauging stations. The stations with label are mentioned in the chapter Method calibration and results.

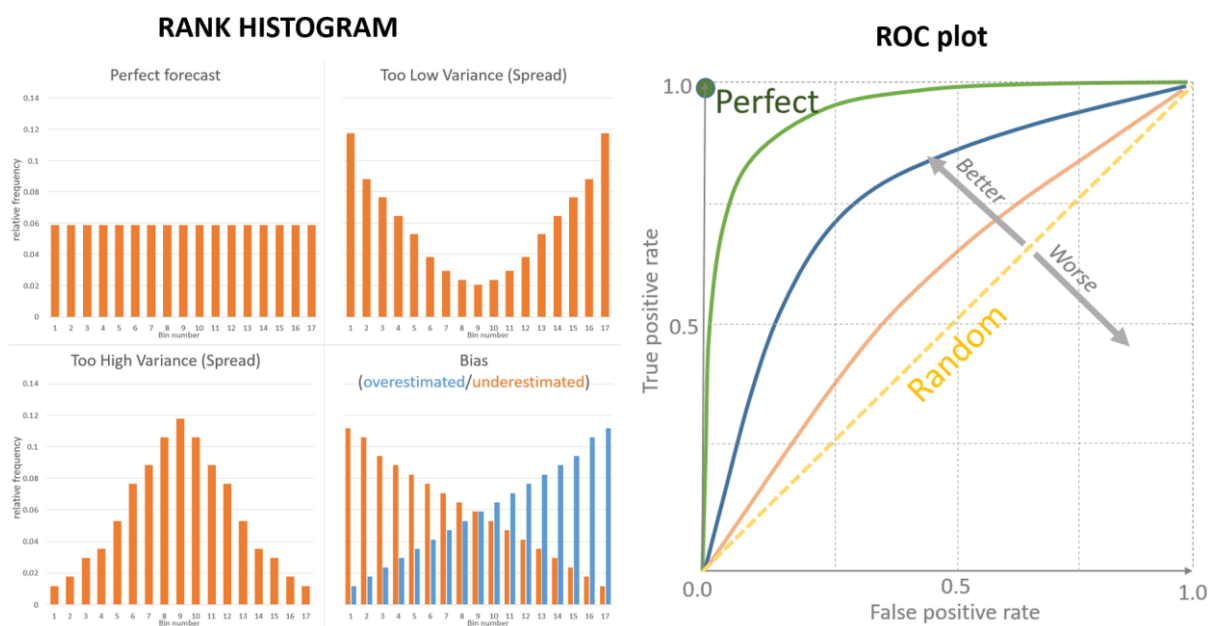


Fig. 3. Basic interpretation of rank histogram and ROC plot.

### Dressing method

Dressing is designed to modify the probabilistic hydrological forecast calculated from the meteorological forecast ensemble. The uncertainty of hydrological modelling is expressed by an error model, which is derived from the statistical distribution of deviations between historical flow forecasts and the observed flow for different lead times.

Historical flow forecasts were calculated by replacing the predicted precipitation with observed precipitation to clear the influence of precipitation forecast uncertainty

on forecast error. The method of calculating historical forecasts as well as a number of forecasts is essential for the successful application of the dressing method. Historical forecasts should well represent the uncertainty of hydrological modelling in real-time operations and should cover as many runoff variants as possible. Because the AquaLog hydrological forecasting system is built on continuous models, we assume that deviations of automatically calculated historical forecasts from the observed flow well represent the uncertainty of hydrological modelling. Uncertainty is expressed as a whole without distinguishing between individual

sources of uncertainty (input data, initial conditions, model structure, operational control, etc.).

*Error model*

Although historical forecasts are not affected by uncertain precipitation prediction, the magnitude of the errors of historical forecasts significantly increases with the lead-time. This is due to two facts. (1) The forecast is in the last phase of the calculation assimilated to the last observed flow, which eliminates the error in short lead-time. (2) The forecast for downstream water gauging stations is in short advance based on a more reliable channel routing model with input of observed discharge from the upper station. After exceeding the travel time of water among two water gauging stations the observed discharge is replaced with simulated discharge, which contains errors from the less reliable rainfall-runoff model. It is obvious that specific error models for different lead-time as well as for different water gauging stations are required.

Error models were constructed according to the frequency of flow multiplicative deviations  $Qdif$ :

$$Qdif_p = \frac{Qobs_p}{Qsim_p} \quad (1)$$

where

$Qsim_p$  – is the forecasted flow in prediction lead time  $p$ ,

$Qobs_p$  – is the observed flow in prediction lead time  $p$ .

With a short lead time, most of the deviations  $Qdif$  derived from the historical forecasts are close to number one. With the increasing lead, the standard deviation, as well as the variance of deviations, increase (see Fig. 4). For some water gauging profiles, there is an uneven distribution of overestimated and underestimated forecasts in the error models. It indicates systematic bias, which is related to the calibration of the hydrological model. The error model created in this way adjusts

the ensemble prediction in two ways. (1) It expands the variance of the hydrological ensemble calculated according to precipitation variants. (2) It corrects the systematic error of the hydrological model (bias).

Pagano (2012) uses one error model for each water gauging profile. The advantage of this approach is a small fluctuation of the error models because they are calculated from a large number of historical forecasts. One set of error models for each forecasting point also facilitates the application of the method to daily operation. In fact, it is clear that the uncertainty of the hydrological model differs for different runoff phases. The increase of forecast errors with a lead-time for the period without precipitation with steady river discharge and for the period when heavy precipitation is expected varies significantly.

The dynamic construction of the error model proved to be a suitable solution to this problem. For each hydrological forecast, a number of the most similar historical forecasts are selected. The specific error model is built from this selection. This means that the error model differs not only for each water gauging profile and the lead-time but also according to the type of runoff phase. The dressing method is combined with the method of the historical analogue (Li, 2017). Nash-Sutcliffe coefficient was chosen as a criterion for the selection of historical forecast analogues. Its calculation is based on equation (2):

$$NS = 1 - \frac{\sum_{i=1}^N (S_i - O_i)^2}{\sum_{i=1}^N (O_i - \bar{O})^2} \quad (2)$$

where

$S_i$  – is the discharge of the current forecast at the time  $i$ ,

$O_i$  – is the discharge of the historical forecast at the time  $i$ ,

$\bar{O}$  – is the average discharge of the historical forecast.

The unique error model for each forecast is more correct because it doesn't mix different runoff phases with different errors into one error model. The other advantage

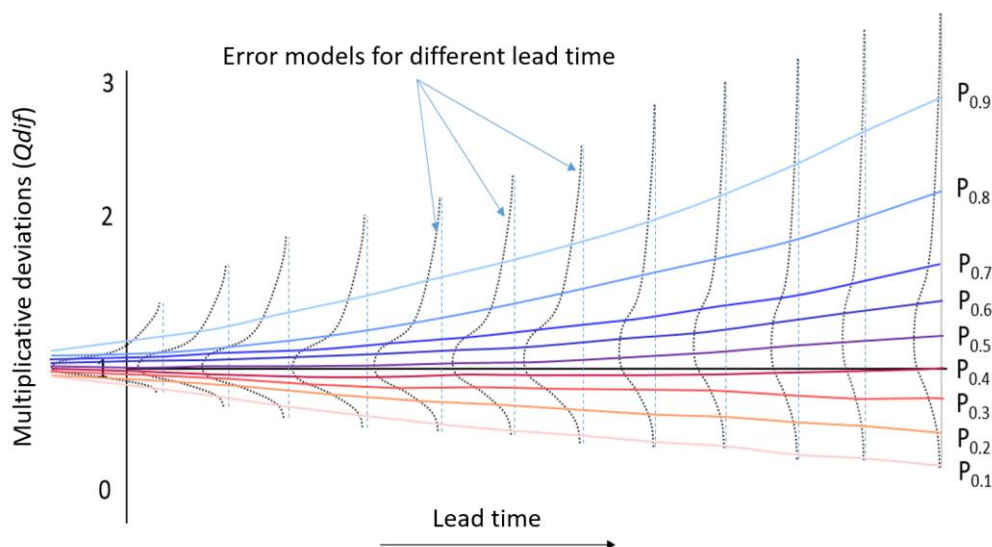


Fig. 4. Error model (distribution of frequency of multiplicative deviations  $Qdif$ ) for different lead time. Coloured lines indicate percentiles of the distribution of deviations.

of dynamic construction of the error model is the elimination of forecasts which are not suitable for the dressing method, i.e. forecasts that don't have a sufficient number of similar historical predictions (Fig.5). The time development of these forecasts is so dynamic that it is difficult to find enough similar historical forecasts. Error models built from lower numbers or less similar discharges can give too large variance and unreal estimation of forecast uncertainty. Testing the method proved that the vast majority of removed forecasts was from the high flow period when the dominant source of uncertainty is the quantitative precipitation forecast, and therefore the original ensemble, based on variants of precipitation forecasting, usually provides a sufficient estimate of forecast uncertainty.

The successful application of the method is related to the setting of the minimum value of the NS coefficient, the number of historical floods required for the error model and the length of the processed time series. The minimum value of the NS separates historical forecasts suitable and not suitable for the error model. The number of chosen historical forecasts determines the reliability of the error model and the length of the time series of the forecast has a similar effect. In the case of forecasts with a very short lead-time, the length of time series should be extended to include observed data because autocorrelation between the observed and the predicted flow is usually very strong.

Setting the method, which means a high degree of similarity between the adjusted forecast and historical forecasts, gives a better chance for a more accurate estimate of the uncertainty of hydrological modelling, on the other hand, it reduces the number of forecasts that can be processed by the method. Finding the optimal compromise between the number of processed predictions and the success of the method was the subject of method calibration.

#### *From error model to ensemble forecast*

The error model was expressed by 9 levels of probability of exceeding from the deviations  $Q_{dif}$  ordered by size. The levels correspond to percentiles  $P_{0.1}$ ;  $P_{0.2}$ ;  $P_{0.3}$  to  $P_{0.9}$  (see Fig. 3). Each hydrological forecast (each member of the forecast ensemble) was divided into 9 forecasts multiplying the flow by nine  $Q_{dif}$  values for each lead time of the forecast. This created a new ensemble nine-time larger than the original ensemble. For example in the case of hydrological forecast ensemble based on 17-member precipitation variants from ALADIN-LAEF system extended 153-member was created.

However, the number of members of the hydrological forecast ensemble should not change after post-processing for two reasons. (1) Some forecasts are not suitable for the dressing method due to too few similar historical forecasts. (2) Post-processing, in general, should not affect further processing of forecasts (publications, archiving). For these reasons, the next step is to reduce the number of ensemble members to the original count. From the several tested procedures,

a simple percentile selection method was finally chosen. The members of the extended ensemble were sorted by the size based on the selected criteria (average flow, or maximum flow, or a combination of multiple indicators) and every 9th member was chosen. The disadvantage of this approach is that new ensemble members don't have to be derived from the same member in the original ensemble. Therefore some variants, typically with secondary waves, may not appear in the new ensemble. However, the variance of the predictions according to the selected criterion (average flow, maximum flow, etc.) is expressed correctly.

#### *Method calibration and results*

Calibration and testing of the post-processing method dressing with a dynamically generated error model consisted of (1) finding optimal parameters for building the error models (2) comparison of the assessment of original and modified hydrological ensemble forecast.

The set of historical hydrological forecasts covered of 2780 episodes from the period 2012 to 2020. They were calculated for 40 forecasted points in the Upper Vltava river basin as a time series of discharge values with 1 hour time step and 66 hours lead time. The time series of predicted discharge started always at 7:00 AM, which is the time zero of real-time forecast. This may be important in building an error model because some forecast errors can be affected by the daily development of weather, especially air temperature. The minimum number of historical forecasts required for the building of the error model was set at 20 cases. Forecasts were compared without including any section of observed flows that precedes the predictions. Calibration was focused on finding the optimal size of the NS coefficient. For the calibration and the testing of the performance of the method, 270 ensemble hydrological forecasts calculated in real-time operation in the years 2020 to 2021 were used. These ensembles were based on 17 variants of precipitation from the ALADIN-LAEF forecast system with a time step of 1 hour and 66 hours lead-time.

With a high degree of similarity ( $NS > 0.7$ ) between the adjusted forecast and its historical analogues, the best statistics of improvement were obtained. Unfortunately, the rate of forecasts that were adjusted by post-processing fell to units of per cent. For the criterion of low degree of similarity ( $NS > 0$ ), between 95 and 99% of all forecasts have already been adjusted by dressing method. However, in this case, the variance of the error models was too large and they produced worse results, especially in the too-large spread of the adjusted ensemble of hydrological forecasts. The size of NS between 0.2 and 0.3 turned out to be the optimal value, which allowed the adjustment of approximately half of the predictions.

The success of river flow forecast can be viewed in different ways and there isn't one perfect evaluation criterion. Therefore three statistical methods were selected for verification of dressing. The positive effect of the adjustment of forecasts was reflected above all in the widening of the spread of ensemble members.

Insufficient spread of original ensemble forecast caused that there were too frequent cases where the observed flow was behind the edge of the ensemble members. It is manifested as too big bars in the rank histogram (Fig. 6). After applying dressing with appropriate parameters the frequency of position of observed discharge between members ensemble forecast was more equal. Methods based on the evaluation of the probability of

exceeding a certain discharge threshold showed significant improvement in the area of average and below-average flow. Furthermore, there was a high rate of adjusted forecasts in this interval of discharge. Towards higher flows, the rate of adjusted forecasts decreases and the effect of post-processing disappears (Fig. 7). The percentage of adjusted forecasts, as well as improvement rate, varies among water gauging profiles.

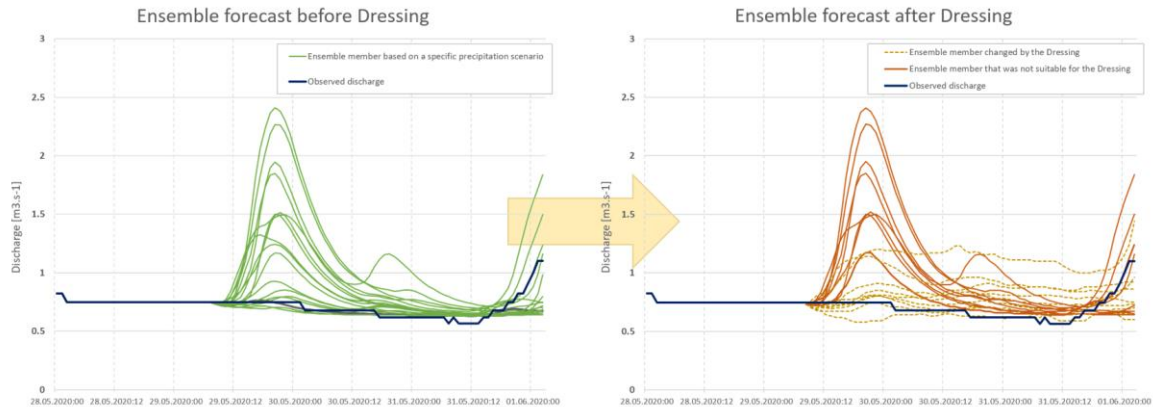


Fig. 5. Example of post-processing with the Dressing method where some of the original member weren't processed because of weak error model.



Fig. 6. Rank histograms of the frequency of the observed average discharge between 17 members of forecasted ensemble of average discharge. Comparison of real-time forecast and the forecast adjusted by post-processing.

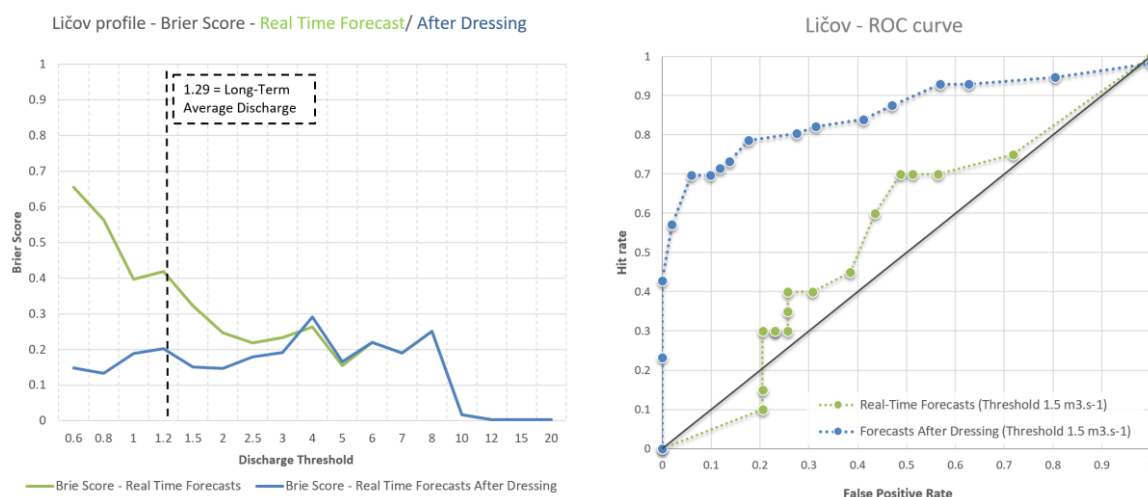


Fig. 7. Brier Score and ROC curve for ensemble hydrological forecasts for Ličov water gauging station (basin area 126 km<sup>2</sup>). Comparison of evaluation of original real time forecasts and adjusted forecasts by dressing method.

It is related to different variability rainfall-runoff conditions and the influence of water constructions (weirs, dams).

### Discussion

The estimation of hydrological modelling uncertainty using the dressing method depends largely on the extent of the archive of historical forecasts and on the fact whether historical forecasts correspond the uncertainty of hydrological modelling of real-time operations. The archive of 2780 historical forecasts for a period of 9 years provided a sufficient database for post-processing forecasts with little variability, mostly average or below-average flows. Better results can be expected by expanding this archive because it should cause more similarity between the current forecast and historical analogues.

Historical forecasts in which the precipitation forecast is replaced by observed precipitation cannot be calculated in real-time operation but must be prepared in automatic calculation afterwards. Forecasting systems where the operation is highly interactive, e.g the hydrologist significantly interferes with the setting of the initial conditions, or even the parameters of the hydrological model and adjusting the forecast are not suitable for the application of this method. This is because a significant part of the uncertainty of hydrological modelling is associated with hydrologist decision-making, which cannot be transferred to the automatic calculation of historical forecasts. However, the development of hydrological forecasting models, especially the increase of their spatial resolution, leads to more automatic real-time operations.

Recalculation of historical forecasts even in very complex hydrological model is possible. In comparison with numerical meteorological models, which are extremely demanding on the computing capacity of

computers it is relatively easy and quick to update the archive of historical forecasts in case of changes in the structure of the model or its parameters. These facts open up space for more frequent use of post-processing methods.

### Conclusion

The post-processing method dressing with a dynamically compiled run-time error model is a functional tool for adjusting ensemble hydrological forecasts which are based only on ensemble precipitation forecasts. Methods increase the success of hydrological ensemble predictions by including uncertainty of hydrological modelling. This uncertainty is derived from deviations of historical forecasts with a similar pattern of simulated discharge and observation. Historical forecasts must represent solely possible errors of the hydrological forecasting system as a whole without the influence of precipitation forecast uncertainty.

Testing the effect of dressing on the short-term ensemble's hydrological forecasting method demonstrated a significant improvement in the success of the forecast adjustment. Above all, there was a positive spreading of the variance of the forecast ensemble and also a slight correction of the systematic bias of the flow from hydrological model resimulation. The change was particularly noticeable in the area of average and below-average flows, where hydrological modelling is the dominant source of uncertainty. For forecasts with higher flows and with rising river levels, there wasn't a sufficient number of similar situations in the database of historical forecasts and therefore no adjustment by the dressing method was possible. However, the most of rejected forecasts were runoff episodes where the dominant source of uncertainty is the precipitation forecast, which is covered in the ensemble's meteorological forecast input.

The method is suitable for the operational operation of hydrological services using automatic or semi-automatic forecasting systems. The application of the method into a hydrological forecasting system is simple and can be implemented without disrupting already established processes.

## References

- Burnash, R., J., C. (1995): The NWS river forecast system – Catchment modeling, in: Computer models of watershed hydrology, edited by: Singh, V. P., Water Resources Publicat., Highlands Ranch, Colorado, U.S.A., 311–366.
- Demargne, J., Wu, L., Regonda, S., Brown, J., Lee, H., He, M., Seo, D. J., Hartman, R., Herr, H. D., Fresch, M., Schaake, J., Zhu, Y. (2013): The science of NOAA's operational hydrologic ensemble forecast service. Bull. American Meteorological Society, 130611111953000. <http://journals.ametsoc.org/doi/abs/10.1175/BAMS-D-12-00081.1>.
- Krejčí, J., Zezulák, J. (2009): The use of hydrological system AquaLog for flood warning service in the Czech Republic. [online]. Regional Workshop on Hydrological Forecasting and Real Time Data Management At: Dubrovnik [cit. 30.6.2011] z <https://www.researchgate.net/publication/301358002>.
- Krzysztofowicz, R (1999): Bayesian theory of probabilistic forecasting via deterministic hydrologic model, Water Resources Research 35 (9), 2739–2750.
- Li, W., Duan, Q., Miao, C., Ye, A., Gong, W., Di, Z. (2017): A review on statistical postprocessing methods for hydrometeorological ensemble forecasting. WIREs Water, e1246. <https://doi.org/10.1002/wat2.1246>.
- Pagano, T., C., Shrestha, D., L., Wang, Q., J., Robertson, D., Hapuarachchi, P. (2012): Ensemble dressing for hydrological applications, In: Hydrological Processes, Special issue S173 Hydrological Ensemble Prediction Systems (HEPS).
- Schaake, J., Perica, S., Mullusky, M., Demargne, J., Welles, E., Wu, L. (2004): Pre-processing of atmospheric forcing for ensemble streamflow prediction., In: 17th Conference on Probability and Statistics in the Atmospheric Sciences, AMS.
- Verkade, J. S., Brownd, J. D., Davids, F., Reggiani, P., Weertsaf, A. H. (2017): Estimating predictive hydrological uncertainty by dressing deterministic and ensemble forecasts; a comparison, with application to Meuse and Rhine. Journal of Hydrology, Volume 555, December 2017, Pages 257–277, <https://doi.org/10.1016/j.jhydrol.2017.10.024>
- WMO (2021) Guidelines on Ensemble Prediction System Postprocessing, WMO no-1284, edition 2021, pages 46, ISBN 978-92-63-11254-5

RNDr. Tomáš Vlasák, PhD. (\*corresponding author, email: [tomas.vlasak@chmi.cz](mailto:tomas.vlasak@chmi.cz))  
Ing. Jakub Krejčí, PhD., MSc.  
Czech Hydrometeorological Institute  
Na Šabatce 17  
140 00 Praha 4  
Czech Republic

## Snow cover in the Ukrainian Carpathians

Viktor I. VYSHNEVSKYI\*, Olena A. DONICH

Based on the results of regular monitoring during 1961–2020, the main features of snow cover in the Ukrainian Carpathians were determined. The observation data at the meteorological stations, mainly located at high altitude, show an increasing trend in snow cover depth in winter and in the first half of spring. At the same time, there is a decrease in snow cover duration at low altitudes and an increase at high altitudes. General trends for the mountain area are higher air temperature and lower wind speed. Simultaneously precipitation changes are small or absent. It has been shown that decrease of wind speed over the last decades should be taken into account to determine the actual changes in snow cover. As a result of this decrease, the snow cover depth in the mountains became more uniform than at the beginning of the observations: larger on mountain tops and smaller in ravines and mountain forests. This means that in general, the snow cover depth and snow water equivalent in the mountains are stable. This was confirmed by the fact that during spring flood the water runoff of local rivers remained without essential changes.

KEY WORDS: snow cover, air temperature, precipitation, wind speed, river runoff, the Ukrainian Carpathians

### Introduction

Climate change in the mountains, in particular of air temperature and snow cover is a popular issue of many scientific studies. Their results showed a trend towards temperature increase (Holko et al., 2020; Marin et al., 2014; Marty and Meister, 2012; Migala et al., 2016; Tomczyk et al., 2021; Vyshnevskyi and Donich, 2021). This increase has been accelerating in recent decades. In particular, the winter of 2019/2020 in Central Europe was much warmer than usual. This could not but affect the snow cover.

The increase of air temperature can give ground for considering a possible decreasing trend in snow cover depth. At the same time, the changes of snow cover depth and its duration are not quite obvious, partly due to essential variability of these parameters. Moreover, in some cases, research results are contradictory.

The study (Tomczyk et al., 2021) showed the decrease in the number of days with snow cover for the most of Poland, except for the mountain region, where there was an increase, but not statistically significant. A decrease in snow cover depth was determined at low, and an increase – at high altitudes. The authors (Tomczyk et al., 2021) consider that the duration of snow cover strongly depends on the temperature, and the snow cover depth depends on the amount of precipitation in the form of snowfall.

Some other results were obtained for the neighboring area in the Tatra Mountains (Holko et al., 2020). At the station, located at an altitude of 1778 m a.s.l., there is

a slight declining tendency of snow cover and at the station with an altitude of 1991 m a.s.l. no changes are noticeable. Simultaneously the duration of snow cover at both stations remained unchanged. A decreasing tendency for the snow cover and the water in it during 1951–2017 was obtained in a study (Fontrodona et al., 2018) on the main part of Europe. At the same time for the coldest areas in Europe, an increase in mean and maximum snow depths is observed. The study (Bulygina, et al., 2009) carried out as to territory of Russia showed the decrease of snow cover on its larger part except Central Siberia and the coast of the Sea of Okhotsk, where it increased. Negative temporal trends in snow cover depth were found in Norway for low altitude stations and positive trends were indicated for the stations over 850 m a.s.l. (Skaugen et al., 2012). Studies (Marty and Meister, 2012) in the Swiss Alps found no changes in snow depth in mid-winter. However, there is a decreasing trend in snow cover depth during the snowmelt period in the spring and summer months.

The dependence of snow cover parameters on important factors has been studied in (Malgorzata, 2002). It was determined that in mountain conditions they have a worse correlation than in lowland ones.

Some studies of snow cover are grounded on remote sensing data. The article (Notarnicola, 2020) contains the statement about significant negative trends in snow area and snow cover depth in the European Alps and the Carpathian Mountains during 2000–2018. The same results were shown in the study (Dong and Menzel, 2019)

carried out for the central European region covered by low mountains.

The precipitation, in particular, in the cold period, generally did not change essentially (Repel et al., 2021; Rožnovský et al., 2020; Kubiak-Wojcicka, 2020).

Many studies show the decrease tendency of wind speed (Birsan et al., 2020; Marin et al., 2014; Spinoni et al., 2015; Vyshnevskiy and Donich, 2021). It is important that the decrease of maximum monthly wind speed exceeds the decrease of mean monthly wind speed. This decrease is more pronounced during the months with the highest wind speed (Birsan et al., 2020).

The study (Grünewald et al., 2014) shows the possibility of wind to redistribute the snow from exposed to sheltered locations. The erosion of snow by the wind is the largest at high altitudes, as wind speed increases with elevation.

Despite some climate changes, in particular snow cover, the river runoff during spring flooding is rather stable. In some European regions there is a trend towards earlier spring floods, in some – to later ones (Blöschl et al., 2017). The studies (Halmová and Pekárová, 2020; Holko et al., 2020; Gorbachova et al., 2018; Bačová Mitková and Halmová, 2020; Mostowik et al., 2019) show that the changes of maximum discharges and runoff volume during spring flood in the Carpathians Mountains are small or absent. As can be seen, there is a problem with finding factors that affect both snow cover and river runoff during spring flood. In our opinion, the uncertainty regarding changes in snow cover depth and river runoff is due to ignoring of some factors, including the changes of wind speed during the last decades. So, the main goal of this study is to specify the real changes in snow depth in the Ukrainian Carpathians as an important factor influencing river runoff.

## The study area

The studied area of the Ukrainian Carpathians is the central part of the Carpathian Mountains. The total length of these mountains is about 240 km, the width is 50 km, the largest altitude is 2061 m a.s.l. (Hoverla Mountain). The characteristic feature of these mountains is the presence of ridges, which go almost parallel to each other. The highest ridge, where Hoverla Mountain is located, has the name of Chornohora or Chornohirskiy Ridge. The second by altitude is Svidovets Ridge with the highest altitude of 1883 m a.s.l., located a little bit northwest from Chornohirskiy Ridge. The volumetric image of the Ukrainian Carpathians, created on the basis of Shuttle Radar Topography Mission (SRTM) digital elevation model, is shown in Fig. 1.

## Methodology and data

In the Ukrainian Carpathians there are about a dozen meteorological stations at different altitudes. Only two of them are located at a rather high altitude. The first station Plai is located on the southwestern macroslope of the mountains; its altitude is 1331.5 m a.s.l. The second station Pozhezhevska with the altitude of 1451 m a.s.l. is located on the northeastern macroslope on the distance 2.6 km from Hoverla Mountain. The other stations are located at low-mountain terrain; their altitudes range from 432 to 762.5 m a.s.l. Typically, these stations are located in river valleys on the outskirts of local towns and villages (Table 1).

In addition to measuring the parameters of the snow cover parameters (dates of its formation, depth and dates of its disappearance), these meteorological stations measure many other parameters: air temperature,

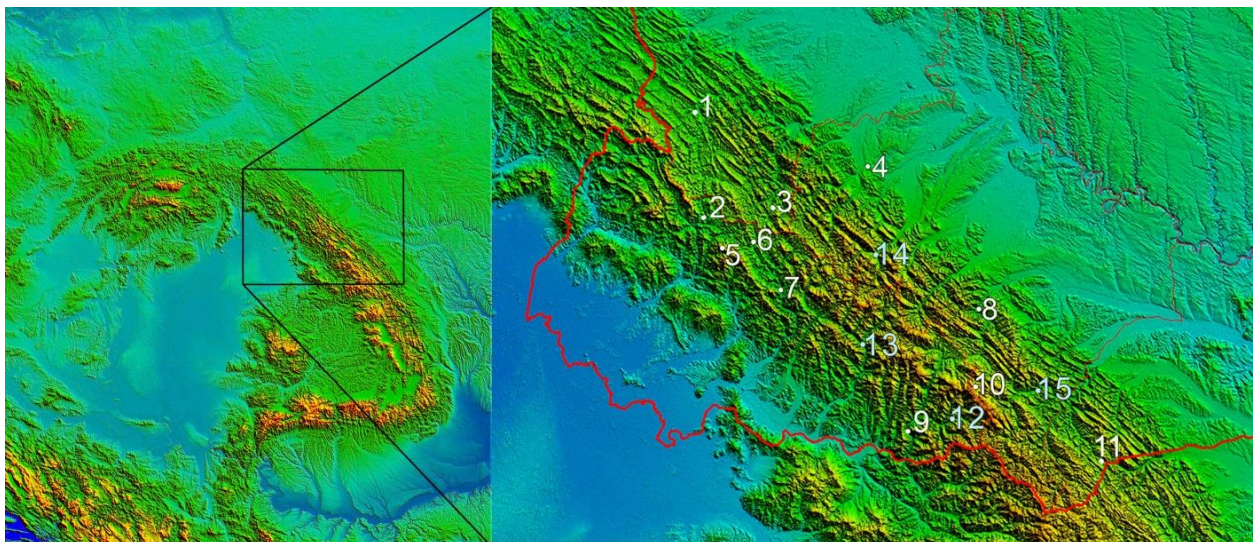


Fig. 1. Volumetric image of the Carpathian Mountains with location of the meteorological stations in its Ukrainian part (1 – Turka, 2 – Nyzhni Vorota, 3 – Slavske, 4 – Dolyna, 5 – Plai, 6 – Nyzhnii Studenyi, 7 – Mezhihiria, 8 – Yaremche, 9 – Rakhiv, 10 – Pozhezhevska, 11 – Seliatyn) and studied hydrological stations (12 – Bila Tysa – Luhi, 13 – Teresva – Ust-Chorna, 14 – Limnitsa – Osmoloda, 15 – Chornyi Cheremosh – Verkhovyna).

precipitation, wind speed, etc. Relevant meteorological parameters were processed for the period 1961–2020. In many cases the data for the periods of 1961–1990 and 1991–2020 were analyzed separately.

Certain attention was also paid to the river runoff – mainly to the inner year distribution. Changes in river runoff and possible factors that may cause them were analyzed. The remote sensing data (mainly of Landsat satellites) were also used in the study.

## Results

### Snow cover depth

The largest snow depth in the Ukrainian Carpathians is observed at the meteorological stations Plai and Pozhezhevka, located at the largest altitude. During 1991–2020 the mean snow depth at the meteorological station Plai in the third decade of February, when it is the largest, is 47 cm. In turn, the mean snow depth at the meteorological station Pozhezhevka in the third decade of March, when it is the largest, reaches 43 cm. The mean snow depth among the largest measured values at these meteorological stations is 74 and 79 cm respectively.

During 1991–2020 the largest snow depth was registered at the end of the cold and snowy winter of 1998/1999.

That winter the mean snow depth among the largest measured ones at 11 meteorological stations was 106 cm. The lowest value was observed in winter 2015/2016, when it was 20 cm.

The available data show that snow cover depth during the period of 1961–2020 slightly changed. At stations located in low-mountain terrain a small snow depth decrease is observed in December and January. Simultaneously, is observed a small increase during the period from February till the middle of April. The changes at the highest stations are much more obvious. There is a significant increase in snow cover depth, especially in winter and in the first half of spring (Fig. 2).

As can be seen in Fig. 2, the largest snow cover depth in the last three decades is observed somewhat later than before. The obtained result gives possibility to make the conclusion that snow cover depth in the Ukrainian Carpathians has an increasing trend. This result coincides with results published in the articles (Tomczyk et al., 2021; Skaugen et al., 2012), but it is different from other ones obtained in other regions – mainly at lowland conditions. Therefore, this issue is considered in more detail in the discussion. The relationship between snow cover depth and snow cover duration at the neighboring stations is generally weak. It is stronger for the snow cover duration and it is weak (almost absent) when concerning the snow cover depth.

**Table 1.** The parameters of meteorological stations in the Ukrainian Carpathians

N <sup>o</sup>	Name	Altitude [m a.s.l.]	Latitude	Longitude
1	Turka	592.4	N49°09'01"	E23°01'47"
2	Nyzhni Vorota	488.7	N48°46'30"	E23°05'52"
3	Slavske	593.6	N48°50'31"	E23°26'57"
4	Dolyna	467.6	N48°58'37"	E23°59'52"
5	Plai	1331.5	N48°40'03"	E23°11'53"
6	Nyzhnii Studenyi	611.4	N48°42'04"	E23°21'57"
7	Mezhihiria	455.4	N48°31'37"	E23°30'17"
8	Yaremche	531.3	N48°27'10"	E24°33'12"
9	Rakhiv	432.1	N48°02'52"	E24°11'54"
10	Pozhezhevka	1451	N48°09'14"	E24°32'04"
11	Seliatyn	762.5	N47°52'36"	E25°12'59"

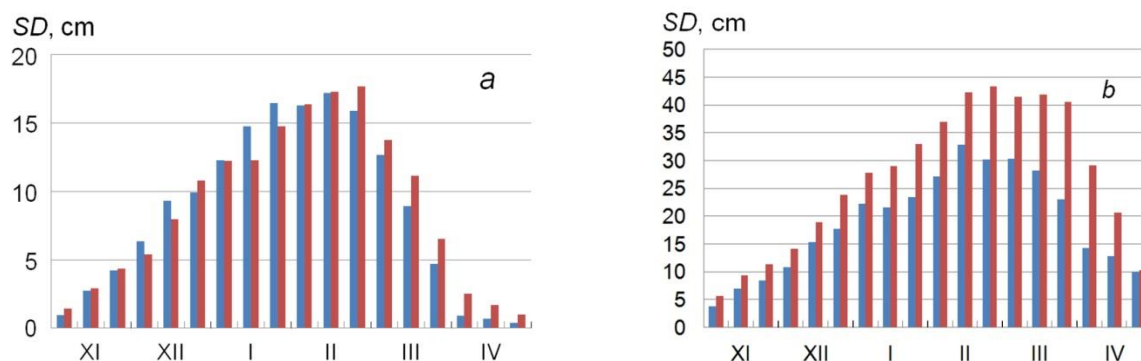


**Fig. 2.** The mean snow depth in the Ukrainian Carpathians: a) – at 9 meteorological stations in low-mountain terrain, b) – at highest Plai and Pozhezhevka stations; left columns – during 1961–1990, right columns – during 1991–2020.

**Snow cover duration**

Data on snow cover, as well as data on the formation, duration and disappearance of snow cover depend on the altitude. This dependence is much stronger than the dependence on latitude. The longest snow cover duration (SCD) is observed at the highest meteorological stations Plai and Pozhezhevska, where during 1991–2020 it was 157 and 158 days, respectively. In the previous period of 1961–1990 this duration at both stations was the same – 153 days. Thus, we see a small increase. The increasing trend in the snow cover depth and duration at Pozhezhevska station in 1961–2010 was also identified in the study (Błażejczyk and Skrynyk, 2019). The snow cover duration at the meteorological stations in low-mountain terrain is much smaller. Thus, at Mezhihiria station (southwestern macroslope of the mountains) in 1961–1990 it was 99 days, in 1991–2020 it was 92 days. In turn, at Yaremche station (northeastern macroslope of the mountains) in 1961–1990 it was 98 days and in 1991–2020 it was 91 days. Over the last 30 years, a decrease in the duration of snow cover has been observed at all low-lying meteorological stations (Fig. 3).

The snow cover duration correlates with the cold period duration, which at low altitude commonly lasts from December till February and at high altitude – from the second part of November till the end of March. Very long period with snow was observed in cold period of 1995–1996, which was caused by the cold November in 1995. That winter the snow cover duration at Pozhezhevska station reached 185 days. On the other hand, the shortest periods were observed in cold periods 2000–2001 and 2019–2020. During winter of 2019–2020 the mean air temperature at the meteorological stations, located at low altitude, was higher than 0°C. As a result, the snow cover duration was about twice shorter than usual.

The snow cover in the mountains was studied with the use of satellite images of Landsat satellites, which have spatial resolution 30 m. The available satellite images prove the essential impact of altitude on snow cover formation and melting. Generally, the formation of snow cover starts on the Chornohorskyi Ridge, which is the highest. Almost simultaneously, it is formed on the Svydavets Ridge, which is located nearby – a little bit to the northwest. The longest duration of snow cover is observed on these ridges as well (Fig. 4).

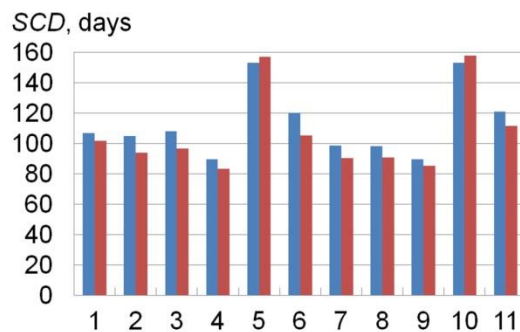


Fig. 3. The snow cover duration at meteorological stations in the Ukrainian Carpathians: 1 – Turka, 2 – Nyzhni Vorota, 3 – Slavske, 4 – Dolyna, 5 – Plai, 6 – Nyzhni Studenyi, 7 – Mezhihiria, 8 – Yaremche, 9 – Rakhiv, 10 – Pozhezhevska, 11 – Seliatyn; left columns – during 1961–1990, right columns – during 1991–2020.

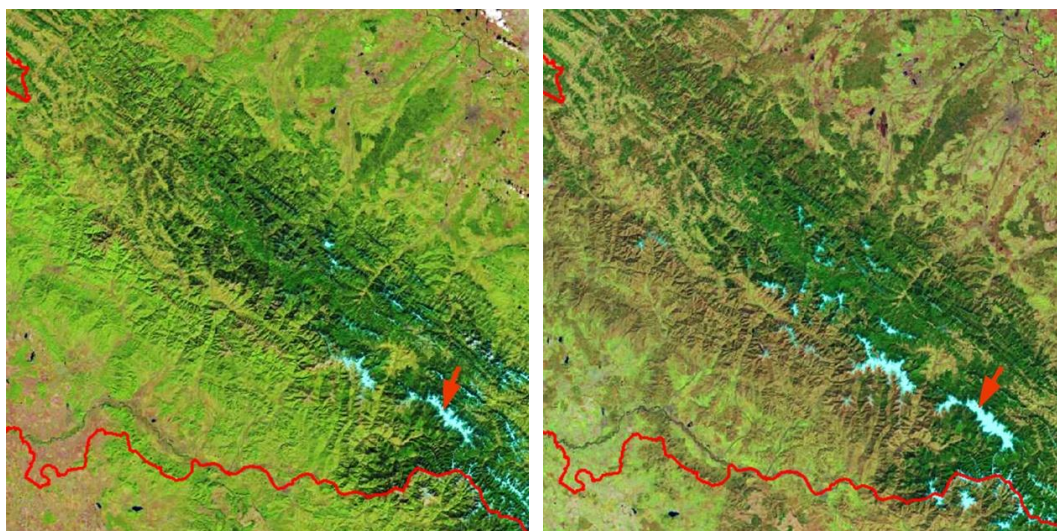


Fig. 4. The snow cover in the Ukrainian Carpathians: on the left – on 05.10.2013, on the right – on 30.03.2014 (the Chornohirskyi Ridge is shown by arrow).

In cold spring, snow cover in the mountains can be observed until May or even until the first half of June. In particular, the existence of snow can be seen in a satellite image obtained on June 11, 1985. At this time, the remnants of snow are observed not on the mountain tops, but on their northern and northeastern slopes. This fact is confirmed by actual observations and satellite images. A study (Vyshneskyi and Shevchuk, 2017), conducted using the thermal channel B10 of the Landsat 8 satellite, showed that the lowest surface temperature in the day time is observed on the northern and northeastern slopes of the mountains.

### Air temperature

Among factors which influence snow cover depth is air temperature. As in many regions in the world, in the Ukrainian Carpathians a vivid increasing trend in air temperatures is observed. That refers the stations located both at low and high altitude (Fig. 5).

As can be seen on Fig. 5, the increase in mean air temperature during the period of 1961–2020 is about 2°C. The increase at the meteorological stations, located

at the low altitude, is some larger than those ones located at the high altitude.

The mean annual air temperature at all 11 meteorological stations in 1961–1990 was 5.6°C, and in 1991–2020 it was 6.6°C.

Considering the question of snow cover depth, it is important to analyze the air temperature in the cold period. These data show that the increase of air temperature at low altitude is larger, than at high altitude. At the same time, at high altitudes, the increase in air temperature in summer is more noticeable (Fig. 6).

The similar results as to the seasonal features were described in many other papers (Rangwala and Miller, 2012; Spinoni et al, 2015). The study (Rangwala and Miller, 2012) showed that in the Swiss Alps the rate of temperature rise in the summer period is the largest and in the autumn period is the lowest.

The increase in temperature in January (the coldest month of the year) at the stations, located at a rather small altitude, in most cases has the range of 0.5–0.6°C per decade. In turn, at the highest stations Plai and Pozhezhevskya the increase is much smaller – 0.15–0.2°C per decade.

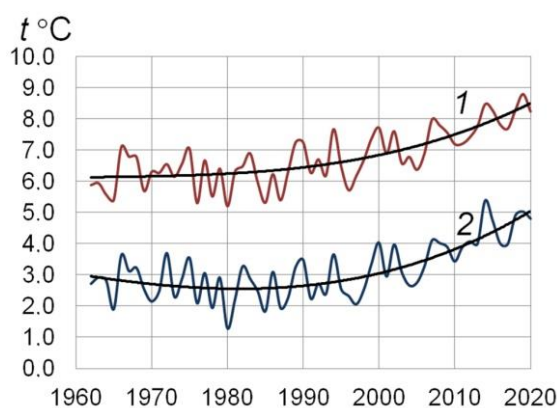


Fig. 5. The increase in mean annual air temperature in the Ukrainian Carpathians during 1961–2020: 1 – at 9 meteorological stations, located at the low altitude, 2 – at two ones, located at the high altitude.

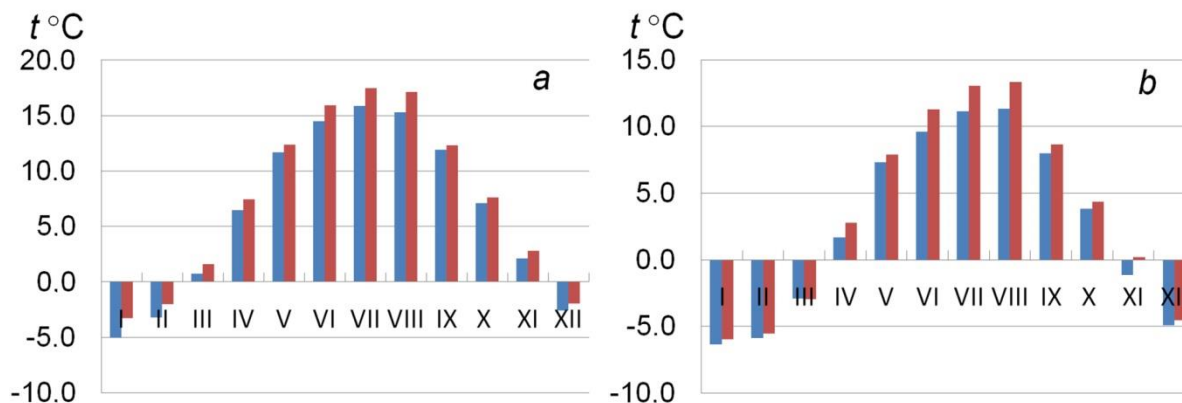


Fig. 6. The increase in mean monthly air temperature in the Ukrainian Carpathians: a) – at 9 meteorological stations, located in low-mountain terrain, b) – at highest Plai and Pozhezhevskya stations. Left columns – during 1961–1990, right columns – during 1991–2020.

The increase in air temperature has some impact on the plants, in particular on the forest. On the large altitude it is observed the increase of forest area. In particular it can be seen in satellite images of the surrounding of the Pozhezhevsk station (Fig. 7).

### Precipitation

Another factor which has influence on the snow depth is precipitation. This parameter in the Ukrainian Carpathians is uneven in space and in time. It depends on the altitude and location of the meteorological stations as to the mountains ridges. The largest amount of annual precipitation is observed at the meteorological stations Plai and Pozhezhevsk, which are at the largest altitudes. During 1961–1990, the mean amount of precipitation at these stations was 1641 and 1436 mm, in 1991–2020, respectively, 1451 and 1536 mm. At the same time, the lowest precipitation is observed at the meteorological stations Dolyna and Seliatyn, where it is about 1.5 times smaller. Generally, the changes in the amount of precipitation during 1961–2020 are not large (Fig. 8). The comparison of data for the periods of 1961–1990 and 1991–2020 shows the small increasing trend in the amount of precipitation in February and March that

can be the reason of snow cover increase in this period. At the same time, these changes are not statistically significant.

The tendency of winter precipitation increase is also observed in the Bieszczady Mountains, located to the northwest of the Ukrainian Carpathians (Mostowik et al., 2019).

### Wind speed (WS)

The important factor which can influence the snow cover depth is the wind speed. Nevertheless, this influence is generally ignored. However, its value in the mountains is much larger (about twice or even more) than at the lowland. At the Pozhezhevsk meteorological station the mean annual wind speed in 1991–2020 was  $5.5 \text{ m s}^{-1}$  or about twice larger than at lowland. Almost the same is the wind speed at Plai station –  $5.3 \text{ m s}^{-1}$ . It is important that during the observation period started in 1961, wind speed essentially decreased. This decrease is observed throughout the year, but in the second half of the year it is the largest (Fig. 9). The decrease of wind speed is observed at low located stations as well, but the changes are smaller, than at the high located stations.

The similar results as to the decrease in wind speed were

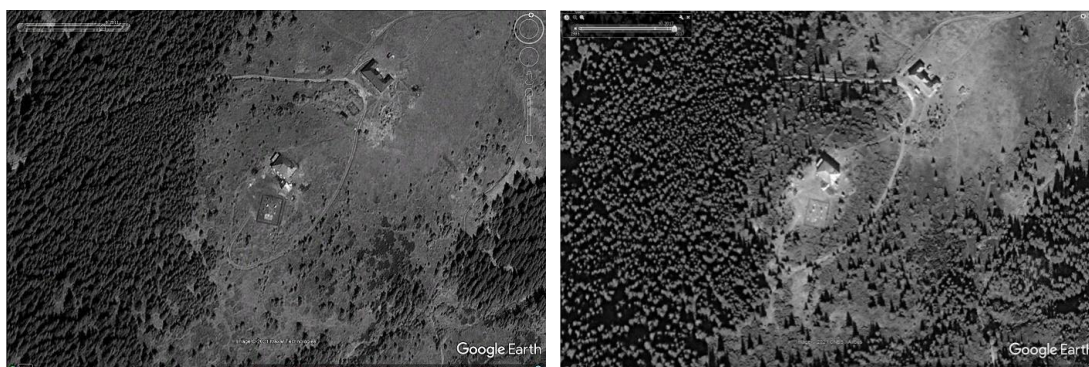


Fig. 7. The changes of forest spread nearby Pozhezhevsk station (in the centre): on the left – on 06.08.2011, on the right – on 01.10.2017.

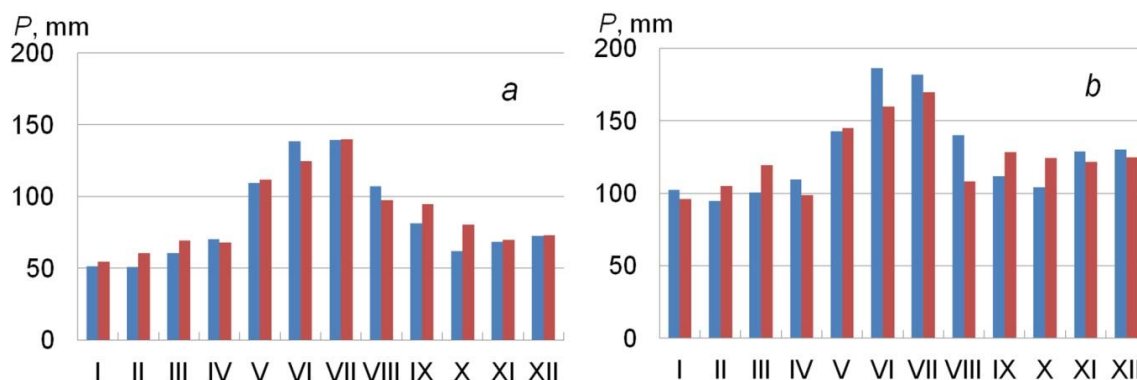


Fig. 8. The mean monthly amount of precipitation in the Ukrainian Carpathians: a) – at 9 meteorological stations, located in low-mountain terrain, b) – at highest Plai and Pozhezhevsk stations. Left columns – during 1961–1990, right columns – during 1991–2020.

obtained in many other regions of the world including the Carpathian Mountains (Birsan et al., 2020; Marin et al., 2014; Spinoni et al., 2015).

**The river runoff**

The analyses of river runoff can help to evaluate the obtained results as to the changes of snow cover depth in the Carpathian Mountains. It would be logical to assume that the increase of snow cover depth must cause the increase of river runoff during the spring flood.

In order to evaluate the impact of snow cover changes on

the river runoff the data of 4 local rivers with rather high river basins were processed. Two river basins (Bila Tysa – Luhi and Teresva – Ust-Chorna) are located on the southwestern macroslope and two ones (Limnitsa – Osmoloda and Chornyi Cheremosh – Verkhovyna) are located on the northeastern macroslope. The mean altitude of these river basins has range 1100–1200 m a.s.l. The available data of these rivers show that water runoff during spring flood practically did not change. At the same time, there is small increase in period January–March. The changes of runoff volume during the period from March till May in a whole are very small (Fig. 10).

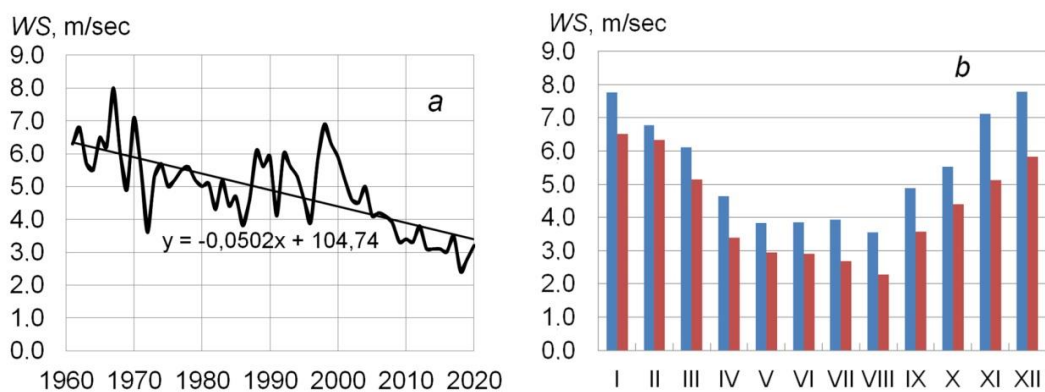


Fig. 9. The changes of wind speed at the Pozhezhevsk station: a) – mean annual values, b) – by months (left columns – 1961–1990, right columns – 1991–2020).

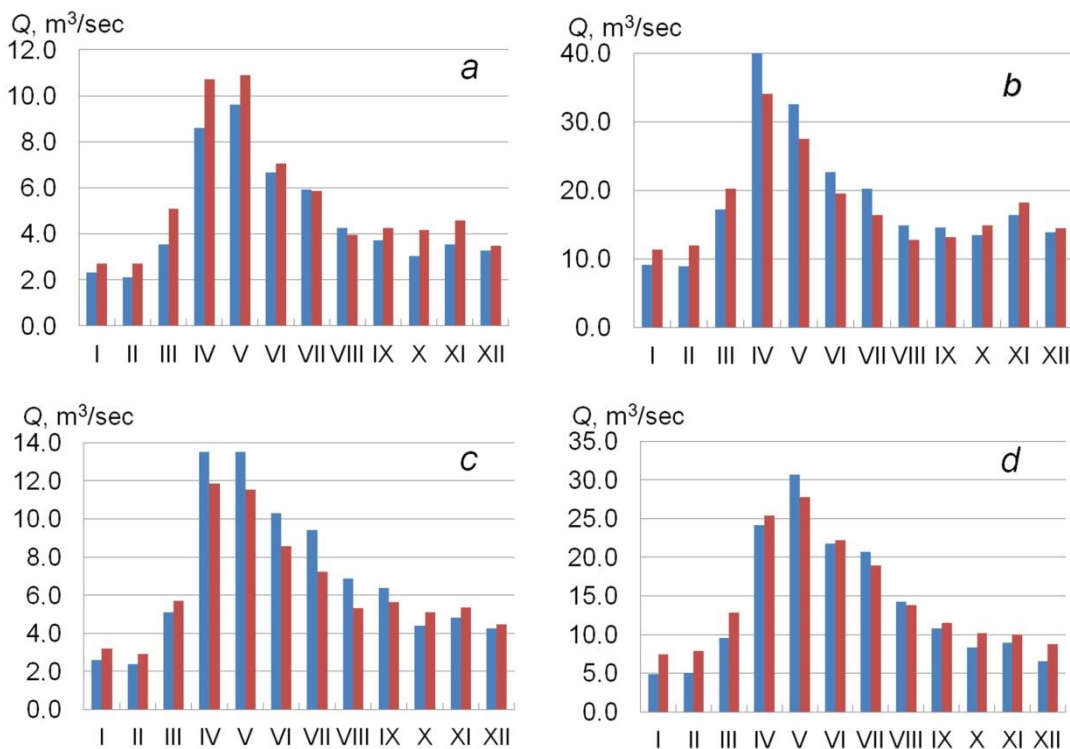


Fig. 10. Intra-annual distribution of water discharge on the Ukrainian Carpathians rivers: a) – Bila Tysa – Luhi, b) – Teresva – Ust-Chorna, c) – Limnitsa – Osmoloda, d) – Chornyi Cheremosh – Verkhovyna (left columns – 1961–1990, right columns – 1991–2020).

These data show that generally, the volume of water in the snow cover did not change. It is possible to assume that the earlier melting of snow cover is observed due to the impact of air temperature increase partly during winter thaws. It is the reason of river runoff increase in this period.

**Discussion**

The available data show that the changes of snow cover on the different altitudes are different. In fact the different is not only altitude, but surroundings. The meteorological stations Plai and Pozhezhevska are located at the tops of mountains, the others – mainly inside the river valleys, where the wind speed is much smaller.

It is well known (Grünewald et al., 2014), that under the influence of wind the snow cover depth is greater in ravines and river valleys, as well as in forests and bushes. The difference in snow depth increases with the increase of wind speed. When the wind speed is small, the snow cover depth becomes uniform.

Special observations near the both highest meteorological stations show the possibility of snow cover depth up to 2 or even 3 m. At the same time, the snow depth at the meteorological sites is essentially smaller.

It means that decrease of wind speed can change the distribution of snow cover in the mountains, making it more uniform: larger on the tops of mountains and smaller in ravines, river valleys, forests and bushes.

To check this idea we analyzed the impact of precipitation and wind speed on snow cover depth – more correctly, its change ( $\Delta SD$ ) during winter months. The impact of precipitation on the change of snow cover depth is direct, and the impact of wind speed is opposite. On a whole, these dependences are not strong, but their comparison for the periods of 1961–1990 and 1991–2020 shows some differences. The correlation between precipitation and the change of snow cover depth during

the last three decades became closer than in the previous period (Fig. 11).

On the other hand, the impact of wind speed on the change of snow cover depth in 1961–1990 was larger than in 1991–2020.

The regressive analyses shows the same result as to the influence of precipitation and wind speed on the change of snow cover depth: the correlation between snow cover depth and precipitation is positive, between snow cover depth and wind speed is negative.

The effect of wind speed on snow cover also is seen in the example of the relationships between the snow cover depth and the duration of snow cover at neighboring stations. Over the last three decades, the correlation has become closer than during the first three decades. First of all it concerns the stations, located in low-mountain terrain.

It can be added that strong wind can blow off the existing snow cover with the speed that exceeds the speed of melting process. This can be seen in the example of the conditions observed at the Pozhezhevska station in March 2006. After a heavy snowfall on March 4–7, 2006, the snow cover depth here reached 121 cm. On March 9, 2006, a strong wind with an average daily speed of 8 m/sec caused the snow cover decrease from 121 cm to 101 cm. Next day strong wind reduced the snow cover from 101 cm to 75 cm and then to 69 cm. We add that during this period the air temperature was much lower than 0°C (Fig. 12).

This case shows the great impact of wind speed on the snow cover depth in the mountains. Obviously, in the highest mountains, this impact is even greater. Thus, the essential decrease of wind speed during the last 60 years is a very important factor influencing snow cover redistribution in the mountains. In our opinion, some decrease of wind speed in the mountains can be the result of altitude increase of forest spread. As can be seen in Fig. 7 this altitude is really increasing.

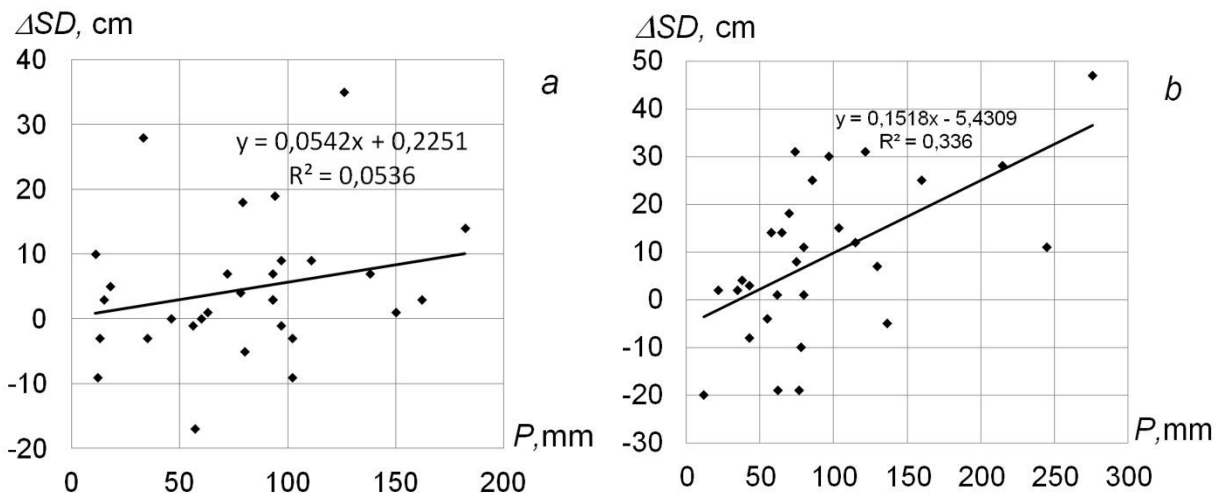


Fig. 11. The correlation between precipitation and the changes of snow cover depth at Pozhezhevska station in January: a) – 1961–1990, b) – 1991–2020.

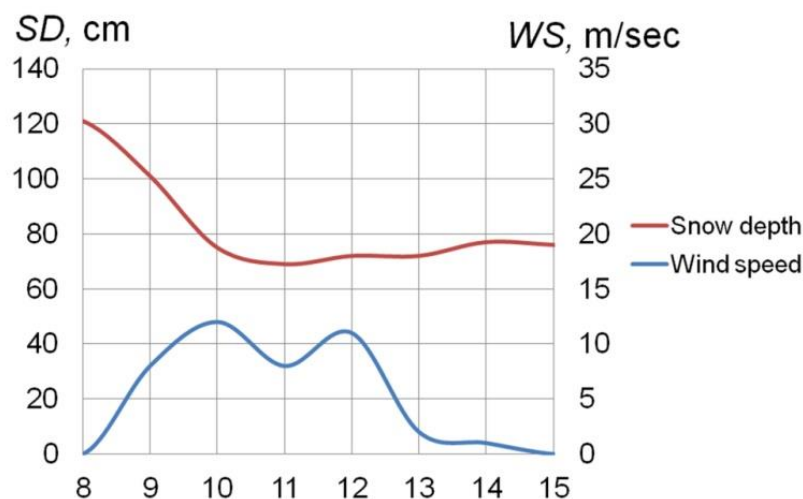


Fig. 12. The changes of snow cover depth and wind speed at Pozhezhevka station on March 8–15, 2006.

## Conclusions

Monitoring at the meteorological stations in the Ukrainian Carpathians, especially at high altitudes, show an increasing trend in snow cover depth. Simultaneously it is observed the increase of air temperature and the decrease of wind speed. However, when assessing changes in the snow cover depth, it is necessary to take into account the effect of wind. Strong wind causes the significant redistribution of snow across the territory and this is the reason of snow cover decrease on the mountain tops and its increase in ravines, river valleys and forests. The observed decrease in wind speed in recent decades is accompanied by the alignment of the snow cover depth in the mountains. The absence of noticeable changes in snow cover in the mountains is confirmed by data on river runoff. The river runoff during the spring flood practically has not changed.

These results will be more visible in case of treatment of data observed not only at meteorological stations but in mountain ravines, river valleys and forests.

## References

- Birsan, M.-V., Nita, I.-A., Cracian, A., Craciun, A., Sfica, L., Radu, C., Szep, R., Kefesztes, A., Micheu, M. M. (2020): Observed changes in mean and maximum monthly wind speed over Romania since AD 1961. *Romanian Reports in Physics*, 72, 702, 1–11.
- Błażejczyk, K., Skrynyk, O. (2019): Principal features of Chornohora climate (Ukrainian Carpathians). *Bulletin of Geography. Physical Geography Series*, No. 17. 61–76. <http://dx.doi.org/10.2478/bgeo-2019-0015>.
- Blöschl, G., Hall, J., Parajka, J., Perdigao, R. A. P., Merz, B., Arheimer, B., Aronica, G. T., Bilbashi, A., Bonacci, O., Živković, B. et al. (2017): Changing climate shifts timing of European floods. *Science* 357, 588–590. DOI: 10.1126/science.aan2506.
- Bulygina, O. N., Razuvaev, V. N., Korshunova, N. N. (2009): Changes in snow cover over Northern Eurasia in the last decades. *Environ. Res. Lett.* 4, 045026. DOI:10.1088/1748-9326/4/4/045026.
- Dong, C., Menzel, L. (2019): Recent snow cover changes over central European low mountain ranges. *Hydrol. Process*, 24, 321–338. <https://doi.org/10.1002/hyp.13586>.
- Gorbachova, L., Zabolotnia, T., Khrystyuk, B. (2018): Homogeneity and stationarity analysis of the snow-rain floods in the Danube Basin within Ukraine. *Acta Hydrologica Slovaca*. 19, 1, 35–41.
- Grünewald, T., Bühler, Y., Lehning, M. (2014): Elevation dependency of mountain snow depth. *The Cryosphere*, 8, 2381–2394, DOI:10.5194/tc-8-2381-2014.
- Fontrudona Bach, A., van der Schrier, G., Melsen, L. A., Klein Tank, A. M. G.; Teuling, A. J. (2018): Widespread and accelerated decrease of observed mean and extreme snow depth over Europe. *Geophys. Res. Lett.* 45, 312–319. <https://doi.org/10.1029/2018GL079799>.
- Halmová, D., Pekárová, P. (2020): Runoff regime changes in the Slovak Danube River tributaries. *Acta Hydrol. Slov.* 21, 1, 9–18. DOI: 10.31577/ahs-2020-0021.01.0002.
- Holko, L., Slezciak, P., Danko, M., Bičárová, S., Pociask-Karteczka, J. (2020): Analysis of changes in hydrological cycle of a pristine mountain catchment. 1. Water balance components and snow cover. *J. Hydrol. Hydromech.*, 68, 2, 180–191. DOI: 10.2478/johh-2020-0010.
- Kubiak-Wojcicka, K. (2020): Variability of air temperature, precipitation and outflows in the Vistula Basin (Poland). *Resources* 9, 103, 1–26. DOI.org/10.3390/resources 9090103.
- Malgorzata, F. (2002): Long-term variability in reconstructed and observed snow cover over the last 100 winter seasons in Cracow and Zakopane (southern Poland). *Climate Research*. 19: 247–256. DOI:10.3354/cr019247.
- Marin, L., Birsan, M.-V., Bojaru, R., Dumitrescu, A., Dumitrescu, A., Micu, D.M., Manea, A. (2014): An overview of annual climatic changes in Romania: trends in air temperature, precipitation, sunshine hours, cloud cover, relative humidity and wind speed during the 1961–2013 period. *Carpathian Journal of Earth and Environmental Sciences*, November, 9, 4, 253–258.
- Marty, C., Meister, R. (2012): Long-term snow and weather observations at Weissfluhjoch and its relation to other high-altitude observatories in the Alps. *Theor. Appl.*

- Climatol. 110, 573–583.
- Migala, K., Urban, G., Tomczynski, K. (2016): Long-term air temperature variation in the Karkonosze mountains according to atmospheric circulation. *Theoretical and Applied Climatology* 125: 337–351.
- Báčová Mitková, V., Halmová, D. (2020): Analysis of the runoff volumes of the wave belongs to maximum annual discharges. *Acta Hydrologica Slovaca*. 21, 1, 9–18 21, 2, 188–196. DOI: 10.31577/ahs-2020-0021.02.0023
- Mostowik, K., Siwek, J., Kisiel, M., Kowalik, K., Krzysik, M., Plenzler, J., Rzonca, B. (2019): Runoff trends in a changing climate in the Eastern Carpathians (Bieszczady Mountains, Poland). *Catena*, 182. DOI.org/10.1016/j.catena.2019.10417.
- Notarnicola, C. (2020): Hotspots of snow cover changes in global mountain regions over 2000–2018. *Remote Sensing of Environment*. 243, 1–19. doi.org/10.1016/j.rse.2020.111781.
- Rangwala, I., Miller, J. R. (2012): Climate change in mountains: a review of elevation-dependent warming and its possible causes. *Climatic Change*. DOI 10.1007/s10584-012-0419-3.
- Repel, A., Zelenáková, M., Jothiprakash, V., Hlavatá, H., Blišťan, P., Gargar, I., Purcz, P. (2021): Long-term analysis of precipitation in Slovakia. *Water*, 13, 952. <https://doi.org/10.3390/w13070952>
- Rožnovský, J., Střeščík, J., Štěpánek, P., Zahradníček, P. (2020): The dynamics of annual and seasonal precipitation totals in the Czech Republic during 1961–2019. *Acta Hydrologica Slovaca*. 21, No. 2, 197–204. DOI: 10.31577/ahs-2020-0021.02.0024.
- Skaugen, T., Stranden, H. B., Saloranta, T. (2012): Trends in snow water equivalent in Norway (1931–2009). *Hydrol. Res.* 43, 489–499. <https://doi.org/10.2166/nh.2012.109>.
- Spinoni, J., Szalai, S., Szentimrey, T., Lakatos, M., Bihari, Z., Nagy, A., Németh, Á., Kovács, T., Mihic, D., Dacic, M., Petrovic, P. et al. (2015): Climate of the Carpathian Region in the period 1961–2010: climatologies and trends of 10 variables. *Int. J. Climatol.* 35: 1322–1341. DOI: 10.1002/joc.4059.
- Tomczyk, A. M., Bednorz, E., Szyga-Pluta, K. (2021): Changes in air temperature and snow cover in winter in Poland. *Atmosphere*, 12, 68. <https://doi.org/10.3390/atmos12010068>.
- Vyshnevskiy, V. I., Donich, O. A. (2021): Climate change in the Ukrainian Carpathians and its possible impact on river runoff. *Acta Hydrologica Slovaca*. 22, No. 1, 3–13. DOI: 10.31577/ahs-2021-0022.01.0001.
- Vyshnevskiy, V. I., Shevchuk, S. (2017): The use of remote sensing technologies for the estimation of the Carpathian Mountains land surface temperature. XXVII Conference of the Danubian countries on hydrological forecasting and hydrological bases of water management. 26–28 September 2017, Golden Sands, Bulgaria. P. 610–615.

Prof. Viktor I. Vyshnevskiy (\*corresponding author e-mail: vishnev.v@gmail.com)  
National Aviation University  
Liubomyra Huzara Ave, 1  
03058, Kyiv  
Ukraine

Ing. Olena A. Donich  
Central Geophysical Observatory  
Nauka Ave, 39  
03028, Kyiv  
Ukraine

## Climatology of the extreme heavy precipitation events in Slovakia in the 1951–2020 period

Ladislav MARKOVIČ\*, Pavel FAŠKO, Jozef PECHO

In this study, we investigate extreme heavy precipitation events in the Slovak Republic in the period 1951–2020 in terms of their spatial and temporal distribution with goal to create dynamic-climatological analysis of those patterns of the atmospheric circulation that can eventually lead to the occurrence of the extreme multi-day precipitation events. Heavy precipitation is defined as maximum precipitation total over five consecutive days (Rx5D) where a non-zero daily precipitation total must be recorded every day of selected 5-day period. Spatial and temporal distribution of multiday precipitation totals is affected by many factors, mainly by the processes taking place in the troposphere eventually represented by the synoptic scale atmospheric circulation and by the orographic diversity of the area, which together significantly affects distribution of precipitation in the selected area. Our study is therefore constructed as an analysis of relationships between localized tropospheric circulation defined by the Czechoslovak catalogue of the typified synoptic situations (Brádka, 1968), the predominant wind patterns and the spatiotemporal distribution of Rx5D.

KEY WORDS: extreme precipitation, precipitation events, dynamic climatology

### Introduction

Current changes in the global climate system, which are strongly correlated to the ongoing human-caused climate change, have an undeniable impact on the mean state of the climate. Long-term increase of the global temperature particularly well expressed in the Arctic and Polar regions of the oceans in the Northern hemisphere can be directly linked to the continually diminishing sea ice areas (Bintanja et al., 2013; Vihma, 2014). It is very likely, that the rise in the ocean surface temperature in the North Atlantic Ocean and the Arctic Ocean affects the dynamics of atmospheric flows and consequently, the processes of genesis, vertical and horizontal dimensions, stability, and patterns of movement of low- and high-pressure areas. Warner (2018) proposes that there is a strong positive correlation between the October sea ice extent and the DJF (December – January – February) values of the NAO index (North Atlantic index). This can, via presupposed stratospheric path, impact the strength of the polar stratospheric vortex, specifically to cause its weakening, which is subsequently manifested in the troposphere by weakening of zonal winds and more pronounced meandering the jet stream. These modifications in the synoptic scale atmospheric circulation might lead to a change in the distribution of precipitation during the year in Slovakia, displaying as an increase in the share of convective based stormy downpours in the total precipitation sums (Faško et al., 2015; Markovič et al.,

2016) and the increasing extremity of precipitation events. Better understanding of the established circulation patterns associated with the extreme heavy multiday precipitation events can help us correctly and more precisely access and model trends and risks linked to human-caused climate change.

In Slovakia, general studies have been previously published that dealt with multi-day precipitation totals (Lapin et al. 2004; Stehlová et al., 2001; Jurčová et al., 2002; Gaál and Lapin, 2002) however, these studies using shorter time series of daily precipitation were mostly very localized and due to the limited number of precipitation stations with processed maximum multiday precipitation totals and time-consuming process of obtaining this data, only limited set of precipitation stations with authentic data has been used in the analysis. Dynamic-climatological analysis of extreme precipitation events was previously published only for maximum 2-day precipitation totals (Markovič, 2019). Our study uses new authentic data set of maximum 5-day precipitation totals (Rx5D) from 486 precipitation stations owned and operated by Slovak Hydrometeorological Institute (SHMI), with available, complete, and consistent time series of daily precipitation from the period 1951–2020. Our spatiotemporal climatological analysis of the extreme heavy precipitation events in Slovakia is constructed as a causal analysis of relationships between spatially localized tropospheric circulation, defined by the Czechoslovak catalogue of the typified synoptic situations (Brádka,

1968), the predominant atmospheric flow and the spatial and temporal distribution of maximum 5-day precipitation totals.

### Data and study area

For needs of our analysis it was essential to create new Rx5D data set obtained from the network of precipitation stations operated by the SHMI performing precipitation observations during the 1951–2020 period (Fig. 1). Eventually, 486 stations with mean elevation 375 meters a.s.l. were selected, excluding those, which could not be incorporated due to the data inconsistency or due to short, incomplete, or unreliable time series of observations. Small portion of time series selected for the analysis still contained brief interruptions. Missing data, however, did not in any case exceed 5% of the total number of Rx5D for each station, and therefore could be fixed or calculated by using an expert approach based on the regression analysis and analogy between data measured at geographically related stations. From selected precipitation stations were prepared Rx5D maps. Spatial and vertical distribution of precipitation stations has proven to be inadequate for used interpolation tool. To improve the vertical distribution calculated for selected set of stations, resulting in a more realistic spatial distribution of Rx5D within the territory of Slovakia, there were (only in the process of creating maps) used 60 supplementary (virtual) points. (Fig. 1) These points were located in the mountain areas, at elevations over 500 meters above the sea level with mean elevation 1049 meters a.s.l. 31 additional points were

placed in positions located at the elevation between 500–1000 meters. Remaining 29 points were placed in the elevations between 1000–2000 meters. Exact placements of supplementary points were identified using method based on expert spatial analysis of the existing field of precipitation stations conducted by Dr. Pavel Faško.

### Maximum multiday precipitation totals

The sums of multi-day atmospheric precipitation totals can be calculated by two slightly different methods – the standard and the modified method (Lapin et al., 2004). Standard processing method of multi-day precipitation totals represents situations where a non-zero daily precipitation total must be recorded every day of selected  $n$ -day period. Possible occurrence of day (or days) during which the precipitation was not registered, or its amount was not measurable (0.0 mm) means, that the total precipitation amount for the considered period is excluded from the analysis. Such a relatively strict view of multi-day continuous precipitation totals is particularly preferred in hydrological treatments. In climatology, on the other hand, it is also interesting and helpful to include precipitation periods incorporating one day without registered precipitation, but which could not be the first or last day of this selected  $n$ -day period, because in that case we would be only dealing with shortened  $n-1$  day period. This correction, of course, does not apply to 2-day totals. The monthly maximum sum of Rx5D therefore represents the highest value of all 5-day sums calculated from five successive days with

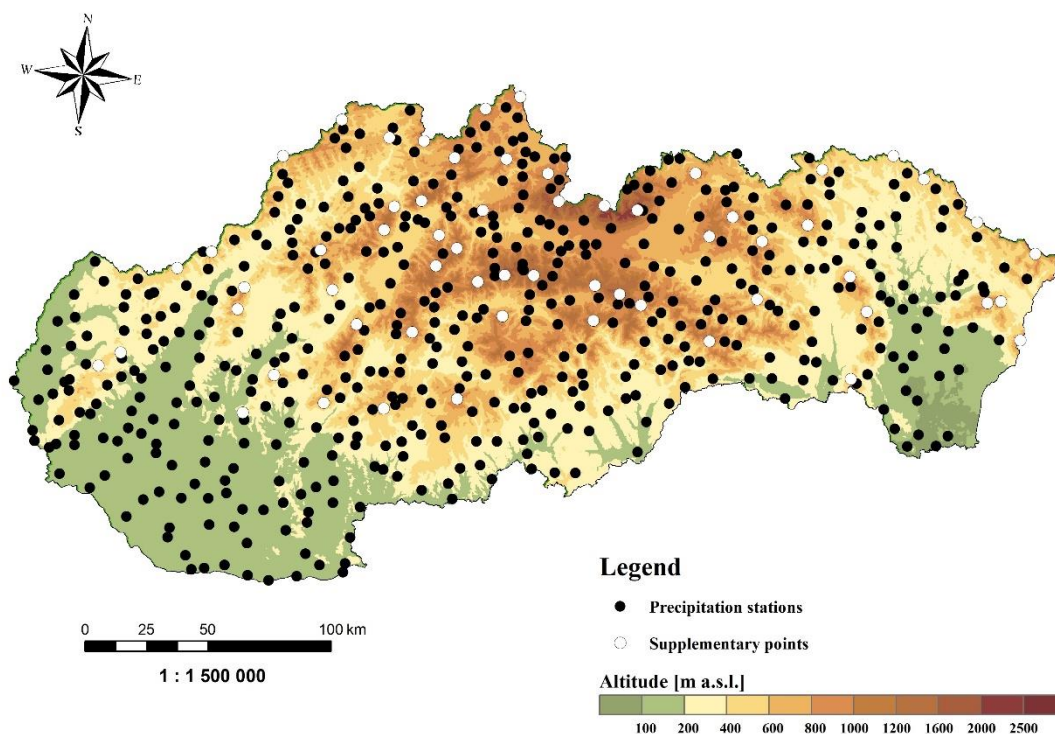


Fig. 1. Selected precipitation stations and supplementary points within the territory of Slovakia.

the observed non-zero precipitation totals over the period of one month. Sums of Rx5D measured at the turn of months was assigned to the month with higher share on total precipitation sum. This approach was also applied to maximum totals that occurred at the turn of years meaning, that there was the possibility that they could, in some cases, be also comprised of data outside of selected 1951–2020 period – data measured in December 1950 and January 2021, which were therefore subsequently included in our study.

## Methodology

Our paper deals with a climatology of the extreme heavy precipitation events in within the network of precipitation stations operated by the SHMI. Presented methodology has been chosen to provide a more comprehensive view of the issue by not only identifying situations with recorded highest Rx5D, but also directly incorporating the necessary condition of sufficiently large area of their distribution presented as a mean spatial value of the monthly Rx5D.

### *Selection of the significant maximum 5-day precipitation totals*

The method used in the process of selecting significant multi-day precipitation events was based on the analysis of mean monthly values of the maximum multi-day totals earned in a given month for each year of analysis as simple average of all station values. If, in any given year, the station did not record 5-day total and hence also the Rx5D, zero value was assigned to this station for the sake of preserving constant number of station values included in each step the analysis. After calculating the average monthly maximum values for the complete set of stations for all years in the 1951–2020 period, we defined the 5 highest values in each month of the calendar year and, together with the year of occurrence, there were selected for a subsequent synoptic analysis. This selection method eventually aggregated 60 different cases available for the consequent annual and half year occurrence analysis of significant weather conditions assigned to the surveyed Rx5Ds.

### *Identification of the period of occurrence*

Occurrence of the extreme heavy precipitation events have been identified within the selected 5 years with the highest average sums. Previously calculated Rx5D were station-wide assigned to corresponding dates, based on regional analysis conducted using precipitation reports and databased datasets from selected profile stations in each river basin determined by station's designators. The final extent of each selected heavy precipitation event has thus been set within 5 to 8-day period.

### *Assignment of typified synoptic situation*

Process of defining the days, from which was each

selected multi-day situation constituted, was followed by assignment to the corresponding typified synoptic situation. Data sources selected for identification process were represented by specialized calendars of analyzed synoptic situations containing analysis on day-to-day basis. For the period 1951–1990 a calendar elaborated for the territory of former Czechoslovakia (ČHMÚ, 2017) was used, and since 1991 a calendar of situations identified exclusively for the territory of Slovakia (SHMÚ, 2021) was applied. Publication of each annual calendar is necessarily preceded by mutual communication between the Czech Hydrometeorological Institute and the SHMI. In these analyzes, however, are for technical reasons, not identified divisions among the synoptic situations of the same circulating type following directly one after another. The general large scale circulation typification used for the territory of Czechoslovakia and later of independent Slovakia is already from the process of its creation hampered by inaccuracies and the larger the territory we try to include under a narrowly defined typified situation, the greater are the potential detection inaccuracies. We have tried to minimize this impending identification errors with a detailed study of daily totals within multi-day precipitation situation, to ascertain given significant weather situation because, in most cases these large-scale circulating units are not stationary. Great diversity and dynamics of atmospheric processes often results in the extended stay period of selected 5-day precipitation situations over the territory of Slovakia and thus, in many cases, subsequently leads to detection of two, exceptionally, up to three influencing typified situations. In the final process of assessing the occurrence of typified conditions, there have been, after analyzing daily totals, selected one, if necessary two or three influencing situations. This approach allowed us to create the input set containing 99 influencing typified synoptic situations assigned to the set of 60 cases consisting of the five heavy precipitation events with the highest spatial means. This dataset was subsequently used in the impact analysis between typified synoptic situations and the spatial distribution of the maximum sums of Rx5Ds. More accurate identification of atmospheric circulation was achieved by the archived reanalyzed large-scale maps of geopotential levels 850 hPa and 500 hPa created by the US Global Circular Model - GFS or by the US Office for Ocean and Atmosphere (NOAA) (Wetterzentrale, 2021).

## Results and discussion

The highest values of Rx5d exceeded 250 millimeters and were measured at precipitation stations located in the mountainous areas in the northern part of Slovakia at elevation over 600 meters a.s.l. Absolute maximum value of Rx5d, accounted for 274.7 mm, was measured in May 2014 in Tatranská Javorina on the northern slopes of the Belianske Tatry mountain range. Rx5Ds over 200 millimeters were detected only on 33 stations (7%) in the January–December period with only 4 stations exceeding this Rx5D value in the cold half-year (October

–March). Furthermore, it can be said, that the Rx5Ds greater than 100 millimeters was at least once recorded at 466 stations, representing almost 96% of the whole set. Spatiotemporal analysis of annual and seasonal maximum Rx5d (Fig. 2) points to the fact, that higher values of Rx5D were in the period 1951–2020 generally achieved in the warm half-year (April–September) (Fig. 3) with significantly pronounced orographic – windward and leeward effects during the cold half-year (October–March) (Fig. 4). Domains with high total values – over 180 millimeters are concentrated mostly in the mountainous northern parts, in the Vysoké Tatry and Západné Tatry mountain ranges, in the north parts of Orava and Kysuce regions and in the southwestern Slovakia in the Malé Karpaty mountain range. However, a relatively large region with high annual Rx5D values is localized also in the northeastern part of the republic. Most of the area of Slovakia is contained in a value range from 110 to 160 millimeters. Isolated areas of the lowest calculated values – under 100 millimeters, are situated mostly in the west on the Podunajská nížina lowland. Spatial distribution of Rx5Ds during warm half year (Fig. 3) resembles overall annual distribution. During the cold half-year are generally observed lower absolute values (Fig. 4), Areas of the highest achieved values – above 140 mm – are in the cold half-year, unlike in the previous cases, located mainly in the central part of the territory, namely in the region containing western parts of Nízke Tatry mountain range and Veľká Fatra mountain range. Areas with high values are also situated in its west and southeast neighborhoods. Relatively extensive area with sums below 80 millimeters is located in the southeast part of the territory in

the Východoslovenská nížina lowland.

### Maximum mean values

The analysis of the highest values of the Rx5Ds can provide a good point of view on the distribution of extreme values, but it is not necessarily suitable for a large-scale study dealing with the effects of the significant typified synoptic situations on the spatio-temporal distribution of the extreme heavy precipitation events. Use of mean values calculated for a complete set of 486 precipitation stations represents a relatively simple and accurate means for determining precipitation events with greater spatial impact. Calculated mean value and accuracy of the detection of the real extreme precipitation event is greatly dependent on the number of stations reaching Rx5D simultaneously. Mean value of the maximum precipitation totals from the complete set of 486 precipitation stations used as a measure to detect the occurrence of the spatially significant precipitation events reached its highest values within the May–October period. The highest mean value and at same time, the only total with value in the 90-millimeter range, was recorded only recently in October 2020 with mean Rx5d value 90.0 millimeters. The second (80.7 mm) and third (78.3 mm) highest values were calculated for July 16 to July 21, 1997 and July 16 to July 22, 2001 respectively. (Table 1) Within the entire set comprised of 720 values of mean monthly Rx5Ds, values greater than 50 millimeters were achieved only 18 times, of which 6 in July and 5 in October. Values greater than 50 millimeters were never, within this data set, recorded in the period from January to April.

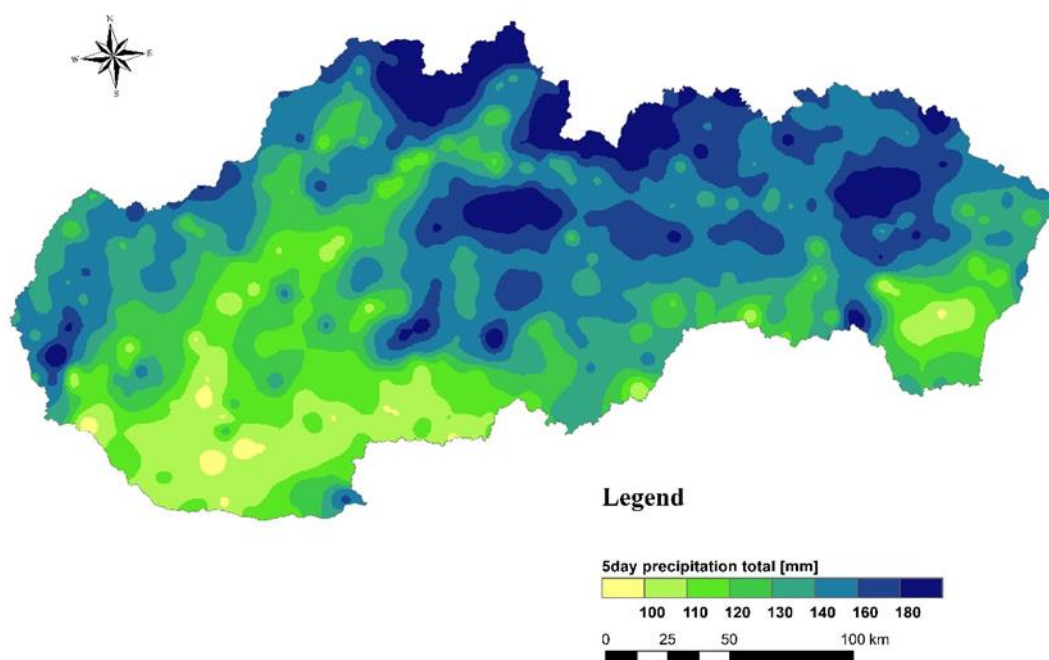


Fig. 2. Maximum 5-day precipitation totals in Slovakia in the 1951–2020 period.

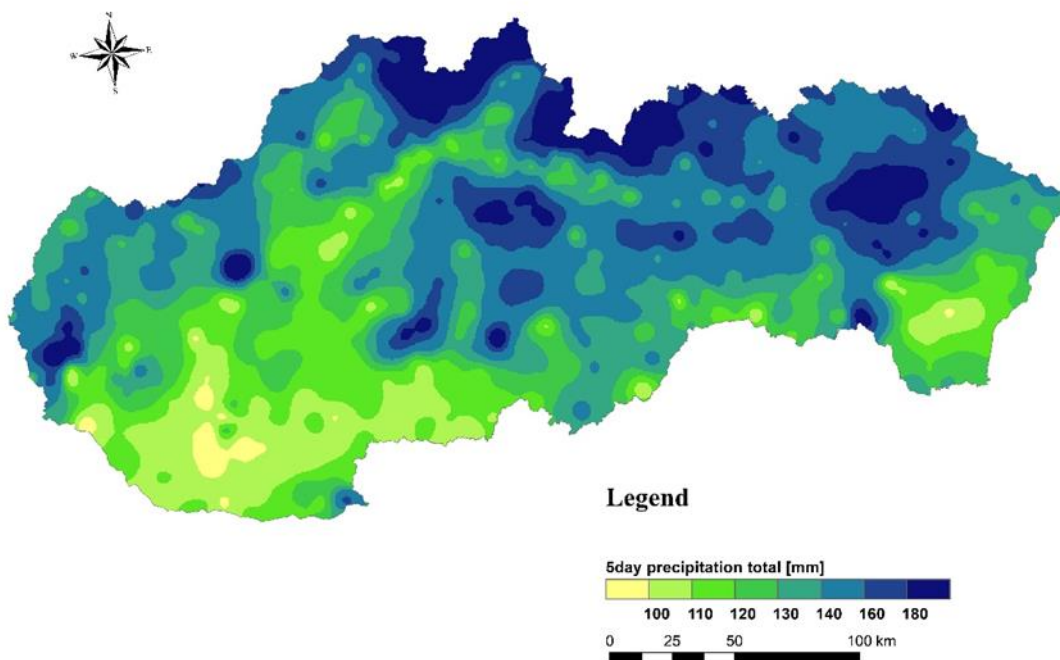


Fig. 3. Maximum 5-day precipitation totals during the warm half-year in Slovakia in the 1951–2020 period.

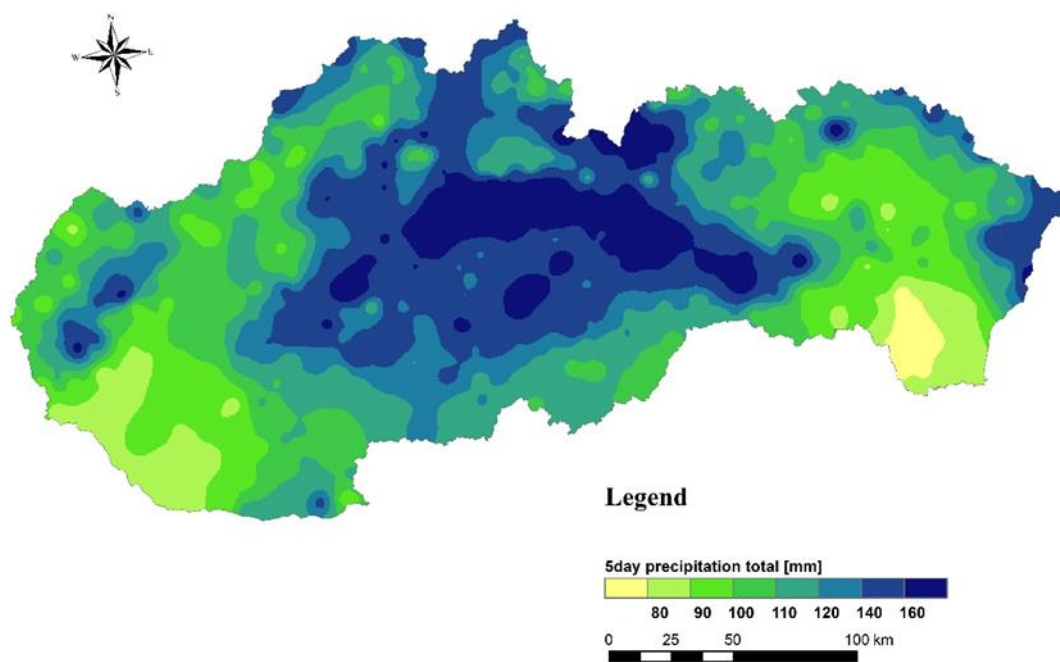


Fig. 4. Maximum 5-day precipitation totals during the cold half-year in Slovakia in the 1951–2020 period.

**Dynamical-climatological analysis of maximum average values**

Form of a cluster analysis was selected to maintain the transparency and informative value of obtained results. Clusters were based on the relative geographic position of the typified synoptic situation in relation to the territory of Slovakia. Using this approach, 25 typified synoptic situations were clustered to the 9 main groups (clusters). These clusters consisted of one, two or three typified situations. We subsequently obtained 7 clusters for cyclonic types – 1. trough of low pressure over the central Europe and trough moving over the central Europe (B/Bp), 2. cyclone over the central Europe (C), 3. the upper-level cyclone (Cv), 4. eastern cyclonic situation (Ec), 5. northern cyclonic situations (Nc/NEc/NWc), 6. southern cyclonic situations (SEc/SWc) and 7. western cyclonic situations (Wc/Wcs).

Anticyclonic and transient situations were thus each assigned into its own one cluster – 8. entrance to the frontal zone (Vfz) and 9. anticyclonic situations. In section of our analysis, we worked with the collection of 60 cases consisting of five Rx5D events with the highest spatial mean values for each month of year. Considering, that the extent of each selected extreme heavy event has been previously set within 5 to 8-day period each event could be represented by up to three typified situations. The final analyzed input set consisted of 98 individual typified synoptic situations – 21 one-situation events, 37 two-situation events and 1 three-situation event. Relative dominance of the B/Bp and Nc/NEc/NWc clusters with exactly the same relative occurrence (29%) was observed when analyzing relative occurrence of significant synoptic types during events with the highest calculated mean values, regardless of the month of their occurrence (Fig. 5). Significant relative representation

**Table 1. Ranking of the 10 highest mean monthly values of the Rx5D in Slovakia in the 1951–2020 period**

Rank	Mean [mm]	Year	Month	Date	Situation	Max [mm]
1	90.0	2020	October	10. – 17.	NWc-C	174.3
2	80.7	1997	July	16. – 21.	C-NEc	253.6
3	78.3	2001	July	16. – 22.	B-Bp	274.0
4	77.2	1984	September	21. – 25.	B	219.7
5	74.5	1980	October	08. – 12.	B-Bp	268.8
6	72.2	2010	May	13. – 18.	B-NEc	219.7
7	65.5	2007	September	04. – 08.	Ec	215.8
8	62.4	2011	July	18. – 22.	B-C	155.2
9	61.3	1960	July	23. – 27.	C	229.6
10	59.8	1964	October	09. – 15.	B-C	211.6

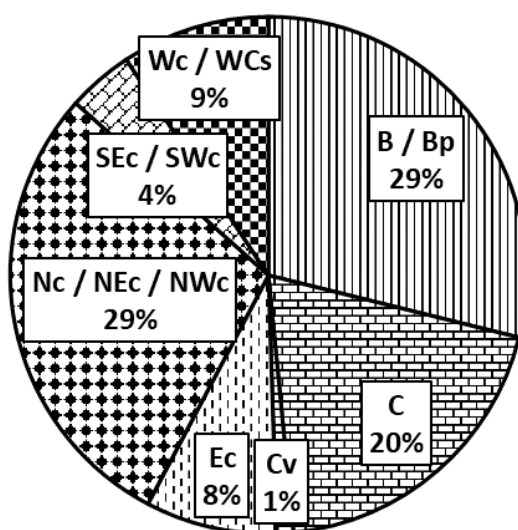


Fig. 5. Relative representation of typified synoptic situation on occurrence of highest average Rx5D [%] from January to December in Slovakia in the 1951–2020 period.

was also observed in case of cyclonic circulation types with central position C (20%). No other cluster managed to reach at least 10% relative occurrence. The highest spatial mean value 90.0 millimeters measured during heavy precipitation event form 10. to 17. October 2020 occurred during NWc situation transitioning into C situation.

The cluster-based analysis of the absolute frequency of occurrences of the typified synoptic situations during the months of calendar year (Fig. 6) provides more detailed look on their temporal distribution. From 2 to 6 detected influencing clusters were identified for each month of the year, the most (6) in March. February, April, May, and August recorded 5 clusters, and the least (2) were

recorded in November, which also saw considerable prevalence of a Nc/NEc/NWc cluster.

A better view on distribution, and the possible change in the impact of selected clustered circulating types during year can be achieved by a separate analysis using, in climatology common division into the warm half-year (April–September) (Fig. 7 left) and the cold half-year (October–March) (Fig. 7 right).

In the warm half-year cluster B/Bp maintained its most influential position with 6% increase in the relative occurrence. Cyclonic situation with a central orientation (C) increased its occurrence and become the second most prevalent circulation type (3% increase). Increase in the relative occurrence was detected for circulation

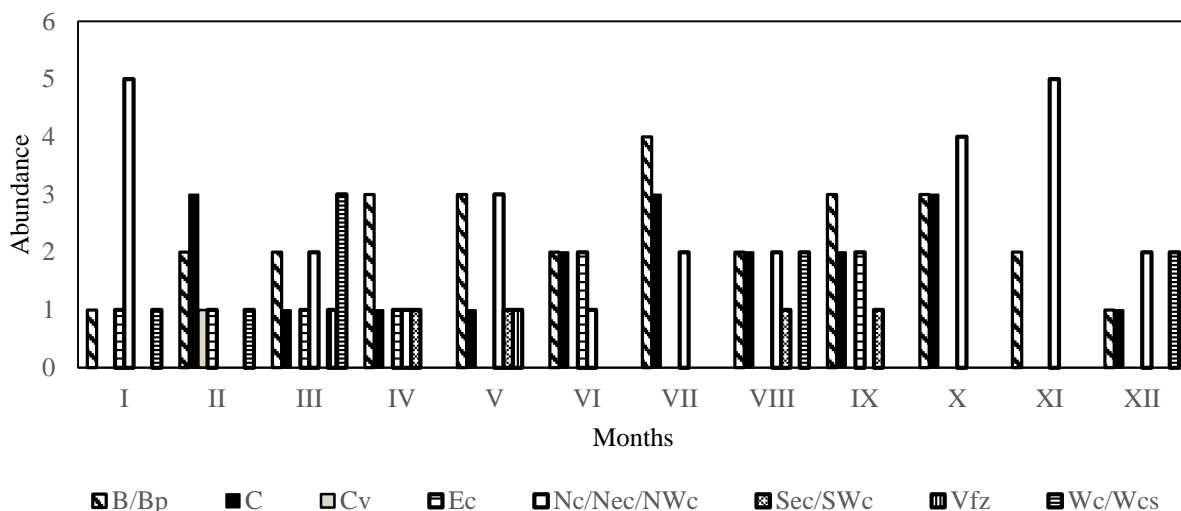


Fig. 6. Absolute frequency of occurrences of the typified synoptic situations during the months of calendar year from January to December in Slovakia in the 1951–2020 period

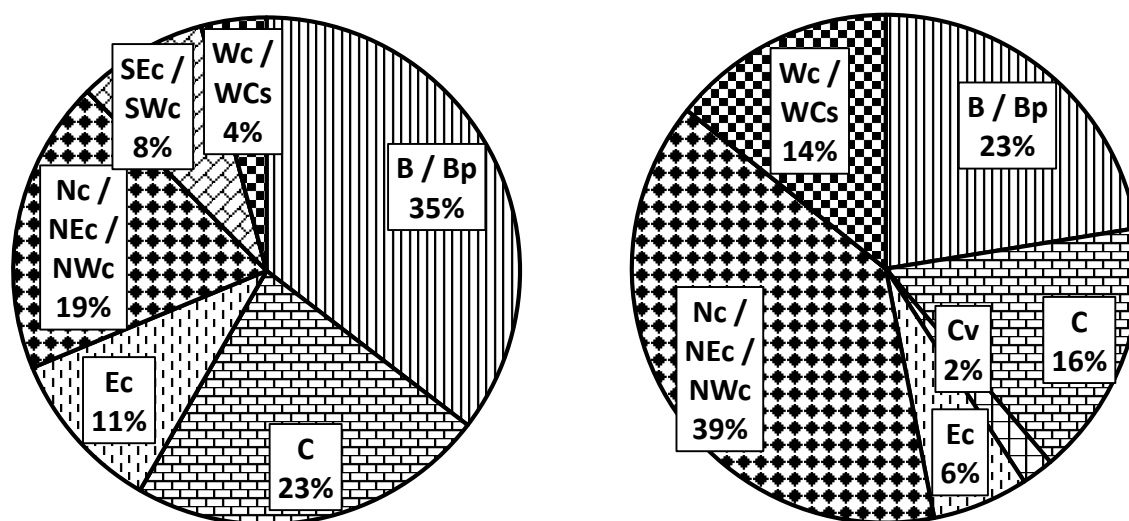


Fig. 7. Relative representation of the typified synoptic situations on occurrence of the highest average Rx5D [%] in the warm half-year (left) and cold half-year (right) in Slovakia in the 1951–2020 period.

clusters Ec (3% increase) and SEc/SWc (4% increase) while western cyclonic situations occurrence decreased by 5%. It can be also further noted, that, during this period, Cv circulation type didn't even participate in the genesis of situations with highest maximum precipitation totals.

Summer months of July and August can be presented as a typical period, during which can be observed large-scale atmospheric circulation necessary for occurrence of the extreme precipitation events with a good spatial distribution. Summer months are usually characterized by high percentage of the convective precipitation, but warm and humid atmosphere can during favorable atmospheric circulation provide ideal condition for heavy precipitation events influencing even lowland areas. Spatial distribution of stations with the highest values of the Rx5Ds calculated for five situations with the highest mean values is displayed in the Fig. 8. Most stations are in the mountain areas in the central part of the territory with a patch of stations located in the eastern part of Slovakia, even in the Východoslovenská nížina lowland. This heavy precipitation event occurred during situation Bp transitioning into NEc situation in 2004. Heavy precipitation event in 1997 (C-NEc), significantly impacted even areas in the west of Slovakia in the Malé Karpaty mountain range, Biele Karpaty mountain range

and Javorníky mountain range.

In the cold half-year can be observed a significantly different relative distribution of clusters detected during heavy precipitation events (Fig. 7). Unlike in the warmer half-year, in this part of year there was recorded (in comparison to the year-round relative distribution) a significant increase in the relative representation of Nc/NEc/NWc cluster (10% increase), which means, that this cluster become the most prevalent with relative occurrence of 39%. Decrease in the relative occurrence was detected for cluster B/Bp (6% decrease) and C (4% decrease) (but during the month of January February and March, even the highest average values during these circulation types. Cyclonic circulation cluster with the southern orientation SEc/SWc didn't even participate in the genesis of the extreme heavy precipitation.

The spatial distribution of the maximum values calculated for 5 events with highest mean maximum precipitation totals displayed for October (Fig. 9) represents a typical placement on the southern westward slopes in the mountainous regions in the central part of Slovakia during wide range of synoptic situations. The absolutely highest mean value calculated for the whole Rx5D data set was set during NWc-C extreme heavy precipitation event in October 2020.

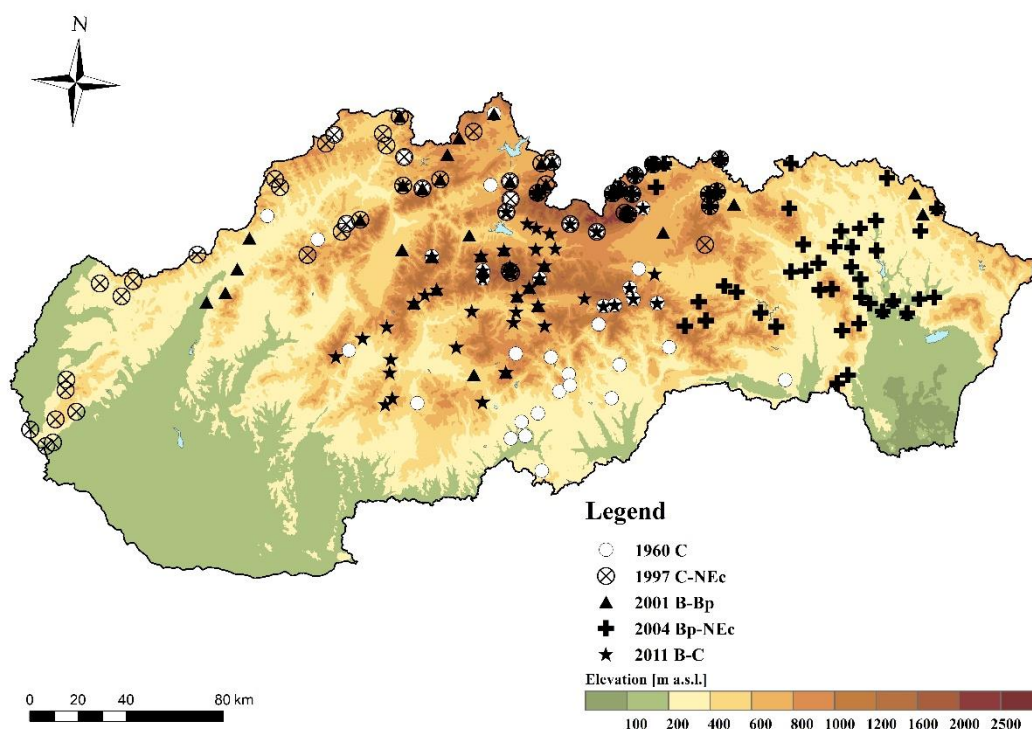


Fig. 8. Placement of 50 stations with the highest Rx5D measured during occurrence of typified synoptic situations with the highest calculated mean values in Slovakia in July in the 1951–2020 period.

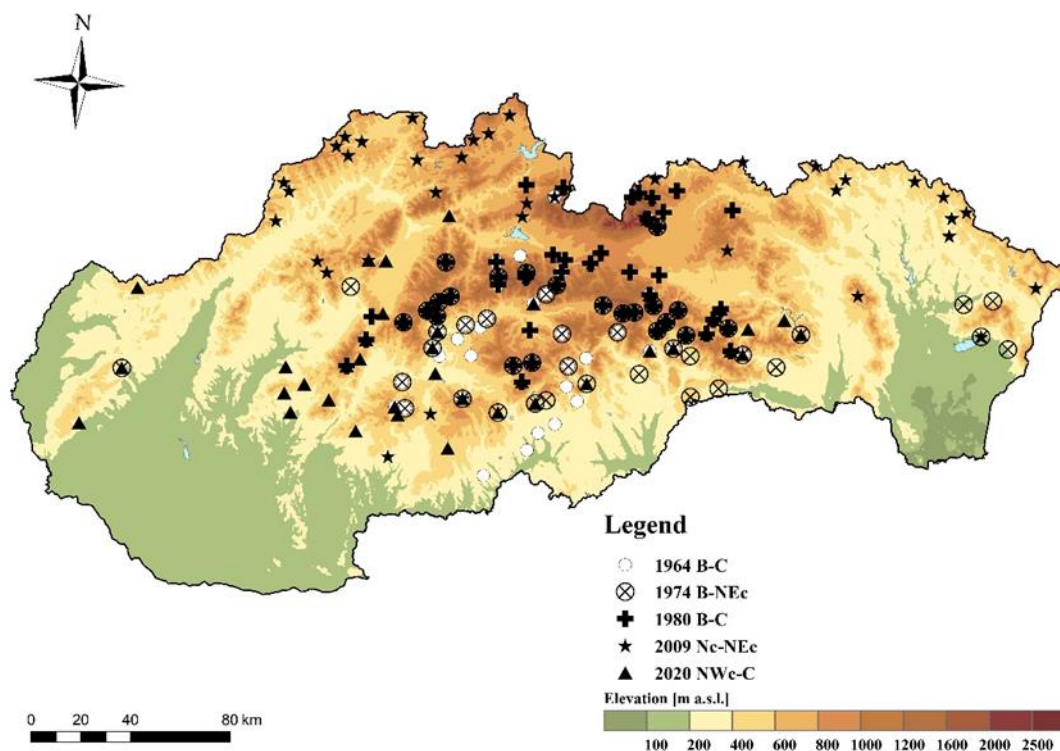


Fig. 9. Placement of 50 stations with the highest Rx5D measured during occurrence of typified synoptic situations with the highest calculated mean values in Slovakia in October in the 1951–2020 period.

## Conclusion

Spatiotemporal analysis of annual and seasonal maximum Rx5d points to the fact, that higher values in the period 1951–2020 of Rx5d were generally achieved in the warm half-year (April–September) with significantly pronounced orographic – windward and leeward effects during the cold half-year (October–March). Mean value of the maximum precipitation totals from the complete set of 486 precipitation stations used as a measure to detect the occurrence of the spatially significant precipitation events reached its highest values within the May – October period. The highest mean value was recorded during heavy precipitation event in October 2020 with mean Rx5d value 90.0 millimeters. The maximum mean values, independent of the month of occurrence, were recorded during the presence of the typified synoptic situations characterized as low-pressure trough (B/Bp) and the cyclonic situations with northern orientation (Nc/NWc/NEc). Changes in the spatial distribution of Rx5d during the year were clearly identified in the separate warm half-year (April–September) and cold half-year (October–March) analyzes. Spatially significant precipitations events recorded in the warm half-year were, in more than 1/2 of the identified events, caused by the cyclonic situations with central position (C) and by the low-pressure trough (B/Bp). Cold half-year is, on the other hand, defined by a dominant influence of the cyclonic situations with

northern orientation (Nc/NWc/NEc) complemented by the low-pressure troughs (B/Bp).

Our analysis highlights the fact, that regional Czechoslovak typification of significant synoptic situations can, despite its often-present subjectivity, provide very good results that correlate with the long-term climatological knowledge of atmospheric circulation over the territory of Slovakia. It also provides good basis for the future objective dynamic-climatological analysis.

## Acknowledgement

*This work was supported by the Slovak Research and Development Agency under the Contract no. APVV-19-0340. This publication is the result of the project implementation: „Scientific support of climate change adaptation in agriculture and mitigation of soil degradation” (ITMS2014+313011W580) supported by the Integrated Infrastructure Operational Programme funded by the ERDF.*

## References

- Bintanja, R., Van Oldenborgh, G. J., Drijfhout, S. S., Wouters, B., Katsman, C. A. (2013): Important role for ocean warming and increased iceshelf melt in Antarctic sea-ice expansion, *Nature Geoscience* 6, 376–379.
- Brádka, J., (1968): *Typizace v meteorologii*, Meteorologické

- Zprávy, Český hydrometeorologický ústav, Praha.
- ČHMÚ (2017): Typizace povětrnostních situací pro území České republiky, Kalendář pro jednotlivé roky, Praha, dostupné online: <http://portal.chmi.cz/historicka-data/pocasi/typizace-povetrnostnich-situaci>.
- Faško, P., Šťastný, P., Švec, M., Kajaba, P. (2015): Výskyt a priestorové rozloženie vysokých denných a viacdenných úhrnov zrážok na Slovensku, Manažment povodí a povodňových rizík 2015 a Hydrologické dni 2015, ÚH SAV, Bratislava.
- Gaál, L., Lapin, M. (2002): Extreme several day precipitation totals at the Hurbanovo observatory (Slovakia) during the 20th century. Contributions to Geophysics and Geodesy, vol. 32 no. 3, 197–213.
- Jurčová, S., Kohnová, S., Szolgay, J., Gaál, L. (2002): K výberu vhodnej distribučnej funkcie maximálnych 5- denných úhrnov zrážok, Acta Hydrologica Slovaca, vol. 3, no. 2, 165–173.
- Lapin, M., Gaál, L., Faško, P. (2004): Maximálne viacdenné úhrny zrážok na Slovensku, Seminár „Extrémy počasi a podnebí“, Brno, 2004, ISBN 80-86690-12-1.
- Markovič, L., Faško, P., Bochníček, O. (2016): Zmeny dlhodobých priemerných mesačných a ročných úhrnov atmosférických zrážok na Slovensku. Acta Hydrologica Slovaca, č. 2, 2016, ÚH SAV, Bratislava, 235–242.
- Markovič, L. (2019): Dynamic-climatological analysis of the maximum 2-day precipitation totals in Slovakia. Meteorologický časopis. Bratislava: Slovenský hydrometeorologický ústav, 22(1), 31–38. ISSN 1335-339X.
- Stehlová, K., Kohnová, S., Szolgay, J. (2001): Analýza dvojdňových úhrnov zrážok v oblasti horného Hrona, Acta Hydrologica Slovaca, vol. 2, no. 1, 167–174.
- SHMÚ (2021): Typy poveternostných situácií, Slovenský hydrometeorologický ústav, Bratislava, dostupné online: <http://www.shmu.sk/sk/?page=8>.
- Vihma, T., (2014): Effects of Arctic Sea Ice Decline on Weather and Climate: A Review, Surveys in Geophysics, Volume 35, Issue 5, 1175–1214.
- Warner, J. (2018): Arctic sea ice – a driver of the winter NAO?, Weather, vol. 73, 307–310.
- Wetterzentrale (2021): NOAA 20th century, online: <https://www.wetterzentrale.de/en/reanalysis.php?model=noaa>.

Mgr. Ladislav Markovič (\*corresponding author, e-mail: [ladislav.markovic@shmu.sk](mailto:ladislav.markovic@shmu.sk))

RNDr. Pavel Faško, CSc.

Mgr. Jozef Pecho

Slovak Hydrometeorological Institute

Jeséniova 17

833 15 Bratislava

Slovak Republic

**Assessment of time course of water and air temperature in the locality of the Turček reservoir during its operation in the period 2005–2019**

Adrian VARGA\*, Yveta VELÍSKOVÁ

In the future, during the ongoing climate change, water reservoirs will play an important role in the provision of raw water for the subsequent production of drinking water for the inhabitants of Slovakia. The Turček water reservoir is the fifth largest water reservoir in Slovakia with a total volume of 9.9 mil. m<sup>3</sup>, which is used for the production of drinking water for the towns Prievidza, Žiar nad Hronom, Handlová and a connection to the water mains of the Žamovica district is also planned. The paper deals with the trend analysis of water and air temperatures data for a selected period of time (2005–2019). We used the non-parametric Mann-Kendall test, which is one of the most widely used nonparametric tests to detect significant trends over time. The results of this test answer the question if there existed a significant trend for mentioned temperatures in this locality or not. Analysis confirmed that it is not possible to determine a significant trend at the significance level of 5%. Anyway, value of annual air temperature increased by 0.57°C during the study period 2005–2019.

KEY WORDS: climate change, air temperature, water temperature, Turček water reservoir, trend analysis

### Introduction

Slovakia is the country with rich water resources. Both the surface water and the groundwater resources ensure the current and also potential needs of the country in the future. However, they are distributed unequally over the Slovak territory. The distribution depends on natural conditions – mostly on geomorphologic, geological, hydrogeological and climatic ones (Zeľeňáková and Fendeková, 2018; Rončák and Šurda, 2019).

Water resources are limited and are facing issues that are caused by over-exploitation, continuous human pressure and also climate changing, which could have serious consequences on quality of water (Shevah, 2015), an essential resource for human health, ecosystems and the economy. Degradation of water quality can result in human exposure to harmful diseases and toxic chemicals (Hu and Cheng, 2013), reduced productivity and diversity of ecosystems and damage to aquaculture, agriculture and other water-related industries (Kaiblinger et al., 2009).

Reservoirs are important sources of drinking water in most parts of the world. Like other water body, reservoirs are also impacted by climate change. This is reflected, for example, in changes of physical properties such as increasing surface water temperature, decreasing ice cover duration, changing stratification or in biological effects such as changes in the phytoplankton community and in increasing risk of cyanobacteria blooms. Climate

change also amplifies processes leading to eutrophication of water bodies which might reinforce global warming. (Feldbauer et al., 2020). Reservoirs respond differently to climate change compared to lakes because storage and outflow are actively managed (Hayes et al., 2017; Bednárová et al., 2021). The operational parameters associated with reservoir control are: the withdrawal rate or quantity, the withdrawal schedule, and the withdrawal depth. The withdrawal depth directly influences storage or dissipation of heat and material, thermal stability, and thus resistance to mixing (Kennedy, 1999). In drinking water reservoirs, adaptation of withdrawal depth is used as a tool to optimize raw water quality for drinking water production (Cáceres et al., 2018).

The aim of this study is to analyze the time course of water temperature and air temperature in this locality as a starting point for assessing the possible impacts of climate change on the water quality in this water body.

### *Water reservoirs for drinking water production in Slovakia*

Water reservoirs intended for the supply of water to the inhabitants have their peculiarities – specific operating conditions that allow raw water to be treated and converted into drinking water. So far, eight water reservoirs have been built in Slovakia, the basic data of which are given in Table 1 (Slovak association of water experts, 2020).

As can be seen from the Table 1 all these reservoirs were built in the 20th century during the period of years 1965 – 1998 with the exception of the Rozgrund reservoir (it was built in the 18th century). From a historical point of view, the Rozgrund reservoir deserves primary and special attention. It was built in the years 1743–1744. The project was elaborated by Samuel Mikovíni in 1741 and under his leadership the construction was also realized (Slovak association of water experts, 2020).

### Trends of climate changes in Slovakia

By the document of the Ministry of Environment of the Slovak Republic (MESR, 2018), the climate change in Slovakia during the period 1881–2017, was manifested as follows:

- the average annual air temperature increased by about 1.73°C;
- spatially different trend of annual total atmospheric precipitation on average by about 0.5% (in the south of the Slovak Republic the decrease was sometimes more than 10%, in the north and northeast seldom total precipitation increased by 3%); decrease in relative humidity (in the south of Slovakia since 1900 by 5%, to other territory less);
- a decrease of values of all snow cover characteristics up to an altitude of 1000m at almost the whole territory of the Slovak Republic (in spite of this, an increasing was recorded at a higher altitude);
- increase of potential evaporation and decrease of soil moisture - characteristics of water evaporation from soil and plants, soil moisture, sunlight confirm that especially the south of Slovakia gradually dries out.

Global warming has manifested itself in Slovakia by maintaining the average annual air temperature over the last 100 years by 1.1°C. These data were observed in the oldest Slovak weather station in Hurbanovo, in which the monitoring has been ongoing since 1871 and continuously since 1901. The period of the warmest 12 years was recorded in the early 1990s. At the same time, atmospheric precipitation increased by an average of 5.6%.

Regional differences were recognized between the southern and northern parts of the Slovakia territory. In the south of Slovakia the decrease was 10%, while in

the north and northeast it was 5%. The manifestation of climate change is primarily a reduction of relative humidity (up to 5%). Similarly, the snow cover decreased in almost the whole territory of Slovakia (SHMI, 2021).

### Impacts of climate change on water quality

Impacts of climate change on water quality with regards to the water reservoirs for supply of the population with drinking water were described and summarized by (Hosaka, 2009) as follows:

- Increase in frequency of turbid water inflow due to increase in heavy rain;
- Stagnation of circulation in reservoir due to global warming;
- Increased risk of toxic chemicals in raw water due to increase in vermin;
- Increase in production of trihalomethane due to water temperature rise;
- Increased risk in pathogenic microorganisms in tap water due to water temperature rise.

Future climate change scenarios also foresee a decrease in water quality due to higher concentrations of pollutants and sediments, through reduced dilution as a result of less water in the rivers and reservoirs. Larger runoff events in winter due to more extreme rainfall events may lead to higher sediment and nutrient loads into streams and reservoirs (Whitehead et al., 2009).

The synergistic effect of a decrease in atmospheric precipitation and an increase in temperature disrupts the natural water cycle. Long-term river flows have been on a declining trend since 1980, with the exception of the Danube River. Already in 1997 it was estimated by (Marečková et al., 1997) that by the scenarios for the time horizons of 2010, 2030 and 2075, the capacity of surface water reserves will decrease to 12.05, 11.05 and 9.42 billion m<sup>3</sup>, with the reduction of flows by 4, 12 and 25%. Due to global warming, the surface water temperature of a reservoir in winter does not lower as much as it had before, and as a result, it does not complete circulation in the reservoir bottom. Therefore, nutrition salts elute from sediments at the reservoir bottom, deteriorating the water quality and resulting in phenomena such as water-bloom (Hosaka, 2009). Such phenomenon is already observed in several lakes and reservoirs.

**Table 1. Summary of water reservoirs in Slovakia used as a source of drinking water (source: Slovak association of water experts, 2020)**

Reservoir	Basin	Total volume [mil.m <sup>3</sup> ]	Year of commissioning
Rozgrund	Hron	0.5	1774
Hriňová	Hron	7.6	1965
Klenovec	Slaná	6.7	1974
Bukovec	Bodva	21.4	1976
Starina	Bodrog	47	1988
Nová Bystrica	Váh	31.6	1989
Málinec	Ipeľ	21.5	1993
Turček	Váh	9.9	1998
Tichý potok	Poprad	24	?

## Material and methods

### Description of study area

The Turček reservoir is located at the confluence of the Turiec and the Ružový streams above the village of Turček village (48°45'50.4"N 18°56'13.2"E). The dam profile is situated in the valley below the confluence of both streams. The width of the valley is approximately 120 m and the altitude in the dam profile localization is 719 m a.s.l. The dam of the Turček reservoir is sprinkled, the length of the crown of the dam is 287.6 m and its height is 59 m (Chmelár, 1998). The total volume of the reservoir is 10.6 mil. m<sup>3</sup>, while its storage content is 9.9 mil. m<sup>3</sup>, (the reservoir is filled twice a year) and the constant volume is 0.3 mil. m<sup>3</sup> of water. The average amount of water supplied to the water treatment plant is 15.8 mil. m<sup>3</sup>/year. The total catchment area is 29.5 km<sup>2</sup>.

### Theoretical background of data processing

The Mann-Kendall nonparametric test (M-K test) is one of the most widely used nonparametric tests for significant trends detection in a time series. Nonparametric tests are more suitable for detection of the trends in the hydrological time series, which are usually irregular with many extremes (Hamed, 2008; Yue et al., 2003; Gilbert, 1987 cited by Bačová Mitková and Halmová, 2021).

This statistical method was also well described in Wang et al. (2020):

The Mann-Kendall trend test (Mann, 1945; Kendall, 1975) is based on the correlation between the ranks and sequences of a time series. For a given time series  $\{X_i, i = 1, 2, \dots, n\}$ , the null hypothesis  $H_0$  assumes it is independently distributed, and the alternative hypothesis  $H_1$  is that there exists a monotonic trend. The test statistic  $S$  is given by:

$$S = \sum_{i=0}^{n-1} \sum_{j=i+1}^n \text{sgn}(X_j - X_i) \quad (1)$$

where

$X_i$  and  $X_j$  – are the values of sequence  $i, j$ ;

$n$  – is the length of the time series;

$$\text{sgn}(\theta) = \begin{cases} 1, & \text{if } \theta < 0 \\ 0, & \text{if } \theta = 0 \\ -1, & \text{if } \theta \geq 0 \end{cases} \quad (2)$$

Mann (1945) and Kendall (1975) have documented that the statistic  $S$  is approximately normally distributed when  $n \geq 8$ , with the mean and the variance of statistics  $S$  as follows:

$$E(S) = 0 \quad (3)$$

$$V(S) = \frac{n(n-1)(2n+5) - \sum_{i=1}^m T_i i(i-1)(2i+5)}{18} \quad (4)$$

where

$T_i$  – is the number of data in the tied group;

$m$  – is the number of groups of tied ranks.

The standardized test statistic  $Z$  is computed by

$$Z = \begin{cases} \frac{S-1}{\sqrt{V(S)}} & S > 0 \\ 0 & S = 0 \\ \frac{S+1}{\sqrt{V(S)}} & S < 0 \end{cases} \quad (5)$$

The standardized MK statistic  $Z$  follows the standard normal distribution with  $E(Z)=0$  and  $V(Z)=1$ , and the null hypothesis is rejected if the absolute value of  $Z$  is larger than the theoretical value  $Z_{1-\alpha/2}$  (for two-tailed test) or  $Z_{1-\alpha}$  (for one-tailed test), where  $\alpha$  is the statistical significance level concerned.

## Results and discussions

Time series of data (type of weather, precipitations, inflows, outflows, temperature of air and water, etc.) were obtained from the operator of this reservoir – Slovenský vodohospodársky podnik, š.p. (Slovak Water Management Enterprise, state enterprise). These data are monitored and recorded every day at 6:30 AM, in some cases even several times per day. This study analyses trend of temperature of water and air in the Turček reservoir locality.

All data were digitized and processed in spreadsheet software and analysis was performed through XLSTAT. The overall course of mean monthly air and water temperatures and trend lines for the whole period 2005–2019 can be seen in Fig. 1. The course of the mean monthly temperature values in the period 2005–2019 is shown in Fig. 2 for each month separately.

As it can be seen, the value of average annual temperature of water oscillated in the period 2005–2017 between 2.2–3.8°C, only in the last two years is starting to rise more rapidly. The value of average annual temperature of air fluctuated in the range of 2°C, but no longer is lasting steeper increase visible. However, both parameters show a gradual increase in values, temperature of air slightly steeper than water temperature. What can be also seen from Fig. 1 is the fact that the change in trend between these parameters occurs with postponement on 3 years in average.

### M-K trend test

The M-K trend test with 5% level of significance was used for detection of the significance in long-term trends of air and water temperature (Fig. 2). This significance level means that there is a 5% probability that we make a mistake if we reject the hypothesis  $H_0$  ( $H_0$  = There is no trend in the series).

Table 2 summarizes results of the Mann-Kendal trend test such as  $S$ ,  $VAR(S)$ ,  $Z$ ,  $p$ -value for each month in seasons: November–January, February–April, May–July, August–October.

Table 3 shows results of MK test for two seasons into

which the year was divided: 1. from November to April and 2. from May to October.

The results of the M-K analysis in the Fig. 2 and summarized in tables showed that there was no significant trend in the majority of months using the 5%

significance level. The data analysis in this study shows decreasing air temperature trends in January, May, July, and September, the rest of the months have a rising trend. The most significant trend at 5% significance level is in July (negative) and in August (positive). The total mean

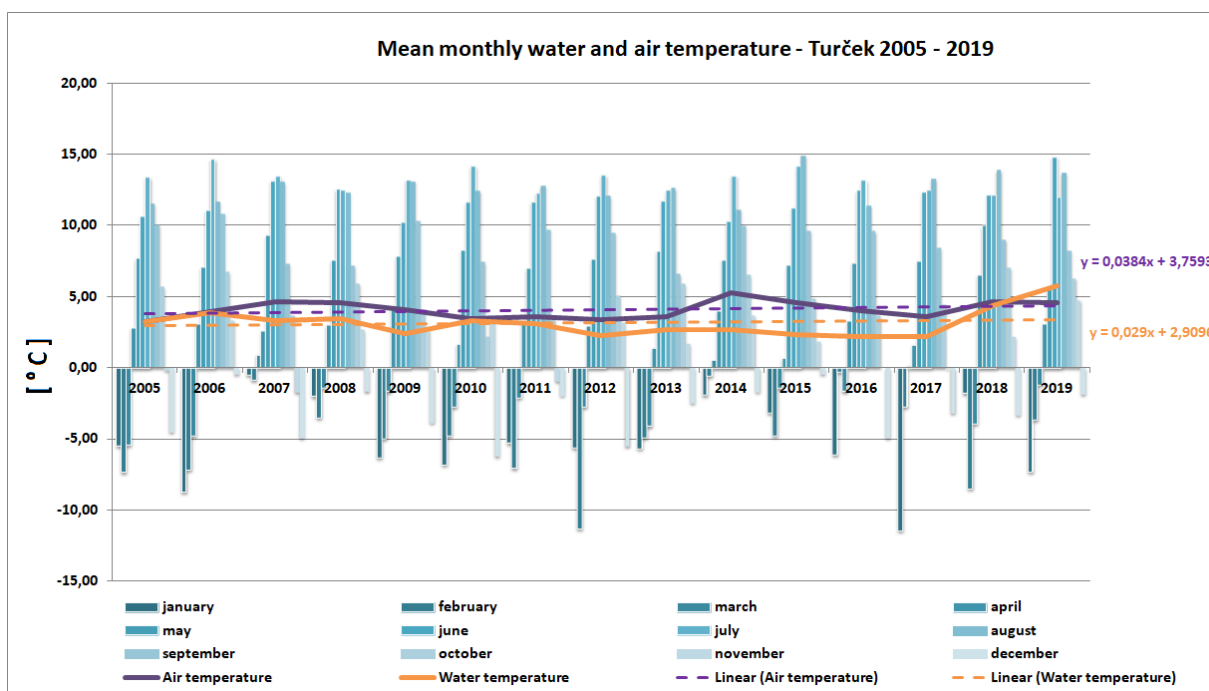


Fig. 1. Time course of Mean monthly air and water temperatures in the period 2005–2019.

Table 2. Results of M-K trend analysis for mean monthly air and water temperatures, significance 5%

Mann-Kendall trend test results						
1. November–January	Air XI.	Water XI.	Air XII.	Water XII.	Air I.	Water I.
Kendall's tau	0.134	0.181	0.077	0.162	-0.086	-0.314
S	14.000	19.000	8.000	17.000	-9.000	-33.000
VAR(S)	407.333	408.333	407.333	408.333	408.333	408.333
p-value (Two-tailed)	0.519	0.373	0.729	0.428	0.692	0.113
Z	0.644	0.891	0.347	0.792	-0.396	-1.584
1. February–April	Air II.	Water II.	Air III.	Water III.	Air IV.	Water IV.
Kendall's tau	0.191	-0.077	0.183	0.105	0.048	0.067
S	20.000	-8.000	19.000	11.000	5.000	7.000
VAR(S)	407.333	407.333	406.333	408.333	408.333	408.333
p-value (Two-tailed)	0.346	0.729	0.372	0.621	0.843	0.767
Z	0.941	-0.347	0.893	0.495	0.198	0.297
2. May–July	Air V.	Water V.	Air VI.	Water VI.	Air VII.	Water VII.
Kendall's tau	-0.162	-0.086	0.287	-0.067	-0.387	-0.010
S	-17.000	-9.000	30.000	-7.000	-40.000	-1.000
VAR(S)	408.333	408.333	407.333	408.333	404.667	408.333
p-value (Two-tailed)	0.428	0.692	0.151	0.767	0.053	1.000
Z	-0.792	-0.396	1.437	-0.297	-1.939	0.000
2. August–October	Air VIII.	Water VIII.	Air IX.	Water IX.	Air X.	Water X.
Kendall's tau	0.314	-0.257	-0.219	-0.276	0.115	-0.181
S	33.000	-27.000	-23.000	-29.000	12.000	-19.000
VAR(S)	408.333	408.333	408.333	408.333	407.333	408.333
p-value (Two-tailed)	0.113	0.198	0.276	0.166	0.586	0.373
Z	1.584	-1.287	-1.089	-1.386	0.545	-0.891

monthly air temperature for the period 2005–2019 shows a temperature increasing by  $0.57^{\circ}\text{C}$ .

In the case of water temperature the situation is very similar. Analysis of month data shows that there was no significant trend in the majority of months using the 5% significance level. Increasing trend occurs in March, April, November and December, in July no trend exists and in the rest months there are decreasing trends for the research period. The most significant trend at 5% significance level is in January (negative) and in November (positive). Total rise of water temperature is  $0.33^{\circ}\text{C}/\text{period}$ .

M-K trend test results for two different seasons of the year show that in the period November–April (could be named as a winter period) the more significant trend exists for air temperature with positive value. On the other side, for the period May–October (could be named as a summer period) the more significant trend occurs for water temperature with negative value.

According to the Report on the state of the environment of the Slovak Republic (2017), since 1951 the annual air temperature in Liptovský Hrádok (640 m above sea level – a.s.l.) represents a statistically significant upward trend in the linear trend until 2017 (an increase of  $2.0^{\circ}\text{C}$ ). Liptovský Hrádok is located at a similar altitude as Turček, so it is presented here to compare what trends in air temperature are in similar localities.

In the study made by Ceppi et al. (2012), where the trend analysis of air temperatures in Switzerland from 1959 to 2008 was described, all seasonal trends are positive and mostly significant with an annual average warming rate of  $0.35^{\circ}\text{C}/\text{decade}$  ( $\sim 1.6$  times the northern hemispheric

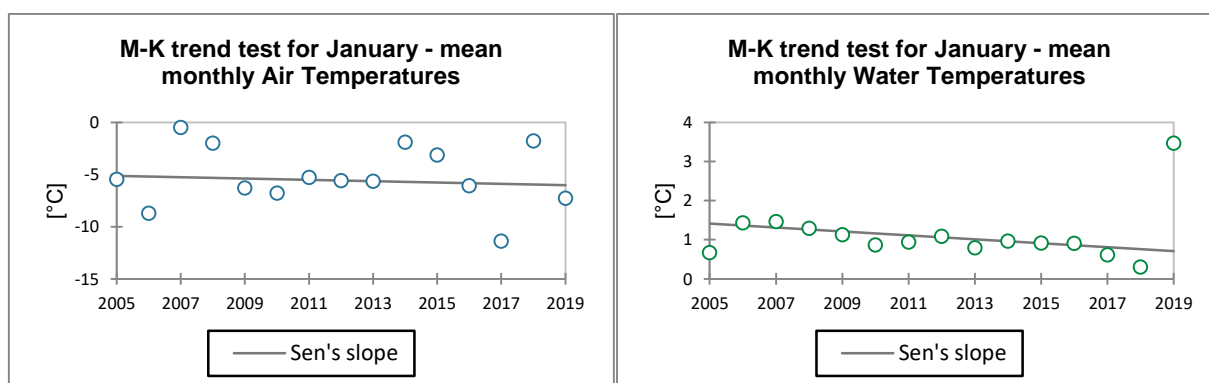
warming rate), ranging from  $0.17^{\circ}\text{C}$  in autumn to  $0.48^{\circ}\text{C}/\text{decade}$  in summer. Altitude-dependent trends are found in autumn and early winter where the trends are stronger at low altitudes ( $<800$  m a.s.l.), and in spring where slightly stronger trends are found at altitudes close to the snow line.

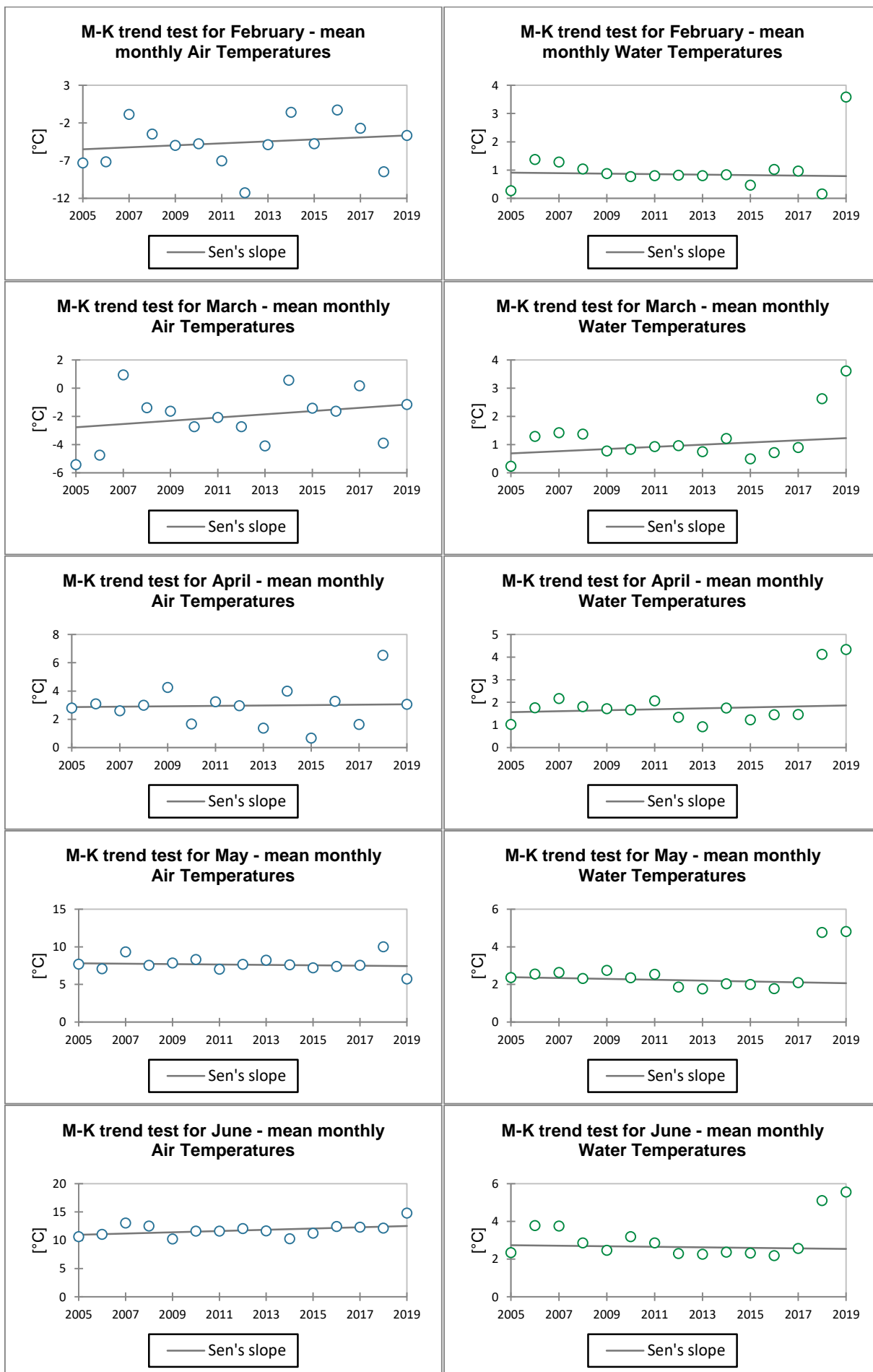
Ohmura (2012) points to temperature trends in different regions of the Earth, for example trends  $0.37^{\circ}\text{C}/\text{decade}$  at Choibalsan (Mongolia, 747 m a.s.l.) for last 40 years (1970–2010) for comparison in our case the air temperature rises by  $0.57^{\circ}\text{C}$  in 15 years as our values are not affected by older values when the air temperature was lower,  $0.09^{\circ}\text{C}/\text{decade}$  for Hami (China, 739 m a.s.l.) for period 1959–2005, these data are used as an example of the globally rising trend of air temperature at a similar altitude as Turček. Summing up the analyses of the 18 groups of stations in 10 regions, there is a general tendency that the amplitude of climate change is larger at high altitudes in comparison with low lands.

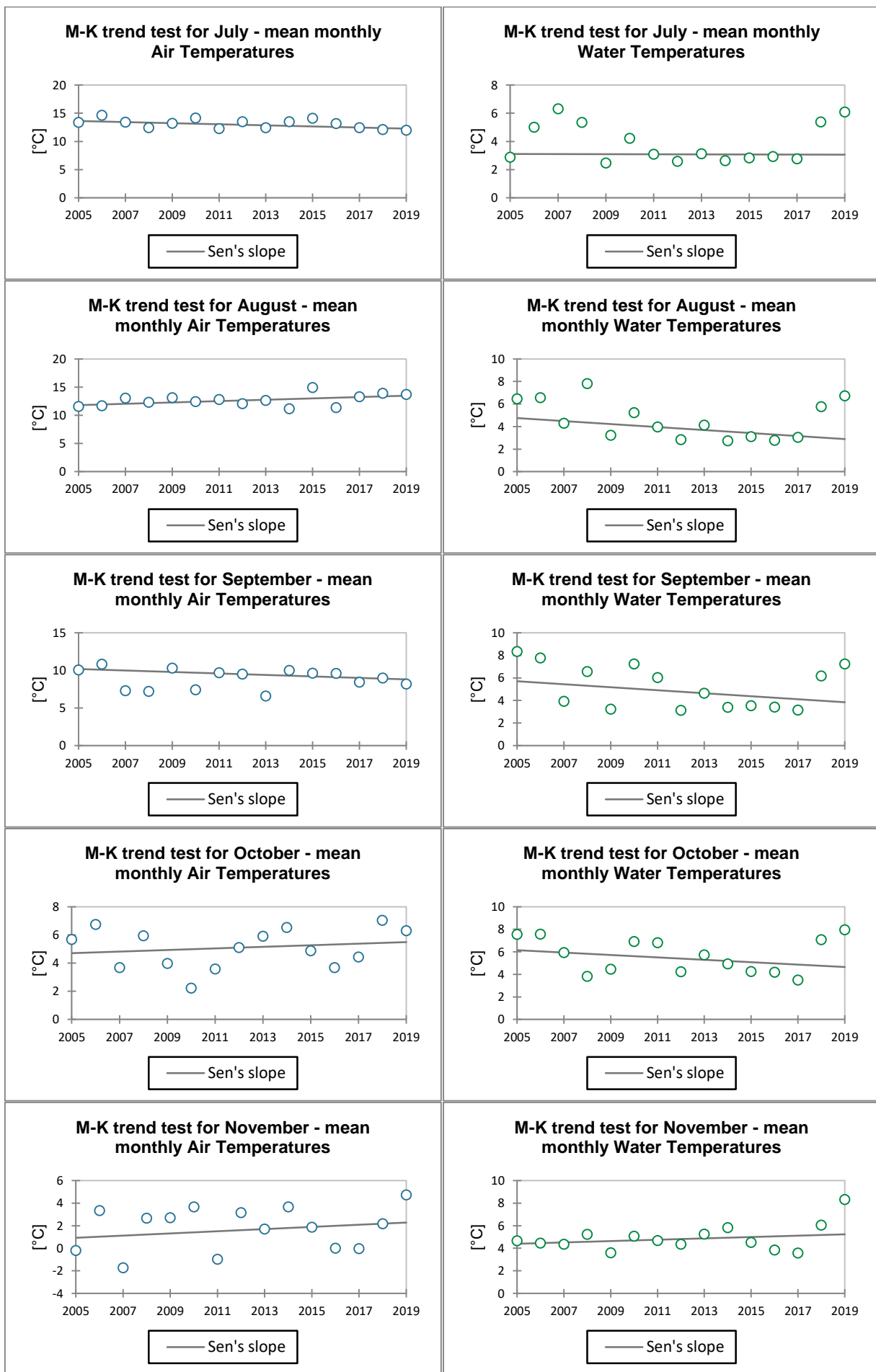
Báčová Mitková and Halmová (2021) used Mann-Kendall's analysis on hydrological and climatic indicators in the Váh river basin. Their results show an increasing trend of air temperature for Liptovský Hrádok. According to their results, the trend of rising air temperature from 2005–2014 is around  $0.25^{\circ}\text{C}$ , but it is necessary to add that it is valid for the period of analysis from 1951 to 2014. Although our research period is 2005–2019, our results show the upward trend, too. Also according to a report from Enviroportal (2016), the air temperature in Liptovský Hrádok increased by  $0.3^{\circ}\text{C}$  in the period 2005–2015. On the other hand, annual air temperature data from the meteorological station Liesek

**Table 3. Results of M-K trend analysis for significance 5%**

M-K trend test results for 2 periods XI.–IV., V.–X.				
periods	November–April		May–October	
temperatures	Air	Water	Air	Water
Kendall's tau	0.200	-0.010	0.105	-0.257
<i>S</i>	21.000	-1.000	11.000	-27.000
<i>Z</i>	0.989744	0	0.494872	-1.28667
<i>VAR(S)</i>	408.333	408.333	408.333	408.333
<i>p</i> -value (Two-tailed)	0.322	1.000	0.621	0.198







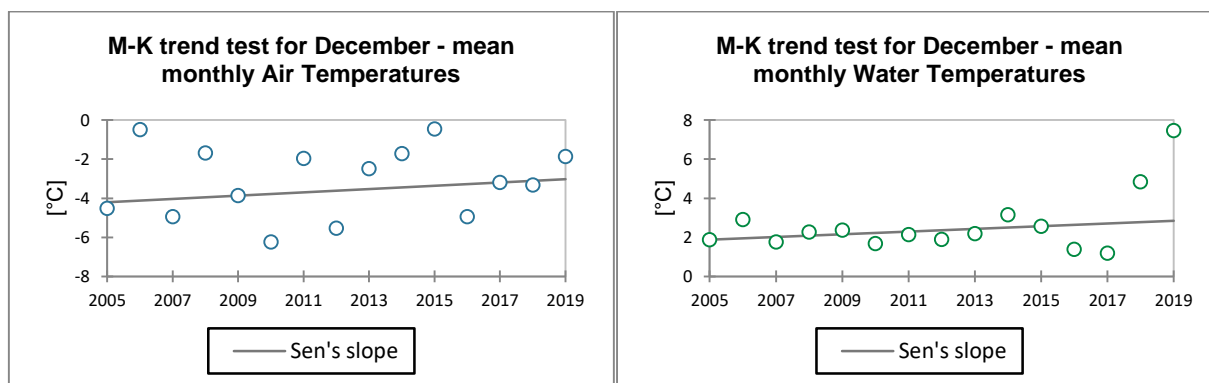


Fig. 2. Mann-Kendall trend test for mean monthly water and air temperatures, significance=5%.

(692 m a.s.l.) show a rising temperature trend of  $0.98^{\circ}\text{C}$  for the period 2006–2019 and for the station Poprad–Gánovce (694 m a.s.l.) air temperature trend increases by  $0.8^{\circ}\text{C}$  for the period 2011–2020. According to data from these 2 meteorological stations, we can see from the trends that average air temperature in Turček is lower.

## Conclusion

The overall trend for water and air temperature is rising during studied period. As we can see in various studies in various parts of the world with a similar altitude as the Turček locality, air temperatures are rising in general although some months have decreasing trends. More significance levels should be used for more telling results, because no significant trend was received at the 5% significance level. Each calculated  $p$ -value was greater than the significance value alpha, which means that we cannot reject the null hypothesis that there is no trend in the data. Air temperature increased by  $0.57^{\circ}\text{C}$  during the study period 2005–2019.

## Acknowledgments

*This work was supported by the project APVV – 18-0205 and by the Scientific Grant Agency VEGA – grant number VEGA 2/0085/20.*

## References

- Bednárová E., Škvarka J., Václavík, P., Poárová, J. (2021): Water management system Liptovská Mara – Bešeňová in the context of climate change. *Acta Hydrologica Slovaca*, Vol. 22, No. 1, 2021, 15–21. DOI: 10.31577/ahs-2021-0022.01.0002
- Cáceres, L., Méndez, D., Fernández, J., Marcé, R. (2018): From end-of-pipe to nature based solutions: a simple statistical tool for maximizing the ecosystem services provided by reservoirs for drinking water treatment. *Water Resour Manag* 32(4):1307–1323. <https://doi.org/10.1007/s11269-017-1871-7>
- Ceppi, P. Scherrer, S. C., Fischer, A. M., Appenzeller, CH. (2012): Revisiting Swiss temperature trends 1959–2008. *Int. J. Climatol.*, 32 (2), 203–213.
- ENVIROPORTAL (2016): Trend of changes in average air temperature and precipitation. <https://www.enviroportal.sk/indicator/detail?id=3101&print=yes> (in Slovak)
- Feldbauer, J., Kneis, D., Hegewald, T. Berendonk, T. U., Petzoldt, T. (2020): Managing climate change in drinking water reservoirs: potentials and limitations of dynamic withdrawal strategies. *Environ Sci Eur* 32, 48 <https://doi.org/10.1186/s12302-020-00324-7>
- Gilbert, R. O. (1987): *Statistical Methods for Environmental Pollution Monitoring*. New York: John Wiley & Sons, Inc.
- Hamed, K. H. (2008): Trend detection in hydrologic data: The Mann-Kendall trend test under the scaling hypothesis. *Journal of Hydrology*, 349(3–4), 350–363.
- Hayes, N. M., Deemer, B. R., Corman, J. R., Razavi, N. R., Strock, K. E. (2017): Key differences between lakes and reservoirs modify climate signals: a case for a new conceptual model. *Limnol Oceanogr Lett* 2(2):47–62.
- Hosaka, Y. (2009): Impacts of Climate Change on Water Quality <https://www.niph.go.jp/soshiki/suido/pdf/h21JPUS/abstract/r2-1.pdf>
- Hu, Y. N., Cheng, H. F. (2013): Water pollution during China's industrial transition. *Environmental Developm.*, 8, 57–73. doi:10.1016/j.envdev.2013.06.001
- Chmelár, V. (1998), *Water reservoir Turček*. Žilina: Electa. <https://www.obecturcek.sk/vodarenska-nadrz-turcek/> (in Slovak) ISBN 80-88689-07-4.
- Kaiblinger, C., Anneville, O., Taddonleke, R., Rimet, F., Druart, J. C., Guillard, J., Dokulil, M. T. (2009): Central European water quality indices applied to long-term data from peri-alpine lakes: Test and possible improvements. *Hydrobiologia*, 633, 67–74. doi:10.1007/s10750-009-9877-7
- Kendall, M. G. (1975): *Rank Correlation Methods*. New York, NY: Oxford University Press.
- Kennedy, R. H. (1999): Reservoir design and operation: limnological implications and management opportunities. In: Tundisi J. G., Straškraba M., eds. *Theoretical reservoir ecology and its applications*.
- Mann, H. B. (1945): Nonparametric tests against trend. *Econometrica* 13, 245–259. doi: 10.2307/1907187
- Marečková, K., Lapin, M., Minárik, B., Mojík, I., Závadský, I., Závadský, D., Zuzula, I. (1997): *Territorial study of Slovakia*, Final report, U.S. Country Studies Program, Ministry of environment of The Slovak Republic, Slovak Hydrometeorological Institute, Bratislava 1997, 108 p. (in Slovak)
- MESR – Ministry of Environment of the Slovak Republic (2018): *Strategy for the Adaptation of the Slovak Republic*

- to the Adverse Consequences of Climate Change – Update [https://www.minzp.sk/files/sea/strategia-adaptacie-sr-nepriaznive-dosledky-zmeny-klimy-aktualizacia\\_2018/strategia-adaptacie-sr-nepriaznive-dosledky-zmeny-klimy-aktualizacia\\_2018.pdf](https://www.minzp.sk/files/sea/strategia-adaptacie-sr-nepriaznive-dosledky-zmeny-klimy-aktualizacia_2018/strategia-adaptacie-sr-nepriaznive-dosledky-zmeny-klimy-aktualizacia_2018.pdf)
- Mitková, V., Halmová, D. (2021): Statistical Analysis and Trend Detection of the Hydrological Extremes in the Váh River at Liptovský Mikuláš. *Acta Horticulturae et Regioecturae*, 24(s1) 80–89. <https://doi.org/10.2478/ahr-2021-0013>
- Ohmura, A. (2012): Enhanced temperature variability in high-altitude climate change. *Theor Appl Climatol* 110, 499–508. <https://doi.org/10.1007/s00704-012-0687-x>
- Report on the state of the environment of the Slovak Republic (2017): Slovak Environment Agency <https://www.enviroportal.sk/uploads/report/8282.pdf> (in Slovak)
- Rončák, P., Šurda, P. (2019): Water balance estimation under a changing climate in the Turiec River basin, *Acta Hydrologica Slovaca*, Vol. 20, No. 2, 2019, 160–165. DOI: 10.31577/ahs-2019-0020.02.0019
- Slovak association of water experts (2020): Development of water and drinking water supply reservoirs in Slovakia [https://savesk.sk/wp-content/uploads/2020/07/Vy%CC%81voj-vodny%CC%81ch-a-vod.-na%CC%81drz%CC%8Ce\\_c%CC%8C%81a%CC%81nok.pdf](https://savesk.sk/wp-content/uploads/2020/07/Vy%CC%81voj-vodny%CC%81ch-a-vod.-na%CC%81drz%CC%8Ce_c%CC%8C%81a%CC%81nok.pdf)
- Shevah, Y. (2015): Water resources, water scarcity challenges, and perspectives. *Water Challenges and Solutions on a Global Scale*, American Chemical Society, 185.
- SHMI – Slovak Hydro-Meteorological Institute (2021): Manifestations of climate change in Slovakia <https://www.shmu.sk/sk/?page=1379>
- Wang, F. Shao, W., Yu, H., Kan, G., He, X., Zhang, D., Ren, M., Wang, G. (2020): Re-evaluation of the Power of the Mann-Kendall Test for Detecting Monotonic Trends in Hydrometeorological Time Series <https://doi.org/10.3389/feart.2020.00014>
- Whitehead, P. G., Wilby, R. L., Battarbee R. W., Kernan, M., Wade, A. J. (2009): A review of the potential impacts of climate change on surface water quality, *Hydrol. Sci. J.*, 54, 101–123.
- Yue, S., Pilon, P., Phinney, B. (2003): Canadian streamflow trend detection: impacts of serial and cross-correlation. *Hydrol. Sci. J.*, 48(1), 51–64.
- Zeleňáková M., Fendeková M. (2018): Key Facts About Water Resources in Slovakia. In: Negm A., Zeleňáková M. (eds) *Water Resources in Slovakia: Part I. The Handbook of Environmental Chemistry*, vol 69. Springer, Cham. [https://doi.org/10.1007/698\\_2017\\_200](https://doi.org/10.1007/698_2017_200)

Ing. Adrián Varga (\*corresponding author, e-mail: [varga@uh.savba.sk](mailto:varga@uh.savba.sk); [xvargaa2@uniag.sk](mailto:xvargaa2@uniag.sk))

Ing. Yvetta Velísková, PhD.

Institute of Hydrology SAS

Dúbravská cesta 9

84104 Bratislava

Slovak Republic

Ing. Adrián Varga

Slovak University of Agriculture

Tulipánová 1117/7

949 76 Nitra

Slovak Republic

## Improvement of design parameters of the sediment reservoirs

Aybek ARIFJANOV\*, Luqmon N. SAMIEV, Tatiana KALETOVÁ

Sediment reservoirs (SR) are an important part of the irrigation systems, and their construction and operation are resource intensive. At present, such facilities are constructed on water structures mainly to deposit sediments in water by slowing down the flow rate. The design form of the SR is frequently rectangular which makes it difficult to control the sedimentation process by sediment fractions along the length of the flow. Based on the results of the theoretical analyses and field experiments, the design parameters of the SR were improved, and a computational method of sediment distribution developed. A new design of the SR, which allows separating the sediments by fractions has been proposed. In the developed SR, muddy water flows into a special reservoir that reduces the flow velocity, and the sediments are separated by fractions along the length of the cross-section, the width of which increases onwards. Large fractions are deposited by the SR itself and are removed from the facility through the sedimentation gallery. Water flowing through the regulated water-releasing gate equals 5% of the water inflowing to the SR.

KEY WORDS: sediment reservoir, sediment trap model, rate of sediment removal, irrigation

### Introduction

In times of high pressure on agriculture and water resources sectors are the raising efficiency of irrigation systems and land reclamation facilities, ensuring reliable operation, modernizing and reducing operational costs highly necessary. Positive solution of these problems is closely connected with sustainable use of water resources and improvement of land reclamation (Arifjanov et al., 2019a; Arifjanov et al., 2019d).

Finding integrated solutions to the abovementioned issues requires the study and management of a sedimentation regime in streams and rivers, thus promoting the efficient use of canals, waterwork facilities, reservoirs and river networks itself. It will also provide a basis for the development of scientifically sound measures that will protect the irrigation canals from sedimentation and allows using the sediments as mineral fertilizers (Arifjanov et al., 2019d; Arifjanov et al., 2019b). Studying hydraulics of the flow and movement of sediments in the sediment-regulating structures in the rivers of Uzbekistan (sediment traps, waterwork facilities, canals and hydraulic structures in the headwater locations) will be the basis for the determination of the parameters of the hydraulic structures and provision of their optimal operation (Arifjanov et al., 2019a; Arifjanov et al., 2019d; Arifjanov et al., 2019b).

Sediment accumulation highly influence the comprehensive benefits of reservoirs and benefits gained from

the water structures related to them (Liu et al., 2018; Tan et al., 2019; Moris, 2020). Therefore, sediment trapping by sediment traps has a high priority in the world because it has significant consequences for downstream structures used for irrigation, municipal water supply and hydropower purposes (Kondolf et al., 2014). Damages caused by sedimentation are:

- the sedimentation of canals and reducing their carrying capacity by 70–80%;
- accumulation of sediments at the intersection of the hydraulic structures complicates water distribution and operation;
- sediments passing through turbines and pumps damage blades, reduce functioning efficiency and their life cycle;
- accumulation of sediments in reservoirs reduces water accumulation capacity and shortens their life cycle;
- sedimentation complicates the design of water structures and increases construction costs (Kondolf et al., 2014; Arifjanov et al., 2019a; Fatxulloev and Gafarova, 2019).

The sediment trapping structures preserve hydraulic facilities, main and distribution irrigation canals from sedimentation. Volume of the sediments deposited before the canals, their composition, characteristics of the irrigation canals and hydraulic machines, and other conditions determine the strategy of coping with sedimentation. Typically, large sediments are removed

from the upstream sections of the waterworks and suspended fine particles flow downstream (Arifjanov et al., 2019c; Jurik et al., 2019). The presence of large-size sediments in river water poses serious problems to the hydraulic engineering facilities and has a significant negative impact on water management in the operation of hydraulic structures and irrigation systems. Data analyses show that the volume of sediments within the large and small irrigation systems during a year is 80 mil m<sup>3</sup>. Considerable amounts of money, labour and material are spending each year to remove these sediments from irrigation systems (Jurik et al., 2019). Therefore, the study of sediment dynamics is of great economic importance.

It is often not advisable to extract out all accumulated sediments of all fractions from water. In cases when sediments are completely removed, the canals will be deepened, i.e., they are deformed and will be saturated again with water and sediments. Excessive removal of sediments can also be harmful: sunlight heats the bottom of the canal, enabling plants to grow and hence, the canal capacity is reduced. Excessively de-sedimented water in mountain rivers and large reservoirs can cause soil erosion in the irrigated lands (Zhang et al., 2016; Fatxulloev and Gafarova, 2019).

The function of the sedimentation facilities like sediment traps (ST) is to deposit excessive sediments in the water courses and to transfer the remaining suspended solids within the saturation boundary to the distribution canals. Such ST are located at the head of the system or used at selected places of network with high number of distributed sediments. Their location and construction also depend on the composition of the particles and the turbidity of the flow (Lu et al., 2019; Jian et al., 2020; Yakovlev et al., 2020). On the other hand, Wang and Kondolf (2014) mentioned that in areas of high sediment yield, sustainable solutions to reservoir sedimentation must focus on passing sediment downstream, not trapping it due to the cost of building and maintaining upstream structures.

By the principle of design and operation, the sedimentation facilities are classified according to the following main criteria (Kondolf et al., 2014; Jurik et al., 2019; Moris, 2020):

- by sedimentation removal method – mechanical excavation, hydraulic flushing and mixing;
- by a mode of hydraulic flushing – periodic and continuous flushing;
- by location - structures on main canal, dispersed headwater structures, non-structural measures;
- by a number of chambers – single chamber, double chamber and multi-chamber;
- by functions of the water management system – energy production, irrigation and municipal water supply;
- by the flow mode in flow chambers – by a linear flow, a transverse circulation.

Sediment traps are installed to protect the main and distribution canals from excessive sediments. The choice of the design of these ST is technically and economically

complex. It is designed within the entire complex of water intake structures. Sediments deposited in the ST inside the irrigation canal network are often mechanically removed by machinery. Nowadays, the method of hydro mechanization has become popular. Hydraulic flushing of sediments is relatively rare due to the difference in water levels in the sedimentation facilities and water courses, and due to the difficulty in generating velocities during sediment flushing.

The grain size of sediment particles tends to decrease along the water flow direction, and in the inlet part of a reservoir higher volume of sediments are deposited than in the outlet part (Bak and Dabkowski, 2013; Jing, et al., 2013). The ST inside irrigation canal networks is designed for the deposition of fine particles, which account for a large portion of the total flow (up to 70%). The saturated suspended fine sediments are typical for flat sections of the river. The Amu Darya River is an example of a water course filled with fine sediments. Fractions of less than 0.01 mm in this river flow constitute 55%, while fractions between 0.1 and 0.05 mm are on average from 26 to 27%, respectively. The number of fractions greater than 0.25 mm are less than 2%. This distribution of suspended sediment fractions is characteristic for the main and distribution irrigation canals, where large particles are deposited due to the installed sedimentation facilities at the headworks (Arifjanov et al., 2019a; Arifjanov et al., 2019d; Arifjanov et al., 2019b). Small-fraction sediments are very useful for irrigated soils as a source of mineral fertilizers (Julien, 2018) and diverting sediment-laden water onto agricultural land to permit deposition of suspended sediments can improve soil fertility (Kondolf et al., 2014).

The reservoir or sediment trap geometry or using an internal or structural barriers can maximize the hydraulic short-circuiting of sediment-laden inflows (Moris, 2020). Therefore, we present a model for periodic flushing of sediments in the reservoir and a developed method of estimating sediment distribution fractions in the proposed model. The newly proposed constant-periodic sediment flushing model depends on the protection of irrigation canals from sedimentation, and from the proper selection of the type and size of the installed sedimentation facility.

## Materials and methods

Based on theoretical and field research, a new design of a constant-periodic sediment flushing reservoir was proposed. Currently, commonly used periodic sediment flushing facilities have various designs; flushing of precipitated sediments in these facilities is as follows: when one of the storage areas becomes full, large particles begin to leak into the canal, an entrance gate in the reservoir is closed, and holes beneath the gate will open. Their widths should only account for the sediment flushing capacity. The amount of water in the flushing area is reduced after opening the gate. The sediments deposited at the bottom pass to the sedimentary gallery and further downstream to the lower part of the canal (Lu et al., 2019).

There are also single-chamber facilities connected with canals, the bottom of which is trapezoidal and attached to each other by a large base, the point of the connection is the threshold, and the bottom area is rectangular (Zhang et al., 2016; Fatxulloev and Gafarova, 2019). The disadvantage of these sedimentation facilities is the difficulty in cleaning sediment deposited in their chambers (Fatxulloev and Gafarova, 2019).

In the first case the sedimentation facility has a permanent cross-section, with no fractional deposition of sediments, and the periodic flushing mode disrupts water supply. In the second case, no sedimentation gallery exists, but fractional sedimentation is controlled. Many years of observations of various sedimentation facilities (in Karshi, Termez, Kuyganyar, etc.) have shown that sedimentation occurs mainly at the beginning section of the facility by increasing the transverse cross-sectional surface of the flow (Arifjanov et al., 2019c; Arifjanov et al., 2019d).

However, such a process of sediment deposition along the length of the stream would cause it to lose its ability to control sedimentation by fractions. It can hence be used on irrigated areas but complicates the transport of suspended sediments containing valuable mineral fertilizers. The following design of the constructions are proposed for self-flushing of sediments and for control of fractional deposition and flushing off river sediments. The bottom of the sediment removal reservoir (2) is trapezoidal, constructed at the angle bottom (Fig. 1), the other two parts are made horizontally, with a threshold and a vertical control gate. The size of the gate openings (4) and (5) is determined by the amount of water supplied to the canal and is intended to move the sediments into the sediment gallery (3). The vertical gate (4) is controlled by an automatic device.

The facility operates as follows: the sediments move

through entry canal (1) into the sedimentation reservoir (2), where turbulent movement occurs due to trapezoidal cross-section with separation into fractions. Large fractions of suspended particles settle in the reservoir, while fine-grained sediment particles flow through outflow canal (6) into the second part of the reservoir.

During the operation of the sedimentation reservoir, once the reservoir is filled with sediments, the sediments are thrown into the gallery (3) by opening of a vertical steering gate (4).

The controlled cross-section of the gate is determined based on the water flow. Accordingly, the gate that provides an intensive removal of sediments deposited on cross-section in a vertically controlled gate into a sedimentation gallery creates a downstream flow process. Volume of water through controlled cross-section of the gate ( $Q$ ) equals to 5% of water intake at the head part of the sediment reservoir ( $Q_1$ ):

$$Q = 0.05 \cdot Q_1 \tag{1}$$

This allows the velocity ( $v$ ) of the water to be greater than the rate of flushing out of the sediments ( $v_f$ ):

$$v \gg v_f \tag{2}$$

Water velocity is determined as follows:

$$v = \frac{Q}{A} \tag{3}$$

where

$Q$  – discharge through the controlled gate [ $\text{m}^3 \text{s}^{-1}$ ],

$Q_1$  – discharge into the reservoir [ $\text{m}^3 \text{s}^{-1}$ ],

$A$  – cross-section area of gate opening [ $\text{m}^2$ ]:  $A = bh$ ,

$b$  – width of gate opening [m],

$h$  – height of gate opening [m].

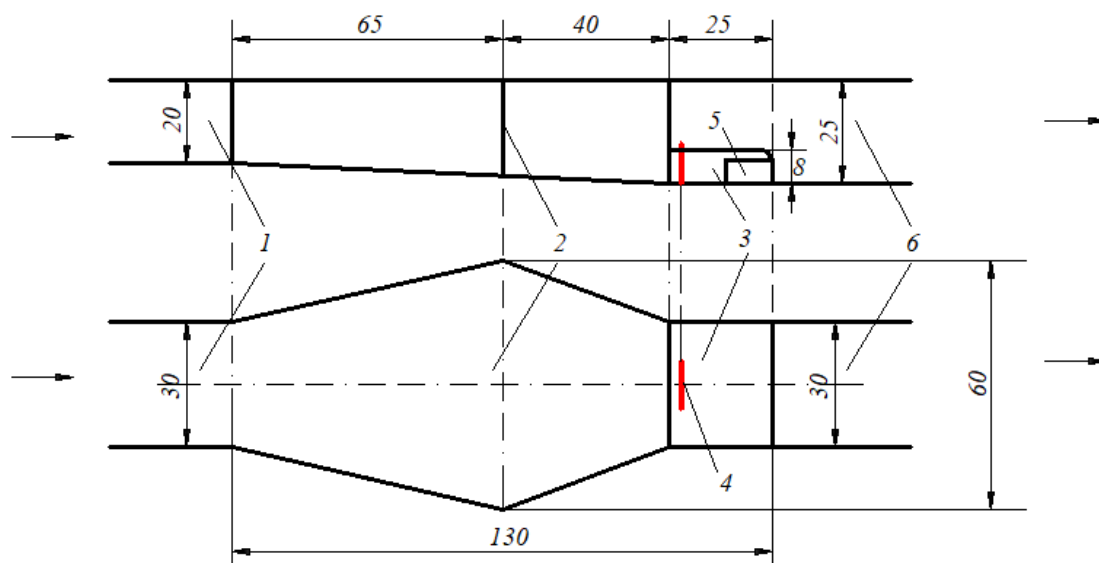


Fig. 1. One-chamber scheme of periodic sediment flushing facility; 1 – entry canal, 2 – sediment reservoir, 3 – flushing gallery, 4 – gate into the sediment gallery, 5 – sediment passing canal to irrigated area, 6 – outflow canal.

The value of the flushing velocity ( $v_f$ ) shall be determined based on the recommendations provided in the “Construction Standards and Regulations” (Building Norms and Regulations, KMK 2.06.03-97). By controlling (opening or closing) the vertical gate, it is possible to achieve the regime required to remove the accumulated sediments.

Based on the research conducted in a newly developed sediment reservoir, a mathematical model of sediment distribution along the length of the stream was developed. Based on this model, the formula for calculating the sediments along the stream flow is:

$$S = S_0 \left( \frac{A_0}{A} \right) \exp \left\{ - \frac{\alpha}{Q^2} \int_0^x \sin \alpha A^2 dx \right\} \quad (4)$$

where

- $S$  – suspended sediments at the entrance to gallery [kg m<sup>-3</sup>],
- $S_0$  – suspended sediments at the entrance to reservoir [kg m<sup>-3</sup>],
- $A_0$  – corresponding cross-sectional area at the entrance to reservoir [m<sup>2</sup>],
- $\alpha$  – parameter characterizing sediments in a stream [-], which can be determined:

$$\alpha = \frac{3g(\rho_t - \rho)}{2\rho_t} \left( \frac{d_0}{d_i} \right)^3 \quad (5)$$

where

- $\rho_t$  – solid particle density [kg m<sup>-3</sup>],
- $\rho$  – fluid density [kg m<sup>-3</sup>],
- $d_i$  – diameter of the sediment particles [m],
- $g$  – acceleration of free fall [m s<sup>-2</sup>],
- $d_0$  – characteristic diameter of the sediment moving at a rate equal to the flow velocity [m].

The advantage of the proposed equation (4) is that the distribution of sediments along the flow length in the equation (4) depends on the variation of the flow hydraulic elements. This allows for a more detailed description of the process.

The abovementioned equation (4) can be calculated by dividing the turbidity distribution in the arbitrary cross-section with a function of river (reservoir) length. In particular cases, changes along the length of the river cross-section ( $A_x$ ) can be estimated as follows:

$$A_x = A_0 + 2 \tan \beta HL \quad (6)$$

where

- $A_x$  – cross-section change [m<sup>2</sup>],
- $\beta$  – angular value of the river slope relative to horizontal level [-],
- $H$  – average depth of flow [m],
- $L$  – length of river or reservoir [m].

To calculate the distribution of sediments along the flow length in the extending cross-section, the expression (6) is placed into the equation (4) and integrate to obtain the following:

$$S = S_0 \left( \frac{A_0}{A} \right) \exp \left\{ - \frac{\alpha(A^3 - A_0^3)}{2Q^2 \tan \beta H} i \right\} \quad (7)$$

where

$i$  – slope of the riverbed [-].

## Results

Based on the research results, the model of a flexible cross-section of the sedimentation reservoir was constructed in the laboratory (Fig. 1 and Fig. 2). The model of the sedimentation reservoir is divided into 4 sections (A, B, C, D) along the length. The distribution of sediment fractions was observed at each cross-sectional site (Fig. 3), and changes of the flow depth were measured (Table 1).

Depend on the above-developed equation (7), calculations were performed for different sediment particles and turbidity levels on the proposed model in the laboratory conditions and applied for the conditions of real sedimentation reservoir. The calculation results for the laboratory model are presented in the Table 1 and for the real reservoir in the Table 2. The calculation presented in the Table 2 are based on the field research made in Fergana valley and was calculated for the parameters of the water intake system of the Sokh canal which is tributary of Great Fergana canal. The rate of sediment removal of particle sizes from 0.01 mm to 0.005 mm vary between 80–97% of the fractions in the total sedimentation in both situations and obtained the ability to keep most fractions in the range of 0.5–0.1 mm in the sediment reservoir. It is possible to see that less than 0.50 percent of this sediment comes out from sediment reservoir. With increasing the  $\tan \beta$  angle of the proposed sediment reservoir model, the process of fractional distribution of suspended sediments in the flow structure will be possible. Based on this, it will be possible to allow the sediments to remain large fractions of suspended sediments larger than 0.1 mm and smaller than 0.01 mm through the structure. The main purpose of avoiding small fractions without holding them in the sediment reservoir was found the presence of microelements in their composition, which can increase soil fertility. The obtained results indicate that it is possible to achieve the desired sediment treatment mode by considering the parameters of flow and river sediments.

Water flow rate in the model was calculated based on the measurement by Thomson weir. The sediment movement and flow rates were calculated in each selected flow section over time. The sediment distribution in the selected flow sections is variable (Fig. 2 and Fig. 3), and the sediments in the flow section A did not settle considerably because of the high flow velocity. The minimum flow velocity is in the flow section C. Due to the changing cross-section in the flow section D the water velocity increases, and the sediments are flushed into the flushing gallery resulting in increased efficiency of flushing of the sediments into a sediment accumulating section. The variability of the cross-section of sediment accumulating section causes sort

**Table 1. Sediment distribution in the sedimentation reservoir model**

$d_i$ [mm]	$d_0$ [mm]	$d_i/d_0$	$Q$ [cm <sup>3</sup> s <sup>-1</sup> ]	$b$ [cm]	$I$	$H$ [cm]	$L$ [cm]	$tg\beta$	$S_0$ [kg m <sup>-3</sup> ]	$S$ [kg m <sup>-3</sup> ]	rate of sediment removal
0.01	0.005	2.0	78.0	31.0	0.0001	1.2	180	0.1	2	1.96	0.97
0.01	0.005	2.0	78.0	31.0	0.0001	1.2	180	0.12	2	1.90	0.89
0.01	0.005	2.0	78.0	31.0	0.0001	1.2	180	0.15	2	1.60	0.80
0.5	0.1	5.0	78.0	31.0	0.0001	1.2	180	0.15	2	1.01	0.51
0.5	0.1	5.0	78.0	31.0	0.0001	1.2	180	0.12	2	0.997	0.50
0.5	0.1	5.0	78.0	31.0	0.0001	1.2	180	0.15	2	0.64	0.32

**Table 2. Sediment distribution in the real sedimentation reservoir**

$d_i$ [mm]	$d_0$ [mm]	$d_i/d_0$	$Q$ [m <sup>3</sup> s <sup>-1</sup> ]	$b$ [m]	$I$	$H$ [m]	$L$ [m]	$tg\beta$	$S_0$ [kg m <sup>-3</sup> ]	$S$ [kg m <sup>-3</sup> ]	rate of sediment removal
0.01	0.005	2.0	30.0	200.0	0.0001	2.0	400.0	0.1	4.0	3.80	0.95
0.01	0.005	2.0	30.0	200.0	0.0001	2.0	400.0	0.12	4.0	3.18	0.80
0.01	0.005	2.0	30.0	200.0	0.0001	2.0	400.0	0.15	4.0	2.92	0.73
0.5	0.1	5.0	30.0	200.0	0.0001	2.0	400.0	0.1	4.0	2.01	0.50
0.5	0.1	5.0	30.0	200.0	0.0001	2.0	400.0	0.12	4.0	1.80	0.45
0.5	0.1	5.0	30.0	200.0	0.0001	2.0	400.0	0.15	4.0	1.55	0.39

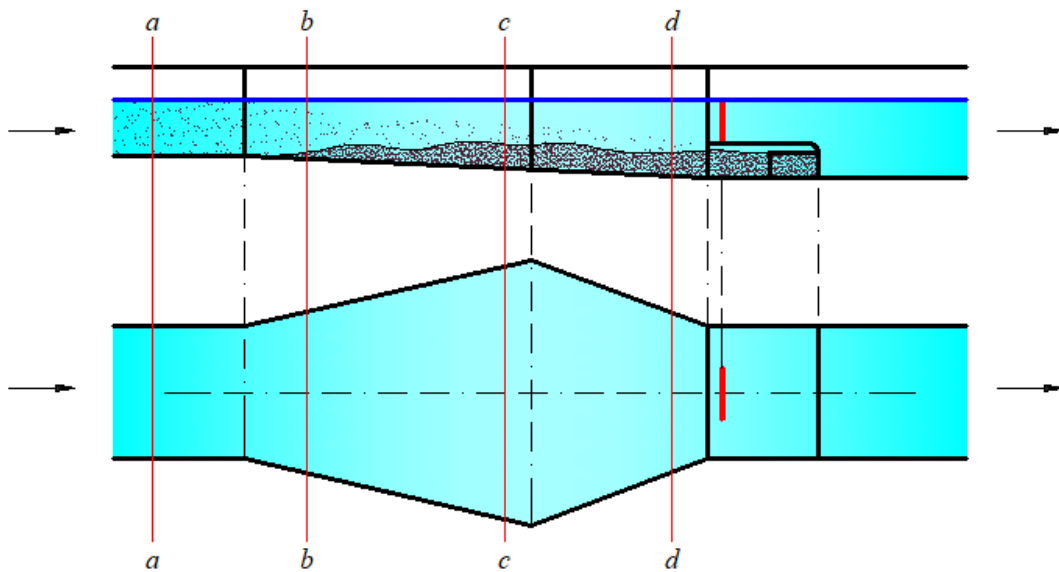


Fig. 2. Laboratory model of the sediment reservoir in lateral view (above) and top view (below).

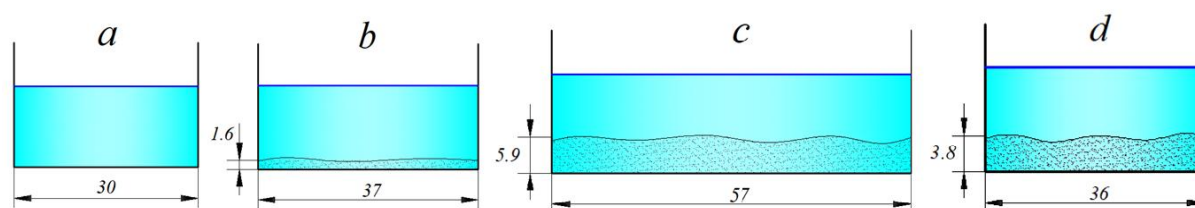


Fig. 3. Distribution of sediments by cross-sections.

of sediments by diameter. This allows the small sediments to flow out of the reservoir.

### Conclusion

Theoretical and laboratory research results allowed improving the constructive parameters of the sediment management structures in rivers. The new design of the sediment reservoirs, which allows separation of river sediments into fractions has been developed. River sediments can be separated by the sediment tank of the new design into fractions, and small fractional particles can be transferred into irrigation fields.

The mathematical model describing the sediment distribution in the developed sediment tank model was improved and a computational method developed. A distinctive feature of this model is the description of the sediment distribution in the stream depending on sediment fractions. Based on the developed calculation method it is possible to predict sedimentation process by considering the uneven flow characteristics in the sediment reservoirs constructed in the irrigation canals. The turbidity distribution for the sediments of different fractions is carried out in fractional order, and the total turbidity is calculated by summing the total sediment volume corresponding to the sediment fractions.

Obtained results allow to conclude that constructing sediment reservoir of variable cross-section allows separating the sedimentation by their fractions. The proposed calculations can be used in any hydraulic facility, reservoirs included, where water purify from river sediments is needed. It is recommended to be used considering the hydraulic and hydrological parameters of the canal under consideration.

The proposed design of the sedimentation reservoir has been recognized by the Intellectual Property Agency as a useful model № FAP 00927 (Arifjanov et al., 2014).

### Acknowledgement

This work was supported by Scientific Grant Agency No. Vega 1/0747/20 and Grant Agency of Slovak University of Agriculture in Nitra No GA 41/2019. We also thanks SAIA, n.o. for the support of research internship in Uzbekistan.

### References

- Arifjanov A. M., Samiev L. N., Akmalov Sh. B. (2014): Periodic detachable single-chamber silencer. Intellectual Property Agency of the Republic of Uzbekistan. Useful model Patent № FAP 00927 Head of Uzbekistan. – Tashkent 20.06.2014y.
- Arifjanov, A., Otaxonov, M., Samiev, L., Akmalov, S. (2019a): Hydraulic calculation of horizontal open drainages. E3S Web of Conferences, 2019, 97, 05039
- Arifjanov, A., Rakhimov, K., Abduraimova, D., Akmalov, S. (2019b): Transportation of river sediments in cylindrical pipeline. IOP Conference Series: Earth and Environmental Science, 2019, 403(1), 012154
- Arifjanov, A., Samiev, L., Akmalov, S. (2019c): Dependence of Fractional Structure of River Sediments on Chemical Composition. International Journal of Innovative Technology and Exploring Engineering, 9, 2646–2649.
- Arifjanov, A., Samiev, L., Apakhodjaeva, T., Akmalov, S. (2019d): Distribution of river sediment in channels. IOP Conference Series: Earth and Environmental Science, 2019, 403(1), 012153
- Bak, L., Dabkowski, S.L. (2013): Spatial distribution of sediments in Suchedniów reservoir. J. Water Land Dev. No. 19 (VII–XII): 13–22. DOI: 10.2478/jwld-2013-0011
- Building Norms and Regulations KMK 2.06.03-97
- Fatxulloev, A., Gafarova A. (2019): Study of the process of cultivation in soil fertile irrigation canals. E3S Web of Conferences, 2019, 97, 05025
- Jian, X., Yang, S., Hong, D., Liang, H., Zhang, S., Fu, H., Zhang, W. (2020): Seasonal geochemical heterogeneity of sediments from a subtropical mountainous river in SE China. Marine Geology, 422, 106120. <https://doi.org/10.1016/j.margeo.2020.106120>
- Jing, H., Li, C., Guo, Y., Zhang, L., Zhu, L., Li, Y. (2013): Modelling of sediment transport and bed deformation in rivers with continuous bends. Journal of Hydrology 499, 224-235, <https://doi.org/10.1016/j.jhydrol.2013.07.005>
- Julien, P. (2018): River Mechanics. Cambridge: Cambridge University Press. 526 p.
- Jurík, E., Zelenáková, M., Kaletová, T., Arifjanov, A. (2019): Small Water Reservoirs: Sources of Water for Irrigation. Handbook of Environmental Chemistry, 69, 97–113.
- Kondolf, G. M. Gao, Y., Annandale, G. W., Morris, G. L., Jiang, E., Zhang, J., Cao, Y., Carling, P., Fu, K., Guo, Q., Hotchkiss, R., Peteuil, C., Sumi, T., Wang, H.-W., Wang, Z., Wei, Z., Wu, B., Wu, C., Yang, C. T. (2014): Sustainable sediment management in reservoirs and regulated rivers: Experiences from five continents. Earth's Future, 2, doi:10.1002/2013EF000184.
- Liu, C., Walling, D. E., He, Y. (2018): Review: The International Sediment Initiative case studies of sediment problems in river basins and their management. International Journal of Sediment Research. 33(2) 216–219. <https://doi.org/10.1016/j.ijsrc.2017.05.005>
- Lu, J., Li, A., Zhang, J., Huang, P. (2019): Yangtze River-derived sediments in the southwestern South Yellow Sea: Provenance discrimination and seasonal transport mechanisms. Journal of Asian Earth Sciences 176, 353–367. <https://doi.org/10.1016/j.jseas.2019.03.007>

- Morris, G. L. (2020): Classification of Management Alternatives to Combat Reservoir Sedimentation. *Water*, 12, 861. <https://doi.org/10.3390/w12030861>
- Tan, G., Chen, P., Deng, J., Xu, Q., Tang, R., Feng, Z., Yi, R. (2019): Review and improvement of conventional models for reservoir sediment trapping efficiency. *Heliyon* 5, e02458. <https://doi.org/10.1016/j.heliyon.2019.e02458>
- Wang, H., Kondolf, G. M. (2014): Upstream sediment-control dams: Five decades of experience in the rapidly eroding Dahan River Basin, Taiwan. *J. Am. Water Resour. Assoc.*, 50, 735–747.
- Yakovlev, E. Y., Malov, A. I., Druzhinin, S. V., Zykova, E. N., Orlov, A. S. (2020): Transformation of the radionuclides composition of river sediments in the area of the exploited Lomonosov diamond deposit (NW Russia). *Journal of Environmental Radioactivity*, 213, 106142, <https://doi.org/10.1016/j.jenvrad.2019.106142>
- Zhang, Q., Gong, Z., Zhang, C., Townend, I., Jin, C., Li, H. (2016): Velocity and sediment surge: What do we see at times of very shallow water on intertidal mudflats? *Continental Shelf Research* 113, 10–20. <https://doi.org/10.1016/j.csr.2015.12.003>

prof. Aybek Arifjanov (\*corresponding author, e-mail: obi-life@mail.ru)  
Dr. Luqmon N. Samiev  
Ing. Tatiana Kaletová, PhD.  
Department of Hydraulics and Hydroinformatics,  
Tashkent Institute of Irrigation and Agricultural Mechanization Engineers,  
39 Kari Niyazov  
Tashkent 100000  
Uzbekistan

Ing. Tatiana Kaletová, PhD.  
Faculty of Horticulture and Landscape Engineering  
Slovak University of Agriculture in Nitra  
Tulipanova 7  
94976 Nitra  
Slovakia

## Statistical analysis of soil water content differences after biochar application and its repeated application during 2020 growing season

Justína VITKOVÁ\*, Peter ŠURDA, Peter RONČÁK, Natália BOTKOVÁ, Anton ZVALA

Soil water content is an important factor influencing crop yield quantity and quality. Extreme meteorological events are more frequent in our geographical conditions in last years and they affect soil water storage. Biochar is an organic material and one of its properties is soil water holding for a longer time. This is one of great benefits during non-precipitation days. Our study is focused on soil water content changes with biochar amendment in comparison to soil without biochar. In addition, we analyzed biochar repeated application as well. It means addition another biochar dose into the soil where the biochar had been applied previously. Our results confirmed positive effect of biochar application and repeated application on soil water content. The soil water regime with biochar repeated application was the most stable in 2020 in comparison to other variants of experiment.

KEY WORDS: biochar, repeated application, soil moisture, statistical analysis

### Introduction

In current times of increasing weather extremes and climate change, is difficult to ensure good-quality and safe agricultural products. It is challenge not only for big farmers, but also for individual persons who tried to grow their own vegetables in good (bio) quality. Soil fertilization is one of possibilities how to improve soil physical and chemical properties and increase an agricultural production. To improve soil properties are used various organic materials, and biochar is one of them. Biochar is carbon-rich porous material produced from biomass by pyrolysis process, what means thermochemical decomposition of organic material at temperatures from 300°C to 1000°C with reduced access of oxygen. The interest of researchers began to focus on applications of burned organic waste into soil in the 80's of the 20th century. They were inspired by Amazon area (Lehmann and Joseph; 2015) where the soils called Terra Preta were made by massive input of wood burnt (similar to biochar). These soils have a high content of organic material and retain a higher production potential than the surrounding soils (Glaser et al., 2003). The soils throughout the world contain specific amounts of biochar as a result of natural events such as natural fires, paleo fires (Kuzyakov et al., 2018) and land use history – deforestation, pre-industrial charcoal kilns and anthropogenic oven mounds (Kuzyakov et al., 2018; Hardy et al., 2017). Biochar may alter the physical properties of the soil, including increasing aeration and

water holding capacity of certain soils (Sohi, 2010). High amounts of biochar added to soil affected soil wettability that influenced soil water retention (Ojeda et al., 2015). Biochar addition has been shown to improve plant growth (Graber et al., 2010), but also stimulate soil microbial activity (Smith et al., 2010). The agronomic value of biochar mainly resides in its value as a fertilizer and its ability to improve soil properties and increase crop production (Subedi et al., 2017; Yu et al., 2019). In Slovakia, we started with biochar experiment in field condition in March of the 2014 and in the 2018 was the same biochar repeatedly applied. The aim of this paper was to evaluate the impact of the biochar application and its repeated application on soil water content of silt loam soil in surface layer during the monitoring time period of the year 2020.

### Material and methods

Our measurements were conducted at the experimental area at Malanta site (Fig. 1). This area belongs to the Slovak University of Agriculture in Nitra, Slovakia. The research site is located 5 km north-east of Nitra city in the Nitra river basin where there is a deficit of soil water available to plants due to dry years (Tarnik and Leitmanova, 2017). The locality is 175 MASL and the soil is classified as a silt loam with content of sand 15.2%, silt 59.9% and clay 24.9% (Simansky and Klimaj, 2017). Our measurements began in March 2014 when certificated biochar was applied to the 0–15 cm soil

depth. Basic biochar characteristics of used biochar are shown in Table 1. A more detailed specification of the experiment foundation was described by Vitkova and Surda (2016) and partial results were published by e.g. Brezianská and Hlaváčiková (2017), Hlaváčiková et al. (2016) or Domanová et al. (2015). The biochar was produced from paper fibre sludge and grain husks in a ratio of 1:1 per weight, at a pyrolysis temperature of 550°C (Vitkova and Surda, 2016). In 2018, the original plots with former biochar application were divided in halves and the same biochar with the same dose was repeatedly applied to one of these halves (Toková et al., 2020). In this paper, we focused on three variants: plots with biochar dose of 20 t ha<sup>-1</sup> applied in 2014 (B20 old), plots with biochar dose of 20 t/ha repeatedly applied in 2018 (B20 new) and plots without biochar (Control). Soil water content was measured by 5TM dielectric sensors (Decagon Devices, USA); data was collected in five minutes interval and stored using the EM 50 data loggers. Two sensors were installed to the depth of 5–10 cm below the soil surface at two B20 old plots, two sensors were installed in the same depth at two B20 new plots and two sensors at two Control plots (four sensors at each variant). We present an average value from all sensors for each variant. The measurements were carried out during the 2020 growing season and the cultivated crop was pea (*Pisum sativum* L.). It was sown on March 20th, but our measurements began later. The monitoring period lasted from April 24th to July 16th. To better evaluate the effect of biochar application in various soil moisture conditions, we have selected (based

on the measured daily precipitation totals) a so-called dry (4.7.2020–10.7.2020) and wet period (5.6.2020–1.6.2020). Differences in group means of soil water content during these periods at all variants of experiment were then compared with each other and tested for statistical significance.

### Statistical analysis

Differences between the measured values of volumetric water content ( $\theta$ ) estimated at different variants of experiment were evaluated using single factor ANOVA with Tukey's Honest Significant Difference (HSD) post-hoc test. The Tukey-Kramer method (also known as Tukey's HSD method) uses the Studentized Range distribution to compute the adjustment to the critical value. The Tukey-Kramer method achieves the exact alpha level (and simultaneous confidence level  $(1 - \alpha)$ ) if the group sample sizes are equal and is conservative if the sample sizes are unequal. The statistical significance in the analysis was defined at  $P < 0.05$ .

### Results and discussion

Growing season in 2020 was well balanced with respect to precipitation, and during the monitoring period was observed dry period and also wet period. Average courses of soil water content values in 5–10 cm depth at plots Control, B20 old and B20 new in comparison to daily precipitation totals are shown at Fig. 2. The lowest values were measured at Control variant, but during

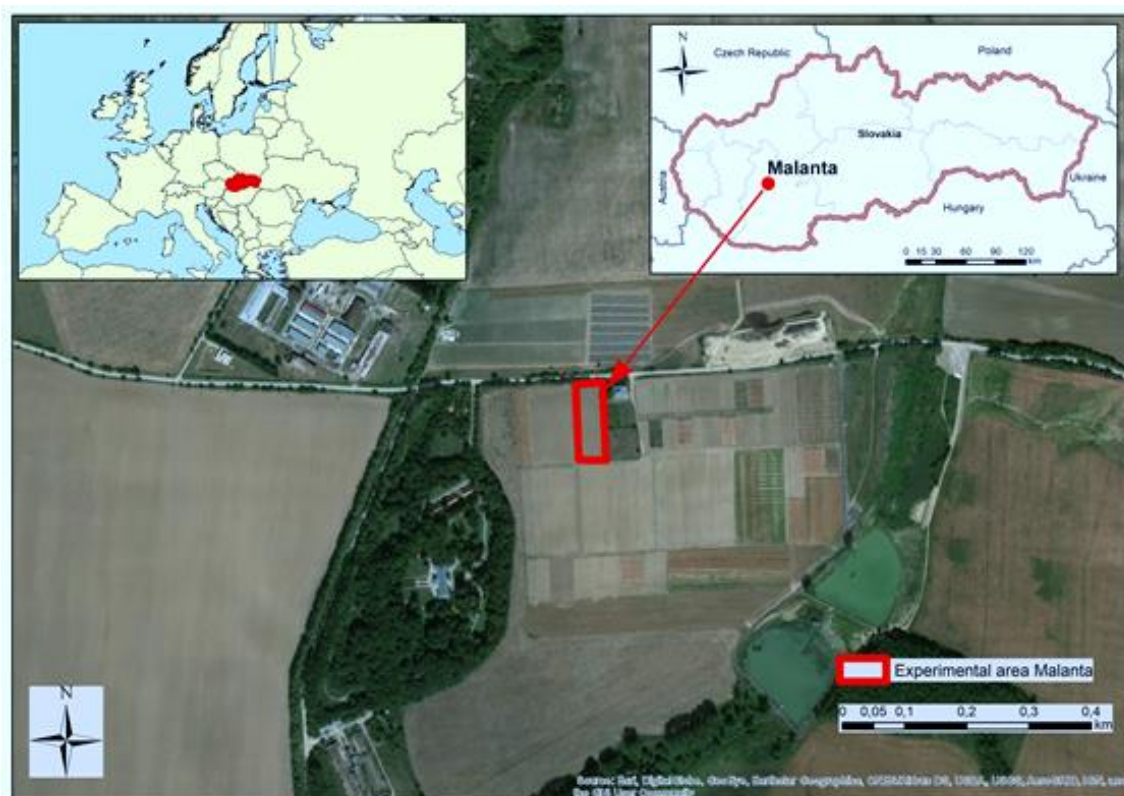


Fig. 1. Experimental area at Malanta site.

**Table 1. Biochar characteristics**

	<b>C</b>	<b>N</b>	<b>H</b>	<b>O</b>	<b>pH<sub>(CaCl<sub>2</sub>)</sub></b>	<b>Ash</b>	<b>SSA</b>
	[%]	[%]	[%]	[%]	[–]	[%]	[m <sup>2</sup> g <sup>-1</sup> ]
<b>Biochar</b>	53.1	1.4	1.84	5.3	8.8	38.3	21.7

(C – carbon, N – nitrogen, H – hydrogen, O – oxygen, pH determined by CaCl<sub>2</sub>, SSA – specific surface area)

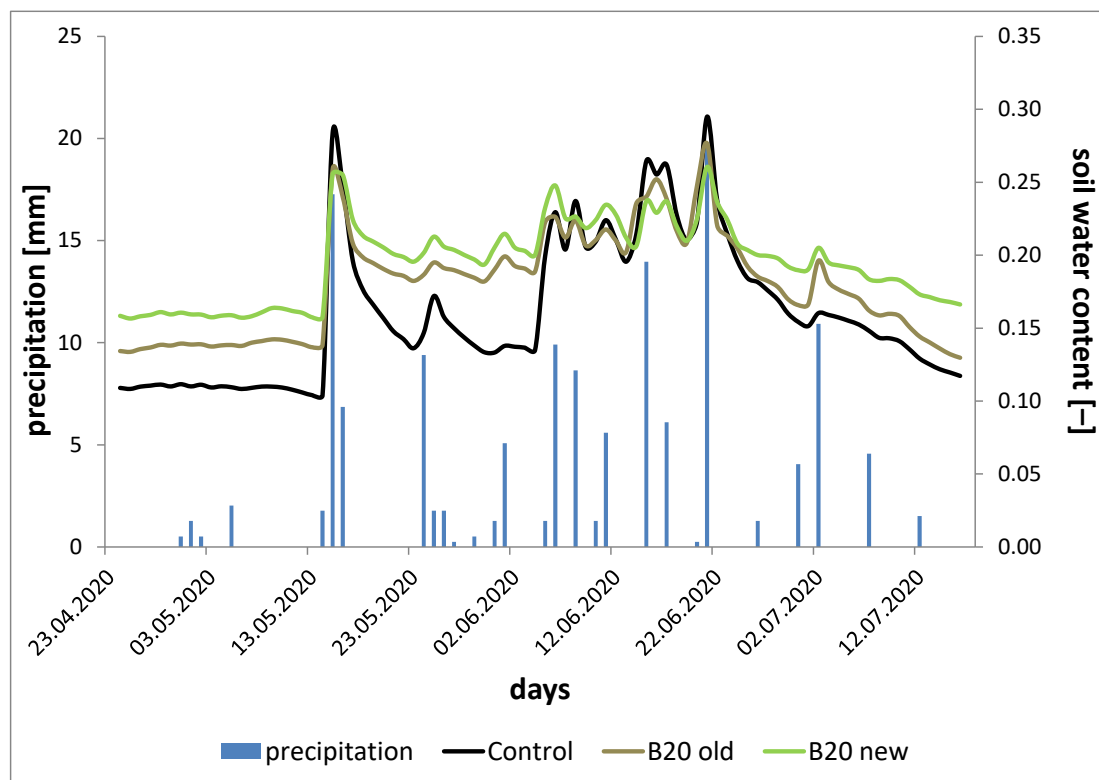


Fig. 2. Courses of measured soil moisture values at plots with old biochar, new biochar and without biochar (Control) during monitoring period.

the wet days were these values the highest. Opposite situation was measured at B20 new variant, where during days without precipitation were measured the highest values of soil water content. Based on these results it can be seen, that soil water content at B20 new variant was the most stable during the monitoring period. For plants (globally, but also for pea grown in 2020) is not important higher amount of soil moisture during wet days, but higher amount of soil moisture during days without precipitations. Soil water content was higher at plots with biochar during dry days of monitoring period, so we can conclude that biochar application had a positive effect on soil water content. Aydin et al. (2020) observed the positive effect of biochar on the alternation of crop yields in the third and fourth year after biochar application into Haplic Luvisol soil, but it also depended significantly on the climatic conditions in the individual year. Higher positive effect of biochar repeated application (B20 new) on crop yield could be also observed during our monitoring period, but our study was not focused on it.

According to values of  $\theta$  at B20 old, B20 new and Control variants of experiment measured during the whole monitoring period, we can state that both minimal (0.101) and maximal (0.427) value of  $\theta$  were measured at Control plot. As a positive effect of the biochar application we can indicate that at B20 old, resp. B20 new the value of  $\theta_{min}$  did not decrease below 0.124 resp. 0.153. Group means of  $\theta$  for whole monitoring period increased in order Control < B20 old < B20 new (Fig. 3a) with statistically significant differences between all variants of experiment (Table 2). During dry period, we found statistically significant differences between all variants of experiment (Table 2) and group means of  $\theta$  increased in the same order as during the whole monitoring period (Fig. 3b). During the wet period we did not found significant difference between the Control and B20 old variant (Fig. 3c); significantly different were B20 new and the remaining two variants. Slightly higher mean value of  $\theta$  was measured on B20 new variant, than on the B20 old and Control.

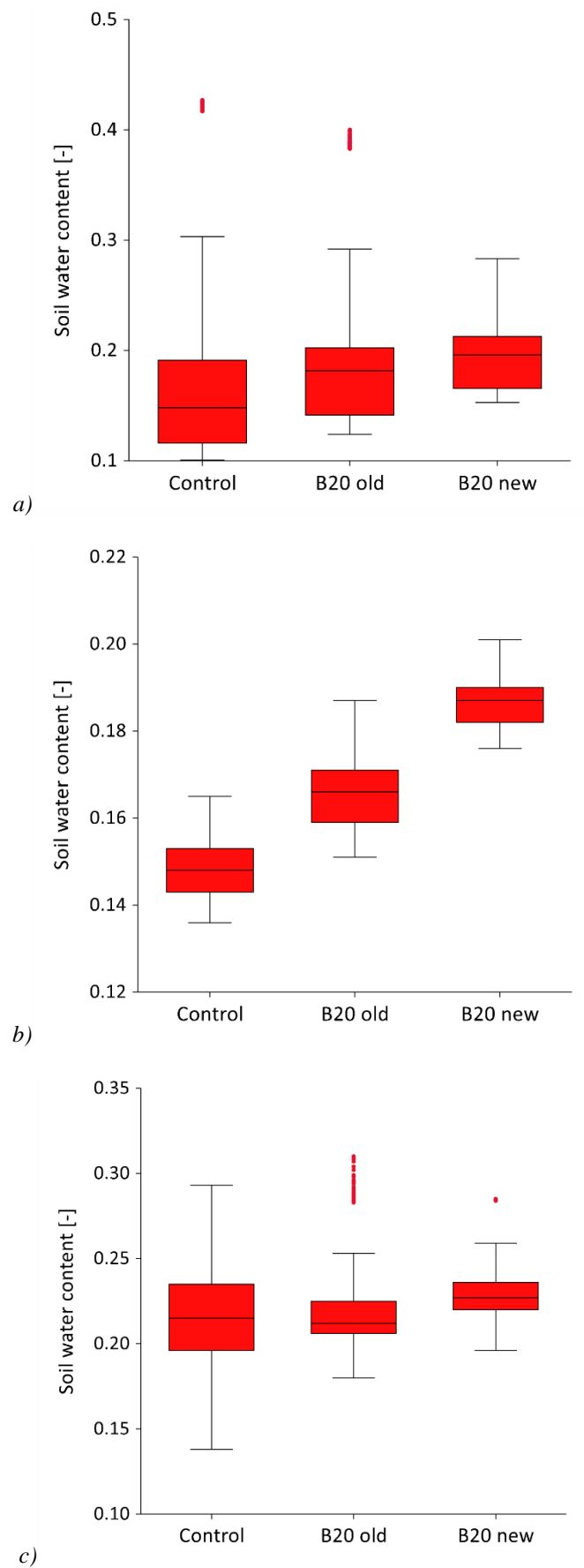


Fig. 3. Box plots with measured values of  $\theta$  during a) whole monitoring period, b) dry period and c) wet period at Control, B20 old and B20 new variants.

**Table 2.** Measured values of volumetric soil water content,  $\theta_{min.}$  – minimal value of  $\theta$ ,  $\theta_{max.}$  – maximal value of  $\theta$ ,  $\theta_{mean}$  ( $\pm$  their standard deviation) – arithmetic mean of  $\theta$  values measured during monitoring period,  $\theta_{dry}$  ( $\pm$  their standard deviation) arithmetic mean of  $\theta$  values measured during dry period 4.7.2020–10.7.2020 and during wet period 5.6.2020–11.6.2020 ( $\theta_{wet}$ ); Arithmetic means with the same letter are not significantly different from each other (Tukey's HSD test,  $P < 0.05$ ).

Plot	$\theta_{min.}$ [-] (N=24023)	$\theta_{max.}$ [-] (N=24023)	$\theta_{mean}$ [-] (N=24023)	$\theta_{dry}$ [-] (N=2016)	$\theta_{wet}$ [-] (N=2016)
Control	0.101	0.427	0.161 $\pm$ 0.0519 <sup>a</sup>	0.149 $\pm$ 0.0070 <sup>a</sup>	0.216 $\pm$ 0.0354 <sup>a</sup>
B20 old	0.124	0.400	0.180 $\pm$ 0.0398 <sup>b</sup>	0.166 $\pm$ 0.0090 <sup>b</sup>	0.217 $\pm$ 0.0206 <sup>a</sup>
B20 new	0.153	0.342	0.195 $\pm$ 0.0297 <sup>c</sup>	0.187 $\pm$ 0.0060 <sup>c</sup>	0.230 $\pm$ 0.0183 <sup>b</sup>

## Conclusion

The application of organic material into the soil has been used for several centuries. In last decades, the interest of scientists has been focused on biochar. Its application into soil can improve its structure and quality thereby also having a positive effect on the crop quantity and quality. Statistically significant differences between all variants of experiment were measured especially during dry period. Repeated application of biochar (B20 new) increased the soil water content at 4% vol. in comparison to Control variant. During the wet period was the different between B20 new and Control variants only 1% vol. It was statistically confirmed that soil water regime was the most stable at B20 new variant (range of values 18.9% vol.) in comparison to B20 old (range of values 27.6% vol.) or Control (range of values 32.6% vol.), respectively. The results of our research at field conditions show that the application of biochar in the soil is very important, especially during dry days.

## Acknowledgement

This work was supported by Scientific Grant Agency No. VEGA 2/0155/21 and by EIG CONCERT-Japan No. EIG JC2019-074.

## References

- Aydin, E., Šimanský, V., Horák, J., Igaz, D. (2020): Potential of Biochar to Alternate Soil Properties and Crop Yields 3 and 4 Years after the Application. *Agronomy*, 10, 889.
- Brezianská, K., Hlaváčiková, H. (2017): Analyse of volume change and soil physical properties of sandy-loam soil and biochar mixtures. *Acta Hydrologica Slovaca*, vol. 18, No. 1, 104–111.
- Domanová, J., Igaz, D., Borza, T., Horák, J. (2015): The retention characteristics of soil after application of biochar. *Acta Hydrologica Slovaca*, vol. 16, No. 2, 193–198.
- Glaser, B., Guggenberger, G., Zech, W. De Lourdes Ruivo, M. (2003): Soil organic matter stability in Amazonian Dark Earths: Origin, Properties, and Management. Kluwer, The Netherlands, 141–158.
- Graber, E. R., Harel, Y. M., Kolton, M., Cytryn, E., Silber, A., David, D. R., Tsechansky, L., Borenshtein, M., Elad, Y. (2010): Biochar impact on development and productivity of pepper and tomato grown in fertigated soilless media. *Plant and Soil*, vol. 337, 481–496.
- Hardy, B.; Cornelis, J. T.; Houben, D.; Leifeld, J.; Lambert, R.; Dufey, J. E. (2017): Evaluation of the long-term effect of biochar on properties of temperate agricultural soil at pre-industrial charcoal kiln sites in Wallonia, Belgium. *Eur. J. Soil Sci.*, 68, 80–89.
- Hlaváčiková, H., Brezianská, K., Novák, V. (2016): Influence of a biochar application on a sandy-loam soil water retention properties. *Acta Hydrologica Slovaca*, vol. 17, No. 2, 279–286.
- Kuzyakov, Y.; Merino, A.; Pereira, P. (2018): Ash and fire, char, and biochar in the environment. *Land Degrad. Dev.*, 29, 2040–2044.
- Lehmann, J., Joseph, S. (2015): Biochar for environmental management: Science, technology and implementation. 2nd ed. London: Routledge, Taylor & Francis Group. 928 pp. ISBN 978-0-415-70415-1.
- Ojeda, G., Mattana, S., Avila, A., Alcaniz, J. M., Volkmann, M., Bachmann, J. (2015): Are soil-water functions affected by biochar application? *Geoderma*, vol. 249–250, 1–11.
- Simansky V., Klimaj A. (2017): How does biochar and biochar with nitrogen fertilization influence soil reaction? *Journal of Ecological Engineering*, vol. 18, 50–54.
- Smith, J. L., Collins, H. P., Bailey, V. L. (2010): The effect of young biochar on soil respiration. *Soil Biology & Biochemistry*, vol. 42, 2345–2347.
- Sohi, S. P. (2010): Appendix 1. Analysis of scientific studies published on the function of char, its quantification, and its stability in soil. In *An Assessment of the Benefits and Issues Associated with the Application of Biochar to Soil*; Shackley, S., Sohi, S.P., Eds.; A Report to the Department for Environment, Food and Rural Affairs and the Department of Energy and Climate Change: London, UK, 1–4.
- Subedi, R.; Bertora, C.; Zavattaro, L.; Grignani, C. (2017): Crop response to soils amended with biochar: Expected benefits and unintended risks. *Ital. J. Agron.*, 12, 161–173.
- Tarnik A., Leitmanova M. (2017): Analysis of the Development of Available Soil Water Storage in the Nitra River Catchment. In *IOP Conference Series: Materials Science and Engineering*, WMCAUS, 245, art No. 062017.

- Toková, L., Igaz, D., Horák, J., Aydin, E. (2020): Effect of Biochar Application and Re-Application on Soil Bulk Density, Porosity, Saturated Hydraulic Conductivity, Water Content and Soil Water Availability in a Silty Loam Haplic Luvisol. *Agronomy*, vol. 10, no. 7, 1005.
- Vitkova J., Surda P. (2016): Soil moisture differences at plots with and without biochar application (in Slovak language), XX. Okresne dni vody: Recenzovany zbornik referatov - Bratislava; Michalovce; Kosice. Institute of Hydrology, Hydrological Research Base in Michalovce, 113–116.
- Yu, H., Zou, W., Chen, J., Chen, H., Yu, Z., Huang, J., Tang, H., Wei, X., Gao, B. (2019): Biochar amendment improves crop production in problem soils: A review. *J. Environ. Manag.*, 232, 8–21.

Ing. Justína Vitková, PhD. (\*corresponding author, e-mail: vitkova@uh.savba.sk)  
Ing. Peter Šurda, PhD.  
Mgr. Peter Rončák, PhD.  
Ing. Natália Botková  
Mgr. Anton Zvala, PhD.  
Institute of Hydrology SAS  
Dúbravská cesta 9  
841 04 Bratislava  
Slovak Republic

Ing. Natália Botková  
Institute of Landscape Engineering  
Faculty of Horticulture and Landscape Engineering  
Slovak University of Agriculture in Nitra  
Tulipánová 7  
949 76 Nitra  
Slovak Republic